NON-LINEAR VIBRATION OF A TRAVELLING BEAM

by

GOUTAM CHAKRABORTY

DEPARTMENT OF MECHANICAL ENGINEERING

INDIAN INSTITUTE OF TECHNOLOGY KANPUR

APRIL, 1999

NON-LINEAR VIBRATION OF A TRAVELLING BEAM

A Thesis Submitted
In Partial Fulfilment of the Requirements
for the Degree of
Doctor of Philosophy

by

Goutam Chakraborty

to the
DEPARTMENT OF MECHANICAL ENGINEERING
INDIAN INSTITUTE OF TECHNOLOGY KANPUR
INDIA
April, 1999

To

the fond memory of my

Grandfather

Certificate

It is to certify that the work contained in the thesis entitled **Non-linear Vibration of a Travelling Beam** by Goutam Chakraborty, has been carried out under my supervision and that this work has not been submitted elsewhere for a degree.

A. K. Mallik 28/4/99

Department of Mechanical Engineering

IIT Kanpur

April, 1999

Acknowledgment

No amount of words will ever be able to express how much I owe to my thesis supervisor Prof. A. K. Mallik. Refraining then from the vain attempt, let me only say that if the present work has any little worth, it is solely due to his constant encouragement, helpful suggestions and fruitful criticism.

I would like to thank Prof. H. Hatwal for his active interest during the initial phase of this research. Thank also goes to Prof. N. S. Vyas, Professor-in-charge of the Vibration Laboratory, for providing a very lively working atmosphere.

I am thankful for the help I got from Mr. M. M. Singh and my kind-hearted colleagues Messrs Goutam Pohit, Ahmed Ali Khan, Animesh Chatterjee, Chandrasekhar and Neeraj.

Plenty of familiar faces, whose friendship always brought happiness into my life at IITK, smilingly crowd in the memory. Let them shine forever from their right place!

Finally, I pay homage to my parents who, by all means, encouraged me since my childhood to learn ever more.

Goutam Chakraborty

Synopsis

A number of real-life systems, like a band-saw, a magnetic tape, a power transmission belt, an overhead cable for aerial tramways, a flexible manipulator arm having prismatic joint etc., can be modelled as axially travelling continua. With increasing axial speed, the productivity increases but the performance deteriorates due to the transverse vibration caused by external or parametric excitations. The separation-of-variable method, a well-known tool for the analysis of an axially stationary member, cannot be applied for a travelling member due to the presence of the 'gyroscopic' term. Further, unlike in a stationary medium, the natures of the propagating transverse waves in a travelling medium become complicated to form a clear physical idea. These complications are further enhanced in a dispersive medium.

In addition to the above difficulties, the analysis also becomes cumbersome due to the presence of geometrical non-linear terms, which are significant during large oscillations at high axial speeds. Such large oscillations are caused by resonance or hard non-resonant excitations. The non-linear terms are important not only for obtaining quantitatively accurate resuls but also for explaining several phenomena which cannot be predicted from a linear analysis. Furthermore, any measure based upon a linear model to control the unwanted vibration may turn out to be ineffective in the presence of non-linear terms.

The aim of the thesis is to study the effects of non-linearities on the transverse

vibration of an Euler-Bernoulli beam moving over two simple supports. Various operating conditions generating different kinds of excitations are considered. Compared to the vast amount of literature available on the linear vibration of travelling continua (discussed in Chapter 1), the non-linear oscilations of a travelling beam have so far received less attention.

The non-linear equation of motion is derived in Chapter 2. Since the small non-linear term in the equation of motion is considered as a perturbation to the linear equation, a detailed knowledge of the linear system is essential. The rest of Chapter 2 is devoted to study the free and forced linear vibrations by two apparently distinct methods, namely the 'modal' analysis and the 'wave-propagation method'. While the discussion of the former is limited to the existing results, the latter method is developed for the first time. The numerical results obtained from these two methods are compared. Damping is not considered unless the presence of the damping term changes the qualitative behaviour of the system.

In Chapter 3, a simple and computationally efficient method of obtaining the near-resonance response of a non-linear continuous system is presented. The method is elucidated, for the sake of simplicity, with an axially stationary beam having either simply-supported or clamped-clamped boundary conditions. The non-linear normal modes of the beam are derived first by perturbing the linear normal modes and then also using the wave-propagation method. These non-linear normal modes are subsequently used to obtain the near-resonance response. The results so obtained are then compared with the experimental results available in the literature. The efficacy of the present method over the Galerkin's technique is highlighted.

The results of Chapters 2 and 3 are extended in Chapter 4 to derive the response of the non-linear travelling beam under both resonant and hard non-resonant excitations. A concept of non-linear complex normal mode is first presented. The near-resonance

response is subsequently obtained using these non-linear complex normal modes. The methods of deriving both the non-linear complex modes and the near-resonance response closely resemble those outlined in Chapter 3. Like in any other non-linear system, multiple values are obtained for the near-resonance response. However, all of these values are not physically realizable. The physically observable results are delineated by carrying out a stability analysis. When the excitation is hard non-resonant one, the modal method encounters difficulties. The method of wave-propagation, derived for the linear system in Chapter 2, has been effectively extended for such a situation.

Chapter 5 deals with the effects of the non-linear term on a parametrically excited travelling beam. The source of the parametric excitation is taken to be the tension fluctuation due to the unbalance in one of the pulleys which is mounted on an axially-flexible support. Single or multiple limit cycles, generated by the combination of non-linearity and parametric excitation in the presence of small viscous damping, are obtained using the non-linear complex normal modes. The stable limit cycles are identified by carrying out a stability analysis. The response of the beam to simultaneous parametric and external harmonic excitations is also obtained. The non-linear complex normal modes are used for this purpose. Again a stability analysis for determining the physically observable solutions is presented.

The stability of an accelerating or decelerating non-linear beam is presented in Chapter 6. This situation arises during the starting or stopping phases. A Lyapunov's stability analysis is first carried out to study the stability characteristics of the beam having any arbitrary acceleration. For a decelerating beam, the stability is determined using a perturbation technique based on Multiple Time Scale (MTS) method. The uniform deceleration which alters the magnitude of the uniform axial speed but not the direction of axial movement is considered as a small perturbation.

A controller to reduce the vibration of a non-linear beam moving with uniform

axial speed is discussed in Chapter 7. A passive controller in the form of a roller guide is proposed. The finite compliance of the guide in the transverse direction, and the frictional force appearing at the guide-beam interface and acting in the axial direction are incorporated. The results of the linear analysis, for both free and forced vibrations, are used to obtain the non-linear complex normal modes that are subsequently utilised to get the near-resonance response. The effectiveness of the roller in reducing the amplitudes of both linear and non-linear vibrations of the beam under harmonic excitation has been brought out with the help of numerical examples.

The main conclusions of the present work are summarized in Chapter 8. Some directions for further research are also mentioned therein. The major conclusions of the analyses presented in the thesis can be summarized as listed below:

(i) The natures of the waves associated with the free modal vibration of a travelling beam change depending upon the relations between various system parameters. During linear modal vibration, either two propagating and two evanescent waves (one of each kind in both upstream and downstream directions) or four propagating waves (one in the upstream direction and the remaining three in the downstream direction) appear depending on the axial speed. The well-known 'phase-closure' principle is satisfied for both the cases. The 'phase-closure' principle is also satisfied during non-linear modal oscillations of such a beam.

(ii) The near-resonance response to an external harmonic and/or parametric excitation can be obtained easily using the non-linear complex normal modes. This method is computationally more efficient than the commonly-used Galerkin's technique.

(iii) The steady-state response of the beam to a non-resonant hard excitation can be obtained by wave-propagation analysis. In this method, a closed form transfer function, i.e., the Laplace transform of a point-impulse response, is first obtained. The linear response obtained using this transfer function is then perturbed to get the effects of

the small non-linear term. The present method is shown to be more accurate and computationally more efficient than either Galerkin's technique or non-linear complex modal analysis.

(iv) The non-linear natural frequencies of a travelling beam increase with the amplitude of vibration. The 'jump' of the amplitude of the response envelope can be observed under a near-resonant excitation. Further, one or multiple 'limit cycle's of the amplitude of the response envelope are possible when the beam is parametrically excited. These three phenomena show striking resemblance with those exhibited by a hard Duffing oscillator.

(v) For a parametrically excited travelling beam with an external harmonic excitation, the effects of various system parameters depend on the relative strengths of the two forms of excitation. Moreover, a particular phase relationship between the two forms of excitations (whose frequencies are related) results in a minimum value of the steady-state response.

(vi) A continuously accelerating beam remains stable, but for a decelerating beam instability may appear depending upon the magnitudes of damping and deceleration. However, the amplitude of a decelerating beam does not grow unboundedly and the beam regains its stability in the long run. The non-linear term does not play any role so far as the stability is concerned. It merely changes the frequencies of oscillations.

(vii) An intermediate guide can be effectively used as a passive controller of vibration. The choice of the suitable guide-location plays a very important role in reducing the level of vibration. The guide also has a stabilizing effect so far as the divergence instability is concerned. But the frictional force between the guide and beam may add to instability. Thus, to use the controller effectively, the friction has to be minimised. Towards this end, a roller-guide is suggested.

Contents

List of Figures

List of Symbols

A	area of cross-section of the beam
E	Young's modulus of the beam material
I_z	second moment of area of cross-section about the neutral axis
$k_f^*/2$	stiffness of the roller-guide
$K_f/2$	non-dimensional stiffness of the guide
$N^*/2$	precompression of the guide
$N/2$	non-dimensional precompression of the guide
R^*	pulley radius
R	non-dimensional pulley radius
T_0^*	initial tension in the beam
T_0	non-dimensional tension
T_j^*	tension in the j-th span in a constrained beam, where $j = 1, 2$
ΔT	difference between the tensions in different spans ($=T_2 - T_1$)
c^*	axial speed
c	non-dimensional axial speed
c'	$=c/\sqrt{T_0 + \pi^2}$
d^*	location of the guide
d	non-dimensional location of the guide
e_1^*	eccentricity of the unbalanced mass
e_1	non-dimensional eccentricity
f^*	transverse force per unit length
f	non-dimensional transverse force per unit length
i	$=\sqrt{-1}$
k_p^*	stiffness of the flexible pulley-foundation
k_p	non-dimensional pulley-support stiffness
k	$k_p/(1 + k_p)\ (0 \leq k \leq 1)$
l	length of the beam
m^*	eccentric unbalanced mass
m	non-dimensional pulley unbalance
r	radius of gyration of the beam cross-section $= \sqrt{I_z/A}$

t	time
u^*	longitudinal displacement of the beam
u	non-dimensional longitudinal displacement
w^*	transverse displacement of the beam
w	non-dimensional transverse displacement
x	non-dimensional distance
Ω^*, Ω_f^*	frequencies of external harmonic excitation
Ω, Ω_f	non-dimensional frequencies of excitation
$2\Omega_p^*$	rotational speed of the pulley
$2\Omega_p$	non-dimensional rotational speed of the pulley
Φ	n-th linear complex modal vector
Ψ	n-th non-linear complex modal vector
α	factor governing uniform acceleration/deceleration
γ	slenderness ratio, $r/l \ll 1$
δ, μ	factors governing viscous damping
ϵ	$= \gamma^2/2$
ξ	axial distance of a point on the beam from the left support
θ_f	phase relationship between parametric and external harmonicexcitation
μ_f	coefficient of dynamic friction
ω_n^l	natural frequency corresponding to the n-th linear mode
ω_n	natural frequency corresponding to n-th non-linear normal mode
ϕ_n^*	$= \sqrt{(\phi_n^R)^2 + (\phi_n^I)^2}$
ϕ_n	n-th linear complex normal mode $= \phi_n^R + i\phi_n^I$
ψ_n	n-th non-linear complex normal mode $= \psi_n^R + i\psi_n^I$
ρ	density of the beam material
τ	non-dimensional time

Chapter 1

INTRODUCTION

1.1 Introduction

A number of appliances in diverse fields of engineering are modelled as axially moving continua. Some of the common examples are saw-bands used in forest industries, magnetic tapes in tape-recorders and computers, travelling threadlines in textile industries, belt-drives in automobiles, flexible manipulator arms having prismatic joints, etc. High productivity often requires these systems to operate at the highest possible speed. However, at a high speed, the performance deteriorates primarily due to vibrations of the moving element in a direction orthogonal to that of the axial movement. The presence of the 'gyroscopic term' in the equation of motion of transverse oscillation of such systems makes the problem quite different from that of an axially stationary slender member. For the latter case, a great variety of mathematical tools have been developed over the centuries. Further, the close relationship between the vibration of and wave propagations in axially stationary members has helped the researchers to gain insight into their oscillatory behaviour. But even a simplistic linear model of a travelling continuous system presents some difficulties as the separation of variable

method, a well-known tool for solving a boundary value problem, is not applicable in this situation. The nature of the propagating transverse waves in a travelling medium, especially if it is dispersive in nature like a beam, becomes complicated to form a clear physical idea. These difficulties have motivated researchers to give special attention to this class of systems.

Apart from the technical difficulties mentioned above, the real situation is further complicated by the inevitable presence of various non-linear terms at different levels of approximation. Depending upon their sources, these non-linear terms are of two kinds: one appearing due to material non-linearities, i.e., non-linear variation of stress with strain, and the other resulting from geometric non-linearities i.e., non-linear strain-displacement relationship. While the former depends upon the material properties of the vibrating medium, the latter is encountered during large-amplitude oscillations, for example, due to resonance or non-resonant hard excitations. The importance of the geometrical non-linearities increases with increasing axial speed of a travelling member. The results of a non-linear analysis not only quantitatively differ from that obtained by a linear analysis, certain phenomena observable in real life can never be explained from a linear analysis. Furthermore, a control measure based only upon the approximate linear model may turn out to be ineffective in the presence of non-linear terms.

For a continuous system, the non-linear analysis becomes increasingly difficult due to modal coupling. The linear vibration analysis of a continuous system is usually carried out by mathematically discretizing the equation of motion, to a set of infinitely many decoupled simple equations, with the help of orthogonal normal modes. Such modal decoupling is generally not possible in the non-linear case. Some simplifications are achieved during resonant vibrations, when the contributions to the overall response from one or few linear modes are orders of magnitude higher than those from the others. But the analysis becomes cumbersome during a non-resonant large oscillation,

especially due to a high-frequency excitation, when a good number of modes contribute significantly to the response.

The aim of this thesis is to study the effects of non-linear terms on the vibrations of a travelling beam operating under various conditions. To this end, special analytical tools for solving the problems under consideration have been devised. The physical understanding of the oscillatory behaviour has been enhanced by explaining both the free and forced vibrations in terms of various waves propagating in this dispersive medium. An easily implementable passive controller has also been suggested to reduce the non-linear vibration of such a system.

1.2 Literature Review

Following Aitken's earliest experiment on the vibrations of a travelling belt, researchers have been trying to understand and control the dynamics of travelling continuous systems [1]. These efforts have been compiled in several review articles [2]- [6]. A very rich literature also exists for the closely related problem of vibration of pipes, where the axial material movement is maintained by the fluid flow [7].

As mentioned in Section 1.1, the vibration of a moving medium, whether supported at one or both ends, differs from that of an axially stationary medium. While both the mass and energy of the span are conserved in a stationary member, the energy of a travelling member is not conserved [8]- [11]. Further, if the support is only at one end, the length of the span and hence, the oscillatory mass changes as the member moves. Thus, the axially moving systems can be divided into two categories, one having 'fixed span' and the other with 'variable span'. These two kinds of system have been treated separately in the literature.

1.2.1 Free Vibration

1.2.1.1 Strings and Cables

Free linear vibration of a string travelling over two supports has been studied analytically [12]- [16]. The theory of wave propagation has also been used [9, 17]. Following the works of Meirovitch [18, 19] and other researchers [20] in the field of linear gyroscopic systems, the modal oscillation of a travelling string has been studied in terms of the complex normal modes. Here the waves in the upstream and downstream directions travel with different speeds. Consequently a standing envelope rather than a standing mode is formed. The impossibility of the standing modes is also evident from the equation of motion, where the temporal and the spatial variables are coupled through the Coriolis component in the transverse force, known as the 'gyroscopic' term in the literature. The centrifugal force, on the other hand, compels the natural frequencies to decrease with increasing axial speed until a 'critical' speed is reached when all of them vanish simultaneously. At this critical speed, no wave can propagate in the upstream direction.

Systems like continuously-supported conveyer belts, air-guided magnetic tapes, translating paper-pulp sheets supported by air-jets etc. are modelled as an axially moving string having intermediate spring supports. The nature of the propagating waves and thus the dynamics of such systems are quite different from those of the systems supported only at the ends of the span [21]- [27]. For example, in a travelling string elastically supported over a part of the span, the harmonic nature of the time-response is lost if the frequencies of the propagating waves become smaller than a 'cut-off' frequency [21, 28]. However, the 'critical' speeds of these systems are not altered. On the other hand, the dry frictional force present in the intermediate supports like capstans, cylinders, eyelets, read/erase heads, rollers etc., reduces the critical

speed significantly [29]. Studies with various other constraints reveal that while a pure elastic constraint increases the natural frequencies, an inertia constraint in the form of a stationary point mass has a reverse effect [26, 30]. The well-known 'eigenvalue-inclusion principle' holds good for both these cases [30]. The complicated situation with both kinds of constraints has also been analysed [31].

The dynamics of a translating cable has also received attention [32]- [36]. Due to the presence of a small sag, the natural frequencies of such a system do not always decrease monotonically with increasing axial speed. The angle of inclination of the cable, caused by a difference in the heights of the end supports, may change the dynamics significantly [33]. For a small axial speed, the equilibrium configuration of a sagged cable is unique and is known as the 'minimum catenary'. But for a sufficiently large translating speed, a second arch-like equilibrium configuration, known as the 'maximum catenary', becomes stable [35, 36].

1.2.1.2 Beams

The vibration problem of a travelling beam was first studied in 1965 with reference to a saw-band which was modelled as an Euler-Bernoulli beam travelling over two frictionless simple supports [37]. This and subsequent analyses have shown that the natural frequencies of such a beam, like those of a string, decrease with increasing axial speed [38]- [40]. But, unlike in a string, there exist different critical speeds for different complex modes of the travelling beam. The compressive load, generated due to the centrifugal force at any of these critical speeds, becomes equal to the Euler buckling load for the corresponding mode. These critical speeds, however, increase if the beam is driven by pulleys having finite support compliance in the axial direction [37]. Studies on the vibrations of travelling beams having non-trivial equilibrium configuration have also been carried out [41, 42]. The static deflection of the beam from the trivial con-

figuration is due to manufacturing flaws, finite end-curvatures because of the pulleys, etc. The natural frequencies of the odd order modes of such a beam do not vanish at any speed, though the natural frequencies of the even order modes disappear at the critical speeds.

For an unguided saw-band driven by pulleys, the vibrational energy does no longer remain confined to any of the two identical spans but gets transferred from one span to the other periodically [43, 44]. Consequently, introduction of damping in one span helps to damp out the oscillations in the other [45]. The periodic transfer of energy among the spans, known as the 'beating phenomenon', is absent if the band is replaced by a srting [43]. The band/wheel system has been studied using two different models. In one model, the non-trivial static equilibrium configurations of the spans, due to the finite end-curvatures at and near the pulleys, are taken into account and the linearized equations of motion of both the transverse and longitudinal vibrations of the two spans have been obtained [44]. The longitudinal vibration, which affects the pulleys, plays a significant role in coupling the oscillatory motions of the two spans. The other simplified model assumes the trivial equilibrium configurations of the spans and the coupling is manifested through the slope- and moment-continuity at each adjascent end [46, 47]. It may be mentioned that in reference [46], the boundary conditions are incomplete (only six of the required eight conditions are presented). Analyses of both the above models show that the frequencies of a band/wheel system appear in groups, each consisting of two closely separated frequencies. The difference between the two frequencies of any such group governs the frequency at which energy is exchanged between the spans. The effects of various parameters like band tension, axial speed, pulley radii, etc., on the vibration coupling have been reported. The coupling decreases with increasing pulley radii and/or the tensions in the bands. As the axial speed is increased, the coupling first decreases until the spans get decoupled for a particular

mode (i.e., two frequencies belonging to a group become identical). If the axial speed is increased further the coupling gets stronger. The decoupling corresponds to the intersection of the frequency vs. axial speed plots. However, a slight disorder in the spans, for example, due to a difference in the initial band tensions, may introduce a new phenomenon, known as 'frequency-loci veering' or 'curve veering' [48]. As the name suggests, the two frequencies, in stead of becoming equal, abruptly veer away from each other. The aforesaid curve veering results in 'vibration localization' or 'mode localization' in one of the two spans [47, 49]. This kind of localization of oscillatory motion has been observed in various physical and engineering systems consisting of periodic elements with disorder [50]- [54]. It may be worthwhile to note that the localization occurs also in a friction guided travelling string [29].

1.2.1.3 Strings/Beams with Attached Systems

The dynamics of a travelling member changes significantly if a rigid or flexible body is attached thereto. Examples of such a system include an aerial tramway, a ski-lift, a monocable ropeway, a conveyer belt, a saw-band having material imperfections like weld-melts, etc. The non-harmonic nature of the response during free vibration of such a system has been confirmed by both exact and approximate analyses [55]- [57]. In the exact analysis, the unknown force between the string and the appendage is solved by formulating a Volterra equation of the first kind. In the approximate method, the inhomogeneity in the mass distribution is considered as a small perturbation to the original system. Theoretical as well as experimental results show that the amplitude of vibration of a string having an attached body is more than that of a string without any appendage. Thus, for safe operation of such a system, the axial speed must be restricted to a value much lower than the critical speed.

1.2.2 Vibration due to External/Parametric Excitations

The responses of a constrained or unconstrained travelling continuous system to force/displacement excitations have been obtained by three different methods, namely, Galerkin's technique or the assumed mode method [58], the exact modal analysis [16, 59] and the transfer-function method [60]- [63]. In the first method, the equations of motion are discretized, with the help of the modes of an axially stationary member, to a set of ordinary differential equations in temporal coordinates which are then solved to get the response. However, the implicit assumption of the separation of the spatial and temporal variables results in slow convergence of the series solution. A faster convergence can be achieved by discretizing the equation of motion to several complex ordinary differential equations with the help of the exact complex normal modes [64]. The series form of the response can be altogether avoided by formulating closed-form transfer function (i.e., the Laplace transform of the Green functions) of the travelling member [60, 62]. The response to any arbitrary excitation is then derived with the help of this transfer function. The last method enjoys an added capability of tackling any arbitrary boundary condition. For a travelling string, different terms of the transfer function have been also explained in terms of various propagating waves [63]. The response of the string to a displacement excitation can be very easily obtained using the wave-propagation theory. For a beam, however, the waves are significantly distorted making the wave-propagation analysis difficult. It should be mentioned here that if the load is time-invariant, the problem of wave propagation does not arise and the exact response can be easily obtained [65].

Apart from direct external excitations, the travelling members are often subjected to parametric excitations. Such excitations are caused by the fluctuations in either tension [66, 67] or axial speed [68]- [71] of the members. For a travelling string

(especially V-belts), the tension fluctuations are caused mainly by the belt-defects, whereas the eccentricities of one or both the pulleys may periodically change the tension of a saw-band. The parametric fluctuations in the belt-drive of an automobile occur through velocity modulations due to the fluctuating turning moment of the engine. Various aspects of a parametrically excited travelling system have been reported in the literature [66]- [71]. Both primary and secondary resonances have been studied. The response of a travelling beam having random tension fluctuations has also been obtained using stochastic averaging technique [72]- [74].

1.2.3 Control

It is well known that the vibration deteriorates the overall performance of travelling systems. Further, the bucklng of the travelling beam at a supercritical speed restricts its speed of operation. Thus the objectives of the vibration engineers have been

(i) to increase the critical speed, and

(ii) to reduce the level of vibration in the subcritical speed regime.

As mentioned earlier, the critical speed can be increased by mounting the pulleys flexibly on the foundation [37]. Other methods like increasing the band tension by heating or applying a belt-tensioner system have also been used [75]. A new method of stabilizing the band at critical speed by introducing a parametric excitation has been suggested recently [76]. This method is analogous to stabilizing an inverted pendulum by means of parametric excitation. Different control strategies, both passive and active, are adopted to reduce the unwanted oscillations of a travelling system during operation. Each controller has its own advantages and disadvantages. While the passive controllers are easy to implement, their inability to operate outside certain frequency band-widths limits the application [77]. On the other hand, an active controller, though difficult to implement, can be used for controlling systems subjected

to broad-band excitations [78]. The vibration of a travelling continuous system is passively controlled by letting them pass through a number of hydrodynamic bearings [79, 80]. As the damping force is sensitive to the length rather than the location of a bearing, it can be placed at any convenient position within the span [81, 82, 83]. Active controllers have also been devised by measuring the system-responses with the help of suitably placed sensors and applying necessary excitation (based upon these measurements) through actuators placed at proper locations [84, 85]. The required amount of excitation depends upon various control strategies used. The simplest of such strategies is known as 'modal control' whereby a few of the normal modes are actively controlled [86]- [88]. However, the adverse 'control' and 'observation' spill-over effects of the unmodelled modes may make the controller ineffective [89, 90]. For a travelling beam, the observation spill-over effect, which is more dangerous than the control spill-over effect, may be reduced by using a comb-filter having frequencies that are adaptively changed with the axial speed [91]. Frequency-domain methods of active control have also been tried to control the vibration of both beams and strings [92, 93]. A novel and altogether different approach of controlling the vibtration of a travelling string by absorbing the energies of the associated travelling waves at the boundaries has been proposed [94]- [96]. This type of control is known as 'wave-cancellation' or 'boundary' control and has been applied for many axially stationary systems [97, 98]. Since the corrective measures are taken at the boundaries, the spill-over effects are circumvented altogether. However, if the sensor is placed at any point away from the actuators, detrimental effects may be resulted. This is due to the finite time taken by the waves associated with the transverse vibration to travel from the observer location (wherefrom the information of the oscillatory motion is collected) to the actuator location (where the corrective measure is taken). The problem of the 'non-collocated' controller has been removed by introducing a suitable time delay

between the sensor and the actuator [99]. Other types of controllers are also suggested to achieve specific objectives. As for example, a combination of feedback and feed-forward controllers has been attempted to solve the chain-sprocket mismatch problem which is caused by the boundary oscillations [100].

1.2.4 Free and Forced Vibrations of Systems Having Variable Span

So far the discussion has been restricted to fixed-span travelling members. However, during vibrations of a robot arm having a prismatic joint or of a flexible appendage in space crafts, the length of the span and hence the inertia changes continuously. These systems are usually modelled as a flexible cantilever beam of variable length and the end load, if any, is considered as a tip mass [101]. The response of a beam with either monotonically or periodically changing length is obtained by various methods, namely, Galerkin's technique using time-dependent assumed modes [101, 102], finite element method with time-dependent elements [103], analytical method [104, 105] by transforming the time-dependent boundary conditions to the time-invariant ones, etc. The periodic response of a beam with monotonically increasing or decreasing length is not possible due to the non-conservative nature of the system. The amplitude of the end point of the beam, moving with either uniform or non-uniform speed, increases during retraction (i.e., when the length is shortened) and decreases during extrusion (i.e., when the span lengthens) and the frequencies of oscillation change significantly. Even the presence of a tip mass or the flexibility of the channel which controls the movements of the beam does not alter the stability characteristics [106]. It has been proved mathematically that these stability characteristics are ubiquitous for any system having continuously expanding or contracting domain [107]. It should be mentioned that the

reverse trend obtained in reference [102] is the result of an incorrect formulation of the equation of motion and is erroneous. For a uniformly extruding beam, the flutter instability has been reported if the speed is increased beyond a certain value [106]. Similarly, for a uniformly retreating beam, the stability is regained beyond the same speed. Parametric vibrations have been observed in a beam having periodic axial speed [104, 105, 102]. The vibrations of a beam during simultaneous axial movement and rotation about a transverse axis have also been studied [108]. It is apparent from the above discussion that a travelling continuous system having a single support can be unstable quite often. However, very few researchers have addressed the problem of controlling these instabilities. A variable order adaptive controller has been proposed for this purpose [109].

1.2.5 Effect of Non-Linearities

The above discussion points out the richness of literature devoted to various aspects of the linear vibrations of travelling continua. Nonetheless, the effects of the geometrical non-linear terms become substantial as the axial speed of the travelling member approaches the critical value. It has been noticed long back that the non-linear terms significantly affect the characteristics of the hyperbolic equation of motion of a travelling string [110]. Further, different phenomena observed experimentally cannot be explained from the linear theory. For example, the shape of the response envelope of a boundary-excited string travelling at a subcritical speed is identical to the first mode. The amplitude of vibration, however, increases continuously until the critical speed is reached, when the amplitude decreases suddenly and the higher modes are generated [111]. Furthermore, if a point harmonic forcing is applied within the span, the string then beyond a certain axial speed, starts oscillating in a direction perpendicular to the plane of excitation. These two phenomena known, respectively, as 'mode-jumping' and

'ballooning' cannot be explained by the linear theory [111]- [113]. In order to explain these experimentally observed phenomena, a non-linear model of the travelling string, neglecting the longitudinal oscillation, has been suggested [111]. More accurate models of non-linear string and beam, simply-supported at both ends, have been subsequently developed [114]. Free vibrations of travelling continuous systems have been studied following these models. Non-linear dynamics of a travelling cable has also been studied [115, 116]. The effects of the non-linear terms on the natural frequencies of axially moving members are obtained by using Galerkin's technique with the linear normal modes of both axially stationary and travelling systems as the basis functions. This is followed by either a harmonic balance method or a perturbation technique [114, 117]. These studies reveal the hardening nature of the non-linearities. In reference [117], the analysis has been extended to the supercritical speed regime.

The modal coupling during the non-linear oscillation restricts the analysis of the forced response to the near-resonance conditions. Consequently, the near-resonance response of a travelling string, to a harmonic displacement excitation at the boundary with a frequency close to the first natural frequency, has been obtained both analytically and experimentally [118]. A perturbation method was used. The Galerkin's technique followed by harmonic balance method has also been used towards this end [119, 120]. It should be pointed out that a one-term approximation in this method gives wrong answers since the effect of the gyroscopic term is not included. The 'modal jumping' or 'ballooning' has not been considered in the above references. Although various authors deal with the latter phenomenon [112, 113], the explanation of the former has been attempted only numerically [111].

For a travelling beam having a single fixed support, different approaches are taken to derive the non-linear equation of motion. A modified version of the Hamilton's principle, suitable for the systems with changing mass has been used by several researchers

[121]- [124]. A new way of formulating the equation of motion, within the framework of Kane's dynamical theory, has also been reported [125, 126]. In this method the uniform axial motion of the beam is taken as a constraint [127, 128]. The free vibrational analysis of the non-linear equation of motion shows that the non-linear terms do not change the stability characteristics predicted by a linear analysis [129]. The effects of the non-linearities are felt in the variation of frequency-contents of the time response.

However, as mentioned in Section 1.1, the non-linear terms may change the dynamic behaviour drastically from that predicted by linear theories. The major qualitative changes can be summarized as follows:

(i) The non-linear terms couple the vibrations of the two spans in a serpentine belt-drive which are assumed to be decoupled in the linear model [130].

(ii) The harmonic edge loading, meant to excite the torsional oscillation in a travelling beam, introduces large transverse vibration [131]. This phenomenon, known as 'autoparametric excitation' (or 'internal resonance') is possible only due to non-linear coupling between the transverse and torsional oscillations.

(iii) Contrary to the prediction by a linear theory, the non-linear term restricts the exponential growth of the vibration amplitude of a parametrically excited string to 'limit cycles' [132].

(iv) The analysis of free vibration neglecting the non-linearities leads to the prediction of flutter in a simply-supported beam travelling at a supercritical speed [16]. This prediction is, however, wrong [133]. Although the proof has been given for a simply-supported pipe, this is true for a travelling beam as well.

(v) Chaotic response has also been observed for a parametrically excited travelling beam [76]. This phenomenon can never be explained by a linear theory [134].

From the above discussion, it is apparent that the omission of the non-linear terms can lead to erroneous results. Although some progress has been made towards under-

standing the effects of non-linearities on the oscillatory motion of a travelling string, the study is far from being complete so far as the travelling beams are concerned. Finally, the controllers proposed for the travelling continuous systems should be re-examined to adjudge their efficacies in the presence of the non-linear terms.

1.3 Objective and Scope of the Present Work

The major objective of the present thesis is to inquire into the effects of the geometric non-linearities on the vibration of an Euler-Bernoulli beam moving over two simple supports. Various operating conditions generating different types of excitations are considered. The non-linear equation of motion is derived in Chapter 2. Since the small non-linear term in the equation of motion is considered as a perturbation to the linear equation, a detailed knowledge of the linear system is essential. The rest of Chapter 2 is devoted to study the free and forced linear vibrations by two apparently distinct methods, namely the 'modal analysis' and the 'wave-propagation method'. While the discussion of the former is limited to the existing results, the latter method is developed for the first time. The numerical results obtained from these two methods are compared. Damping is neither considered here nor will be considerd later except during the occasions where the presence of a damping term changes the qualitative behaviour of the system.

In Chapter 3, a simple and computationally efficient method of obtaining the near-resonance response of a non-linear continuous system is presented. The method is elucidated, for the sake of simplicity, with an axially stationary beam having either simply-supported or clamped-clamped boundary conditions. The non-linear normal modes of the beam, similar to the linear normal modes, are first derived using a perturbation as well as the wave-propagation method. These non-linear normal modes

are subsequently used to obtain the near-resonance response. The results so obtained are then compared with experimental results available in the literature. The efficacy of the present method over the Galerkin's technique is highlighted.

The results of Chapters 2 and 3 are extended in Chapter 4 to derive the response of the non-linear travelling beam under both resonant and hard non-resonant excitations. A concept of non-linear complex normal mode is first presented. The near-resonance response has been subsequently obtained using these non-linear complex normal modes. The methods of deriving both the non-linear complex modes and the near-resonance response resemble closely the procedure outlined in Chapter 3. Like in any other non-linear system multiple values are obtained for the near-resonance response. However, all of these values are not physically realisable. The physically observable results are delineated by carrying out a stability analysis. When the excitation is hard non-resonant one, the modal method encounters difficulties. The method of wave-propagation, derived for the linear system in Chapter 2, has been effectively extended for such a situation.

Chapter 5 deals with the effects of the non-linear term on a parametrically excited travelling beam. The source of the parametric excitation is taken to be the tension fluctuation due to the unbalance in one of the pulleys which is mounted on an axially-flexible support. Single or multiple limit cycles, generated by the combination of non-linearity and parametric excitation in the presence of small viscous damping, are obtained using the non-linear complex normal modes. The stable limit cycles are separated from the unstable ones by carrying out a stability analysis. The response of the beam to simultaneous parametric and external harmonic excitations is also obtained. The non-linear complex normal modes are once again used for that purpose. In this case too, a stability analysis to determine the physically observable solutions is presented.

The stability of an accelerating or decelerating non-linear beam is presented in Chapter 6. This situation arises during the starting or stopping phases. A Lyapunov's stability analysis is first carried out to study the stability characteristics of the beam having any arbitrary acceleration. For a decelerating beam, the stability is determined using a perturbation technique based on Multiple-Time-Scale (MTS) method. The uniform deceleration is taken as a small perturbation to the uniform axial speed.

A controller to reduce the vibration of a non-linear beam moving with uniform axial speed is discussed in Chapter 7. A passive controller in the form of a roller guide is proposed. The finite compliance of the guide in the transverse direction, and the frictional force appearing at the guide-beam interface and acting in the axial direction are incorporated. The results of the linear analysis, for both free and forced vibrations, are used to obtain the non-linear complex normal modes that are subsequently utilised to get the near-resonance response. The effectiveness of the roller in reducing the amplitudes of both linear and non-linear vibrations of the beam under harmonic excitation has been brought out with the help of numerical examples.

The main conclusions of the present work are summarized in Chapter 8. Some directions for further research are also mentioned therein.

Chapter 2

LINEAR VIBRATION OF A TRAVELLING BEAM

2.1 Introduction

First, the equation of motion for the transverse vibration of a simply-supported travelling beam including the non-linear term is derived in Section 2.2. Considering the physical nature of the problem, the equation of motion has been simplified from the more accurate results reported by Thurman and Mote [114]. For a slender beam, the non-linear term can be taken as a small perturbation to the linear equation. Therefore, before embarking on the non-linear analysis, the linear anlysis is presented in this chapter.

The linear free vibration of a travelling beam has been studied by various analytical techniques that are suitable for solving a differential equation with given boundary conditions [16], [37]- [42]. The major objective is to determine the natural frequencies and mode shapes. The connection between the vibration of and the wave propagation in continuous systems provides better understanding of the oscillatory motions. It is

well known that in an axially stationary string, two waves, travelling in the opposite directions at the same speed, are reflected at the boundaries to generate the normal modes of vibration. The free vibration of an axially stationary Euler-Bernoulli beam has also been studied using the wave-propagation approach. A 'phase-closure principle' has been derived [135] that shows that the normal modes correspond to a phase change of an integer multiple of 2π for the propagating as well as the evanescent waves, as they return to their starting point after traversing to and fro once across the span. The phase-closure principle still remains valid during the modal vibrations of an axially moving string [9], where the speed of the wave propagation does not remain equal in the upstream and downstream directions. Owing to the dispersive nature of the medium, the wave propagation in an axially moving beam is more complicated. Consequently, only an approximate, rather than the exact, result has been obtained for the natural frequencies of such a beam [40].

Forced vibrations of a travelling continuous system are usually studied using Galerkin's technique [58] or modal analysis [16]. In these methods, the equation of motion (which is a partial differential equation) is discretized into a set of countably infinite number of uncoupled ordinary differential equations. This is achieved by assuming the spatial distribution of the response in terms of various orthogonal (or 'basis') functions. In practical situations, only the first few terms corresponding to the lower modes are considered. The error due to this modal truncation can be eliminated by constructing a closed-form transfer function (i.e., the Laplace transform of the Green's function) by analytically solving the boundary value problem [60, 61]. An interpretation of the transfer function of an axially moving string, in terms of the waves propagating in two opposite directions [63] without distortion, simplifies the computation of the response to any displacement excitation. However, in a beam, where the wave propagation gets significantly complicated, the determination of the response by the wave-propagation

theory is difficult.

The free and forced vibrations of a travelling beam are studied using modal analysis and the wave-propagation theory in Sections 2.3 and 2.4, respectively. The details of the modal analysis, easily available in the open literature, are omitted. But the method based on wave propagation is carried out in details. The frequency equation of the free modal vibration of the beam is derived using the phase-closure principle. Since the characters of the waves change drastically as the axial speed is increased beyond a certain value, the phase-closure principle is applied differently in these two speed regimes. The justifications of some approximate methods for obtaining the natural frequencies are also discussed. In the presence of an external forcing, the closed-form transfer function is first obtained using the wave-propagation theory, which is then used to determine the response to any arbitrary excitation. Numerical results obtained from the above two methods are compared by evaluating the response to a point harmonic excitation. The efficacy of the wave-propagation method for determining the forced response is clearly brought out. However, it should be mentioned that both the methods are important for carrying out the non-linear analysis presented later. The modal analysis is more suitable when the beam is resonantly excited whereas the wave-propagation method is advantageous if the beam is subjected to a hard, non-resonant excitation.

2.2 Equation of Motion

In this section, the equation of motion of the undamped, planar, transverse vibration of a slender beam, (see Figure 2.1) having an initial tension T_0^* and moving axially with a uniform speed c^* between two stationary and widely separated frictionless supports, is derived retaining the geometric non-linear terms. To this end, the following

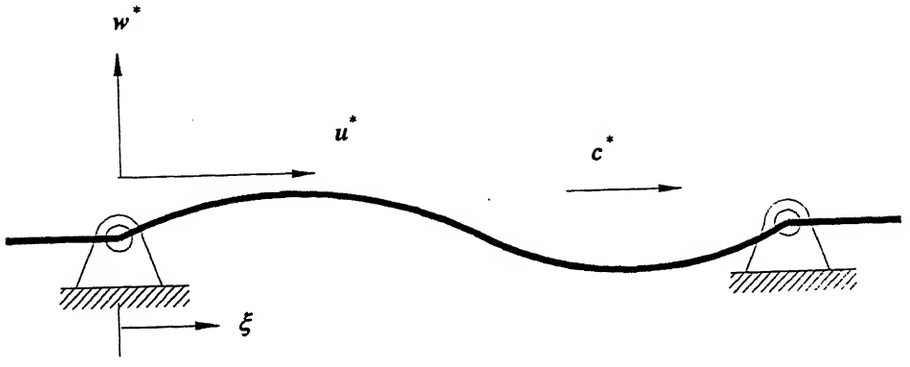

Figure 2.1: Schematic diagram of a travelling beam.

assumptions are made:

(i) The amplitude of the longitudinal vibration, $u^*(\xi,t)$, is order of magnitude smaller than the amplitude of transverse vibration, $w^*(\xi,t)$. Mathematically, $u^*(\xi,t) = O(w^*(\xi,t))^2$, where ξ represents the distance measured along the direction of axial movement, in a stationary reference frame, and t denotes the time.

(ii) The radius of gyration of the beam cross-section, r, is much smaller compared to the span length l (i.e., $r \ll l$).

(iii) The frictionless supports prevent the longitudinal oscillation and act as simple supports so far as the transverse vibration is concerned [114].

With these assumptions, the equations of motion of the coupled longitudinal and transverse vibrations of the beam are [114]:

$$\rho A\left[\frac{\partial^2 u^*}{\partial t^2}+2c^*\frac{\partial^2 u^*}{\partial \xi \partial t}+c^{*2}\frac{\partial^2 u^*}{\partial \xi^2}\right]-EA\frac{\partial^2 u^*}{\partial \xi^2}=(EA-T_0^*)\frac{\partial w^*}{\partial \xi}\frac{\partial^2 w^*}{\partial \xi^2}, \tag{2.1}$$

and

$$\rho A\left[\frac{\partial^2 w^*}{\partial t^2}+2c^*\frac{\partial^2 w^*}{\partial \xi \partial t}+c^{*2}\frac{\partial^2 w^*}{\partial \xi^2}\right]-T_0^*\frac{\partial^2 w^*}{\partial \xi^2}+EI_z\frac{\partial^4 w^*}{\partial \xi^4}$$

$$= (EA - T_0^*)\frac{\partial}{\partial \xi}[(\frac{\partial u^*}{\partial \xi})(\frac{\partial w^*}{\partial \xi}) + \frac{1}{2}(\frac{\partial w^*}{\partial \xi})^3] \,, \tag{2.2}$$

where the area of the beam cross-section is A with second moment about the neutral axis $I_z = Ar^2$, ρ and E are, respectively, the density and Young's modulus of the beam material.

The boundary conditions are given by

$$u^*(0,t) = u^*(l,t) = 0, \tag{2.3}$$

$$w^*(0,t) = w^*(l,t) = 0 \tag{2.4}$$

and

$$\frac{\partial^2 w^*(0,t)}{\partial \xi^2} = \frac{\partial^2 w^*(l,t)}{\partial \xi^2} = 0. \tag{2.5}$$

Using the following non-dimensional parameters,

$$u = u^*/l, \;\; \gamma = \frac{r}{l}, \;\; w = w^*/(l\gamma^2), \;\; x = \xi/l, \;\; \tau = \frac{1}{l}(\frac{E}{\rho})^{1/2}\gamma t,$$

$$c = c^*(\frac{E}{\rho})^{-1/2}\frac{1}{\gamma}, \;\; \text{and} \;\; T_0 = \frac{T_0^*}{EA\gamma^2}, \tag{2.6}$$

equations (2.1)-(2.5) can be rewritten, respectively, as

$$\left[\frac{\partial^2 u}{\partial \tau^2} + 2c\frac{\partial^2 u}{\partial x \partial \tau} + c^2\frac{\partial^2 u}{\partial x^2}\right] - \frac{1}{\gamma^2}\frac{\partial^2 u}{\partial x^2} = \gamma^2(1 - \gamma^2 T_0)\frac{\partial w}{\partial x}\frac{\partial^2 w}{\partial x^2}, \tag{2.7}$$

$$\frac{\partial^2 w}{\partial \tau^2} + 2c\frac{\partial^2 w}{\partial x \partial \tau} + (c^2 - T_0)\frac{\partial^2 w}{\partial x^2} + \frac{\partial^4 w}{\partial x^4} = (1 - \gamma^2 T_0)\frac{\partial}{\partial x}\left[\frac{1}{\gamma^2}(\frac{\partial u}{\partial x})(\frac{\partial w}{\partial x}) + \frac{\gamma^2}{2}(\frac{\partial w}{\partial x})^3\right], \tag{2.8}$$

$$u(0,\tau) = u(1,\tau) = 0, \tag{2.9}$$

$$w(0,\tau) = w(1,\tau) = 0 \tag{2.10}$$

and

$$\frac{\partial^2 w(0,\tau)}{\partial x^2} = \frac{\partial^2 w(1,\tau)}{\partial x^2} = 0. \tag{2.11}$$

The non-dimensional axial speed, c, has been obtained using the longitudinal wave speed and the slenderness ratio γ. The significance of the inclusion of γ will be apparent during the non-linear analysis in terms of the small parameter $(\gamma^2/2)$.

For a slender beam, i.e., with $\gamma \ll 1$, one can neglect the longitudinal inertia term in equation (2.7) and gets (neglecting terms of order higher than γ^2) the following equation:

$$-\frac{1}{\gamma^2}\frac{\partial^2 u}{\partial x^2} = \gamma^2 \frac{\partial w}{\partial x}\frac{\partial^2 w}{\partial x^2},$$

which, when integrated twice with respect to x, yields

$$u(x,\tau) = -\frac{\gamma^4}{2}\int_0^x \left(\frac{\partial w}{\partial x_1}\right)^2 \mathrm{d}x_1 + x f_1'(\tau) + f_2'(\tau). \tag{2.12}$$

Ensuring $u(x,\tau)$ satisfies the boundary conditions given by equation (2.9), the constants of integration $f_1'(\tau)$ and $f_2'(\tau)$ are obtained as

$$f_2'(\tau) = 0 \text{ and } f_1'(\tau) = \frac{\gamma^4}{2}\int_0^1 (\frac{\partial w}{\partial x})^2 \,\mathrm{d}x. \tag{2.13}$$

Now substituting equations (2.12) and (2.13) into equation (2.8), one gets

$$\frac{\partial^2 w}{\partial \tau^2} + 2c\frac{\partial^2 w}{\partial x \partial \tau} + (c^2 - T_0)\frac{\partial^2 w}{\partial x^2} + \frac{\partial^4 w}{\partial x^4} = \epsilon \left[\int_0^1 (\frac{\partial w}{\partial x})^2 \,\mathrm{d}x\right] \frac{\partial^2 w}{\partial x^2}, \tag{2.14}$$

where $\epsilon (= \frac{\gamma^2}{2})$ is a small parameter, i.e., $\epsilon \ll 1$. Finally, equation (2.14) together with the boundary conditions (2.10) and (2.11) describe the non-linear transverse vibration of the travelling beam.

The equation of motion in the presence of a non-dimensional external force $f(x,\tau)$ is

$$\frac{\partial^2 w}{\partial \tau^2} + 2c\frac{\partial^2 w}{\partial x \partial \tau} + (c^2 - T_0)\frac{\partial^2 w}{\partial x^2} + \frac{\partial^4 w}{\partial x^4} = \epsilon \left[\int_0^1 (\frac{\partial w}{\partial x})^2 \,\mathrm{d}x\right] \frac{\partial^2 w}{\partial x^2} + f(x,\tau), \tag{2.15}$$

where $f(x,\tau) = f^*(x,t)l/(EA\gamma^4)$ with $f^*(x,t)$ as the transverse external force per unit length at the location x.

For the gyroscopic system under discussion, equations (2.14) and (2.15) are often recast in the following state-space form [16] :

$$\mathrm{A}\frac{\partial W}{\partial \tau} + \mathrm{B}W = \epsilon \mathrm{N} \tag{2.16}$$

and

$$\mathrm{A}\frac{\partial W}{\partial \tau} + \mathrm{B}W = \epsilon \mathrm{N} + \mathrm{f}, \tag{2.17}$$

where

$$\mathrm{A} = \begin{bmatrix} I & 0 \\ 0 & K \end{bmatrix}, \ \mathrm{B} = \begin{bmatrix} G & K \\ -K & 0 \end{bmatrix}, \ \mathrm{W} = \begin{Bmatrix} \frac{\partial W}{\partial \tau} \\ W \end{Bmatrix}, \ \mathrm{f} = \begin{Bmatrix} f(x,\tau) \\ 0 \end{Bmatrix},$$

and

$$\mathrm{N} = \left\{ \left(\int_0^1 \left(\frac{\partial w_2}{\partial x} \right)^2 \mathrm{d}x \right) \frac{\partial^2 w_2}{\partial x^2}, 0 \right\}^T,$$

with $K \equiv (c^2 - T_0)\partial^2/\partial x^2 + \partial^4/\partial x^4$, $G \equiv 2c\partial/\partial x$ and I as the identity operator.

Both forms of the equations of motion, (i.e., the partial differential equations and the state-space form) are useful depending on the method of subsequent analysis as will be seen later.

In this chapter, the linear analysis of the free and forced vibrations (i.e., with $\epsilon = 0$ in equations (2.16) and (2.17)) are presented. In what follows, the free vibration is first studied using both modal analysis and wave-propagation approach. The response of the beam to external force excitations is next obtained again using both these methods.

2.3 Free Vibration

As mentioned in Chapter 1, the transverse waves in a travelling beam move with different speeds in opposite directions. Consequently, no standing (stationary) mode exists even for the linear vibration. However, the situations still exist when all the points

of the beam undergo harmonic oscillation with same frequency. These frequencies are called natural frequencies of the travelling beam. These natural frequencies and the corresponding complex normal modes can be obtained by either direct modal analysis or wave-propagation method as detailed below.

2.3.1 Modal Analysis

The linear normal modes of a travelling beam differ from those of an axially stationary beam in the sense that in case of the former, the phase difference between the oscillatory displacement and velocity at any point depends on the axial coordinate x. This implies the importance of considering both the displacement and velocity at a point during the modal responses of a travelling beam. This fact is taken into account by treating the displacement and velocity as two independent quantities, which can be done by recasting the equation of motion in the state-space form (i.e., equation (2.16) with $\epsilon = 0$) as shown below :

$$\mathbf{A}\frac{\partial W}{\partial \tau} + \mathbf{B}W = 0. \tag{2.18}$$

For a harmonic solution, the response vector $W(x,\tau)$ can be assumed as

$$W(x,\tau) = \frac{a}{2}\Phi(x)e^{i\omega^l\tau} + \frac{\overline{a}}{2}\overline{\Phi}(x)e^{-i\omega^l\tau}, \tag{2.19}$$

where $i = \sqrt{-1}$ and $\Phi = \left\{ \begin{array}{c} i\omega^l\phi \\ \phi \end{array} \right\}$. The bar at the top indicates the complex conjugate.

Substituting equation (2.19) in equation (2.18) and equating the coefficients of $e^{i\omega^l\tau}$ and $e^{-i\omega^l\tau}$, separately, from both sides, one obtains the following equation and its complex conjugate :

$$i\omega^l\mathbf{A}\Phi + \mathbf{B}\Phi = 0, \tag{2.20}$$

where the partial derivatives in **A** and **B** are replaced by total derivatives. It can be verified that equation (2.20) is equivalent to the following equation :

$$-(\omega^l)^2\phi + 2ic\omega^l\frac{\mathrm{d}\phi}{\mathrm{d}x} + (c^2 - T_0)\frac{\mathrm{d}^2\phi}{\mathrm{d}x^2} + \frac{\mathrm{d}^4\phi}{\mathrm{d}x^4} = 0, \tag{2.21}$$

and the boundary conditions are

$$\phi(0) = \phi(1) = 0, \quad \frac{\mathrm{d}^2\phi(0)}{\mathrm{d}x^2} = \frac{\mathrm{d}^2\phi(1)}{\mathrm{d}x^2} = 0. \tag{2.22}$$

A set of values of the natural frequencies, ω^l and the corresponding complex normal mode shapes, $\phi(x)$, can be obtained by solving equations (2.21) and (2.22). Assuming $\phi(x)$ in the following form

$$\phi(x) = \sum_{j=1}^{4} A_j e^{ik_j x},$$

and substituting it in the boundary conditions the following frequency equation is finally obtained:

$$\det \begin{vmatrix} 1 & 1 & 1 & 1 \\ k_1^2 & k_2^2 & k_3^2 & k_4^2 \\ e^{ik_1} & e^{ik_2} & e^{ik_3} & e^{ik_4} \\ k_1^2 e^{ik_1} & k_2^2 e^{ik_2} & k_3^2 e^{ik_3} & k_4^2 e^{ik_4} \end{vmatrix} = 0, \tag{2.23}$$

where k_j's $(j = 1, 2, 3, 4)$ are the roots of the algebraic equation

$$-(\omega^l)^2 - 2c\omega^l k - (c^2 - T_0)k^2 + k^4 = 0. \tag{2.24}$$

The n-th natural frequency and the corresponding normal mode, denoted by ω_n^l and ϕ_n, respectively, are obtained by (numerically) solving equations (2.23) and (2.24) simultaneously. It can be shown that for the special case $T_0 = 0$, equation (2.23) takes the following simple form

$$c^2\sigma\delta_1\left[\cos c - \cos\frac{\sigma}{2}\cosh\frac{\delta_1}{2}\right] + \left[c^4 - 8(\omega_n^l)^2\right]\sin\frac{\sigma}{2}\sinh\frac{\delta_1}{2} = 0, \tag{2.25}$$

if $c < 2\sqrt{\omega_n^l}$ and

$$c^2\sigma\delta_2\left[\cos c - \cos\frac{\sigma}{2}\cos\frac{\delta_2}{2}\right] + \left[4c^2\omega_n^l - \frac{c^4}{2}\right]\sin\frac{\sigma}{2}\sin\frac{\delta_2}{2} = 0, \tag{2.26}$$

if $2\sqrt{\omega_n^l} < c < (c_{cr})_1 (= \pi)$, where $\delta_1 = \sqrt{4\omega_n^l - c^2}$, $\delta_2 = \sqrt{c^2 - 4\omega_n^l}$ and $\sigma = \sqrt{c^2 + \omega_n^l}$.

The linear analysis remains valid so long as the axial speed is less than the lowest critical speed, $(c_{cr})_1$. For a tensioned beam [114] $(c_{cr})_1 = \sqrt{T_0 + \pi^2}$.

Attention may be drawn to the fact, that the frequency equation for $c < 2\sqrt{\omega_n^l}$ was also obtained in reference [39] (see equation (7) therein). However, that equation, in terms of the symbols used in the present work, turns out to be

$$c^2\sigma\delta_1\left[\cos c - \cos\frac{\sigma}{2}\cosh\frac{\delta_1}{2}\right] - 16\omega_n^l\sin\frac{\sigma}{2}\sinh\frac{\delta_1}{2} = 0.$$

This equation is erroneous and should be replaced by equation (2.25).

The well-known orthogonality relations [16], satisfied by the complex normal modes ϕ_n's, are given by the following complex inner products:

$$\int_0^1 \Phi_m^T \mathbf{A}\Phi_n \, dx = 0 \text{ for all } m \text{ and } n, \tag{2.27}$$

and

$$\int_0^1 \overline{\Phi}_m^T \mathbf{A}\Phi_n \, dx = 0 \text{ for all } m \neq n. \tag{2.28}$$

Using the expansion theorem [18], any non-dimensional vector $V = \begin{Bmatrix} \nu_1(x) \\ \nu_2(x) \end{Bmatrix}$ satisfying the boundary conditions can be expanded in terms of the complex normal modes as

$$V = \sum_{n=1}^{\infty}(a_n\Phi_n + b_n\overline{\Phi}_n),$$

where a_n and b_n are obtained, with the help of the orthogonality relations, as

$$a_n = \frac{\int_0^1 \overline{\Phi}_n^T \mathbf{A} V \, dx}{\int_0^1 \overline{\Phi}_n^T \mathbf{A}\Phi_n \, dx},$$

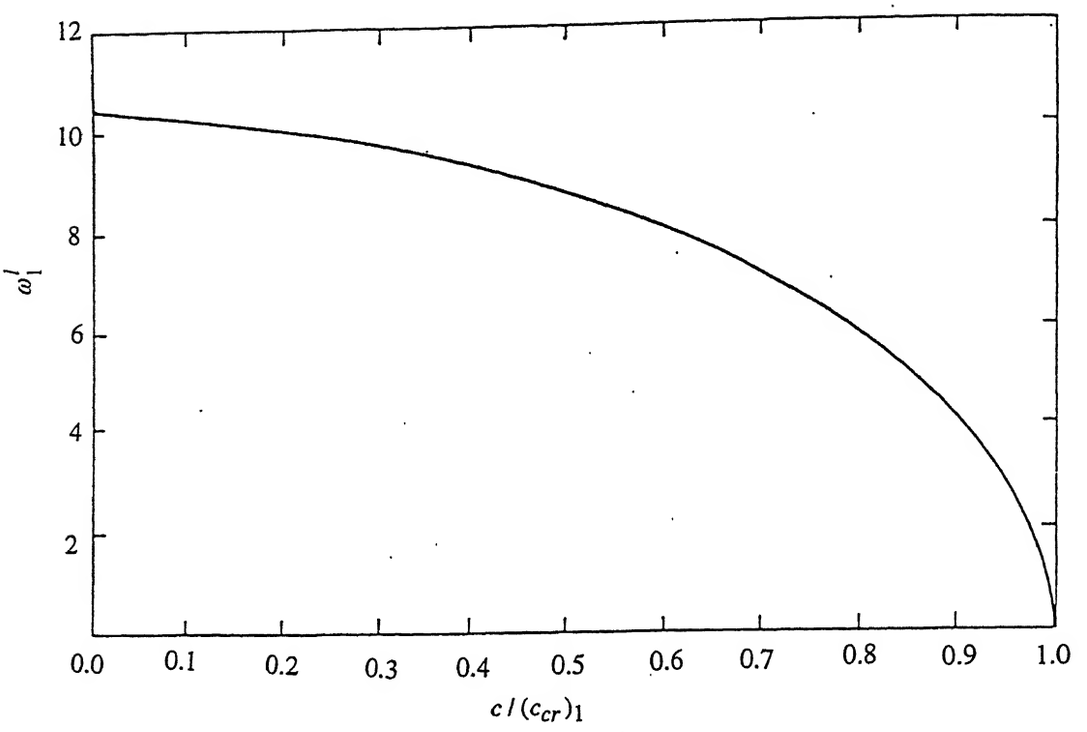

Figure 2.2: Variation of the first linear natural frequency with axial speed. $T_0 = 1.0$.

and

$$b_n = \frac{\int_0^1 \Phi_n^T \mathbf{A} V \, \mathrm{d}x}{\int_0^1 \overline{\Phi}_n^T \mathbf{A} \Phi_n \, \mathrm{d}x}.$$

2.3.2 Numerical Results and Discussion

In this section, some numerical results obtained from the theoretical analysis presented in Section 2.3.1 are discussed. The variation of the first linear natural frequency (ω_1^l) with the travelling speed, c, is plotted in Figure 2.2. The zero value of ω_1^l at $c = (c_{cr})_1$ implies the divergence or buckling instability. Figures 2.3 and 2.4 show the real and imaginary parts of the first and second complex normal mode shapes, i.e., $\phi_1(x)$ and $\phi_2(x)$, respectively, for three values of the travelling speed. The real and imaginary parts are neither symmetric nor antisymmetric about the mid-point.

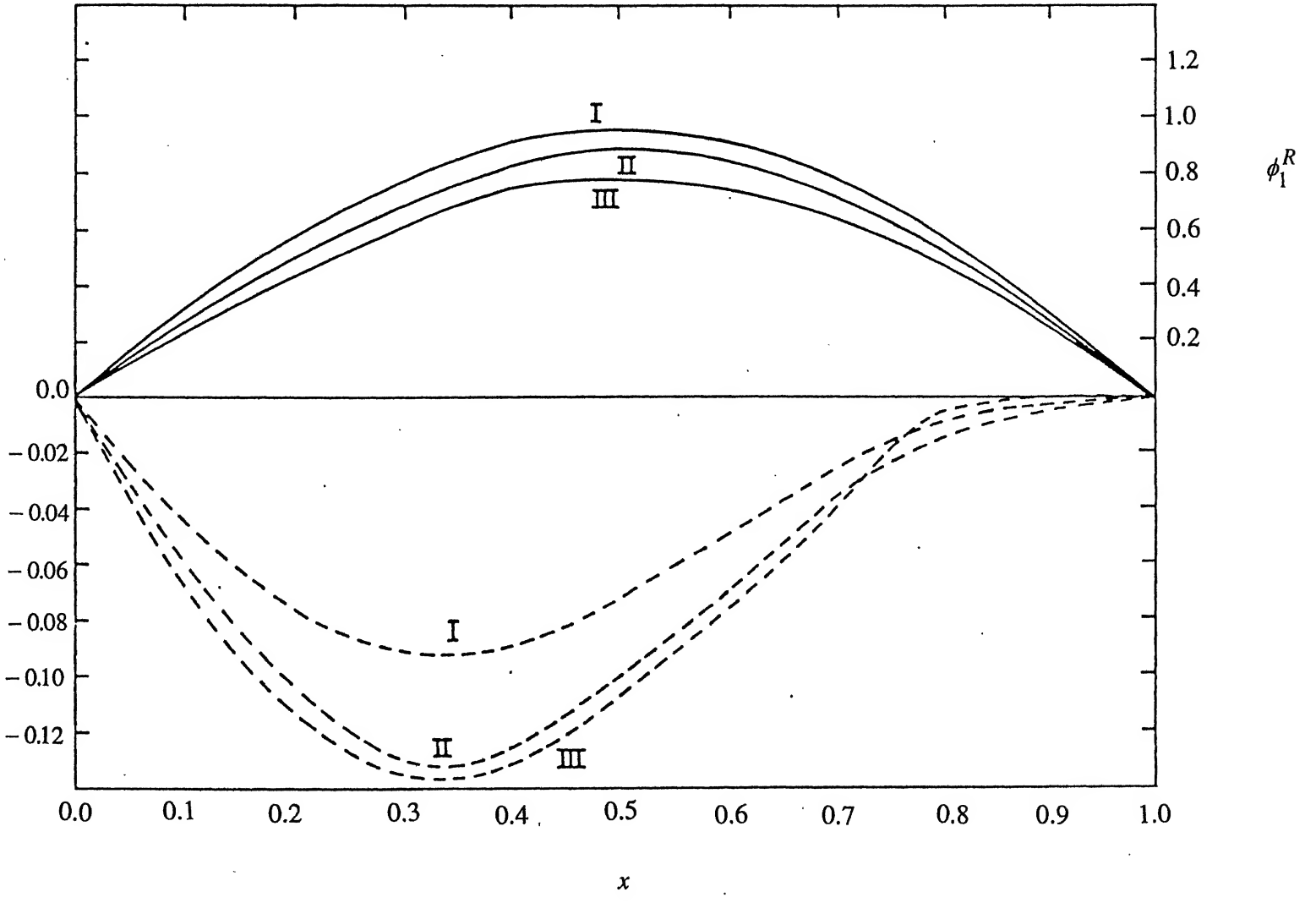

Figure 2.3: First linear complex mode shape . —— : real part, – – – : imaginary part; $T_0 = 1.0$. I : $c = 0.3(c_{cr})_1$, II : $c = 0.5(c_{cr})_1$, III : $c = 0.7(c_{cr})_1$.

2.3.3 Wave-Propagation Analysis

In this section, the free vibration of the travelling beam is re-examined using the wave-propagation theory. To this end, first the harmonic waves associated with the modal vibration of a simply-supported travelling beam are considered. The study is then extended to set up both the approximate and exact frequency equations.

2.3.4 Wave Propagation and Reflection at a Boundary

The equation of motion for linear oscillation is obtained by putting $\epsilon = 0$ in equation (2.14), as

$$\frac{\partial^2 w}{\partial \tau^2} + 2c\frac{\partial^2 w}{\partial x \partial \tau} + (c^2 - T_0)\frac{\partial^2 w}{\partial x^2} + \frac{\partial^4 w}{\partial x^4} = 0. \tag{2.29}$$

To study the harmonic wave propagation, the response of the beam is assumed as

$$w(x, \tau) = a e^{i\omega' \tau} e^{ikx}. \tag{2.30}$$

Substitution of equation (2.30) into equation (2.29) leads to same algebraic equation (2.24). Using Descartes' rule [136], it can be seen that the roots of this quartic equation (in the wave number k) belong to one of the following categories :

(i) one pair of real roots (with one negative (k_1, say) and the other positive (k_2, say)) with the other roots as complex conjugates (k_3 and k_4, say),

(ii) four real roots with one positive (k_2, say) and the other three negative (k_1, k_3 and k_4, say).

In what follows, for the sake of algebraic simplicity, the analysis is carried on with $T_0 = 0$. However, the nature of the wave propagation remains the same for all values of T_0.

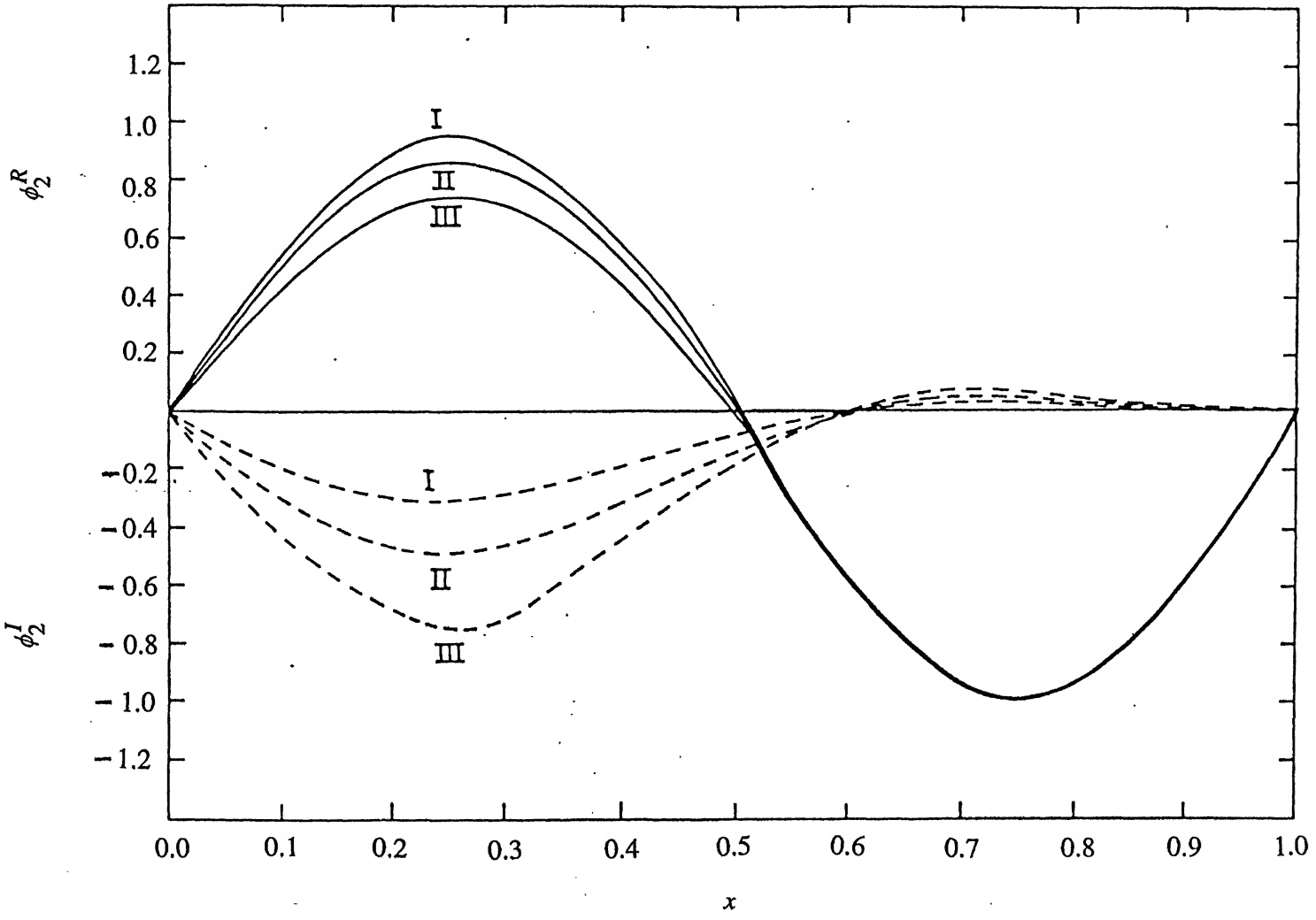

Figure 2.4: Second linear complex mode shape. —— : real part, − − − : imaginary part; $T_0 = 1.0$. I : $c = 0.3(c_{cr})_1$, II : $c = 0.5(c_{cr})_1$, III : $c = 0.7(c_{cr})_1$.

For $T_0 = 0$, the roots k_j's $(j = 1, 2, 3, 4)$ are obtained as

$$k_1 = c/2 - \sqrt{\omega^l + c^2/4}, \qquad k_2 = c/2 + \sqrt{\omega^l + c^2/4}$$

$$k_3 = -c/2 + i\sqrt{\omega^l - c^2/4} \quad \text{and} \quad k_4 = -c/2 - i\sqrt{\omega^l - c^2/4}. \tag{2.31}$$

Thus, the response is given by

$$w(x, \tau) = \left[A_1 e^{ik_1 x} + A_2 e^{ik_2 x} + A_3 e^{ik_3 x} + A_4 e^{ik_4 x}\right] e^{i\omega^l \tau}. \tag{2.32}$$

The wave numbers k_1 and k_2 correspond to the waves propagating along the downstream and upstream directions, respectively, and will be denoted as A_1- and A_2-waves. Their phase velocities CP_1 and CP_2 differ by

$$CP_1 - CP_2 = \left|\frac{\omega^l}{k_1}\right| - \left|\frac{\omega^l}{k_2}\right| = c.$$

For $c < 2\sqrt{\omega^l}$, the other two waves i.e., the A_3- and A_4-waves can be called 'evanescent waves', since their group velocities become imaginary (implying no propagation of energy) as shown below :

$$CG_3 = \frac{\partial \omega^l}{\partial k_3} = -2i\sqrt{\omega^l - c^2/4}, \quad CG_4 = \frac{\partial \omega^l}{\partial k_4} = 2i\sqrt{\omega^l - c^2/4}.$$

It should be noted that unlike in an axially stationary beam $(c = 0)$ [135], in the present case, the phases of the evanescent waves change as they move along the beam. However, for $c \geq 2\sqrt{\omega^l}$, all the group velocities are real and both the A_3- and A_4-waves become downstream propagating waves. The existence of such four propagating waves has been reported in reference [10]. Since the wave-propagation characteristics change drastically in the two velocity regimes mentioned above, the phase-closure principle is applied separately for these cases, namely for $0 < c < c_d$ and $c_d < c < (c_{cr})_1 = \pi$ with $c_d = 2\sqrt{\omega^l}$. But before applying the phase-closure principle, the reflection of waves at the boundaries with simple supports are briefly discussed.

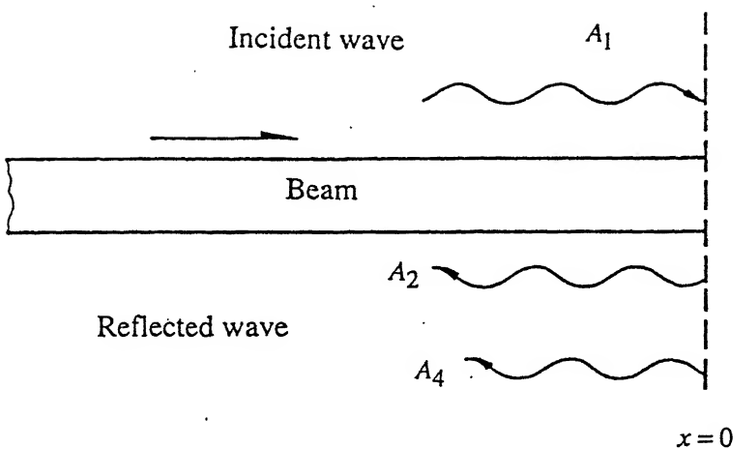

Figure 2.5: Reflection of wave at a simple support.

Reflection of waves for $0 < c < c_d$:

If the downstream propagating wave i.e., the A_1-wave is the only wave impinging upon a boundary (see Figure 2.5), then the reflected waves will be both the upstream propagating (A_2-) and evanescent (A_4-) waves. The total displacement at a point is

$$w(x,\tau) = \left[A_1 e^{ik_1 x} + A_2 e^{ik_2 x} + A_4 e^{ik_4 x}\right] e^{i\omega' \tau},$$

which together with the boundary conditions

$$w(0,\tau) = \frac{\partial^2 w}{\partial x^2}(0,\tau) = 0,$$

give the following relations

$$A_1 + A_2 + A_4 = 0 \tag{2.33}$$

and

$$k_1^2 A_1 + k_2^2 A_2 + k_4^2 A_4 = 0. \tag{2.34}$$

Using equations (2.31), (2.33) and (2.34) one obtains

$$A_2 = -\left[\frac{(\omega' - c/2\sqrt{\omega' + c^2/4}) + ic/2\sqrt{\omega' - c^2/4}}{(\omega' + c/2\sqrt{\omega' + c^2/4}) + ic/2\sqrt{\omega' - c^2/4}}\right] A_1 \tag{2.35}$$

and

$$A_4 = -\left[\frac{c\sqrt{\omega^l + c^2/4}}{(\omega^l + c/2\sqrt{\omega^l + c^2/4}) + ic/2\sqrt{\omega^l - c^2/4}}\right] A_1. \tag{2.36}$$

It can be seen that unlike in an axially stationary beam, the phase of the propagating wave does not change by π after reflection at the boundary. The change of phase is given by

$$\begin{aligned} \epsilon_R &= \pi + \left(\tan^{-1}\frac{c/2\sqrt{\omega^l - c^2/4}}{\omega^l - c/2\sqrt{\omega^l + c^2/4}} - \tan^{-1}\frac{c/2\sqrt{\omega^l - c^2/4}}{\omega^l + c/2\sqrt{\omega^l + c^2/4}}\right) \\ &= \pi + \epsilon_1 \end{aligned}$$

where

$$\epsilon_1 = \tan^{-1}\left[\frac{2(c/2)^2\sqrt{(\omega^l)^2 - (c^2/4)^2}}{(\omega^l)^2 + 2(c^2/4)^2}\right]. \tag{2.37}$$

Reflection of waves for $c_d \leq c < \pi$:

In this speed regime, the reflection can be studied by considering only the upstream propagating A_2-wave impinging on the boundary. Three waves will be generated, namely the A_1-, A_3- and A_4-waves. From the boundary conditions one gets

$$(A_1 + A_3 + A_4) = -A_2.$$

Since the A_2-wave is the only wave reflected, the total phase change will be π. The individual phase relationships between the A_1-, A_3- and A_4-waves need not be considered here.

2.3.5 Phase-Closure Principle

In this section, the wave-propagation theory is used to obtain the natural frequencies. In what follows, for $0 < c < c_d$, first the evanescent waves are neglected to obtain the natural frequencies approximately. Then the exact natural frequencies are obtained by

considering the evanescent waves as well. For $c_d \leq c < \pi$, there exists no evanescent wave and the exact natural frequencies are obtained.

Natural frequencies neglecting evanescent waves for $0 < c < c_d$

As explained in Section 2.3.4, the evanescent waves are characterized by their spatial exponential decay in the medium. Consequently, if the wave number of these waves is high, then the decay will be substantial and it is justified to neglect them altogether. In other words, the approximation becomes more accurate while determining the higher order frequencies. However, as can be seen from equation (2.31), the evanescent waves decay less with increasing axial speed. Therefore, the approximate derivation of the natural frequencies neglecting the evanescent waves is valid for low axial speeds.

With the above limitations, the change of phase, as the propagating waves travel once around the span, is

$$\Delta\theta_{phase} = 2(\pi + \epsilon_1) + |k_1| + |k_2|,$$

where the first term (within the parenthesis) in the right hand side signifies the change in the phase due to reflection at the boundaries and the other terms denote the phase changes as the propagating waves move along the beam. According to the phase-closure principle, for the n-th normal mode

$$2(\pi + \epsilon_1) + 2\sqrt{\omega_n^l + c^2/4} = 2(n+1)\pi$$

or

$$\epsilon_1 + \sqrt{\omega_n^l + c^2/4} = n\pi. \tag{2.38}$$

Equation (2.38) together with equation (2.37) can be used to determine the natural frequencies.

If, as a further approximation, ϵ_1 is altogether neglected, the frequency equation becomes

$$\omega_n^l = n^2\pi^2 - \frac{c^2}{4}, \tag{2.39}$$

as obtained by Nelson [40], although from an altogether different approach.

Calculation of the natural frequencies including the evanescent waves for $0 < c < c_d$

In this section, the exact natural frequencies are derived considering the effects of the evanescent waves. For an axially stationary beam, the natural frequencies are obtained by considering the phase closure of either the propagating or the evanescent waves [135]. However, as already mentioned, in a travelling beam, the evanescent waves also contribute to the phase change during propagation. So, the phase-closure principle has to be used by considering both the propagating and the evanescent waves.

Considering both forms of wave, the reflection at the boundaries can be analysed by considering the simple support at any point, say at $x = 0$. The waves must satisfy the relations

$$A_1 + A_2 + A_3 + A_4 = 0 \tag{2.40}$$

and

$$k_1^2 A_1 + k_2^2 A_2 + k_3^2 A_3 + k_4^2 A_4 = 0. \tag{2.41}$$

Using these relations, one can see that if the A_1- and A_3-waves impinge on a simply-supported boundary, the resulting A_2- and A_4-waves are given by

$$\begin{Bmatrix} A_2 \\ A_4 \end{Bmatrix} = -\begin{bmatrix} 1 & 1 \\ k_2^2 & k_4^2 \end{bmatrix}^{-1} \begin{bmatrix} 1 & 1 \\ k_1^2 & k_3^2 \end{bmatrix} \begin{Bmatrix} A_1 \\ A_3 \end{Bmatrix}. \tag{2.42}$$

Similarly,

$$\begin{Bmatrix} A_1 \\ A_3 \end{Bmatrix} = -\begin{bmatrix} 1 & 1 \\ k_1^2 & k_3^2 \end{bmatrix}^{-1} \begin{bmatrix} 1 & 1 \\ k_2^2 & k_4^2 \end{bmatrix} \begin{Bmatrix} A_2 \\ A_4 \end{Bmatrix}. \tag{2.43}$$

Now, to use the phase-closure principle one needs to follow the waves until they reach their starting point after travelling to and fro once along the beam. This is carried out as explained below:

(i) Let A_1- and A_3-waves of respective strengths a_1 and a_3 start from $x = 0$ and travel towards $x = 1$. If the strengths of the waves at $x = 1$ become a_1' and a_3', respectively, one can verify that

$$a_1' = e^{ik_1} a_1,$$

$$a_3' = e^{ik_3} a_3,$$

or in the matrix form

$$\left\{ \begin{array}{c} a_1' \\ a_3' \end{array} \right\} = \left[\begin{array}{cc} e^{ik_1} & 0 \\ 0 & e^{ik_3} \end{array} \right] \left\{ \begin{array}{c} a_1 \\ a_3 \end{array} \right\} = [R_1] \left\{ \begin{array}{c} a_1 \\ a_3 \end{array} \right\}, \quad \text{(say)}.$$

(ii) The A_1- and A_3-waves reflect at the simply-supported boundary placed at $x = 1$ to yield the A_2- and A_4-waves of strengths a_2 and a_4, respectively. Since the phase change due to the reflection is independent of the location of the boundary, the transformation matrix is always given by equation (2.42). Thus,

$$\left\{ \begin{array}{c} a_2 \\ a_4 \end{array} \right\} = [R_2] \left\{ \begin{array}{c} a_1' \\ a_3' \end{array} \right\},$$

with

$$[R_2] = - \left[\begin{array}{cc} 1 & 1 \\ k_2^2 & k_4^2 \end{array} \right]^{-1} \left[\begin{array}{cc} 1 & 1 \\ k_1^2 & k_3^2 \end{array} \right].$$

(iii) The upstream propagating (i.e., the A_2-wave) and evanescent (i.e., the A_4-wave) waves reach from $x = 1$ to $x = 0$ with strengths a_2' and a_4', respectively. The transformation matrix is,

$$[R_3] = \left[\begin{array}{cc} e^{-ik_2} & 0 \\ 0 & e^{-ik_4} \end{array} \right] = \left[\begin{array}{cc} e^{ik_2} & 0 \\ 0 & e^{ik_4} \end{array} \right]^{-1}.$$

(iv) The A_2- and A_4-waves get reflected at $x = 0$ and become the A_1- and A_3-waves with strengths a_1'' and a_3'', respectively. The transformation matrix is given by equation

(2.43). Thus,

$$[R_4] = -\begin{bmatrix} 1 & 1 \\ k_1^2 & k_3^2 \end{bmatrix}^{-1} \begin{bmatrix} 1 & 1 \\ k_2^2 & k_4^2 \end{bmatrix}.$$

The condition for the beam to vibrate in one of its normal modes can be stated as

$$a_1'' = a_1 \tag{2.44}$$

and

$$a_3'' = a_3. \tag{2.45}$$

In terms of the transformation matrices, the phase-closure principle thus yields

$$[R_4][R_3][R_2][R_1] \begin{Bmatrix} a_1 \\ a_3 \end{Bmatrix} = \begin{Bmatrix} a_1 \\ a_3 \end{Bmatrix}. \tag{2.46}$$

For non-trivial solutions of a_1 and a_3, the following condition must be satisfied :

$$\det\ [[R_4][R_3][R_2][R_1] - [I]] = 0. \tag{2.47}$$

As shown in Appendix A, the above equation is same as the frequency equation (2.23).

Calculation of the natural frequencies for $c_d \leq c < \pi$

In this speed regime, three waves, namely the A_1-, A_3- and A_4-waves propagate in the downstream direction and the remaining A_2-wave moves in the opposite direction. When a simply-supported boundary is placed at a point, say $x = 0$, the four waves satisfy the following relations:

$$A_1 + A_2 + A_3 + A_4 = 0$$

and

$$k_1^2 A_1 + k_2^2 A_2 + k_3^2 A_3 + k_4^2 A_4 = 0.$$

If an A_2-wave hits upon the boundary, the resulting A_1-, A_3- and A_4-waves are obtained from the above two equations. But since the number of unknowns exceeds that of the

equations, the strengths of the waves can not be calculated individually. However, their relative strengths A_1/A_4 and A_3/A_4 are obtained as

$$\left\{ \begin{array}{c} A_1/A_4 \\ A_3/A_4 \end{array} \right\} = - \left[\begin{array}{cc} 1 & 1 \\ k_1^2 & k_3^2 \end{array} \right]^{-1} \left[\begin{array}{cc} 1 & 1 \\ k_2^2 & k_4^2 \end{array} \right] \left\{ \begin{array}{c} A_2/A_4 \\ 1 \end{array} \right\}. \tag{2.48}$$

On the other hand, if the propagating A_1-, A_3- and A_4-waves get reflected from the boundary, the resulting A_2-wave can be obtained from the following relation:

$$A_2 = -(A_1 + A_3 + A_4). \tag{2.49}$$

It is to be pointed out that this motion is over-constrained. The waves must also satisfy the following equation due to the disappearance of the bending moments at the simply-supported boundaries:

$$A_1 k_1^2 + A_2 k_2^2 + A_3 k_3^2 + A_4 k_4^2 = 0. \tag{2.50}$$

To get the normal modes, the propagation of the waves is to be followed as detailed below :

(i) Let an A_2-wave of strength a_2 be reflected from the simply-supported boundary placed at $x = 0$. Three waves, namely, the A_1-, A_3- and A_4-waves, are generated. The strengths of these waves can not be determined uniquely, but the relative strengths a_1/a_4 and a_3/a_4 can be obtained in the following matrix form :

$$\left\{ \begin{array}{c} a_1/a_4 \\ a_3/a_4 \end{array} \right\} = - \left[\begin{array}{cc} 1 & 1 \\ k_1^2 & k_3^2 \end{array} \right]^{-1} \left[\begin{array}{cc} 1 & 1 \\ k_2^2 & k_4^2 \end{array} \right] \left\{ \begin{array}{c} a_2/a_4 \\ 1 \end{array} \right\} = [R_1] \left\{ \begin{array}{c} a_2/a_4 \\ 1 \end{array} \right\}.$$

(ii) The above A_1-, A_3- and A_4-waves of respective strengths a_1, a_3 and a_4 start travelling from $x = 0$ and reach $x = 1$ with strengths a_1', a_3' and a_4', respectively. It is seen that

$$a_1' = e^{ik_1} a_1, \quad a_3' = e^{ik_3} a_3, \quad a_4' = e^{ik_4} a_4.$$

Since only the values of the relative strengths a_1/a_4 and a_3/a_4 are known at $x = 0$, the corresponding values at $x = 1$ are obtained as

$$\left\{ \begin{array}{c} a_1'/a_4' \\ a_3'/a_4' \end{array} \right\} = \left[\begin{array}{cc} e^{i(k_1-k_4)} & 0 \\ 0 & e^{i(k_3-k_4)} \end{array} \right] \left\{ \begin{array}{c} a_1/a_4 \\ a_3/a_4 \end{array} \right\} = [R_2] \left\{ \begin{array}{c} a_1/a_4 \\ a_3/a_4 \end{array} \right\}, \text{ (say)}.$$

(iii) The propagating A_1-, A_3- and A_4-waves are reflected from $x = 1$ and produce an A_2-wave of strength a_2'. As equations (2.49) and (2.50) are to be satisfied at the boundary, one gets the following relation in terms of the relative strengths:

$$\left\{ \begin{array}{c} a_2'/a_4' \\ 1 \end{array} \right\} = - \left[\begin{array}{cc} 1 & 1 \\ k_2^2 & k_4^2 \end{array} \right]^{-1} \left[\begin{array}{cc} 1 & 1 \\ k_1^2 & k_3^2 \end{array} \right] \left\{ \begin{array}{c} a_1'/a_4' \\ a_3'/a_4' \end{array} \right\} = [R_3] \left\{ \begin{array}{c} a_1'/a_4' \\ a_3'/a_4' \end{array} \right\}.$$

(iv) Finally the A_2-wave of strength a_2' reaches the point $x = 0$ with strength a_2''. Thus,

$$a_2'' = e^{-ik_2} a_2',$$

from which the following transformation matrix is constructed:

$$\left\{ \begin{array}{c} a_2''/a_4 \\ 1 \end{array} \right\} = \left[\begin{array}{cc} e^{-i(k_2-k_4)} & 0 \\ 0 & 1 \end{array} \right] \left\{ \begin{array}{c} a_2'/a_4' \\ 1 \end{array} \right\} = [R_4] \left\{ \begin{array}{c} a_2'/a_4' \\ 1 \end{array} \right\}.$$

According to the phase-closure principle

$$a_2'' = a_2,$$

or

$$a_2''/a_4 = a_2/a_4.$$

In terms of the transformation matrices, the above requirement is equivalent to

$$[[R_4][R_3][R_2][R_1] - I] \left\{ \begin{array}{c} a_2/a_4 \\ 1 \end{array} \right\} = 0.$$

For non-trivial solutions

$$\det\ [[R_4][R_3][R_2][R_1] - [I]] = 0. \tag{2.51}$$

One can easily verify, following the results given in Appendix A, that equation (2.51) is again identical to the frequency equation (2.23).

2.4 Forced Vibration

In this section, the forced vibration of the travelling beam is studied using the modal analysis as well as the wave-propagation method.

2.4.1 Modal Analysis

The equation of motion of a linear travelling beam, excited by an external force $f(x,\tau)$, can be written, after substituting $\epsilon = 0$ in equation (2.17), as :

$$\mathbf{A}\frac{\partial W}{\partial \tau} + \mathbf{B}W = \mathbf{f}. \tag{2.52}$$

The response $W(x,\tau)$ and the initial conditions are expanded in terms of the complex normal modes in the form

$$W(x,\tau) = \sum_{n=1}^{\infty}(\zeta_n(\tau)\Phi_n + \overline{\zeta}_n(\tau)\overline{\Phi}_n) \tag{2.53}$$

and

$$W(x,0) = \sum_{n=1}^{\infty}(\zeta_n(0)\Phi_n + \overline{\zeta}_n(0)\overline{\Phi}_n). \tag{2.54}$$

Combining equations (2.52) and (2.53) and the orthogonality relations given by equations (2.27) and (2.28), one can easily get the following equation and its complex conjugate

$$\frac{\mathrm{d}\zeta_n}{\mathrm{d}\tau} - i\omega_n^l\zeta_n = \frac{\int_0^1 \overline{\Phi}_n^T\mathbf{f}\,\mathrm{d}x}{\int_0^1 \overline{\Phi}_n^T\mathbf{A}\Phi_n\,\mathrm{d}x}.$$

The above equation can be solved as an initial value problem after obtaining the initial conditions from equation (2.54) and using the orthogonality relations. In what follows, two kinds of forcing, namely, a point-impulse and a harmonic loading, are considered.

For a unit-impulse excitation at point $x = x_0$, i.e., $f(x,\tau) = \delta(\tau-\tau_0)\delta(x-x_0)$ where $\delta(x)$ denotes the Dirac δ-function, the values of $\zeta_n(\tau)$'s with zero initial conditions can be obtained as

$$\zeta_n(\tau) = -i\frac{\left[\int_0^\tau e^{i\omega_n^l(\tau-\tau_1)}\overline{\phi}_n(x_0)\delta(\tau_1-\tau_0)\mathrm{d}\tau_1\right]}{\left[2\omega_n^l\int_0^1\phi_n\overline{\phi}_n\,\mathrm{d}x - 2ic\int_0^1\overline{\phi}_n\frac{\mathrm{d}\phi_n}{\mathrm{d}x}\,\mathrm{d}x\right]},$$

yielding the response as

$$w(x,\tau) = \sum_{n=1}^{\infty}\frac{\phi_n(x)\overline{\phi}_n(x_0)}{2\omega_n^l\int_0^1\phi_n\overline{\phi}_n\,\mathrm{d}x - 2ic\int_0^1\overline{\phi}_n\frac{\mathrm{d}\phi_n}{\mathrm{d}x}\,\mathrm{d}x}e^{i\omega_n^l(\tau-\tau_0)} + c.c. \text{ for } \tau \geq \tau_0. \qquad (2.55)$$

and zero for $\tau < \tau_0$, where *c.c.* denotes the complex conjugate of the preceeding expression.

The steady-state response (neglecting the effects of the transients) of the beam to a harmonic loading $f(x,\tau) = f(x)\cos\Omega\tau$ can be written as

$$W(x,\tau) = \frac{1}{2}\left(P(x)e^{i\Omega\tau} + \overline{P}(x)e^{-i\Omega\tau}\right), \qquad (2.56)$$

where Ω is the non-dimensional frequency obtained from the frequency of excitation, Ω^*, through the relation

$$\Omega^* = \frac{1}{l}\left(\frac{E}{\rho}\right)^{1/2}\gamma\Omega.$$

Following the modal analysis detailed above, one finally gets

$$P = \sum_{n=1}^{\infty}(p_n\Phi_n + q_n\overline{\Phi}_n),$$

where

$$p_n = \frac{2\int_0^1\overline{\Phi}_n^T\mathbf{f}_1\,\mathrm{d}x}{i(\Omega-\omega_n^l)\int_0^1\overline{\Phi}_n^T\mathbf{A}\Phi_n\,\mathrm{d}x}. \qquad (2.57)$$

and

$$q_n = \frac{2\int_0^1 \Phi_n^T \mathbf{f}_1 \, dx}{i(\Omega + \omega_n^l)\int_0^1 \overline{\Phi}_n^T \mathrm{A} \Phi_n \, dx}, \tag{2.58}$$

with $\mathbf{f}_1 = \left\{ \begin{array}{c} f(x)/2 \\ 0 \end{array} \right\}$.

It is to be noted, that for the stationary beam $\phi_n = \overline{\phi}_n$ and $\int_0^1 \overline{\Phi}_n^T \mathrm{A} \Phi_n \, dx = 2(\omega_n^l)^2 \int_0^1 \phi_n^2 \, dx$. Thus, the response expressed by equation (2.56), after expanding Φ_n and $\mathbf{f}_1$, becomes

$$W(x,\tau) = \left(\sum_{n=1}^{\infty} \frac{\int_0^1 \phi_n f(x) \, dx}{[(\omega_n^l)^2 - \Omega^2] \int_0^1 \phi_n^2 \, dx} \right) \cos \Omega \tau,$$

which is well established in the literature [137].

2.4.2 Wave-Propagation Analysis

The response of the travelling beam first to a point impulse excitation and then to any arbitrary excitation are now derived using the principle of wave propagation. To this end, the following observations of the free vibration, presented in Section 2.3.4 are important.

The natures of the waves generated during the free vibration are different in two axial speed regimes, namely, $c < c_d$ and $c \geq c_d$. In the first case, one propagating (A_1-wave) and one evanescent (A_3-wave) waves travel in the downstream direction. Similarly, the upstream waves comprise of one propagating (A_2-wave) and one evanescent (A_4-wave) waves. In the second case, in place of the two evanescent waves, two more downstream propagating waves (A_3- and A_4-waves) are generated. In either case, equation (2.23) is satisfied during a modal vibration.

The easiest way to understand the forced response of a continuous system through wave-propagation approach is to analyse the equation of motion in the frequency domain. This is done by writing the equation of motion in terms of the Laplace transform

of the variables, taken with respect to time, as follows :

$$s^2\hat{w}+2sc\frac{\partial\hat{w}}{\partial x}+(c^2-T_0)\frac{\partial^2\hat{w}}{\partial x^2}+\frac{\partial^4\hat{w}}{\partial x^4}=\hat{f}(x,s)-s\frac{\partial w}{\partial\tau}(x,0)-w(x,0)-2c\frac{\partial w}{\partial x}(x,0), \quad (2.59)$$

where $\hat{w}(x,s)$ and $\hat{f}(x,s)$ are the Laplace transforms of $w(x,\tau)$ and $f(x,\tau)$, respectively. The initial configuration and velocity of the beam are assumed to be trivially zero, i.e., at $\tau = 0$, $w = 0$, $\partial w/\partial\tau = 0$ and $\partial w/\partial x = 0$ for all x. Further, with $f(x,\tau) = \delta(x-x_0)\delta(\tau-\tau_0)$, the equation of motion becomes

$$s^2\hat{w}+2sc\frac{\partial\hat{w}}{\partial x}+(c^2-T_0)\frac{\partial^2\hat{w}}{\partial x^2}+\frac{\partial^4\hat{w}}{\partial x^4}=\delta(x-x_0)e^{-s\tau_0}, \quad (2.60)$$

since $\hat{f}(x,s) = \delta(x-x_0)e^{-s\tau_0}$.

The particular integral of equation (2.60) can be obtained as

$$\hat{w}(x,s)=\sum_{j=1}^{4}\left(\prod_{m=1,m\neq j}^{4}\frac{i}{(k_j^*-k_m^*)}\right)e^{ik_j^*x}\int_0^x e^{-ik_j^*x_1}\delta(x_1-x_0)e^{-s\tau_0}\,dx_1. \quad (2.61)$$

For $x > x_0$, the particular integral becomes

$$\hat{w}(x,s)=\sum_{j=1}^{4}D_j e^{ik_j^*(x-x_0)}, \quad (2.62)$$

where

$$D_j=\prod_{m=1,m\neq j}^{4}\frac{i}{(k_j^*-k_m^*)}e^{-s\tau_0},$$

and k_j^*'s are the roots of the polynomial

$$s^2+2isck^*-(c^2-T_0)(k^*)^2+(k^*)^4=0. \quad (2.63)$$

For any complex value of s, the roots of the above polynomial are either real or complex. Among the complex roots, those having positive (or negative) imaginary parts correspond to the downstream (or upstream) evanescent waves. Of the real roots, the negative ones correspond to the downstream propagating waves and the positive ones to the upstream propagating waves. For $s = i\omega$, the possibilities of the two kinds of

waves are already mentioned in Section 2.3.4. Depending upon the relation between c and ω, either two propagating or four propagating waves may exist.

From the physical nature of the problem, it can be argued that all the terms in the right hand side of equation (2.62) are not present at a point $x > x_0$. At the point $x = x_0$, there exist four waves of strength D_j $(j = 1, 2, 3, 4)$, out of which only those propagating in the downstream direction have an effect on a point lying in the same side of x_0. The effects of the upstream-going waves will not be felt at these points. For example, for $s = i\omega$ ($\omega > 0$ and $c < c_d$) only the contributions of A_1- and A_3-waves are to be retained. But for $c > c_d$, all the downstream propagating waves (i.e., the D_1, D_3 and D_4 terms) contribute to the response at a point $x > x_0$.

Thus, the omission or inclusion of any term of the right hand side of equation (2.62) depends upon the values of k_j^*'s. In the following, the response is calculated only for $s = i\omega$ and $c < c_d$. The other cases may be studied in an analogous manner. The particular integral (see equation (2.62)) now becomes,

$$\hat{w}(x, s) = \sum_{j=1,3} D_j e^{ik_j^*(x-x_0)} \quad \text{for } x \geq x_0, \tag{2.64}$$

The particular integral for $x < x_0$ can be found out by first substituting $x' = -x$ in equation (2.60). Following the same steps carried out for $x > x_0$, and noting that $-k_j^*$'s are the roots of the algebraic equation analogous to equation (2.63), the particular integral is finally obtained as

$$\hat{w}(x, s) = -\sum_{j=1}^{4} D_j e^{ik_j^*(x-x_0)} \quad \text{for } x \leq x_0.$$

Following the same reasoning, used for $x > x_0$, the particular integral in this case has terms corresponding to the waves going only in the upstream direction. For the case considered here ($s = i\omega$ and $c < c_d$),

$$\hat{w}(x, s) = -\sum_{j=2,4} D_j e^{ik_j^*(x-x_0)} \text{ for } x \leq x_0. \tag{2.65}$$

It is to be noted that the particular integral gives the response of the beam only due to the direct influence of the force. However, the waves generated by the external excitation are reflected at the boundaries and new terms appear. These terms are taken care of by retaining the complementary function. The total response is thus given by

$$\hat{w}(x,s) = \sum_{j=1}^{4} C_j e^{ik_j^* x} + \sum_{j=1,3} D_j e^{ik_j^*(x-x_0)} \quad \text{for} \quad x \geq x_0, \tag{2.66}$$

$$= \sum_{j=1}^{4} C_j e^{ik_j^* x} - \sum_{j=2,4} D_j e^{ik_j^*(x-x_0)} \quad \text{for} \quad x \leq x_0. \tag{2.67}$$

One can also verify that the continuity of displacement, slope and moment exist at $x = x_0$. The unknown constants C_j's can be obtained by ensuring that the response satisfies the boundary conditions. This yields

$$0 = [\Delta^*]\{C\} + [F]\{D\} \tag{2.68}$$

where

$$[\Delta^*] = \begin{bmatrix} 1 & 1 & 1 & 1 \\ (k_1^*)^2 & (k_2^*)^2 & (k_3^*)^2 & (k_4^*)^2 \\ e^{ik_1^*} & e^{ik_2^*} & e^{ik_3^*} & e^{ik_4^*} \\ (k_1^*)^2 e^{ik_1^*} & (k_2^*)^2 e^{ik_2^*} & (k_3^*)^2 e^{ik_3^*} & (k_4^*)^2 e^{ik_4^*} \end{bmatrix},$$

$$[F] = \begin{bmatrix} 0 & e^{-ik_2^* x_0} & 0 & e^{-ik_4^* x_0} \\ 0 & (k_2^*)^2 e^{-ik_2^* x_0} & 0 & (k_4^*)^2 e^{-ik_4^* x_0} \\ e^{-ik_1^*(1-x_0)} & 0 & e^{-ik_3^*(1-x_0)} & 0 \\ (k_1^*)^2 e^{-ik_1^*(1-x_0)} & 0 & (k_3^*)^2 e^{-ik_3^*(1-x_0)} & 0 \end{bmatrix},$$

$\{C\} = \{C_1, C_2, C_3, C_4\}^T$ and $\{D\} = \{D_1, -D_2, D_3, -D_4\}^T$. The values of C_j's become

$$\{C\} = -[\Delta^*]^{-1}[F]\{D\} = -[\Delta^*]_{adj}[F]\{D\}/\det[\Delta^*], \tag{2.69}$$

where $[\Delta^*]_{adj}$ is the adjoint matrix of $[\Delta^*]$. Substitution of the values of C_j's into equations (2.66) and (2.67), gives the transfer function for a travelling beam and is denoted by $G(x,\ x_0,\ s)$.

The response of the beam to any arbitrary excitation $f(x,\tau)$ is obtained from the Laplace transform of the response, given by

$$\hat{w}(x,s) = \int_0^1 G(x,\ \zeta,\ s)\hat{f}(\zeta,\ s)\,\mathrm{d}\zeta.$$

To retrieve the time-response $w(x,\tau)$, to a unit impulse excitation, one has to take the inverse Laplace transform of $\hat{w}(x,s)$ as

$$w(x,\tau) = \lim_{Y\to\infty} \frac{1}{2\pi i}\int_{\beta-iY}^{\beta+iY} \hat{w}(x,s)e^{s\tau}\mathrm{d}s,\ \text{ for } \tau > 0 \tag{2.70}$$

where the value of β is so chosen that the integration converges. It is shown below that the integration can also be evaluated using the contour integration theory of complex variable. As seen from equations (2.62)-(2.67), the integrand contains a term $e^{-s\tau_0}$, for which the inverse transformation is carried out separately for $\tau < \tau_0$ and $\tau > \tau_0$.

For $\tau < \tau_0$, the value of β is taken to be negative and the contour is devoid of any singularity (see Figure 2.6). Thus,

$$w(x,\tau) = 0 \text{ for } \tau < \tau_0. \tag{2.71}$$

For $\tau > \tau_0$, one must choose β to be an arbitrary positive number. Since the contour (see Figure 2.7) now contains countably infinite number of singular points, the integration can be performed with the help of the following two theorems [138, 139].

Theorem 1 : Let $f(s)$ be a function which is analytic inside a simple closed path C and on C, except for finitely many singular points $a_1,\ a_2,\ \cdots a_m$ inside C, then

$$\int_C f(s)\mathrm{d}s = 2\pi i \sum_{j=1}^{m} \mathrm{Res}\, f(s)|_{s=a_j},$$

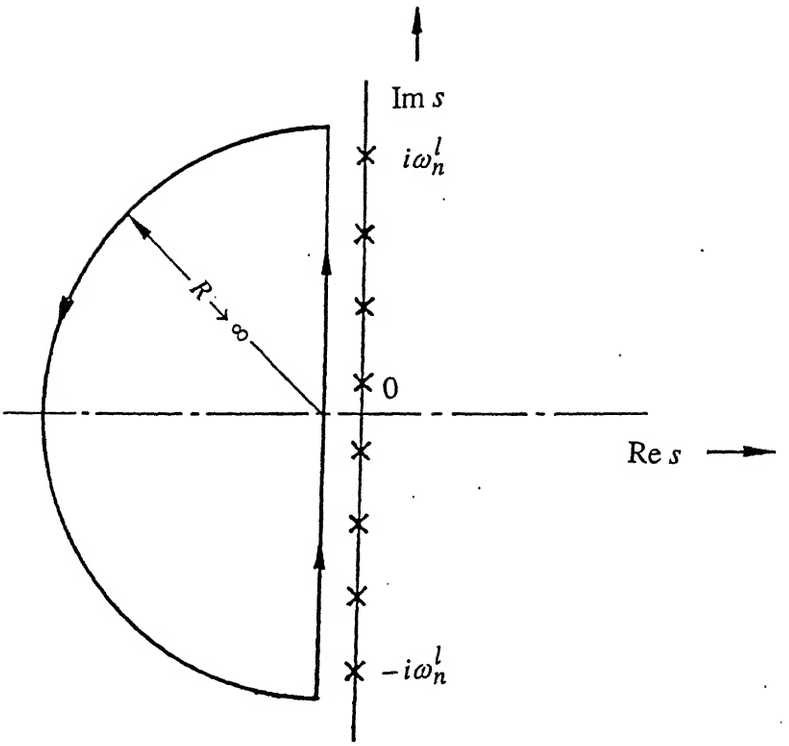

Figure 2.6: Contour of the integration (equation (2.70)) for $\tau < \tau_0$.

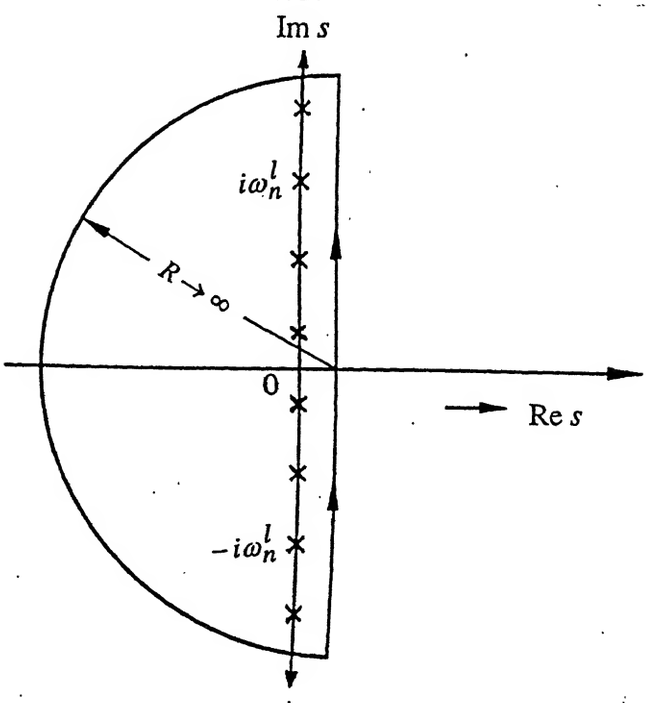

Figure 2.7: Contour of integration (equation (2.70) for $\tau > \tau_0$.

the integral being taken in the counterclockwise sense around the path C [138].

Theorem 2 : If $f_1(s)$ and $f_2(s)$ are analytic in the neighbourhood of s_0 and if $f_1(s_0) \neq 0$ but $f_2(s)$ has a simple pole at s_0, then the residue of $f_1(s)/f_2(s)$ at s_0 is equal to $f_1(s_0)/f_2'(s_0)$ [139].

The integration appearing in equation (2.70), when carried out, yields

$$w(x,\tau) = \sum_{n=1}^{\infty} \left\{ \frac{\sum_{j=1}^{4} C_j e^{ik_j^* x} + \sum_{j=1,3} D_j e^{ik_j^*(x-x_0)}}{\partial(\det[\Delta^*])/\partial s} \right\}\Bigg|_{s=i\omega_n^l} e^{i\omega_n^l(\tau-\tau_0)} + c.c., \quad \text{for } x \geq x_0 \tag{2.72}$$

where the value of the denominator is

$$\frac{\partial}{\partial s}(\det[\Delta^*]) = \sum_{j=1}^{4} \frac{\partial}{\partial k_j^*} \det[\Delta^*] \frac{\mathrm{d}k_j^*}{\mathrm{d}s}.$$

The response can be obtained for $x \leq x_0$, after replacing D_1 and D_3 in equation (2.72) by $-D_2$ and $-D_4$, respectively.

Before considering the steady state response of a travelling beam, it may be worthwhile to mention that the response of a travelling string obtained by the wave-propagation method can be explicitly shown to be identical to equation (2.55). The details of this derivation is given in Appendix B.

The computation of the steady-state response of a travelling beam to a harmonic point load is very convenient by the wave-propagation method. For a linear beam, with a harmonic excitation of frequency Ω (i.e., $f(x,\tau) = F_0\delta(x-x_0)\cos\Omega\tau$), the response is obtained as

$$w(x,\tau) = \frac{F_0}{2} G(x,\, x_0,\, i\Omega) e^{i\Omega\tau} + c.c.. \tag{2.73}$$

It may be noted that the response becomes infinitely large if the beam is resonantly excited with $\Omega = \omega_n^l$ as $\det[\Delta^*] = 0$.

2.4.3 Numerical Results and Discussion

In this section, numerical results of the linear response, obtained by both the wave-propagation method and modal analysis are presented. The initial tension and the axial speed of the beam is taken as $T_0 = 1$ and $c^{'} = c/(c_{cr})_1 = 0.5$ where $(c_{cr})_1 = \sqrt{T_0 + \pi^2}$.

Figure 2.8 shows the variation of $|G(x, x_0, \imath\Omega)|$ with the frequency of excitation (Ω), when an exciting force of unit amplitude is applied at $x_0 = 0.3$ and the response is measured at $x = 0.5$. As shown in the figure, the response amplitude is infinitely large if the excitation frequency, Ω, coincides with one of the natural frequencies of the beam and the point of either excitation or observation does not fall on the nodal points of the corresponding mode. Thus, the response amplitude at $\Omega = \omega_2^l$, as depicted in the figure, is small since the point of measurement coincides with the nodal point where the response envelope corresponding to the second mode attains its minimum value. A large response is obtained for this excitation (i.e., with $\Omega = \omega_2^l$) at any other point. Figure 2.9 shows a large response obtained at $x = 0.75$. It must be pointed out, that an interchange between the positions of excitation and observation leaves the response unaltered. This reciprocity relation has indeed been observed in the numerical computaion.

The response can also be computed in terms of the normal modes, whereby a solution is constructed in a series form. However, only a few terms of the infinite series are usually taken into account. Figure 2.10 shows the displacement profiles, obtained by considering only the first two linear modes of the beam, with an external force $F_0 = 13.22$ and $\Omega = 0.9\omega_1^l$ applied at $x_0 = 1/3$. The four curves in the figure correspond to different time instants during one cycle of excitation. The continuous phase difference along the length of the beam is obvious in this figure.

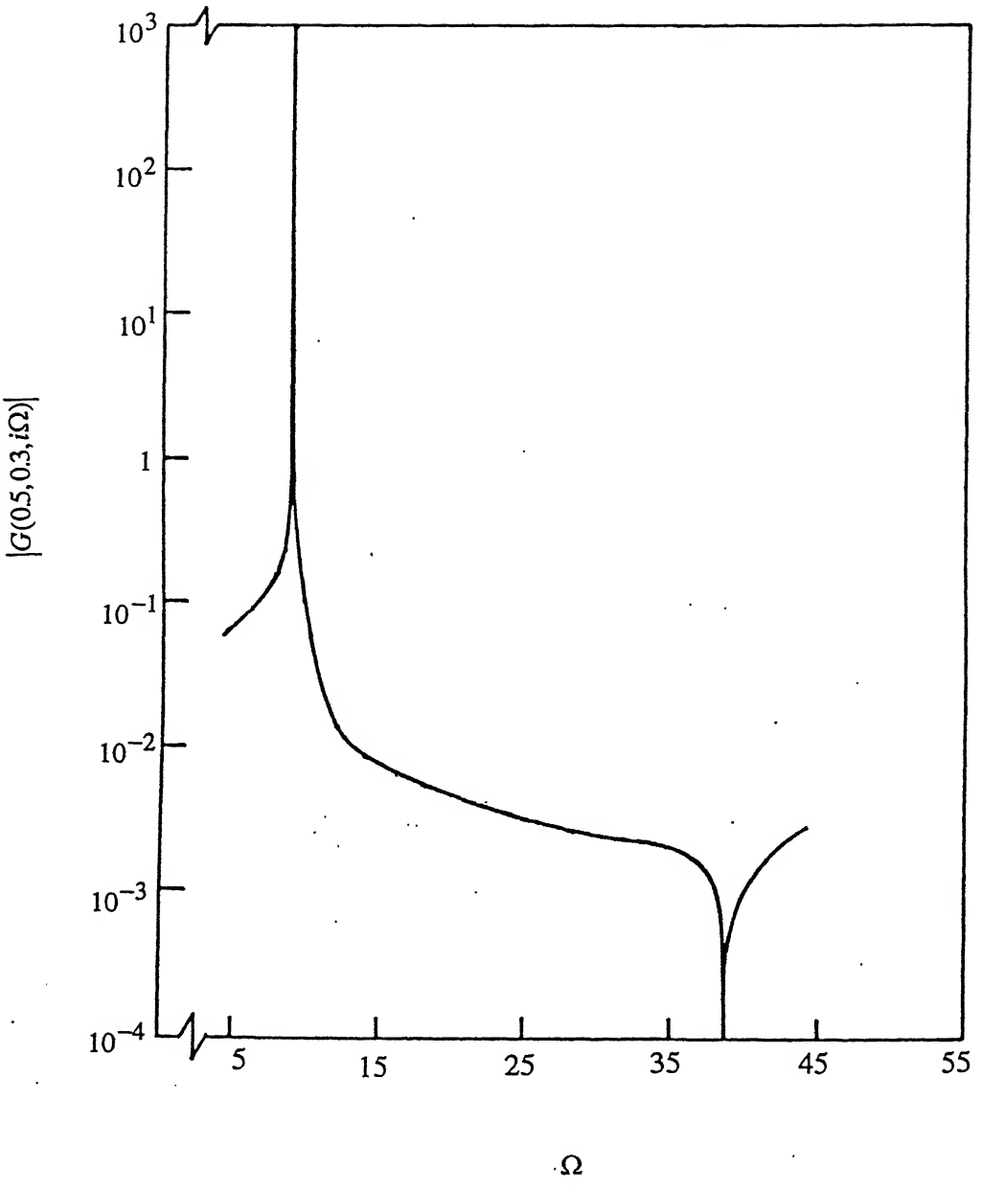

Figure 2.8: Linear frequency response function to a point excitation at $x_0 = 0.3$ measured at $x = 0.5$. $c' = 0.5$.

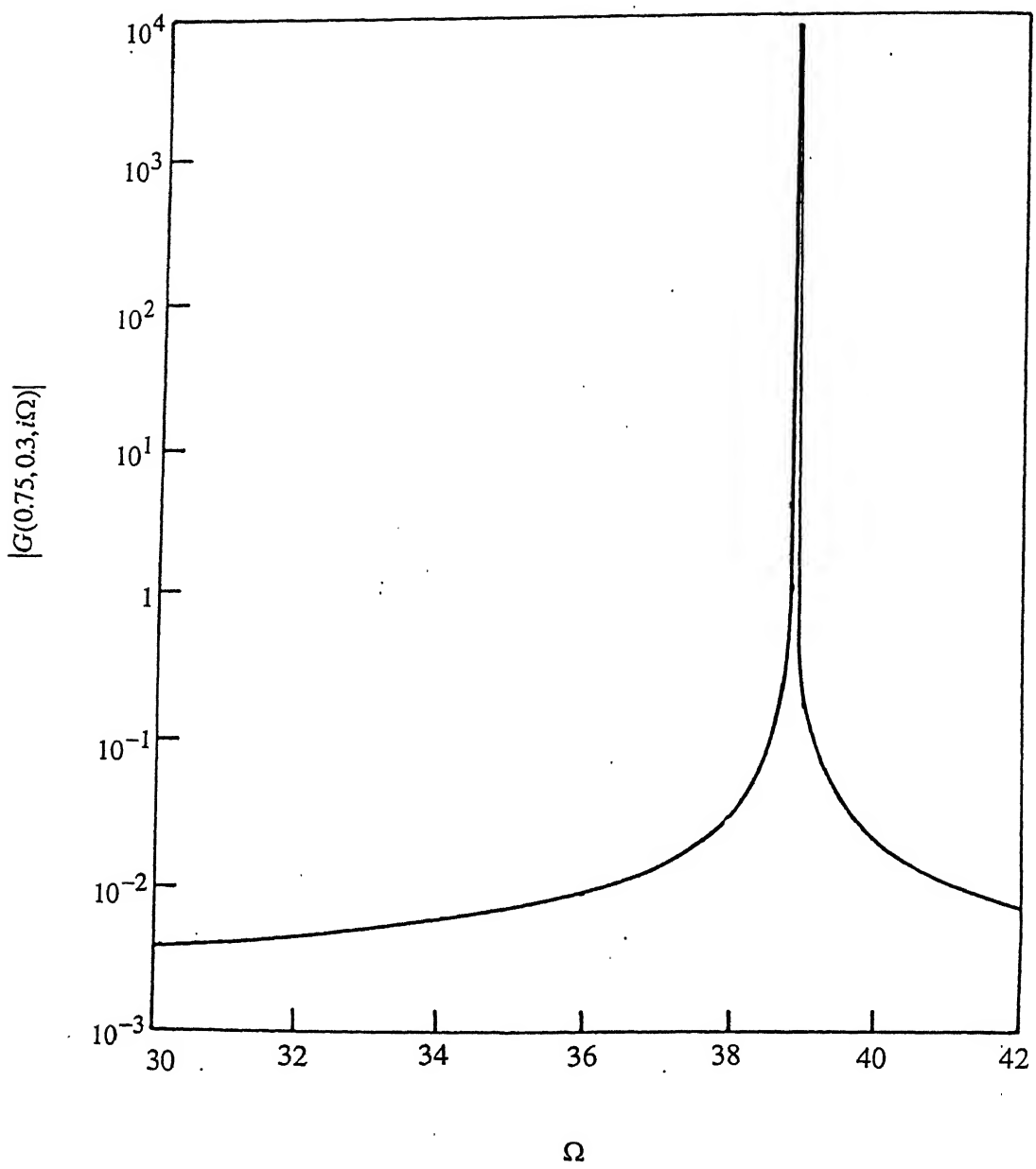

Figure 2.9: Linear frequency response function to a point excitation at $x_0 = 0.3$ measured at $x = 0.75$. $c' = 0.5$.

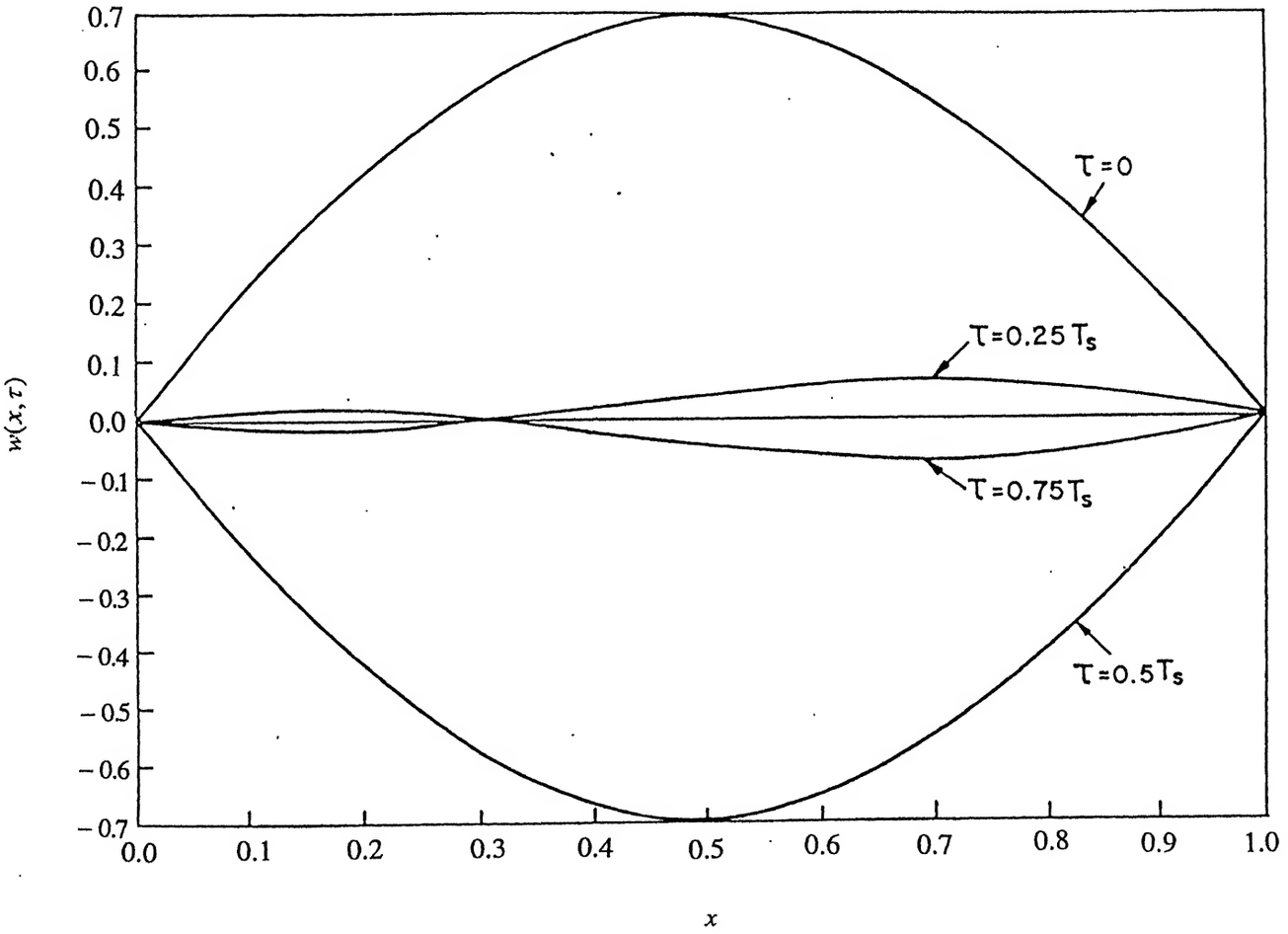

Figure 2.10: Response of a linear travelling beam at four instants of time. $T_0 = 1.0$, T_s = time period of harmonic excitation.

For the excitation frequency close to a natural frequency of the beam, the corresponding normal mode contributes most significantly. But if the excitation frequency is away from any ω_n^l, the effects of all the neighbouring modes become significant. For a high frequency of excitation a large number of modes are to be considered, thus making the computation quite expensive. However, in the wave-propagation method, the response is obtained accurately in the closed form. Figure 2.11 shows the comparative results obtained by the wave-propagation method and also by the one- and two-term modal approximations. For the chosen frequency range, one-term approximation is very crude while addition of another mode makes the result closer to the exact. It has been found that for a frequency $\Omega \approx \omega_1^l$, even the first mode approximation yields quite accurate results.

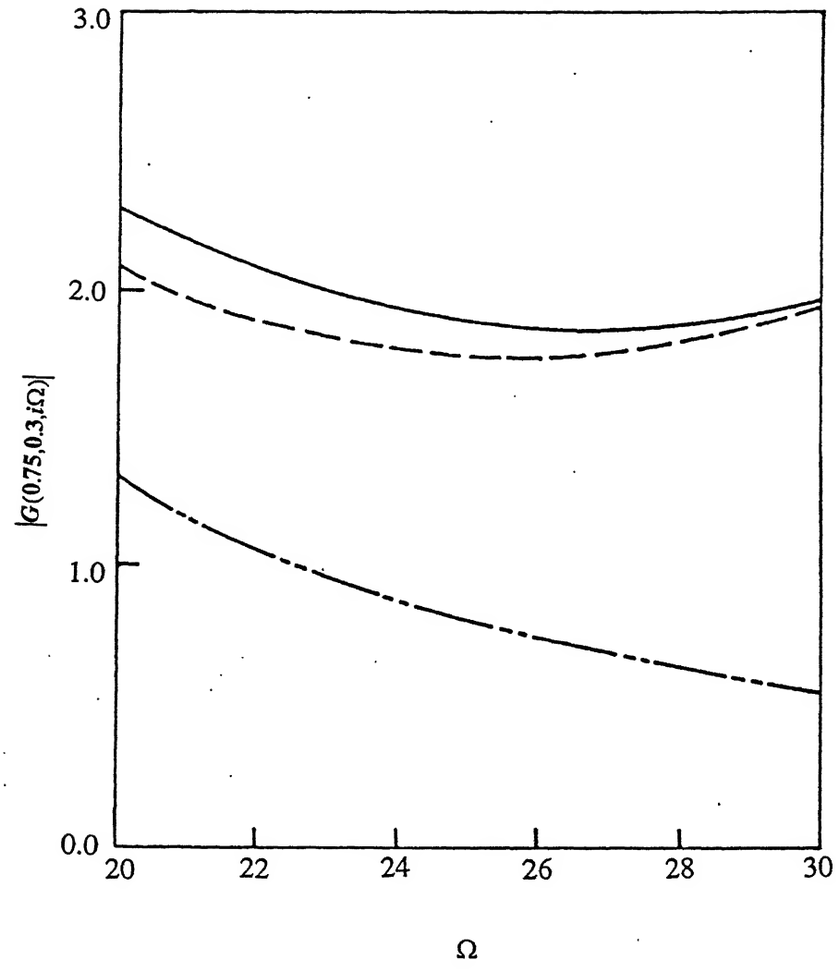

Figure 2.11: Linear frequency response function to a point excitation at $x_0 = 0.3$ measured at $x = 0.5$. $c' = 0.75$. ——— : wave propagation analysis; — - - — : one-term modal analysis; – – – : two-term modal analysis.

Chapter 3

NON-LINEAR NORMAL MODES AND NEAR-RESONANCE RESPONSE

3.1 Introduction

The linear normal modes of a travelleing beam have been derived in Chapter 2. These modes have been subsequently used to obtain the forced response. In the non-linear case (i.e., $\epsilon \neq 0$), such a modal vibration is not possible due to the coupling of the linear modes. Consequently, the analysis of the forced vibration gets complicated. This difficulty is nothing special for the vibration analysis of a travelling member, but appears in almost every non-linear, multi-degrees-of-freedom system. However, periodic solutions exist for the equation of free vibration of even such a non-linear, multi-degrees-of-freedom system. During such a motion all the co-ordinates pass through their equilibrium positions simultaneously and also attain the maximum values simultaneously. This fact, which is true during the modal vibration of a linear system, has

been used to introduce the concept of a 'non-linear normal mode', and a 'non-linear natural frequency'. But generally the 'non-linear normal modes', unlike the linear ones, are not orthogonal to each other. Further, the shapes of the non-linear normal modes as well as the associated natural frequencies are not system properties. Both of these depend on the extent of motion.

The non-linear normal modes of a multi-degree-of-freedom system have been obtained originally using geometric methods [140]. The efficacy of the simple Harmonic Balance Method followed by numerical analysis for obtaining the non-linear normal modes of a multi-degree-of-freedom system has been brought out by Stupnicka [141] with the help of numerous examples. Numerical computation of near-resonance response of such systems, using the non-linear normal modes, is also amply demonstrated in the last reference. The concept of non-linear normal modes for an axially stationary beam (infinite degrees of freedom) with linear boundary conditions have been elaborated by several researchers, like Shaw and Pierre [142], Nayfeh and Nayfeh [143], King and Vakakis [144]. Different methods, namely, the invariant manifold theory [142], the energy method [144] and the multiple-time-scale method [143] have been used to achieve the same goal.

In Section 3.2, a simple method of obtaining the non-linear normal modes of a continuous system is demonstrated with the help of an axially stationary beam, either simply-supported or clamped at both ends and having negligible longitudinal inertia. Towards this end, a combination of harmonic balance and a perturbation technique, instead of using a numerical approach following harmonic balance [141], has been used. Thus, the effects of non-linearities can be very easily tracked to different orders of approximation. The non-linear normal modes are subsequently used in Section 3.3 to obtain the steady-state, near-resonance response for both symmetrically and asymmetrically located harmonic loads. The results obtained by the present method

are compared with those reported in reference [146]. In reference [146], the Galerkin's technique was used for response computation and the results were compared with those obtained experimentally.

In Sections 3.4 and 3.5, the non-linear normal modes and the near-resonance response are recalculated, respectively, taking the longitudinal inertia into consideration. The negligible effect of the longitudinal inertia on the transverse vibration of the beam is clearly brought out.

Thus, the major objectives in this chapter are:

(i) To develop a method for studying the free and forced vibrations of a non-linear continuous system.

(ii) To provide a justification for neglecting the longitudinal inertia term while deriving the non-linear equation of motion of the travelling beam (see Section 2.2).

Although the results are obtained only for an axially stationary beam, the methodology is quite general and will be used again in Chapter 4 to analyse the free and forced vibrations of a non-linear travelling beam.

3.2 Non-linear Normal Modes Neglecting Longitudinal Inertia

In this section, the non-linear normal modes of an axially stationary beam without initial tension are obtained neglecting the effect of longitudinal inertia. The non-linear equation of motion of such a beam, obtained by substituting $c = 0$ and $T_0 = 0$ in equation (2.14), is

$$\frac{\partial^2 w}{\partial \tau^2} + \frac{\partial^4 w}{\partial x^4} = \epsilon \left[\int_0^1 (\frac{\partial w}{\partial x})^2 \, \mathrm{d}x \right] \frac{\partial^2 w}{\partial x^2}. \tag{3.1}$$

The n-th linear normal mode ϕ_n and the corresponding natural frequency ω_n^l ($n = 1, 2, 3, \cdots$) are obtained from the above equation after substituting $\epsilon = 0$. To obtain the non-linear normal modes, the response $w(x, \tau)$ is assumed as

$$w(x, \tau) = a\psi_n(x) \cos \omega_n \tau. \tag{3.2}$$

Substituting equation (3.2) into equation (3.1) and equating the coefficients of $\cos \omega_n \tau$ from both sides, one gets

$$-\omega_n^2 \psi_n + \frac{\mathrm{d}^4 \psi_n}{\mathrm{d}x^4} = \frac{3}{4}\epsilon a^3 \left[\int_0^1 (\frac{\mathrm{d}\psi_n}{\mathrm{d}x})^2 \, \mathrm{d}x\right] \frac{\mathrm{d}^2 \psi_n}{\mathrm{d}x^2}. \tag{3.3}$$

Now, for small non-linearity (i.e., $\epsilon \ll 1$) the n-th non-linear mode ψ_n and the associated non-linear natural frequency ω_n are assumed, respectively, as

$$\psi_n = \phi_n + \epsilon \delta_n^{(1)} + \epsilon^2 \delta_n^{(2)} + \cdots, \tag{3.4}$$

and

$$(\omega_n)^2 = (\omega_n^l)^2 + \epsilon \beta_n^{(1)} + \epsilon^2 \beta_n^{(2)} + \cdots. \tag{3.5}$$

Substituting these expressions into equation (3.3) and subsequently equating the coefficients of the like powers of ϵ from both sides of the resulting equation, one obtains

$$\epsilon^0 \; : \; -(\omega_n^l)^2 \phi_n + \frac{\mathrm{d}^4 \phi_n}{\mathrm{d}x^4} = 0, \tag{3.6}$$

$$\epsilon^1 \; : \; -(\omega_n^l)^2 \delta_n^{(1)} + \frac{\mathrm{d}^4 \delta_n^{(1)}}{\mathrm{d}x^4} = \beta_n^{(1)} \phi_n + \frac{3}{4} a^2 \left[\int_0^1 (\frac{\mathrm{d}\phi_n}{\mathrm{d}x})^2 \, \mathrm{d}x\right] \frac{\mathrm{d}^2 \phi_n}{\mathrm{d}x^2}. \tag{3.7}$$

Equation (3.6) is trivially satisfied. To solve equation (3.7), $\delta_n^{(1)}$ is written in the following series form :

$$\delta_n^{(1)} = \sum_{j=1, j \neq n}^{\infty} \Delta_j^{(1)} \phi_j, \tag{3.8}$$

since the solvability condition [145] of equation (3.7) demands that $\delta_n^{(1)}$ cannot have any contribution from ϕ_n.

Further, one can rewrite the right hand side of equation (3.8) as

$$\beta_n^{(1)}\phi_n + \frac{3}{4}a^2\sum_{j=1}^{\infty}\alpha_j^{(1)}\phi_j, \tag{3.9}$$

where

$$\alpha_j^{(1)} = \frac{\left(\int_0^1 \left(\frac{\mathrm{d}\phi_n}{\mathrm{d}x}\right)^2 \mathrm{d}x\right)\left(\int_0^1 \frac{\mathrm{d}^2\phi_n}{\mathrm{d}x^2}\phi_j\,\mathrm{d}x\right)}{\left(\int_0^1 \phi_j^2 \mathrm{d}x\right)}. \tag{3.10}$$

First equations (3.8)-(3.10) are substituted into equation (3.7), then equating the coefficients of ϕ_j's from both sides of the equation, one gets

$$\beta_n^{(1)} = -\frac{3}{4}a^2\alpha_n^{(1)} \tag{3.11}$$

and

$$\delta_n^{(1)} = \frac{3}{4}a^2\sum_{j\neq n}\frac{\alpha_j^{(1)}\phi_j}{\left[(\omega_j^l)^2 - (\omega_n^l)^2\right]}. \tag{3.12}$$

Thus, the non-linear normal modes and the associated frequencies are obtained as

$$\psi_n = \phi_n + \frac{3}{4}\epsilon a^2\sum_{j\neq n}\frac{\alpha_j^{(1)}\phi_j}{\left[(\omega_j^l)^2 - (\omega_n^l)^2\right]}. \tag{3.13}$$

and

$$(\omega_n)^2 = (\omega_n^l)^2 - \frac{3}{4}\epsilon a^2\alpha_n^{(1)}. \tag{3.14}$$

The amplitude dependence of the non-linear mode shapes and the natural frequencies are clearly exhibited by the above two equations.

Similar to the linear case, the phase-closure principle holds good even during the non-linear modal vibration. This is shown below by recalculating the non-linear normal modes and the natural frequencies using the wave-propagation theory.

3.2.1 Wave-Propagation Approach

To derive the non-linear normal modes, i.e., the shape of the beam which vibrates at a single frequency ω, the response $w(x,\tau)$ given by equation (3.2), is substituted into

equation (3.1) to get

$$\left(-\omega^2\psi + \frac{\mathrm{d}^4\psi}{\mathrm{d}x^4}\right) a\cos\omega\tau = \frac{3}{4}\epsilon a^3 \left[\int_0^1 (\frac{\mathrm{d}\psi}{\mathrm{d}x})^2\,\mathrm{d}x\right] \frac{\mathrm{d}^2\psi}{\mathrm{d}x^2}\cos\omega\tau, \tag{3.15}$$

after neglecting the higher harmonics. For a normal mode to exist, $\psi(x)$ is such that the phase of any wave should change by an integral multiple of 2π by travelling once to and fro along the beam. In the absence of non-linearity (i.e., with $\epsilon = 0$), the phase closure occurs when $\omega = \omega_n^l$ and $\psi = \phi_n$. In general, in the presence of the non-linear term, different linear modes are simultaneously excited. Hence, the normal mode corresponds to the frequency at which the phases of the waves corresponding to all the linear modes are closed simultaneously. Thus, to get the normal oscillation, one has to search for such a frequency. To this end, the following observation from the linear analysis is important.

For the free vibration at any linear mode, say the n-th mode, one can write

$$\phi_n(x) = A_1 e^{-ikx} + A_2 e^{ikx} + A_3 e^{-kx} + A_4 e^{kx},$$

where the wave number $k = \sqrt{\omega_n^l}$ and the coefficients A_1, A_2, A_3 and A_4 bear a constant ratio amongst each other. Thus, four (two propagating and two evanescent) waves of definite wave numbers travel once across the beam in such a way that the phase of each wave gets closed after a time interval $2\pi/\omega_n^l$. However, for a frequency different from ω_n^l, say Ω, the same waves can be closed as they traverse once across the beam only by applying a suitable external force given by

$$f_n = \left[(\omega_n^l)^2 - \Omega^2\right] \phi_n(x) \cos\Omega\tau. \tag{3.16}$$

With the above forcing, the wave numbers and the relative strengths of the constituent waves do not change, but the phase velocity of each wave is changed to

$$CP' = \frac{\Omega}{k} = \frac{\omega_n^l}{k}.\frac{\Omega}{\omega_n^l} = CP \times \frac{\omega_n^l}{\Omega}.$$

where CP is the phase velocity of the wave propagating in the n-th normal mode and having the wave number k.

Now returning to the non-linear case, for weak non-linearity one can write

$$(\omega)^2 = (\omega_n^l)^2 + O(\epsilon) \tag{3.17}$$

and

$$a\psi = \sum_{m=1}^{\infty} a_m \phi_m, \tag{3.18}$$

where $a_n = a$ and $a_m = O(\epsilon)$ for $m \neq n$.

It can be said that the force arising out of the non-linear term (i.e. the right hand side of equation (3.15)) is just suitable for simultaneous application of the phase closure for all the waves participating in various linear modes. Keeping in view equation (3.16) for a linear normal mode and replacing $\phi_n(x)$ by $a\psi(x)$ and Ω by ω one can write

$$\sum_{m=1}^{\infty} \left[(\omega_m^l)^2 - \omega^2\right] a_m \phi_m = \frac{3}{4}\epsilon a^3 \left[\int_0^1 (\frac{\mathrm{d}\psi}{\mathrm{d}x})^2 \,\mathrm{d}x\right] \frac{\mathrm{d}^2\psi}{\mathrm{d}x^2}. \tag{3.19}$$

Applying equations (3.17)-(3.19) together with the orthogonality relationships among the linear modes one gets the following results neglecting terms $O(\epsilon^2)$:

$$\omega^2 = (\omega_n^l)^2 - \frac{3}{4}a^2\epsilon \frac{\left(\int_0^1 \phi_n \frac{\mathrm{d}^2\phi_n}{\mathrm{d}x^2}\,\mathrm{d}x\right)\left(\int_0^1 \left(\frac{\mathrm{d}\phi_n}{\mathrm{d}x}\right)^2 \mathrm{d}x\right)}{\int_0^1 \phi_n^2 \,\mathrm{d}x} \tag{3.20}$$

and

$$a_m = \frac{3}{4}a^3\epsilon \frac{\left(\int_0^1 \phi_m \frac{\mathrm{d}^2\phi_n}{\mathrm{d}x^2}\,\mathrm{d}x\right)\left(\int_0^1 \left(\frac{\mathrm{d}\phi_n}{\mathrm{d}x}\right)^2 \mathrm{d}x\right)}{[(\omega_m^l)^2 - (\omega_n^l)^2]\int_0^1 \phi_m^2 \,\mathrm{d}x}. \tag{3.21}$$

The above equations yield results identical to those given by equations (3.13) and (3.14).

In what follows, the results for simply-supported and clamped-clamped boundary conditions are explicitly obtained.

3.2.2 Simply-Supported Beam

For the simply-supported non-linear beam, the boundary conditions are given by equations (2.10) and (2.11), which are reproduced below:

$$w(0,\tau) = w(1,\tau) = 0, \quad \frac{\partial^2 w(0,\tau)}{\partial x^2} = \frac{\partial^2 w(1,\tau)}{\partial x^2} = 0.$$

In this case,

$$\phi_n = \sin n\pi x \quad \text{and} \quad (\omega_n^l)^2 = (n\pi)^4. \tag{3.22}$$

Substituting equation (3.22) into equations (3.10), (3.13) and (3.14), one gets

$$\alpha_j^{(1)} = 0 \text{ if } j \neq n \text{ and } \alpha_n^{(1)} = -(n\pi)^4/2$$

and

$$\omega_n^2 = (n\pi)^4 \left[1 + \frac{3}{8}\epsilon a^2\right], \quad \psi_n(x) = \phi_n(x). \tag{3.23}$$

Thus, for a simply-supported beam, the non-linear normal modes are the same as the linear normal modes and hence also orthogonal to each other. The above results are well established in the literature [143].

3.2.3 Clamped-Clamped Beam

In this case, the boundary conditions are

$$w(0,\tau) = w(1,\tau) = 0, \quad \frac{\partial w(0,\tau)}{\partial x} = \frac{\partial w(1,\tau)}{\partial x} = 0.$$

The linear modes and the natural frequencies are given by

$$\phi_n = \left[(\sin \mu_n x - \sinh \mu_n x) - \frac{(\sin \mu_n - \sinh \mu_n)}{(\cos \mu_n - \cosh \mu_n)}(\cos \mu_n x - \cosh \mu_n x)\right], \quad (\omega_n^l)^2 = \mu_n^4, \tag{3.24}$$

where μ_n's are the roots of the transcendental equation $\cos \mu_n \cosh \mu_n = 1$. Further, the following relation is satisfied between the normal modes.

$$\int_0^1 \frac{\mathrm{d}^2\phi_n}{\mathrm{d}x^2}\phi_j \, \mathrm{d}x = 0 \quad \text{if } j+n = \text{ odd}. \tag{3.25}$$

Combining equations (3.13), (3.14), (3.24) and (3.25), one finally gets

$$\psi_n = \phi_n + \frac{3}{4}\epsilon a^2 \sum_{j+n=\text{even}, j\neq n} \frac{\alpha_j^{(1)}\phi_j}{\left[(\omega_j^l)^2 - (\omega_n^l)^2\right]}, \tag{3.26}$$

where $\alpha_j^{(1)}$'s are obtained from equation (3.10).

From equation (3.26) one can see that the odd order non-linear normal modes comprise of only odd order linear normal modes and even order non-linear normal modes are given by a combination of only even order linear normal modes. Hence the odd and even order non-linear normal modes are orthogonal to each other.

The non-linear normal modes for the clamped-clamped beam and the corresponding frequencies, taking only the first three linear normal modes into consideration, are obtained up to $o(\epsilon)$ as

$$\psi_1 = \phi_1 + 0.006675\epsilon a^2\phi_3, \quad \omega_1^2 = (\omega_1^l)^2\left[1 + 0.2351\epsilon a^2\right], \tag{3.27}$$

$$\psi_2 = \phi_2, \quad \omega_2^2 = (\omega_2^l)^2\left[1 + 0.41672\epsilon a^2\right], \tag{3.28}$$

$$\psi_3 = \phi_3 - 0.05017\epsilon a^2\phi_1, \quad \omega_3^2 = (\omega_3^l)^2\left[1 + 0.50226\epsilon a^2\right]. \tag{3.29}$$

3.3 Near-Resonance Response Neglecting Longitudinal Inertia

In this section, the near-resonance response of a harmonically excited non-linear beam is derived using the non-linear normal modes. The equation of motion of such a beam

can be written in the following non-dimensional form :

$$\frac{\partial^2 w}{\partial \tau^2} + \frac{\partial^4 w}{\partial x^4} - \epsilon \left[\int_0^1 (\frac{\partial w}{\partial x})^2 \, \mathrm{d}x \right] \frac{\partial^2 w}{\partial x^2} = f(x) \cos \Omega \tau. \tag{3.30}$$

The response can be written as

$$w(x, \tau) = \sum_{j=1}^{\infty} a_j \psi_j(x) \cos \Omega \tau, \tag{3.31}$$

where $\psi_j(x)$ is the j-th non-linear normal mode, derived in the previous section. One should not assume that the non-linear normal modes are orthogonal to each other. When the forcing frequency is close to a linear natural frequency, say, ω_n^l, then the participation of the corresponding non-linear normal mode is largest whereas the other modes participate only weakly. Mathematically this can be written in the following form :

$$\text{when } \Omega = \omega_n^l + \epsilon \Omega_1, \quad a_j = O(\epsilon) = \epsilon b_j, \quad \text{(say), for } j \neq n. \tag{3.32}$$

Substituting equations (3.31) and (3.32) into equation (3.30) and neglecting terms $O(\epsilon^2)$, one obtains

$$a_n \left(-\Omega^2 \psi_n + \frac{\mathrm{d}^4 \psi_n}{\mathrm{d}x^4} \right) \cos \Omega \tau - \epsilon a_n^3 \left[\int_0^1 (\frac{\mathrm{d}\psi_n}{\mathrm{d}x})^2 \, \mathrm{d}x \right] \frac{\mathrm{d}^2 \psi_n}{\mathrm{d}x^2} \cos^3 \Omega \tau$$

$$+ \epsilon \sum_{j \neq n} b_j \left[-\Omega^2 \psi_j + \frac{\mathrm{d}^4 \psi_j}{\mathrm{d}x^4} \right] \cos \Omega \tau = f \cos \Omega \tau. \tag{3.33}$$

Applying the harmonic balance technique to equation (3.33) and substituting equation (3.3), the following result is obtained:

$$a_n \psi_n (\omega_n^2 - \Omega^2) + \epsilon \sum_{j \neq n} b_j \left[-\Omega^2 \psi_j + \frac{\partial^4 \psi_j}{\partial x^4} \right] = f. \tag{3.34}$$

Further, it can be noted from equation (3.13) that

$$\int_0^1 \psi_n \psi_j \, \mathrm{d}x = O(\epsilon), \quad (j \neq n). \tag{3.35}$$

Hence, multiplying equation (3.34) by $\psi_n(x)$ and integrating over x, while neglecting terms $O(\epsilon^2)$, one obtains

$$a_n = \frac{\int_0^1 f(x)\psi_n \, dx}{(\omega_n^2 - \Omega^2)\int_0^1 \psi_n^2 \, dx}. \tag{3.36}$$

Equations (3.14) and (3.36) yield a cubic equation for the determination of a_n.

Since the non-linear frequency is close to the linear natural frequency and the n-th order linear mode of the beam is resonantly excited, one finds $\omega_n^2 - \Omega^2 = O(\epsilon)$. Now multiplying equation (3.34) by ψ_m, $(m \neq n)$, and integrating over x, one gets the following result using equations (3.35) and (3.32) and neglecting terms $O(\epsilon^2)$:

$$a_m = \frac{\int_0^1 f(x)\phi_m \, dx}{((\omega_m^l)^2 - \Omega^2)\int_0^1 \phi_m^2 \, dx}, \qquad (m \neq n). \tag{3.37}$$

It is observed from equation (3.37) that the same expression for a_m $(m \neq n)$ could have been obtained using only the linear theory. Substituting equations (3.36) and (3.37) into equation (3.31), one finally obtains the near-resonance response.

Now a special situation when some non-linear normal modes are orthogonal to each other is discussed. This happens, for example, for all the non-linear modes of a simply-supported beam (see Section 3.2.2) and the non-linear modes of even and odd orders for a clamped-clamped beam (refer Section 3.2.3). In such cases, when two orthogonal non-linear normal modes, say of order n and m are excited, the response can be written as

$$w(x,\tau) = a_n\psi_n \cos \Omega\tau + a_m\psi_m \cos \Omega\tau + \epsilon \sum_{j \neq n,m} b_j\psi_j \cos \Omega\tau, \tag{3.38}$$

with

$$\int_0^1 \psi_n\psi_m \, dx = 0, \quad \int_0^1 \psi_n\psi_j \, dx = O(\epsilon), \quad \int_0^1 \psi_m\psi_j \, dx = O(\epsilon), \quad \text{when } j \neq m, \, n. \tag{3.39}$$

Equation (3.38) is first substituted into equation (3.30). Then considering the fact that

for the cases under discussion, $\int_0^1 \frac{\mathrm{d}\psi_m}{\mathrm{d}x}\frac{\mathrm{d}\psi_n}{\mathrm{d}x}\,\mathrm{d}x = 0$ (for $m \neq n$), one obtains

$$a_n\psi_n(\omega_n^2 - \Omega^2) + a_m\psi_m(\omega_m^2 - \Omega^2) - \frac{3}{4}\epsilon a_n a_m^2\left[\int_0^1 (\frac{\mathrm{d}\psi_m}{\mathrm{d}x})^2\,\mathrm{d}x\right]\frac{\mathrm{d}^2\psi_n}{\mathrm{d}x^2}$$

$$-\frac{3}{4}\epsilon a_m a_n^2\left[\int_0^1 (\frac{\mathrm{d}\psi_n}{\mathrm{d}x})^2\,\mathrm{d}x\right]\frac{\mathrm{d}^2\psi_m}{\mathrm{d}x^2} + \epsilon\sum_{j\neq m,n} b_j\left[-\Omega^2\psi_j + \frac{\mathrm{d}^4\psi_j}{\mathrm{d}x^4}\right] = f, \qquad (3.40)$$

by balancing of harmonics. Multiplying equation (3.40) by ψ_n and ψ_m separately and integrating over x, the following equations are obtained by neglecting terms $O(\epsilon^2)$:

$$a_n(\omega_n^2 - \Omega^2) + \frac{3}{4}\epsilon a_n a_m^2\frac{\left[\int_0^1\left(\frac{\mathrm{d}\phi_n}{\mathrm{d}x}\right)^2\mathrm{d}x\right]\left[\int_0^1\left(\frac{\mathrm{d}\phi_m}{\mathrm{d}x}\right)^2\mathrm{d}x\right]}{\int_0^1\phi_n^2\,\mathrm{d}x} = \frac{\int_0^1 f(x)\psi_n\,\mathrm{d}x}{\int_0^1\psi_n^2\,\mathrm{d}x}, \qquad (3.41)$$

$$a_m(\omega_m^2 - \Omega^2) + \frac{3}{4}\epsilon a_m a_n^2\frac{\left[\int_0^1\left(\frac{\mathrm{d}\phi_n}{\mathrm{d}x}\right)^2\mathrm{d}x\right]\left[\int_0^1\left(\frac{\mathrm{d}\phi_m}{\mathrm{d}x}\right)^2\mathrm{d}x\right]}{\int_0^1\phi_m^2\,\mathrm{d}x} = \frac{\int_0^1 f(x)\psi_m\,\mathrm{d}x}{\int_0^1\psi_m^2\,\mathrm{d}x}. \qquad (3.42)$$

Equations (3.41) and (3.42) can be solved simultaneously to obtain a_n and a_m. It may be noted that even the linear theory can be used to calculate a_j's when $j \neq m, n$.

3.3.1 Numerical Results and Discussion

The non-linear response of a harmonically excited clamped-clamped beam was obtained in reference [146] using the linear modes. The response was assumed to be of the form

$$w(x,\tau) = \sum_{j=1}^{3} A_j^*\phi_j(x)\cos\Omega\tau,$$

and the coefficients A_j^*'s were determined by solving three simultaneous non-linear algebraic equations which were obtained using Galerkin's technique.

From the analysis presented in Section 3.3, one can see the efficacy of using non-linear normal modes for calculating the response of a non-linear system. While the harmonic balance method presented in reference [146] requires solution of three simultaneous non-linear algebraic equations, the present method reduces the computation

to merely solving one cubic equation. Furthermore, in the ordinary harmonic balance method, the number of equations increases proportionately with the number of linear modes considered. But in the method presented here, all the modal participations can be obtained from a single equation.

To illustrate further that both the methods give same results, the near-resonance response of a clamped-clamped beam to a point harmonic excitation are calculated. The beam parameters are taken to be the same as those in reference [146]. To compare the results with those reported in the same reference, the coefficients of the first three linear normal modes (denoted by, say, A_j^*, with $j = 1, 2, 3$) are collected from equations (3.31), (3.36) and (3.37). With a forcing frequency close to the n-th linear natural frequency, the participation of different linear modes are as follows:

$$A_n^* = a_n, \quad A_m^* = a_m + \epsilon\Delta_m^{(1)}, \quad (m \neq n).$$

For the dimensions of the beam treated in reference [146], the non-dimensional parameters are obtained as $\gamma^2 = 2.12 \times 10^{-6}$ and $f(x) = 55624.7775\delta(x - x_0)$, where x_0 is the point of application of the load. When the load is symmetrical about the mid-point of the beam and ψ_n is antisymmetric, the response amplitude is very small (since $a_n = 0$) and can be calculated from the linear theory. The situation is exactly similar when the load is antisymmetric and ψ_n is symmetric. For the simply-supported and clamped-clamped beams, it was seen that ψ_n is symmetric or antisymmetric according to whether n is odd or even, respectively. Thus, from the above argument the non-linear analysis is required only if: (i) n is odd and the load is symmetric about the mid-point i.e., $x = 1/2$; (ii) n is even and the load is antisymmetric about $x = 1/2$; (iii) the load is asymmetric.

Figures 3.1(a) and 3.1(b) show the participation of the first and third linear modes when the first linear mode is resonantly excited by a load at $x = 1/2$. The factor (γ^2),

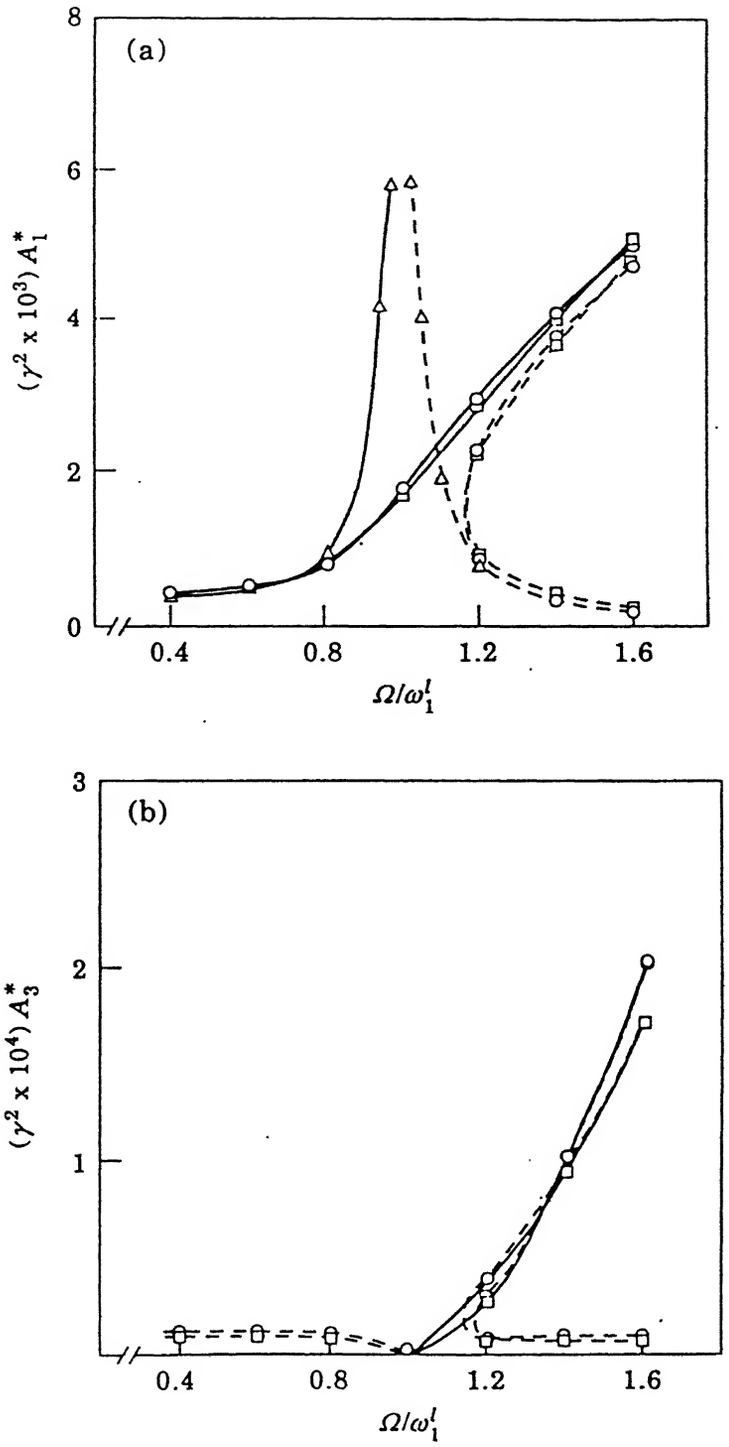

Figure 3.1: (a) Participation of the first mode in the response. (b) Participation of the third mode in the response. △: linear theory,□ : Ref. [146] , ○ : present method; —— : in phase, – – – : out of phase.

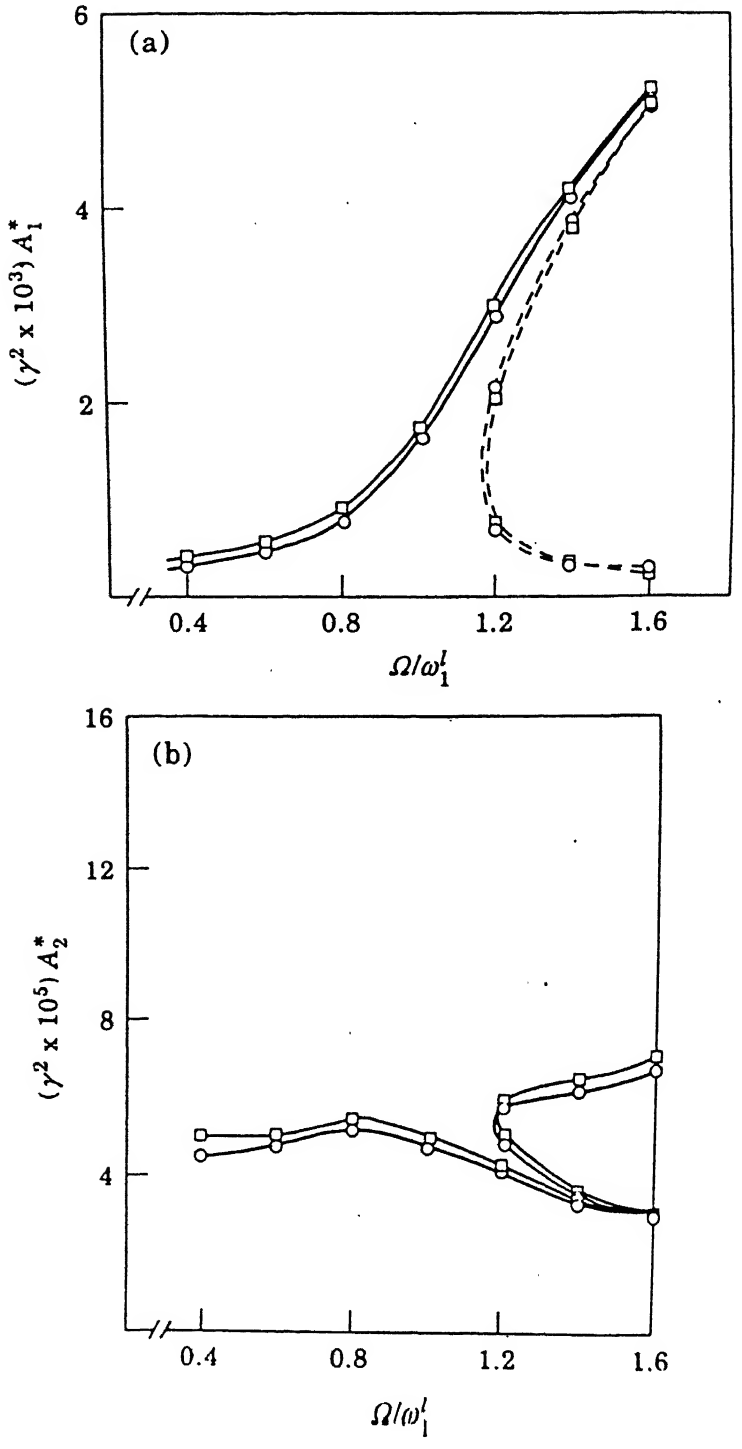

Figure 3.2: (a) Participation of the first mode in the response. (b) Participation of the second mode in the response. □: Ref. [146], ○ : present method; —— : in phase, – – – : out of phase.

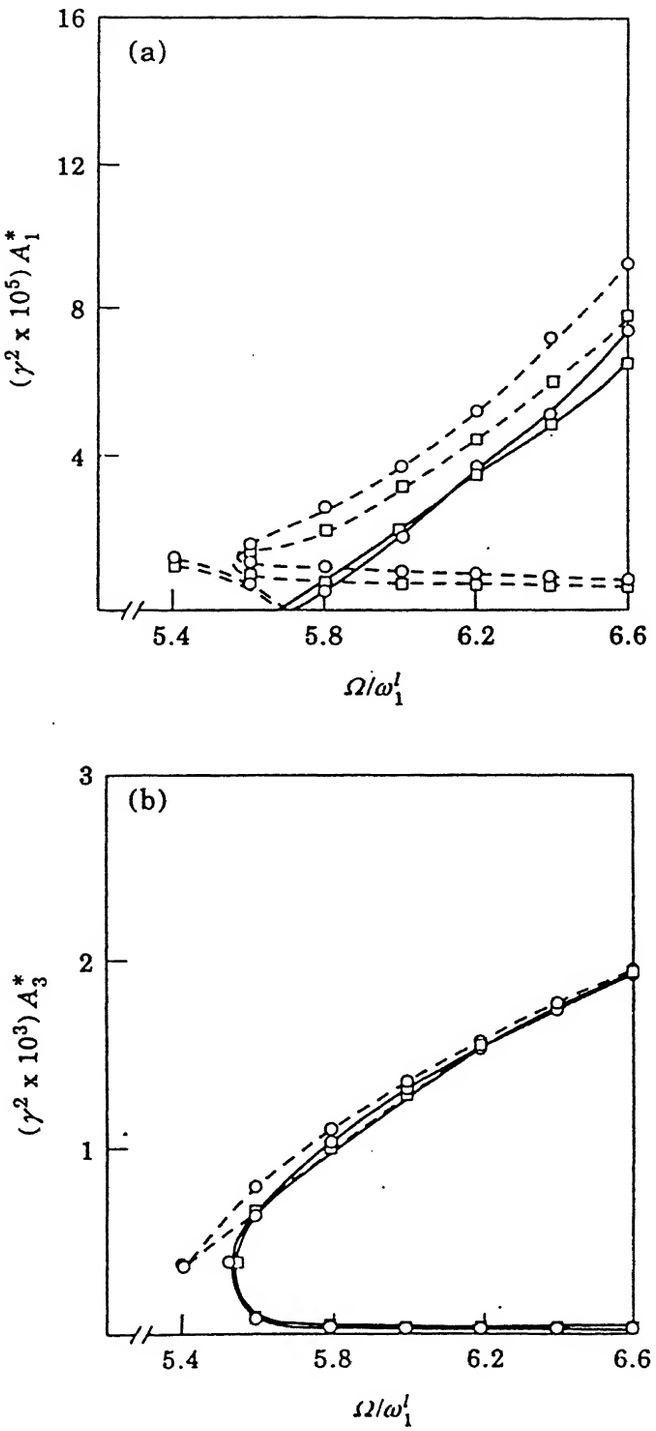

Figure 3.3: (a) Participation of the first mode in the response. (b) Participation of the third mode in the response. □ : Ref. [146], ○ : present method; —— : in phase, – – – : out of phase.

used in the ordinate to compare the results of reference [146] arises because of the difference in the non-dimensionalization procedure. The results of the present analysis are in very good agreement with those of reference [146]. Both the results show marked deviation from the linear theory. It is also to be noted that the experimental data obtained in reference [146] support the theoretical results. Further, like all cases of cubic non-linearity, the intermediate value of the multiple solutions for the periodic response is unstable.

When the first mode is resonantly excited by a point harmonic load applied at $x = 1/4$, both the first and second non-linear normal modes, which are orthogonal to each other, get excited. The response amplitudes in these modes are obtained by solving equations (3.41) and (3.42) and are shown in Figures 3.2(a) and 3.2(b). The results again show excellent agreement with those reported in reference [146].

When the third linear mode is excited by a point harmonic load at $x = 1/2$, the first mode is also excited due to the modal coupling. The modal participation of the first and third linear modes are shown in Figures 3.3(a) and 3.3(b), respectively. The results also show reasonable agreement with those of reference [146].

3.4 Non-Linear Normal Modes Including Longitudinal Inertia

In this section, the non-linear normal modes and the associated natural frequencies of an axially stationary beam are obtained after including the longitudinal inertia. The non-linear normal modes are then used to obtain the near-resonance response in the next section. The equations of motion of the beam, obtained by substituting $c = 0$

and $T_0 = 0$ in equations (2.7) and (2.8), are

$$\frac{\partial^2 u}{\partial \tau^2} - \frac{1}{2\epsilon}\frac{\partial^2 u}{\partial x^2} = 2\epsilon \frac{\partial w}{\partial x}\frac{\partial^2 w}{\partial x^2}, \tag{3.43}$$

and

$$\frac{\partial^2 w}{\partial \tau^2} + \frac{\partial^4 w}{\partial x^4} = \frac{\partial}{\partial x}\left[\frac{1}{2\epsilon}\left(\frac{\partial u}{\partial x}\right)\left(\frac{\partial w}{\partial x}\right) + \epsilon\left(\frac{\partial w}{\partial x}\right)^3\right], \tag{3.44}$$

where $\epsilon = \gamma^2/2$. For obtaining the non-linear normal modes, the response $w(x,\tau)$ assumed to be given by equation (3.2) is substituted into equation (3.43) to yield

$$\frac{\partial^2 u}{\partial \tau^2} - \frac{1}{2\epsilon}\frac{\partial^2 u}{\partial x^2} = \epsilon a^2 \frac{\mathrm{d}\psi_n}{\mathrm{d}x}\frac{\mathrm{d}^2\psi_n}{\mathrm{d}x^2} + \epsilon a^2 \frac{\mathrm{d}\psi_n}{\mathrm{d}x}\frac{\mathrm{d}^2\psi_n}{\mathrm{d}x^2}\cos 2\omega_n \tau. \tag{3.45}$$

The steady-state solution to equation (3.45) is assumed in the form :

$$u(x,\tau) = u_1(x) + u_2(x,\tau), \tag{3.46}$$

where $u_1(x)$ and $u_2(x,\tau)$ are the solutions with only the first and the second term, respectively, on the right hand of equation (3.45). Thus,

$$\frac{\mathrm{d}u_1}{\mathrm{d}x} = -\epsilon^2 a^2 \left(\frac{\mathrm{d}\psi_n}{\mathrm{d}x}\right)^2 + g, \tag{3.47}$$

with g as the constant of integration. Equation (3.47), on integration and after using the boundary conditions that the longitudinal displacement is zero at both $x = 0$ and $x = 1$, yields

$$g = \epsilon^2 a^2 \int_0^1 \left(\frac{\mathrm{d}\psi_n}{\mathrm{d}x}\right)^2 \mathrm{d}x. \tag{3.48}$$

Next, the time-dependent part of u, $u_2(x,\tau)$ is easily obtained as

$$u_2(x,\tau) = \epsilon a^2 \sum_{j=1}^{\infty} \frac{C_j \Gamma_j(x)}{\left(\frac{1}{2\epsilon}\nu_j^2 - 4\omega_n^2\right)} \cos 2\omega_n \tau, \tag{3.49}$$

where

$$C_j = \frac{\int_0^1 \frac{\mathrm{d}\psi_n}{\mathrm{d}x}\frac{\mathrm{d}^2\psi_n}{\mathrm{d}x^2}\Gamma_j \,\mathrm{d}x}{\int_0^1 \Gamma_j^2 \,\mathrm{d}x}, \tag{3.50}$$

and Γ_j's and ν_j's are the linear mode shapes and natural frequencies for the longitudinal vibration, i.e.,

$$\Gamma_j(x) = \sin j\pi x \quad \text{and} \quad \nu_j = j\pi, \quad j = 1, 2, 3, \cdots. \tag{3.51}$$

Substitution of equations (3.2), (3.46)-(3.51) into equation (3.44) yields the following result after balancing the harmonic:

$$a\left(-\omega_n^2\psi_n + \frac{\mathrm{d}^4\psi_n}{\mathrm{d}x^4}\right) = a^3\frac{\mathrm{d}}{\mathrm{d}x}\left[\frac{\epsilon}{4}\left(\frac{\mathrm{d}\psi_n}{\mathrm{d}x}\right)^3 + \frac{\epsilon}{2}\sum_{j=1}^{\infty}\frac{C_j^l\left(\frac{\mathrm{d}\Gamma_j}{\mathrm{d}x}\right)\left(\frac{\mathrm{d}\psi_n}{\mathrm{d}x}\right)}{\nu_j^2}\right]$$

$$+\frac{\epsilon}{2}a^3\left[\int_0^1(\frac{\mathrm{d}\psi_n}{\mathrm{d}x})^2\,\mathrm{d}x\right]\frac{\mathrm{d}^2\psi_n}{\mathrm{d}x^2}. \tag{3.52}$$

For small non-linearities, the non-linear mode ψ_n and the associated frequency ω_n are expanded as in equations (3.4) and (3.5), respectively. Then substituting these into equation (3.52) and subsequently equating the coefficients of the like powers of ϵ from both sides of the resulting equation, one obtains

$$\epsilon^0 \; : \; -(\omega_n^l)^2\phi_n + \frac{\mathrm{d}^4\phi_n}{\mathrm{d}x^4} = 0, \tag{3.53}$$

$$\epsilon^1 \; : \; -(\omega_n^l)^2\delta_n^{(1)} + \frac{\mathrm{d}^4\delta_n^{(1)}}{\mathrm{d}x^4} = \beta_n^{(1)}\phi_n + a^2\frac{\mathrm{d}\Lambda}{\mathrm{d}x} + \frac{1}{2}a^2\left[\int_0^1(\frac{\mathrm{d}\phi_n}{\mathrm{d}x})^2\,\mathrm{d}x\right]\frac{\mathrm{d}^2\phi_n}{\mathrm{d}x^2}, \tag{3.54}$$

where

$$\Lambda = \left[\frac{1}{4}\left(\frac{\mathrm{d}\phi_n}{\mathrm{d}x}\right)^3 + \frac{1}{2}\sum_{j=1}^{\infty}\frac{C_j^l\left(\frac{\mathrm{d}\Gamma_j}{\mathrm{d}x}\right)\left(\frac{\mathrm{d}\phi_n}{\mathrm{d}x}\right)}{\nu_j^2}\right] \tag{3.55}$$

and

$$C_j^l = \frac{\int_0^1 \frac{\mathrm{d}\phi_n}{\mathrm{d}x}\frac{\mathrm{d}^2\phi_n}{\mathrm{d}x^2}\Gamma_j\,\mathrm{d}x}{\int_0^1\Gamma_j^2\,\mathrm{d}x}. \tag{3.56}$$

The solutions to the above equations are carried out by the method described in Section 3.2. The final results are obtained as

$$\psi_n = \phi_n + \epsilon a^2\sum_{j\neq n}\frac{\left(\lambda_j^{(1)} + \frac{\alpha_j^{(1)}}{2}\right)\phi_j}{\left[(\omega_j^l)^2 - (\omega_n^l)^2\right]}, \tag{3.57}$$

and

$$(\omega_n)^2 = (\omega_n^l)^2 - \epsilon a^2 \left(\lambda_n^{(1)} + \frac{\alpha_n^{(1)}}{2} \right), \tag{3.58}$$

where $\alpha_j^{(1)}$'s are given by equation (3.10) and

$$\lambda_j^{(1)} = \frac{\left(\int_0^1 \frac{d\Lambda}{dx} \phi_j \, dx \right)}{\int_0^1 \phi_j^2 \, dx}. \tag{3.59}$$

Now we recalculate the non-linear normal modes and the associated frequencies from equations (3.58) and (3.59) for simply-supported and clamped-clamped end conditions to demonstrate the effect of longitudinal inertia.

3.4.1 Simply-Supported Beam

Substitution of equation (3.22), i.e., the linear normal mode shape and frequency into equations (3.58) and (3.59) yields the following results

$$\omega_n^2 = (n\pi)^4 \left[1 + \frac{3}{8} \epsilon a^2 \right], \quad \psi_n(x) = \phi_n(x), \tag{3.60}$$

which are identical with those given by equation (3.23).

3.4.2 Clamped-Clamped Beam

Using the linear mode shapes and frequencies from equation (3.24), the first three non-linear modes and the corresponding frequencies are obtained as

$$\psi_1 = \phi_1 + 0.006598 \epsilon a^2 \phi_3, \quad \omega_1^2 = (\omega_1^l)^2 \left[1 + 0.2351 \epsilon a^2 \right], \tag{3.61}$$

$$\psi_2 = \phi_2, \quad \omega_2^2 = (\omega_2^l)^2 \left[1 + 0.4169 \epsilon a^2 \right], \tag{3.62}$$

$$\psi_3 = \phi_3 - 0.05062 \epsilon a^2 \phi_1, \quad \omega_3^2 = (\omega_3^l)^2 \left[1 + 0.50225 \epsilon a^2 \right]. \tag{3.63}$$

Comparing equations (3.61)-(3.63) with equations (3.27)-(3.29), one can conclude that the effect of the longitudinal inertia on the non-linear normal modes and frequencies of transverse vibration is negligible.

3.5 Near-Resonance Response Including Longitudinal Inertia

If the beam is excited by a transverse harmonic force, the equations of motion are given by equation (3.43) and

$$\frac{\partial^2 w}{\partial \tau^2} + \frac{\partial^4 w}{\partial x^4} = \frac{\partial}{\partial x}\left[\frac{1}{2\epsilon}(\frac{\partial u}{\partial x})(\frac{\partial w}{\partial x}) + \epsilon(\frac{\partial w}{\partial x})^3\right] + f(x)\cos\Omega\tau. \tag{3.64}$$

When $\Omega = \omega_n^l + \epsilon\Omega_1$, the response, as in Section 3.3, is written in the form:

$$w(x,\tau) = a_n\psi_n \cos\Omega\tau + \epsilon\sum_{j\neq n} b_j\psi_j(x)\cos\Omega\tau. \tag{3.65}$$

Equation (3.65) is first substituted into equation (3.43) and solved for $u(x,\tau)$. The expression for $u(x,\tau)$ thus obtained is then used in equation (3.64). Thereafter, balancing the harmonics and omitting terms $O(\epsilon^2)$, the following equation is obtained:

$$a_n\left(-\Omega^2\psi_n + \frac{\mathrm{d}^4\psi_n}{\mathrm{d}x^4}\right) - a_n^3\frac{\mathrm{d}}{\mathrm{d}x}\left[\frac{\epsilon}{4}\left(\frac{\mathrm{d}\psi_n}{\mathrm{d}x}\right)^3 + \frac{\epsilon}{2}\sum_{j=1}^{\infty}\frac{C_j^l\left(\frac{\mathrm{d}r_j}{\mathrm{d}x}\right)\left(\frac{\mathrm{d}\psi_n}{\mathrm{d}x}\right)}{\nu_j^2}\right]$$

$$-\frac{\epsilon}{2}a_n^3\left[\int_0^1(\frac{\mathrm{d}\psi_n}{\mathrm{d}x})^2\,\mathrm{d}x\right]\frac{\mathrm{d}^2\psi_n}{\mathrm{d}x^2} + \epsilon\sum_{j\neq n} b_j\left[-\Omega^2\psi_j + \frac{\mathrm{d}^4\psi_j}{\mathrm{d}x^4}\right] = f. \tag{3.66}$$

Substituting equation (3.52) into equation (3.66) one gets

$$a_n\psi_n(\omega_n^2 - \Omega^2) + \epsilon\sum_{j\neq n} b_j\left[-\Omega^2\psi_j + \frac{\mathrm{d}^4\psi_j}{\mathrm{d}x^4}\right] = f. \tag{3.67}$$

Using equation (3.35) one finally obtains from equation (3.67)

$$a_n = \frac{\int_0^1 f(x)\psi_n\,\mathrm{d}x}{(\omega_n^2 - \Omega^2)\int_0^1\psi_n^2\,\mathrm{d}x}. \tag{3.68}$$

As noted in Section 3.3, b_j's are obtained from linear analysis with $j \neq n$.

3.5.1 Numerical Results and Discussion

Here the results, reported in Section 3.3, are recalculated taking effects of the longitudinal inertia into consideration. The results are then compared with those of Section 3.3.

Figures 3.4(a) and 3.4(b) show the participations of the first and the third linear modes when the first linear mode is excited by a point load at $x = 1/2$. The effect of longitudinal inertia is seen to be extremely small.

Figures 3.5(a) and 3.5(b) show the participations of the first and the third linear modes when the third linear mode is excited by the same loading. Here also the effect of longitudinal inertia is seen to be negligibly small.

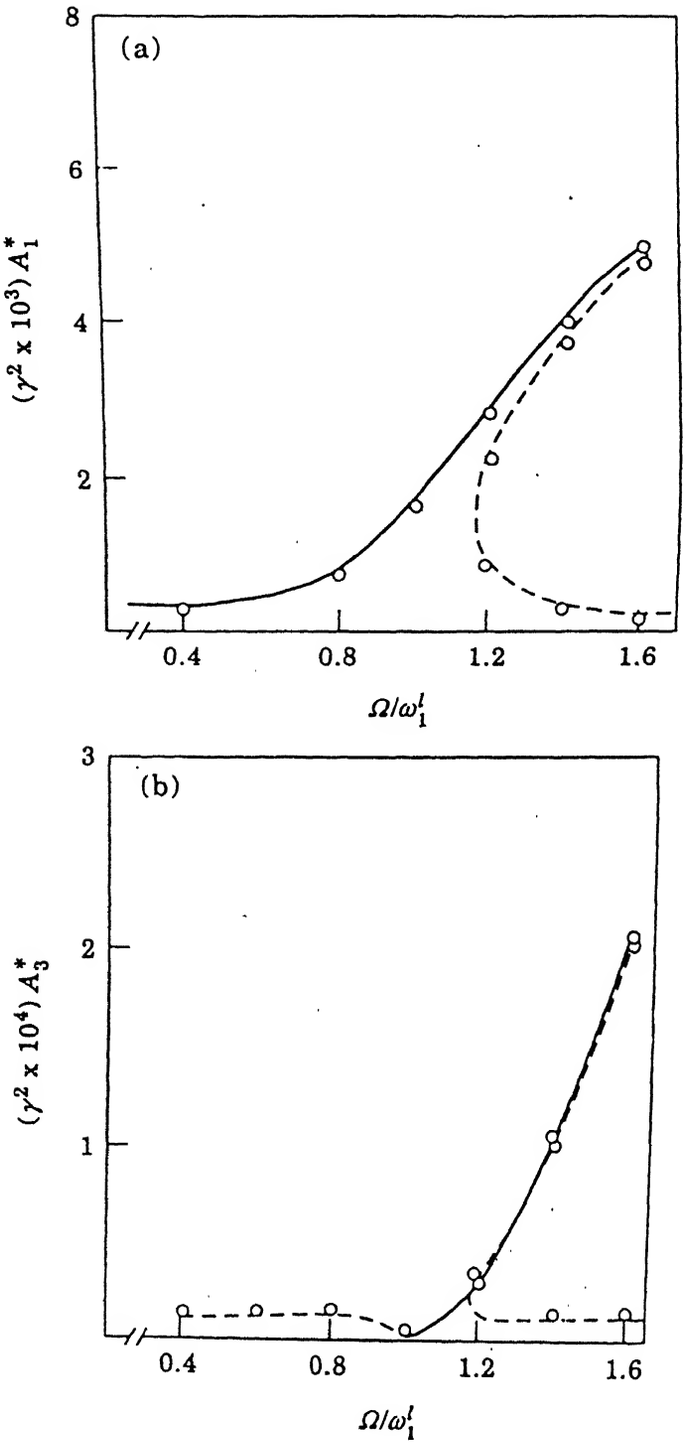

Figure 3.4: (a) Participation of the first mode in the response. (b) Participation of the third mode in the response, —— : in-phase response neglecting longitudinal inertia, – – – : out-of-phase response neglecting longitudinal inertia; ∘ : including longitudinal inertia.

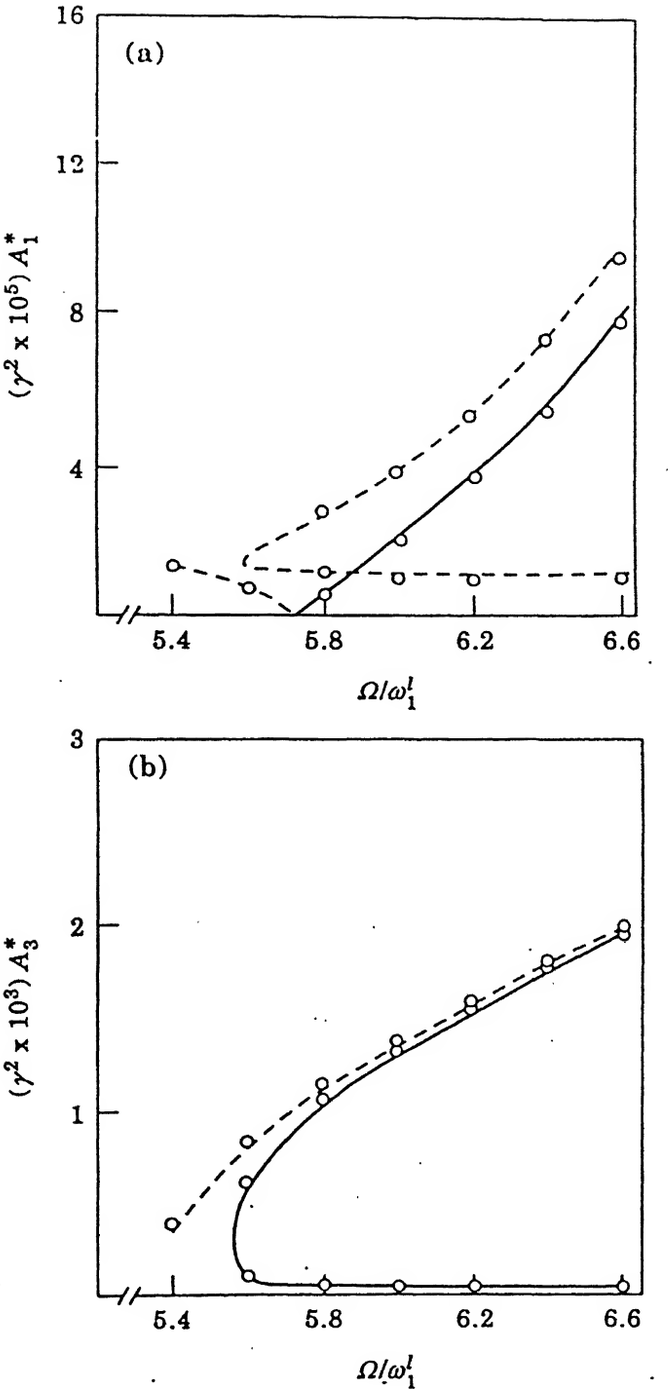

Figure 3.5: (a) Participation of the first mode in the response. (b) Participation of the third mode in the response, —— : in-phase response neglecting longitudinal inertia, – – – : out-of-phase response neglecting longitudinal inertia; o : including longitudinal inertia.

Chapter 4

NON-LINEAR VIBRATION OF A TRAVELLING BEAM

4.1 Introduction

In this chapter, the concept of non-linear normal modes, explained for an axially stationary beam in Chapter 3, is extended to the case of a travelling beam where even a standing linear mode is not possible. However, a complex normal mode can still be derived. Obviously, standing mode is not expected if the non-linearities are included in a travelling beam. Consequently, the existence of 'non-linear complex normal modes' are looked for. Two methods, namely, the modal analysis and wave-propagation approach, are outlined in Section 4.2 to formulate these non-linear complex normal modes. Near-resonance steady-state response to an external harmonic excitation is presented in Section 4.3. Towards this end, the non-linear complex normal modes are used. As expected, the non-linear response has multiple solutions in some ranges of excitation frequency. A stability analysis, required to delineate the stable/unstable solutions, is also carried out in Section 4.3.

For a near-resonant excitation, the contribution of one linear mode is order of magnitude higher than the others and the modal analysis converges quickly. However, for a hard non-resonant excitation, a number of linear modes participate with significant contributions and the modal approach becomes unwieldy. Such an excitation is considered in Section 4.4. The problem of modal coupling is alleviated by taking the linear response in a closed form as obtained in Chapter 2 with the help of the wave-propagation theory. Thereafter, the non-linear response is obtained using a perturbation approach.

4.2 Complex Normal Modes

In this section, the non-linear complex normal modes and the associated non-linear natural frequencies of a simply-supported travelling beam are derived. The equation of motion of the non-linear free vibration is given by equation (2.16) and the boundary conditions by equations (2.10) and (2.11).

To analyse the non-linear free vibration, one can write

$$W(x,\tau) = \frac{a}{2}\Psi_n(x)e^{i\omega_n\tau} + c.c. \tag{4.1}$$

where ω_n is the non-linear natural frequency, and $\Psi_n = \left\{ \begin{array}{c} i\omega_n\psi_n \\ \psi_n \end{array} \right\}$, with ψ_n as the non-linear mode shape, and *c.c.* denotes the complex conjugate of the preceeding expression. Both ω_n and ψ_n are dependent on the complex amplitude a.

Substituting equation (4.1) into the equation of motion (i.e., equation (2.16)) and balancing the first harmonic, (or equating the coefficients of $e^{i\omega_n\tau}$ and $e^{-i\omega_n\tau}$, separately, to zero), one obtains the following complex equation and its conjugate:

$$i\omega_n\frac{a}{2}\mathrm{A}\Psi_n + \frac{a}{2}\mathrm{B}\Psi_n - \epsilon\mathrm{N}_1 = 0, \tag{4.2}$$

where

$$\mathrm{N_1} = \left\{ \frac{a^2\overline{a}}{8} \left(2\frac{\mathrm{d}^2\psi_n}{\mathrm{d}x^2} \int_0^1 \frac{\mathrm{d}\psi_n}{\mathrm{d}x}\frac{\mathrm{d}\overline{\psi}_n}{\mathrm{d}x}\,\mathrm{d}x + \frac{\mathrm{d}^2\overline{\psi}_n}{\mathrm{d}x^2} \int_0^1 \left(\frac{\mathrm{d}\psi_n}{\mathrm{d}x}\right)^2 \mathrm{d}x \right), 0 \right\}^T . \tag{4.3}$$

For weak non-linearity, it can be assumed that the non-linear modes are very close to the linear modes and one can write

$$\Psi_n = \Phi_n + \epsilon\Delta_1^{(n)} + \epsilon^2\Delta_2^{(n)} + \cdots, \tag{4.4}$$

and

$$\omega_n = \omega_n^l + \epsilon\beta_1^{(n)} + \epsilon^2\beta_2^{(n)} + \cdots. \tag{4.5}$$

Substituting equations (4.4) and (4.5) in equation (4.2) and equating the coefficients of like powers of ϵ from both sides, one gets

$$\epsilon^0 \;:\; i\omega_n^l \frac{a}{2}\mathbf{A}\Phi_n + \frac{a}{2}\mathbf{B}\Phi_n = \mathbf{0}, \tag{4.6}$$

$$\epsilon^1 \;:\; i\omega_n^l \frac{a}{2}\mathbf{A}\Delta_1^{(n)} + \frac{a}{2}\mathbf{B}\Delta_1^{(n)} = -i\frac{a}{2}\beta_1^{(n)}\mathbf{A}\Phi_n + \mathrm{N_1}^l, \tag{4.7}$$

where

$$\mathrm{N_1}^l = \left\{ \frac{a^2\overline{a}}{8} \left(2\frac{\mathrm{d}^2\phi_n}{\mathrm{d}x^2} \int_0^1 \frac{\mathrm{d}\phi_n}{\mathrm{d}x}\frac{\mathrm{d}\overline{\phi}_n}{\mathrm{d}x}\,\mathrm{d}x + \frac{\mathrm{d}^2\overline{\phi}_n}{\mathrm{d}x^2} \int_0^1 \left(\frac{\mathrm{d}\phi_n}{\mathrm{d}x}\right)^2 \mathrm{d}x \right), 0 \right\}^T . \tag{4.8}$$

Equation (4.6) is trivially satisfied. To solve equation (4.7), one can expand $\Delta_1^{(n)}$ in terms of the linear modes as

$$\Delta_1^{(n)} = \sum_{m\neq n} (g'_m\Phi_m + \sum_{n=1}^{\infty} h'_m\overline{\Phi}_m), \tag{4.9}$$

since the solvability condition of equation (4.7) demands that $\Delta_1^{(n)}$ can not have any contribution from Φ_n.

The right hand side of equation (4.7) is first expanded in terms of the linear complex normal modes (see Section 2.3.1). Then substituting equation (4.9) into equation (4.7)

and equating the coefficients of Φ_j and $\overline{\Phi}_j$, $(j = 1, 2, 3, \cdots)$ from both sides of the same, one finally gets

$$\beta_1^{(n)} = \frac{2}{ai} \frac{\int_0^1 \overline{\Phi}_n^T \mathbf{N_1}^l \, \mathrm{d}x}{\int_0^1 \overline{\Phi}_n^T \mathbf{A} \Phi_n \, \mathrm{d}x}, \tag{4.10}$$

$$g'_m = \frac{2}{ai} \frac{\int_0^1 \overline{\Phi}_m^T \mathbf{N_1}^l \, \mathrm{d}x}{(\omega_n^l - \omega_m^l) \int_0^1 \overline{\Phi}_m^T \mathbf{A} \Phi_m \, \mathrm{d}x}, \quad m \neq n \tag{4.11}$$

and

$$h'_m = \frac{2}{ai} \frac{\int_0^1 \Phi_m^T \mathbf{N_1}^l \, \mathrm{d}x}{(\omega_n^l + \omega_m^l) \int_0^1 \overline{\Phi}_m^T \mathbf{A} \Phi_m \, \mathrm{d}x}, \quad m = 1, 2, 3, \cdots \tag{4.12}$$

Expanding Φ_n and $\mathbf{N_1}^l$ using equations (2.19) and (4.8), respectively, equations (4.10)-(4.12) take the following forms:

$$\beta_1^{(n)} = -\frac{a\overline{a}}{4} \omega_n^l \frac{\lambda(\overline{\phi}_n, \phi_n)}{\int_0^1 \overline{\Phi}_n^T \mathbf{A} \Phi_n \, \mathrm{d}x}, \tag{4.13}$$

$$g_m = \frac{g'_m}{a\overline{a}} = -\frac{1}{4} \frac{\omega_m^l}{\omega_n^l - \omega_m^l} \frac{\lambda(\overline{\phi}_m, \phi_n)}{\int_0^1 \overline{\Phi}_m^T \mathbf{A} \Phi_m \, \mathrm{d}x}, \quad m \neq n \tag{4.14}$$

and

$$h_m = \frac{g'_m}{a\overline{a}} = \frac{1}{4} \frac{\omega_m^l}{\omega_n^l + \omega_m^l} \frac{\lambda(\phi_m, \phi_n)}{\int_0^1 \overline{\Phi}_m^T \mathbf{A} \Phi_m \, \mathrm{d}x}, \quad m = 1, 2, 3, \cdots \tag{4.15}$$

where

$$\lambda(\phi_m, \phi_n) = 2 \left(\int_0^1 \phi_m \frac{\mathrm{d}^2 \phi_n}{\mathrm{d}x^2} \, \mathrm{d}x \right) \left(\int_0^1 \frac{\mathrm{d}\phi_n}{\mathrm{d}x} \frac{\mathrm{d}\overline{\phi}_n}{\mathrm{d}x} \, \mathrm{d}x \right) + \left(\int_0^1 \phi_m \frac{\mathrm{d}^2 \overline{\phi}_n}{\mathrm{d}x^2} \, \mathrm{d}x \right) \left(\int_0^1 \left(\frac{\mathrm{d}\phi_n}{\mathrm{d}x} \right)^2 \mathrm{d}x \right).$$

Finally, equations (4.13)-(4.15) can be used to write the non-linear normal modes and the associated frequencies as

$$\Psi_n = \Phi_n + \epsilon a \overline{a} \left(\sum_{m \neq n} g_m \Phi_m + \sum_{m=1}^{\infty} h_m \overline{\Phi}_m \right) + O(\epsilon^2) \tag{4.16}$$

and

$$\omega_n = \omega_n^l + \epsilon \beta_1^{(n)} + O(\epsilon^2). \tag{4.17}$$

It can be easily shown from equation (4.13) that for a stationary beam

$$\beta_1^{(n)} = -\frac{3}{8}a^2 \frac{\left(\int_0^1 \phi_n \frac{\mathrm{d}^2\phi_n}{\mathrm{d}x^2}\,\mathrm{d}x\right)\left(\int_0^1 \left(\frac{\mathrm{d}\phi_n}{\mathrm{d}x}\right)^2 \mathrm{d}x\right)}{\omega_n^l \int_0^1 \phi_n^2\,\mathrm{d}x},$$

yielding

$$\omega_n^2 = (\omega_n^l)^2 - \frac{3}{4}a^2\epsilon \frac{\left(\int_0^1 \phi_n \frac{\mathrm{d}^2\phi_n}{\mathrm{d}x^2}\,\mathrm{d}x\right)\left(\int_0^1 \left(\frac{\mathrm{d}\phi_n}{\mathrm{d}x}\right)^2 \mathrm{d}x\right)}{\int_0^1 \phi_n^2\,\mathrm{d}x},$$

a result obtained explicitly in Chapter 3 (see equation (3.20)) with the amplitude a as real.

As in the case of an axially stationary beam, the non-linear complex normal modes of a travelling beam can be derived also by the wave-propagation analysis as presented in the next section.

4.2.1 Wave-Propagation Approach

During vibration in any of the non-linear normal modes, the phases of the waves corresponding to all the linear normal modes get closed. Assuming the non-linear complex modal response as :

$$W(x,\tau) = \frac{a}{2}\Psi_n(x)e^{i\omega\tau} + \frac{\overline{a}}{2}\overline{\Psi}_n(x)e^{-i\omega\tau}, \tag{4.18}$$

the following equation is satisfied during the modal vibration :

$$(i\omega\frac{a}{2}\mathbf{A}\Psi_n + \frac{a}{2}\mathbf{B}\Psi_n)e^{i\omega\tau} - \epsilon\mathbf{N_1}e^{i\omega\tau} = 0. \tag{4.19}$$

where $\mathbf{N_1}$ is given by equation (4.3).

From the linear analysis presented in Chapter 2, it is observed that to close the phases of the waves associated with Φ_n and $\overline{\Phi}_n$ in time $2\pi/\Omega$, the required forces are

$$\{f\} = i(\Omega - \omega_n^l)\mathbf{A}\Phi_n e^{i\Omega\tau}$$

and

$$\{f\} = -i(\Omega + \omega_n^l)\mathbf{A}\overline{\Phi}_n e^{i\Omega\tau},$$

respectively. As the force due to the non-linearity closes the phases of the waves of all the linear modes simultaneously, one can write,

$$\epsilon \mathbf{N}_1 = \sum_{m=1}^{\infty} i(\omega_m^l - \omega)\frac{a_m}{2}\mathbf{A}\Phi_m - \sum_{m=1}^{\infty} i(\omega_m^l + \omega)\frac{b_m}{2}\mathbf{A}\overline{\Phi}_m. \tag{4.20}$$

As in the previous section, for weak non-linearity, one assumes

$$\omega = \omega_n^l + O(\epsilon) \tag{4.21}$$

and

$$a\Psi = \sum_{m=1}^{\infty} a_m \Phi_m + \sum_{m=1}^{\infty} b_m \overline{\Phi}_n, \tag{4.22}$$

where $a_n = a$, $a_m = O(\epsilon)$ for $m \neq n$ and $b_m = O(\epsilon)$ for all m. Combining equations (4.20)-(4.22) and the orthogonality relations, one gets the following results, valid up to $o(\epsilon)$:

$$\omega = \omega_n^l + \frac{2\epsilon}{ai}\frac{\int_0^1 \overline{\Phi}_n^T \mathbf{N}_1^l \, dx}{\int_0^1 \overline{\Phi}_n^T \mathbf{A}\Phi_n \, dx},$$

$$a_m = \frac{2\epsilon}{i}\frac{\int_0^1 \overline{\Phi}_m^T \mathbf{N}_1^l \, dx}{(\omega_n^l - \omega_m^l)\int_0^1 \overline{\Phi}_m^T \mathbf{A}\Phi_m \, dx}, \quad m \neq n$$

and

$$b_m = \frac{2\epsilon}{i}\frac{\int_0^1 \Phi_m^T \mathbf{N}_1^l \, dx}{(\omega_n^l + \omega_m^l)\int_0^1 \overline{\Phi}_m^T \mathbf{A}\Phi_m \, dx}, \quad m = 1, 2, 3, \cdots$$

where $\mathbf{N}_1^l$ is the vector $\mathbf{N_1}$ with ψ_n changed to ϕ_n. It can be verified, by expanding Φ_j's and $\mathbf{N}_1^l$ that the above results are identical to those obtained in Section 4.2.

4.3 Near-Resonance Response

In this section, the non-linear response of a travelling beam, excited harmonically with a frequency very close to one of the linear natural frequencies, is detailed.

The equation of motion (i.e., equation (2.17) is reproduced below :

$$\mathbf{A}\frac{\partial W}{\partial \tau} + \mathbf{B}W - \epsilon \mathbf{N} = \mathbf{f}, \tag{4.23}$$

where

$$\mathbf{f} = \{f(x)\cos\Omega\tau\ ,\ 0\}^T. \tag{4.24}$$

Equation (4.24) can be written as

$$\mathbf{f} = \mathbf{f}_1 e^{i\Omega\tau} + c.c. \tag{4.25}$$

with $\mathbf{f}_1 = \{f(x)/2\ ,\ 0\}^T$.

The principal harmonic response of the beam can be assumed as

$$W(x,\tau) = \frac{1}{2}\left(\Lambda(x)e^{i\Omega\tau} + \overline{\Lambda}(x)e^{-i\Omega\tau}\right). \tag{4.26}$$

Now, in the absence of any internal resonance, if the excitation frequency is very close to a linear natural frequency, then the response contains primarily the corresponding non-linear mode. The contributions of the other non-linear normal modes are very weak. This statement can be expressed mathematically as follows:

When $\Omega = \omega_n^l + \epsilon\Omega_1$,

$$\Lambda = a_n\Psi_n + \sum_{m\neq n}^{\infty} a'_m\Psi_m + \sum_{m=1}^{\infty} b'_m\overline{\Psi}_m + O(\epsilon^2), \tag{4.27}$$

with $a'_m = O(\epsilon) = \epsilon a_m$, (say) and $b'_m = O(\epsilon) = \epsilon b_m$, (say).

Equations (4.26) and (4.27) are then substituted into equation (4.23) and the harmonic balance method (i.e., equate the coefficients of $e^{i\Omega\tau}$ and $e^{-i\Omega\tau}$, separately, from both sides of the equation) is used. Neglecting terms $O(\epsilon^2)$ the following relation and its complex conjugate are obtained:

$$i\Omega\frac{a_n}{2}\mathbf{A}\Psi_n + \frac{a_n}{2}\mathbf{B}\Psi_n - \epsilon\mathbf{N}_1 + \epsilon\left[\sum_{m\neq n}\left(i\Omega\frac{a_m}{2}\mathbf{A}\Phi_m + \frac{a_m}{2}\mathbf{B}\Phi_m\right)\right.$$

$$+\sum_{m=1}^{\infty}\left(i\Omega\frac{b_m}{2}\mathbf{A}\overline{\Phi}_m+\frac{b_m}{2}\mathbf{B}\overline{\Phi}_m\right)\Bigg]=\mathbf{f_1}, \tag{4.28}$$

where $\mathbf{N_1}$ is defined as

$$\mathbf{N_1}=\left\{\frac{a_n^2\overline{a}_n}{8}\left(2\frac{\mathrm{d}^2\psi_n}{\mathrm{d}x^2}\int_0^1\frac{\mathrm{d}\psi_n}{\mathrm{d}x}\frac{\mathrm{d}\overline{\psi}_n}{\mathrm{d}x}\,\mathrm{d}x+\frac{\mathrm{d}^2\overline{\psi}_n}{\mathrm{d}x^2}\int_0^1\left(\frac{\mathrm{d}\psi_n}{\mathrm{d}x}\right)^2\mathrm{d}x\right),0\right\}^T.$$

Substitution of equation (4.2) in equation (4.28) yields

$$i(\Omega-\omega_n)\frac{a_n}{2}\mathbf{A}\Psi_n+\epsilon\left[\sum_{m\neq n}\left(i\Omega\frac{a_m}{2}\mathbf{A}\Phi_m+\frac{a_m}{2}\mathbf{B}\Phi_m\right)+\sum_{m=1}^{\infty}\left(i\Omega\frac{b_m}{2}\mathbf{A}\overline{\Phi}_m+\frac{b_m}{2}\mathbf{B}\overline{\Phi}_m\right)\right]=\mathbf{f_1}. \tag{4.29}$$

Premultiplying equation (4.29) by $\overline{\Psi}_n^T$, and using equation (4.16) and the orthogonality relations (see equations (2.27) and (2.28)), one gets, after neglecting terms $O(\epsilon^2)$,

$$a_n=\frac{2\int_0^1\overline{\Psi}_n^T\mathbf{f_1}\,\mathrm{d}x}{i(\Omega-\omega_n)\int_0^1\overline{\Psi}_n^T\mathbf{A}\Psi_n\,\mathrm{d}x}. \tag{4.30}$$

Since ω_n is related to a_n through equation (4.17), equation (4.30) is a complex cubic equation in a_n. To solve equation (4.30) one can write

$$a_n=\tilde{a}_n e^{i\theta_n}.$$

Now, expanding Ψ_n and $\mathbf{f_1}$ with the help of equations (4.13)-(4.17) and (4.25) and again considering terms up to $o(\epsilon)$, the following results are obtained:

$$\tilde{a}_n(\cos\theta_n+i\sin\theta_n)=\frac{Q+\epsilon\tilde{a}_n^2M}{(\Omega-\omega_n^l-\epsilon\tilde{a}_n^2S)t_n}, \tag{4.31}$$

where

$$Q=-\omega_n^l\int_0^1\overline{\phi}_n f\,\mathrm{d}x,$$

$$M=\left\{-\sum_{m\neq n}\overline{g_m}\omega_m^l\int_0^1\overline{\phi}_m f\,\mathrm{d}x\right\}+\left\{\sum_{m=1}^{\infty}\overline{h_m}\omega_m^l\int_0^1\phi_m f\,\mathrm{d}x\right\},$$

$$S=\frac{\beta_1^{(n)}}{\tilde{a}_n^2}.$$

and

$$t_n = \int_0^1 \overline{\Phi}_n^T \mathrm{A} \Phi_n \, \mathrm{d}x.$$

It is to be observed that Q and M are complex quantities whereas S and t_n are real. So, equating the real and imaginary parts of equation (4.31), one gets

$$\tilde{a}_n \cos\theta_n = \frac{Q^R + \epsilon \tilde{a}_n^2 M^R}{(\Omega - \omega_n^l - \epsilon \tilde{a}_n^2 S) t_n} \tag{4.32}$$

and

$$\tilde{a}_n \sin\theta_n = \frac{Q^I + \epsilon \tilde{a}_n^2 M^I}{(\Omega - \omega_n^l - \epsilon \tilde{a}_n^2 S) t_n}, \tag{4.33}$$

where the superscripts R and I denote the real and imaginary parts, respectively. Squaring equations (4.32) and (4.33) and adding, one gets,

$$\tilde{a}_n^2 = \frac{\left(Q^R + \epsilon \tilde{a}_n^2 M^R\right)^2 + \left(Q^I + \epsilon \tilde{a}_n^2 M^I\right)^2}{(\Omega - \omega_n^l - \epsilon \tilde{a}_n^2 S)^2 t_n^2}. \tag{4.34}$$

Again equation (4.34) is a cubic equation in $\tilde{a}_n^2$. If the externally applied force $f(x)$ is a point load expressed by $F_0 \delta(x - x_0)$, equation (4.34) can be written as

$$A^6 + \left[\frac{2\omega_n^l (1 - r_1)}{S} - \nu\left((M_1^R)^2 + (M_1^I)^2\right)\right] A^4 + \left[\frac{(\omega_n^l)^2 (1 - r_1)^2}{S^2} - 2\nu(M_1^R Q_1^R + M_1^I Q_1^I)\right] A^2$$
$$- \nu\left[(Q_1^R)^2 + (Q_1^I)^2\right] = 0, \tag{4.35}$$

where

$$r_1 = \frac{\Omega}{\omega_n^l}, \; \nu = \left(\frac{F_0}{t_n}\right)^2 \frac{\epsilon}{S^2}, \; A = \sqrt{\epsilon}\tilde{a}_n, \; M_1 = M/F_0, \; Q_1 = Q/F_0.$$

The phase angle θ_n can be obtained from equations (4.32) and (4.33) as

$$\tan\theta_n = \frac{\left(Q^I + \epsilon \tilde{a}_n^2 M^I\right)}{\left(Q^R + \epsilon \tilde{a}_n^2 M^R\right)}. \tag{4.36}$$

Now, to solve for a'_m (appearing in equation (4.27)) from equation (4.29), one premultiplies equation (4.29) by $\overline{\Phi}_m^T$ and uses equations (2.27) and (2.28) to get

$$\epsilon a_m = a'_m = \frac{2\int_0^1 \overline{\Phi}_m^T \mathbf{f}_1 \, \mathrm{d}x}{i(\Omega - \omega_m^l)\int_0^1 \overline{\Phi}_m^T \mathrm{A} \Phi_m \, \mathrm{d}x}; \quad m \neq n. \tag{4.37}$$

In a similar fashion b'_m can be obtained as

$$\epsilon b_m = b'_m = \frac{2\int_0^1 \Phi_m^T \mathbf{f_1}\, dx}{i(\Omega + \omega_m^l)\int_0^1 \overline{\Phi}_m^T \mathbf{A}\Phi_m\, dx}; \quad m = 1, 2\cdots. \tag{4.38}$$

Comparing equations (4.37) and (4.38) with equations (2.57) and (2.58), respectively, one can see that the same expressions for b'_m and a'_m could be obtained using only the linear theory.

Collecting $\tilde{a}_n$, θ_n, a'_m and b'_m from equations (4.34)-(4.38) and putting them into equations (4.26) and (4.27), one gets the non-linear response of a travelling beam to a near-resonance harmonic excitation. Obviously, the linear response, presented in Section 2.4, follows by subtituting $\epsilon = 0$.

Since a continuous phase difference exists in a travelling beam, different sections reach the maximum amplitude at different instants. Hence, a better representation of the response is to show the envelope which bounds the response at all times. When the n-th complex normal mode is excited, the shape of the beam can very well be expressed in the form

$$\begin{aligned} w(x,\tau) &= \frac{\tilde{a}_n}{2} e^{i\theta_n}\phi_n e^{i\Omega\tau} + c.c. + O(\epsilon) \\ &= \tilde{a}_n \phi_n^* \cos(\Omega\tau + \theta_n + \varrho) + O(\epsilon), \end{aligned} \tag{4.39}$$

where

$$\tan\varrho = -\phi_n^I/\phi_n^R \tag{4.40}$$

and

$$\phi_n^* = \sqrt{(\phi_n^R)^2 + (\phi_n^I)^2}.$$

4.3.1 Stability Analysis of Periodic Solutions

As expected for a non-linear system, the possibility of a multi-valued response to a harmonic excitation is observed in Section 4.3. This is manifested as a cubic equation

where $\mathbf{L}_1 = \{l_1(x,\tau)\ ,0\}^T$, with

$$\begin{aligned} l_1(x,\tau) &= \frac{1}{4}\tilde{a}_n^2\left\{3\left(\int_0^1(\frac{\mathrm{d}\phi_n}{\mathrm{d}x})^2\,\mathrm{d}x\right)\frac{\mathrm{d}^2\phi_n}{\mathrm{d}x^2}\right\}e^{2i(\Omega\tau+\theta_n)} \\ &+ \frac{1}{4}\tilde{a}_n^2\left\{\left(\int_0^1(\frac{\mathrm{d}\overline{\phi}_n}{\mathrm{d}x})^2\,\mathrm{d}x\right)\frac{\mathrm{d}^2\phi_n}{\mathrm{d}x^2}+2\left(\int_0^1\frac{\mathrm{d}\overline{\phi}_n}{\mathrm{d}x}\frac{d\phi_n}{dx}\,\mathrm{d}x\right)\frac{\mathrm{d}^2\overline{\phi}_n}{\mathrm{d}x^2}\right\}e^{-2i(\Omega\tau+\theta_n)} \\ &+ \frac{1}{4}\tilde{a}_n^2\left\{2\left(\int_0^1(\frac{\mathrm{d}\phi_n}{\mathrm{d}x})^2\,\mathrm{d}x\right)\frac{\mathrm{d}^2\overline{\phi}_n}{\mathrm{d}x^2}+4\left(\int_0^1\frac{\mathrm{d}\overline{\phi}_n}{\mathrm{d}x}\frac{\mathrm{d}\phi_n}{\mathrm{d}x}\,\mathrm{d}x\right)\frac{\mathrm{d}^2\phi_n}{\mathrm{d}x^2}\right\}. \end{aligned}$$

Applying the orthogonality conditions and equation (2.20) in equation (4.43), one gets the following equation and its complex conjugate:

$$\frac{\mathrm{d}\xi_n}{\mathrm{d}\tau} - i\omega_n^l\xi_n = \epsilon\frac{\int_0^1\overline{\Phi}_n\mathbf{L}_1\,\mathrm{d}x}{\int_0^1\overline{\Phi}_n^T\mathbf{A}\Phi_n\,\mathrm{d}x}\xi_n + \epsilon\frac{\int_0^1\overline{\Phi}_n\overline{\mathbf{L}}_1\,\mathrm{d}x}{\int_0^1\overline{\Phi}_n^T\mathbf{A}\Phi_n\,\mathrm{d}x}\overline{\xi}_n. \tag{4.44}$$

Assuming $\tau' = \Omega\tau + \theta_n$ and $\eta = \frac{\omega_n^l}{\Omega}$, equation (4.44) can be written as

$$\Omega\left[\frac{\mathrm{d}\xi_n}{\mathrm{d}\tau'} - i\eta\xi_n\right] = \epsilon\frac{\int_0^1\overline{\Phi}_n\mathbf{L}'_1\,\mathrm{d}x}{\int_0^1\overline{\Phi}_n^T\mathbf{A}\Phi_n\,\mathrm{d}x}\xi_n + \epsilon\frac{\int_0^1\overline{\Phi}_n\overline{\mathbf{L}'}_1\,\mathrm{d}x}{\int_0^1\overline{\Phi}_n^T\mathbf{A}\Phi_n\,\mathrm{d}x}\overline{\xi}_n, \tag{4.45}$$

where $\mathbf{L}'_1 = \{l_1(x,\tau')\ ,0\}^T$.

Since $\Omega = \omega_n^l + O(\epsilon)$, one can assume

$$\xi_n = \xi_n^{(0)} + \epsilon\xi_n^{(1)} + \cdots \tag{4.46}$$

and

$$\eta = 1 + \epsilon\eta_1 + \cdots. \tag{4.47}$$

Substituting equations (4.46) and (4.47) into equation (4.45) and equating the like powers of ϵ from both sides, the following results are obtained:

$$\epsilon^0 : \ \frac{\mathrm{d}\xi_n^{(0)}}{\mathrm{d}\tau'} - i\xi_n^{(0)} = 0, \tag{4.48}$$

$$\begin{aligned} \epsilon^1 : \ \frac{\mathrm{d}\xi_n^{(1)}}{\mathrm{d}\tau'} - i\xi_n^{(1)} &= i\eta_1\xi_n^{(0)} + \frac{\int_0^1\overline{\Phi}_n\mathbf{L}'_1\,\mathrm{d}x}{\int_0^1\overline{\Phi}_n^T\mathbf{A}\Phi_n\,\mathrm{d}x}\xi_n^{(0)} \\ &+ \frac{\int_0^1\overline{\Phi}_n\mathbf{L}'_1\,\mathrm{d}x}{\omega_n^l\int_0^1\overline{\Phi}_n^T\mathbf{A}\Phi_n\,\mathrm{d}x}\overline{\xi}_n^{(0)}. \end{aligned} \tag{4.49}$$

The solution to equation (4.48) is written as

$$\xi_n^{(0)} = be^{i\tau'},$$

and is substituted into equation (4.49). Writing Φ_n and $\mathbf{L}_1'$ in expanded forms in equation (4.49), it is seen that the secular term in $\xi_n^{(1)}$ can be avoided by choosing η_1 to satisfy

$$(\eta_1 - \Gamma_1)b - \Gamma_2\bar{b} = 0, \tag{4.50}$$

where

$$\Gamma_1 = \tfrac{1}{4}\tilde{a}_n^2\left[2\left(\int_0^1(\frac{\mathrm{d}\phi_n}{\mathrm{d}x})^2\,\mathrm{d}x\right)\left(\int_0^1\frac{\mathrm{d}^2\bar{\phi}_n}{\mathrm{d}x^2}\bar{\phi}_n\,\mathrm{d}x\right)+4\left(\int_0^1\frac{\mathrm{d}\bar{\phi}_n}{\mathrm{d}x}\frac{\mathrm{d}\phi_n}{\mathrm{d}x}\,\mathrm{d}x\right)\left(\int_0^1\frac{\mathrm{d}^2\phi_n}{\mathrm{d}x^2}\bar{\phi}_n\,\mathrm{d}x\right)\right]/t_n$$

$$\Gamma_2 = \tfrac{1}{4}\tilde{a}_n^2\left[\left(\int_0^1(\frac{\mathrm{d}\phi_n}{\mathrm{d}x})^2\,\mathrm{d}x\right)\left(\int_0^1\frac{\mathrm{d}^2\bar{\phi}_n}{\mathrm{d}x^2}\bar{\phi}_n\,\mathrm{d}x\right)+2\left(\int_0^1\frac{\mathrm{d}\bar{\phi}_n}{\mathrm{d}x}\frac{\mathrm{d}\phi_n}{\mathrm{d}x}\,\mathrm{d}x\right)\left(\int_0^1\frac{\mathrm{d}^2\phi_n}{\mathrm{d}x^2}\bar{\phi}_n\,\mathrm{d}x\right)\right]/t_n \tag{4.51}$$

Equation (4.50) is satisfied for $b \neq 0$ if

$$\eta_1 = \Gamma_1 + \Gamma_2 \tag{4.52}$$

or

$$\eta_1 = \Gamma_1 - \Gamma_2. \tag{4.53}$$

Putting $\eta = \frac{\omega_n^l}{\Omega}$ and equations (4.52) and (4.53) in equation (4.47), one gets the bounding frequencies as

$$\Omega' = \omega_n^l - \epsilon(\Gamma_1 + \Gamma_2)\omega_n^l \tag{4.54}$$

and

$$\Omega'' = \omega_n^l - \epsilon(\Gamma_1 - \Gamma_2)\omega_n^l. \tag{4.55}$$

When Γ_1 and Γ_2 are substituted from equation (4.51), the following relation is finally yielded:

$$\Gamma_1 - \Gamma_2 = -\beta_1^{(n)}/\omega_n^l,$$

where $\beta_1^{(n)}$ is given by equation (4.13). This implies that equation (4.55) is nothing but the backbone curve. The primary unstable region is bounded by the two curves, expressed by equations (4.54) and (4.55), in the $\Omega - \tilde{a}_n$ plane.

4.3.2 Numerical Results and Discussion

In this section, some numerical results obtained from the theoretical analysis presented in Sections 4.2 and 4.3 are discussed. The initial tension, T_0 is taken to be unity.

Figure 4.1 shows the amplitude dependence of the first non-linear frequency, expressed as a factor of the first linear natural frequency of a stationary beam (ω_1^0). The non-linear frequency is obtained using equations (4.13) and (4.17) with $\tilde{a}^2 = a\overline{a}$. The figure shows a hardening type non-linear characteristic. Consequently, the non-linearity, as expected, has a stabilizing effect on the divergence instability. The hardening effect becomes more pronounced with increasing travelling speed of the beam.

Using the non-linear normal modes, discussed in Section 4.2, the steady-state response of a travelling beam, excited by a point harmonic load applied at $x_0 = 1/3$, and having a frequency close to the first linear natural frequency (i.e. $n = 1$), is calculated taking the effects of the first two linear modes. The roots of A (i.e. $\tilde{a}_1\sqrt{\epsilon}$) from equation (4.35), for three values of the travelling speed $c' = c/(c_{cr})_1 = 0$, 0.3 and 0.5, with $F_0\sqrt{\epsilon} = 13.22$, are shown in Figure 4.2. The frequency of excitation, Ω, has been expressed as a factor of the first natural frequency of a stationary beam (ω_1^0). Since the mode shape of a travelling beam is not stationary in space, the plot of only $\tilde{a}_1$ becomes meaningless. In order to provide useful information about the response, the positive half of the shape of the response envelope, i.e., $\phi_1^*(x)$, shown in Figure 4.3, is also necessary. It is to be noted that the envelope $\tilde{a}_1\phi_1^*$ bounds the beam displacement within an accuracy of $o(1)$, and different sections of the beam touch the envelope at

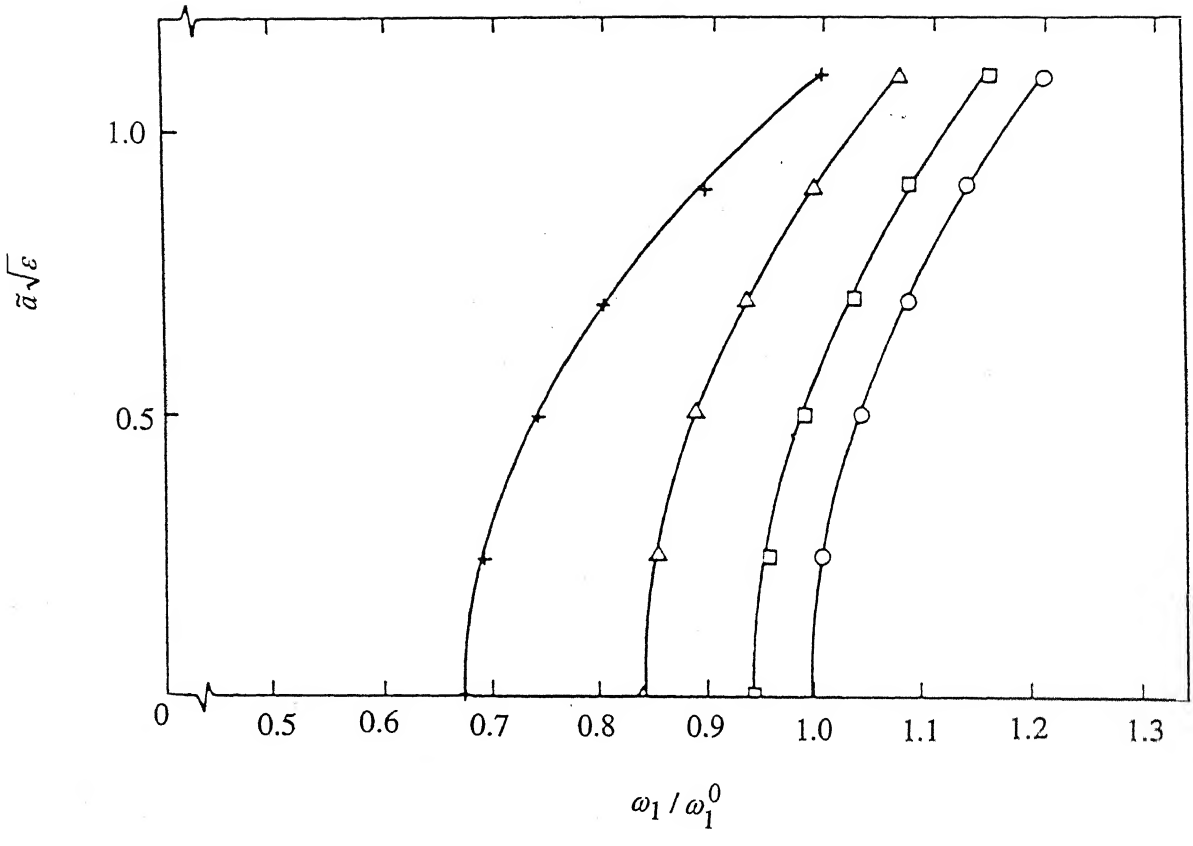

Figure 4.1: Amplitude dependence of first non-linear natural frequency : $T_0 = 1.0$. $\circ$ $c = 0$, $\square$: $c = 0.3(c_{cr})_1$, $\triangle$: $c = 0.5(c_{cr})_1$, $\times$: $c = 0.7(c_{cr})_1$.

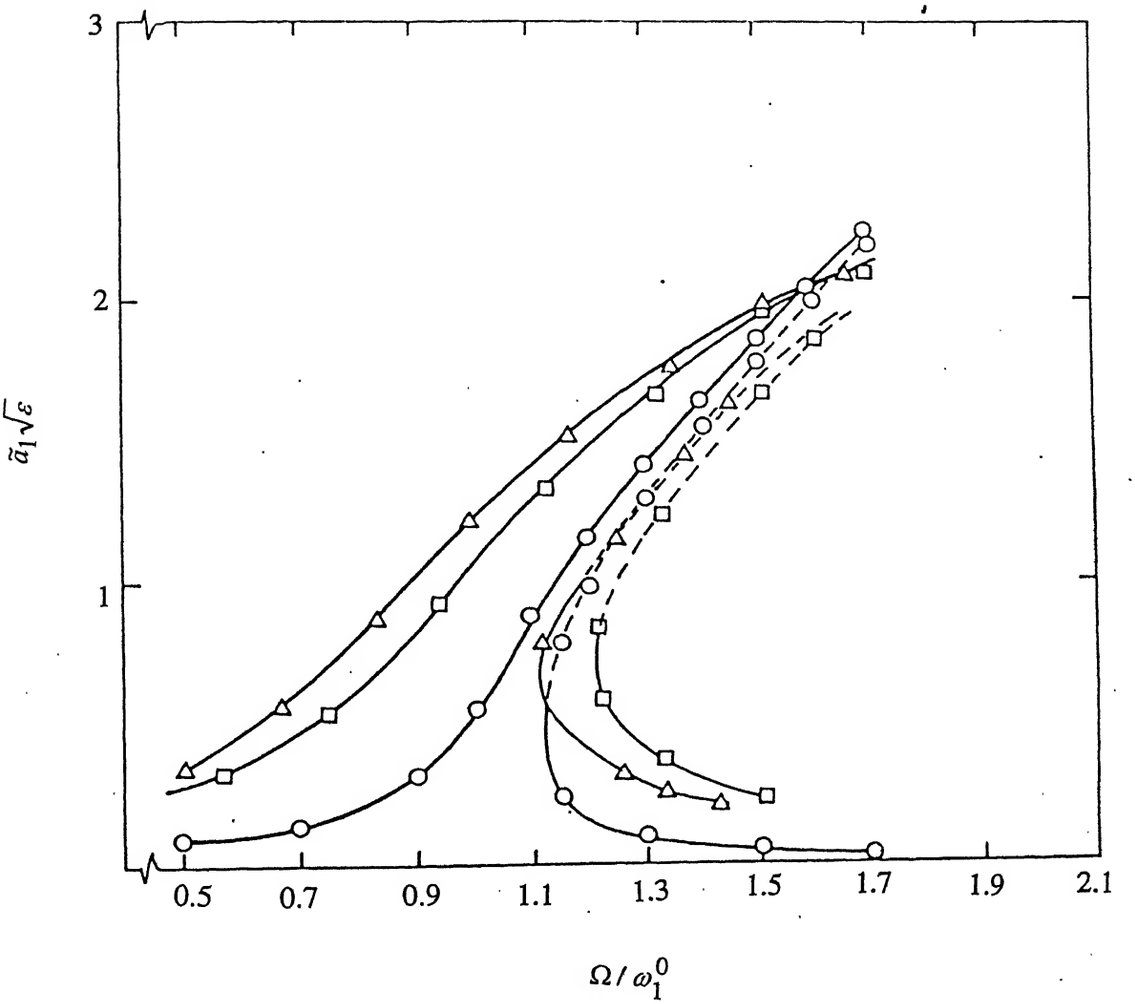

Figure 4.2: Variation of A (equation (4.35)) with forcing frequency when first linear normal mode of a travelling beam is resonantly excited. $T_0 = 1.0$. $\circ$: $c = 0$, $\square$: $c = 0.3(c_{cr})_1$, $\triangle$: $c = 0.5(c_{cr})_1$.

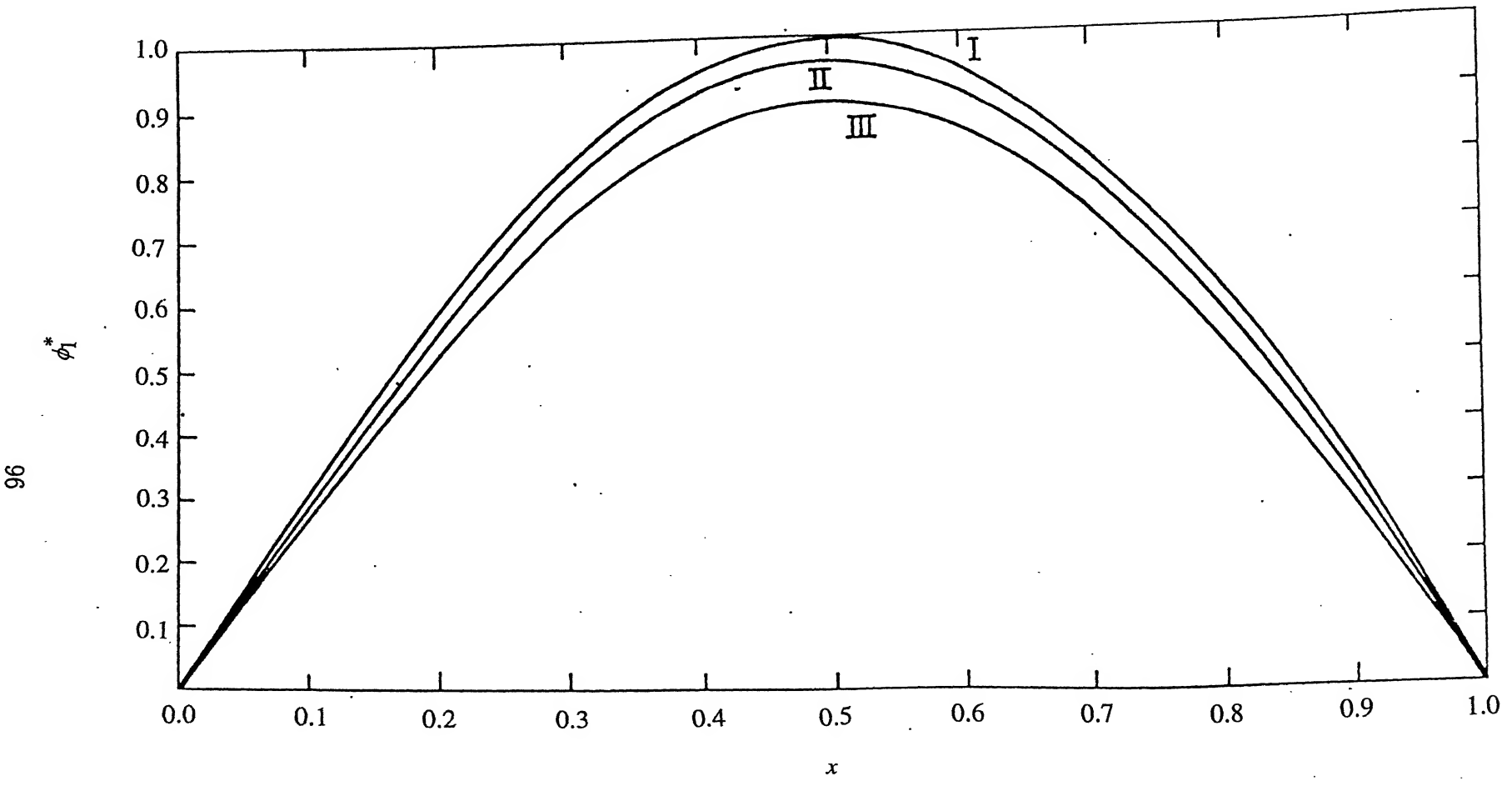

Figure 4.3: Shape of response envelope of a travelling beam when the first linear mode is resonantly excited : $T_0 = 1.0$. I : $c = 0$, II : $c = 0.3(c_{cr})_1$, III : $c = 0.5(c_{cr})_1$.

different instants of time. Hence, Figures 4.2 and 4.3 are to be used together to obtain the response envelope for different travelling speeds and excitation frequencies.

The results of the stability analysis of the steady-state harmonic solution, presented in Section 4.3.1, is shown in Figure 4.4. The frequency response curves for a beam having $c = 0.5(c_{cr})_1$ and $F_0\sqrt{\epsilon} = 12$ and 53 are plotted. The intermediate branches of both the plots, shown by the broken lines, refer to unstable solutions. As explained in Section 4.3.1, the region between the curves, represented by equations (4.54) and (4.55), refers to unstable solutions. These boundary curves are shown by chain lines. The upper boundary of the unstable region, shown in Figure 4.4, represents the backbone curve. The other curve is the locus of the points of vertical tangencies of the frequency response curves.

4.4 Response to Non-Resonant Hard Excitation

In this section, the non-linear stady-state periodic response of the beam subjected to a non-resonant hard excitation is analysed. As the frequency of excitation is away from any of the linear natural frequencies or combinations thereof, various linear modes are excited. Consequently, the modal analysis is not convenient for obtaining the response. In such a situation, the transfer function of the beam, derived in Chapter 2, can be used with great advantage. Since the linear response in the present method, contrary to the modal analysis, is obtained in a closed form, the analysis becomes simplified. Also the error encountered in the modal analysis due to neglecting the higher order modes is avoided.

Let the excitation be of the form $f(x,\tau) = F_0\delta(x - x_0)\cos\Omega\tau$, with F_0 sufficiently large so as to render the effects of the non-linear term in equation (2.15) to become significant, even if the excitation frequency Ω is away from any of the natural frequencies

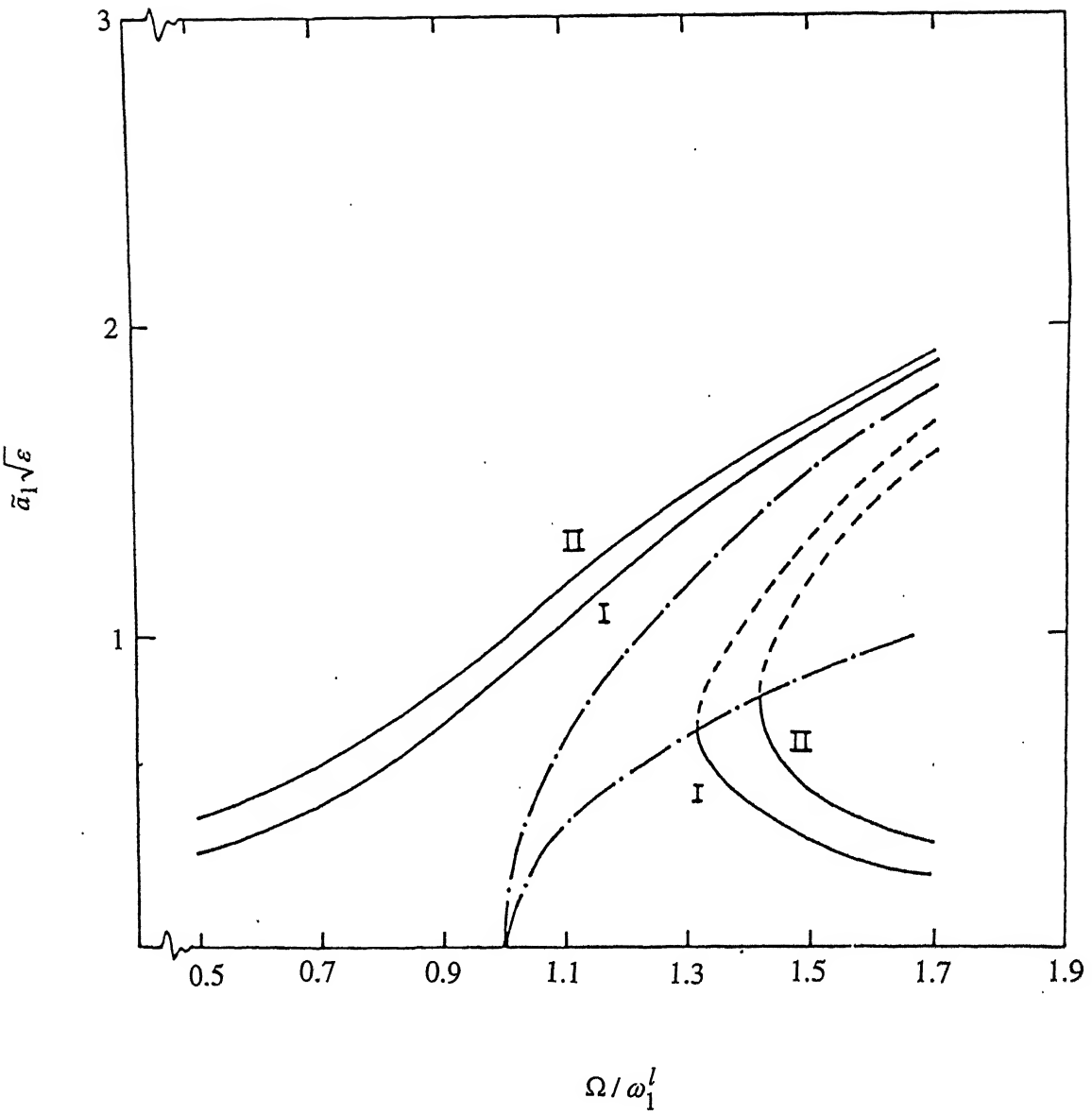

Figure 4.4: Primary unstable region in the frequency-response diagram of a resonantly excited non-linear travelling beam. $T_0 = 1.0$, $c = 0.5(c_{cr})_1$. I : $F_0\sqrt{\epsilon} = 12$, II : $F_0\sqrt{\epsilon} = 53$. —— : stable solutions, – – – : unstable solutions.

or their combinations. The response of $w(x,\tau)$ is sought in the following series form :

$$w(x,\tau) = w_0(x,\tau) + \epsilon w_1(x,\tau) + \cdots. \tag{4.56}$$

It may be pointed out that the above series is valid only for Ω away from any linear natural frequency, ω_n^l. When $\Omega \approx \omega_n^l$, the series diverges.

Substituting equation (4.56) into equation (2.15) and equating the coefficients of the like powers of ϵ from both the sides, the following results are obtained :

$$\epsilon^0 : \quad \frac{\partial^2 w_0}{\partial \tau^2} + 2c\frac{\partial^2 w_0}{\partial x \partial \tau} + (c^2 - T_0)\frac{\partial^2 w_0}{\partial x^2} + \frac{\partial^4 w_0}{\partial x^4} = f(x)\cos\Omega\tau \tag{4.57}$$

$$\epsilon^1 : \quad \frac{\partial^2 w_1}{\partial \tau^2} + 2c\frac{\partial^2 w_1}{\partial x \partial \tau} + (c^2 - T_0)\frac{\partial^2 w_1}{\partial x^2} + \frac{\partial^4 w_1}{\partial x^4} = \left[\int_0^1 (\frac{\partial w_0}{\partial x})^2 \,\mathrm{d}x\right]\frac{\partial^2 w_0}{\partial x^2}. \tag{4.58}$$

Following the procedure outlined in Section 2.4.2, equation (4.57) is solved to yield

$$w_0(x,\tau) = \frac{e^{i\Omega\tau}}{2}\int_0^1 G(x,\ \zeta,\ i\Omega)f(\zeta)\mathrm{d}\zeta + \frac{e^{-i\Omega\tau}}{2}\int_0^1 G(x,\ \zeta,\ -i\Omega)f(\zeta)\mathrm{d}\zeta \tag{4.59}$$

or

$$w_0(x,\tau) = \frac{H(x,\ i\Omega)}{2}e^{i\Omega\tau} + \frac{H(x,\ -i\Omega)}{2}e^{-i\Omega\tau}, \tag{4.60}$$

where

$$H(x,\ i\Omega) = \int_0^1 G(x,\ \zeta,\ i\Omega)f(\zeta)\mathrm{d}\zeta.$$

Solution of equation (4.58) can be obtained by writing the right hand side of the same equation as follows :

$$\left[\int_0^1 (\frac{\partial w_0}{\partial x})^2 \,\mathrm{d}x\right]\frac{\partial^2 w_0}{\partial x^2} = \left[M_1(x)e^{i\Omega\tau} + M_2 e^{3i\Omega\tau}\right] + c.c. \tag{4.61}$$

where

$$M_1(x) = \frac{1}{8}\left[\int_0^1 \left(\frac{\partial H(x,\ i\Omega)}{\partial x}\right)^2 \mathrm{d}x\right]\frac{\partial^2 H(x,\ -i\Omega)}{\partial x^2} + \frac{1}{4}\left[\int_0^1 \frac{\partial H(x,\ i\Omega)}{\partial x}\frac{\partial H(x,\ -i\Omega)}{\partial x}\,\mathrm{d}x\right]$$
$$\times\frac{\partial^2 H(x,\ i\Omega)}{\partial x^2}$$

and

$$M_2(x) = \frac{1}{8}\left[\int_0^1 \left(\frac{\partial H(x,\, i\Omega)}{\partial x}\right)^2 \mathrm{d}x\right] \frac{\partial^2 H(x,\, i\Omega)}{\partial x^2}.$$

With the help of equation (4.61), $w_1(x,\tau)$ is obtained as :

$$w_1(x,\tau) = e^{i\Omega\tau}\int_0^1 G(x,\, \zeta,\, i\Omega)M_1(\zeta)\mathrm{d}\zeta + e^{3i\Omega\tau}\int_0^1 G(x,\, \zeta,\, 3i\Omega)M_2(\zeta)\mathrm{d}\zeta + c.c.. \quad (4.62)$$

Substituting equations (4.60) and (4.62) in equation (4.56), the response of a non-linear beam, up to the term $o(\epsilon)$, is obtained. Further simplification can be obtained if the force is assumed to be a point harmonic one i.e., $f(x) = F_0\delta(x - x_0)$. In that case

$$H(x, i\Omega) = F_0\, G(x,\, x_0,\, i\Omega),$$

and the values of $M_1(x)$ and $M_2(x)$ are evaluated by numerically computing a few definite integrals.

4.4.1 Numerical Results and Discussion

The non-linear response of a beam subjected to a point harmonic excitation is presented in this section. The axial speed, initial tension, amplitude of excitation and the small parameter ϵ are taken as follows :

$$c' = 0.5,\;\; T_0 = 1.0,\;\; F_0 = 1000,\;\; \epsilon = 10^{-2}.$$

The Fourier transform of the response at the point $x = 0.75$ to a non-resonant hard excitation applied at $x_0 = 0.3$ is shown in Figure 4.5. The response has both harmonic and superharmonic components. Figure 4.6 shows the variations of harmonic components ($w_\Omega(x,\tau)$, say) of the response amplitudes, measured at two different locations ($x = 0.5$ and $x = 0.75$) of the beam, to a point excitation having Ω away from both ω_1^l (=8.72855) and ω_2^l (=38.85552). It is seen that the effect of the non-linearity is more

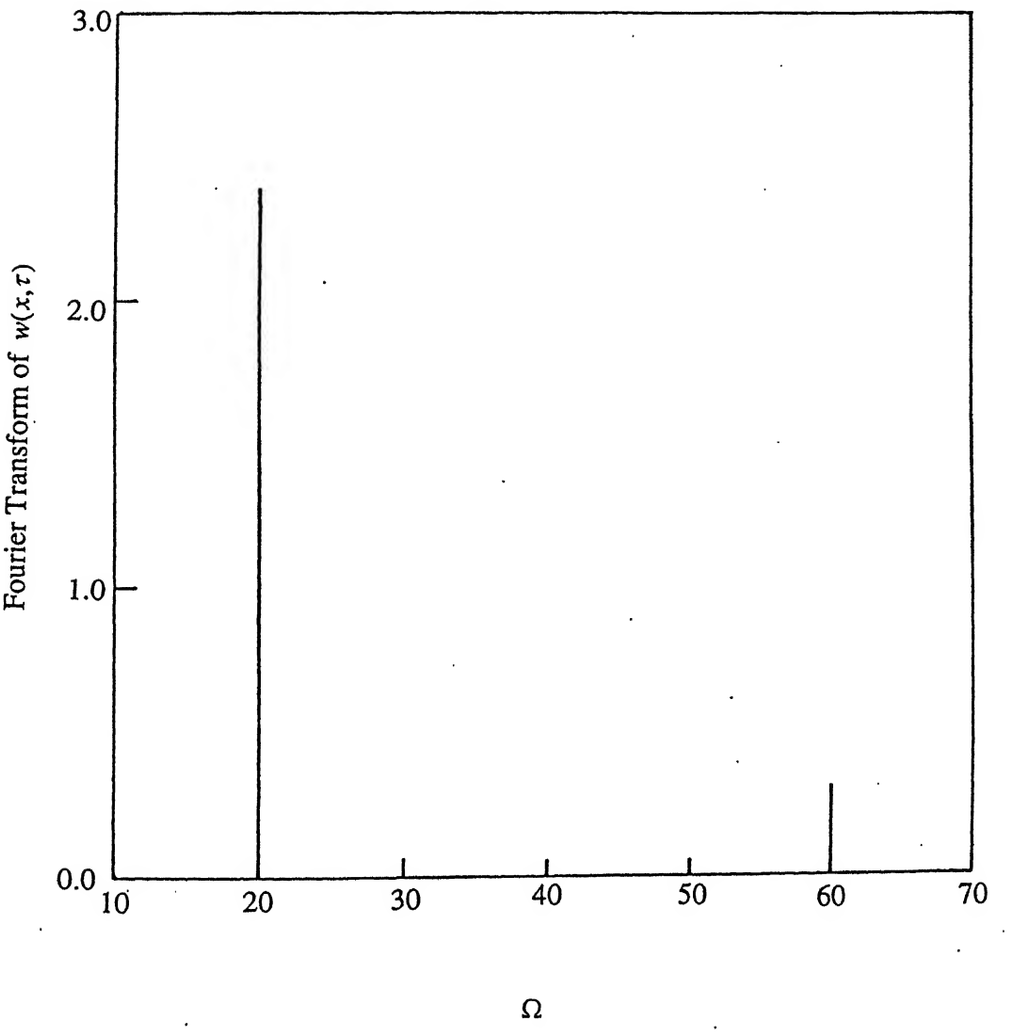

Figure 4.5: Fourier transform of the non-linear response at $x = 0.75$. $F_0 = 1000$, $c' = 0.5$, $\epsilon = 0.01$, $\Omega = 20$, $x_0 = 0.3$.

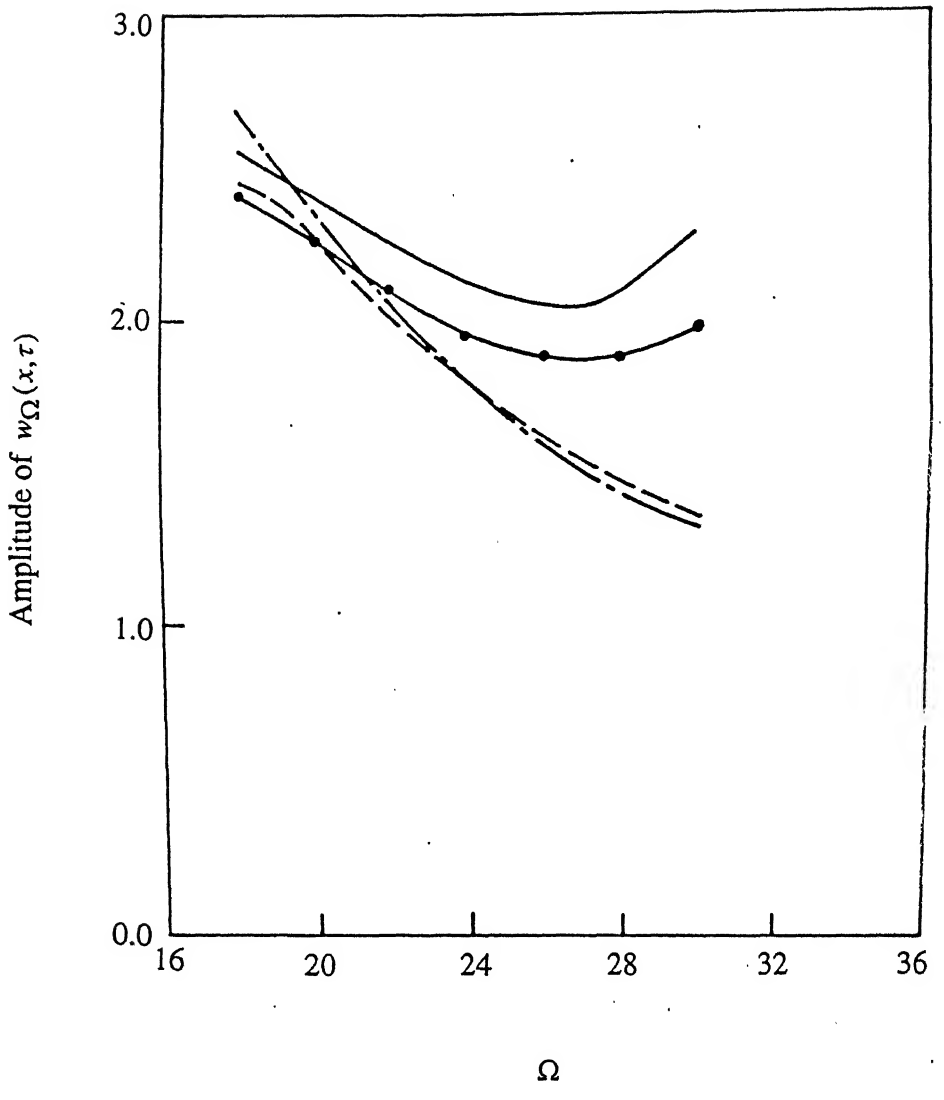

Figure 4.6: Variation of the harmonic components of responses to point harmonic excitation. $F_0 = 1000$, $c' = 0.5$, $\epsilon = 0.01$, $x_0 = 0.3$: —— : non-linear response measured at $x = 0.75$; —•— : linear response measured at $x = 0.75$; – – – : non-linear response measured at $x = 0.5$; — · — : linear response measured at $x = 0.5$.

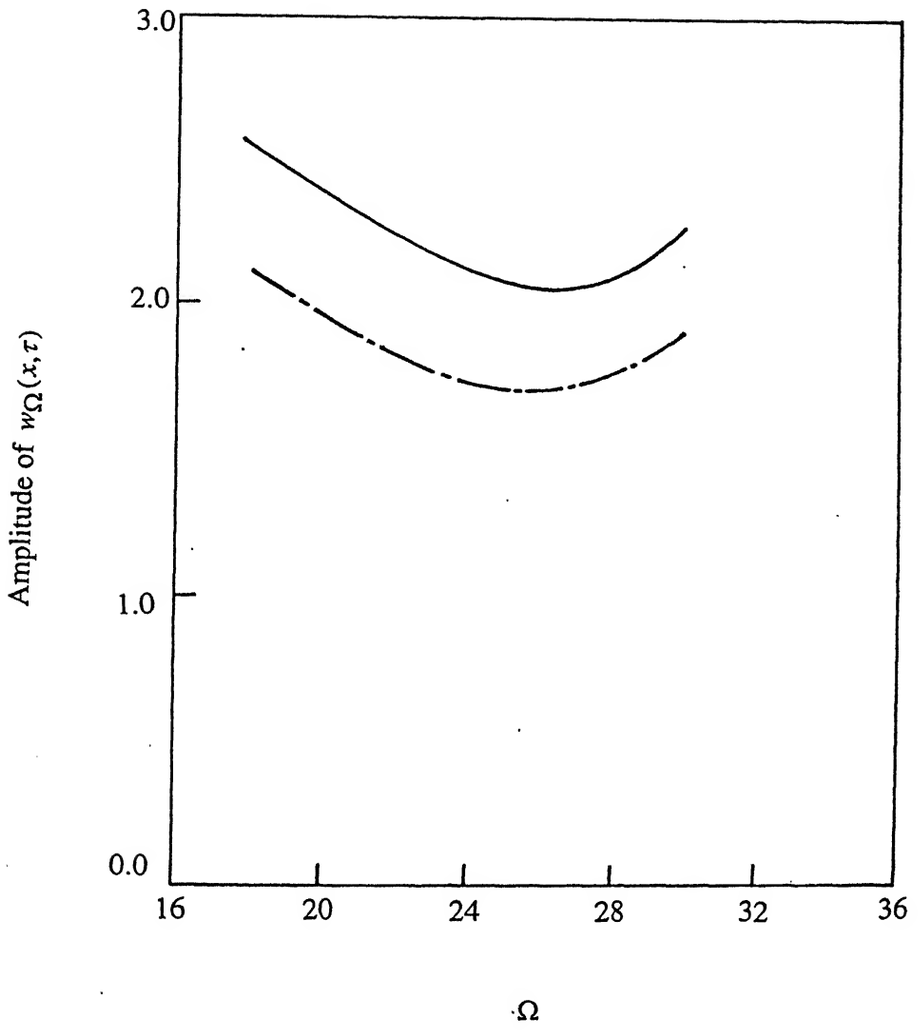

Figure 4.7: Variation of the harmonic components of non-linear responses to point harmonic excitation measured at $x = 0.75$. $F_0 = 1000$, $c' = 0.5$, $\epsilon = 0.01$, $x_0 = 0.3$. —— : wave propagation method; — · — : Galerkin's technique.

pronounced at $x = 0.75$, since the participation of the second mode is stronger for that location.

As discussed earlier, the non-linear response can be obtained by either the wave-propagation method or the Galerkin's technique. Figure 4.7 shows the amplitude of the harmonic component of the response calculated by these two methods. The discrepancy between the results obtained by these two methods is seen to be more than that for a linear beam. This is perhaps due to the coupling between various linear modes in the presence of non-linearity.

Chapter 5

PARAMETRICALLY EXCITED TRAVELLING BEAM WITH AND WITHOUT EXTERNAL FORCING

5.1 Introduction

In the last chapter, the effects of the non-linear term on the forced response of a travelling beam were analysed. In this chapter, another form of excitation, namely, the parametric excitation, is considered.

The axial movement of a travelling beam is normally sustained by rotating pulleys which are either rigidly or flexibly mounted upon the foundation. Normally, a finite pulley-support compliance in the axial direction provides a stabilizing effect to the buckling or divergence instability that occurs in the super-critical speed regime. However, the presence of any rotating unbalance in the flexibly mounted pulleys may

cause parametric excitation, which in turn causes instability in an otherwise stable system. As discussed in Chapter 1, there may be other causes of parametric excitations in various travelling slender members.

Non-linearities have long been recognized to play a significant role in the parametrically excited Duffing oscillator [145]. Whereas the linear analysis predicts an exponential growth of the amplitude of such an oscillator for a range of excitation amplitudes and frequencies, the non-linear terms limit the response to a finite amplitude in the steady-state. These solutions are referred to as 'limit cycles' in the literature. The existence of limit cycles in a travelling string has already been mentioned in Chapter 1.

The response of a Duffing oscillator to simultaneous external and parametric excitations [147, 148] is normally aperiodic. But if the frequency of the two forms of excitation are synchronized, a steady-state harmonic solution is obtained. Superharmonics and subharmonics may also result if some special relationships exist between the frequencies of the two forms of excitation.

After deriving the relevant equations of motion in Section 5.2, the primary resonance of a travelling beam under only parametric excitation including the non-linear effects is presented in Section 5.3. To this end, the concept of non-linear complex normal modes, explained in the previous chapter, has been used. The limit-cycle amplitudes and their stabilities have been given special attention. The excitation of other linear modes besides the primarily excited one has been clearly brought out. Numerical solutions are presented to show the effects of different system parameters (like band-speed, pulley compliance etc.) on the limit-cycle amplitudes. In Section 5.4, the non-linear complex normal modes are again used to obtain the steady-state harmonic response of the beam when both forms of excitation, namely parametric and external harmonic, are simultaneously active.

5.2 Equation of Motion

Consider a travelling slender beam, driven like a belt-pulley system as shown in Figure 5.1. The finite pulley compliance is modelled by a linear spring having stiffness k_p^*. Under the usual assumption $u^* = O(w^*)^2$, the equations of motion for undamped planar vibration including the non-linear terms are:

$$\rho A\left[\frac{\partial^2 u^*}{\partial t^2} + 2c^*\frac{\partial^2 u^*}{\partial \xi \partial t} + c^{*2}\frac{\partial^2 u^*}{\partial \xi^2}\right] - EA\frac{\partial^2 u^*}{\partial \xi^2} = (EA - T^*)\frac{\partial w^*}{\partial \xi}\frac{\partial^2 w^*}{\partial \xi^2} \tag{5.1}$$

and

$$\rho A\left[\frac{\partial^2 w^*}{\partial t^2} + 2c^*\frac{\partial^2 w^*}{\partial \xi \partial t} + c^{*2}\frac{\partial^2 w^*}{\partial \xi^2}\right] - T^*\frac{\partial^2 w^*}{\partial \xi^2} + EI_z\frac{\partial^4 w^*}{\partial \xi^4}$$
$$= (EA - T^*)\frac{\partial}{\partial \xi}\left[\frac{\partial u^*}{\partial \xi}\frac{\partial w^*}{\partial \xi} + \frac{1}{2}\left(\frac{\partial w^*}{\partial \xi}\right)^3\right], \tag{5.2}$$

where T^* is the equilibrium tension in the beam and the other symbols used in equations (5.1) and (5.2) are explained in Chapter 2. The equilibrium tension T^* and the initial tension T_0^* are related as [37]

$$T^* = T_0^* + \eta \rho A c^{*2}, \tag{5.3}$$

where

$$\eta = 1/\left(1 + \frac{k_p^* l}{2AE}\right) \; ; \; 0 \leq \eta \leq 1. \tag{5.4}$$

Neglecting the curvature of the beam beyond the frictionless guides, the boundary conditions can be written as follows:

$$w^*(0,t) = w^*(l,t) = 0, \tag{5.5}$$

$$\frac{\partial^2 w^*(0,t)}{\partial \xi^2} = \frac{\partial^2 w^*(l,t)}{\partial \xi^2} = 0, \tag{5.6}$$

$$u^*(0,t) = 0 \tag{5.7}$$

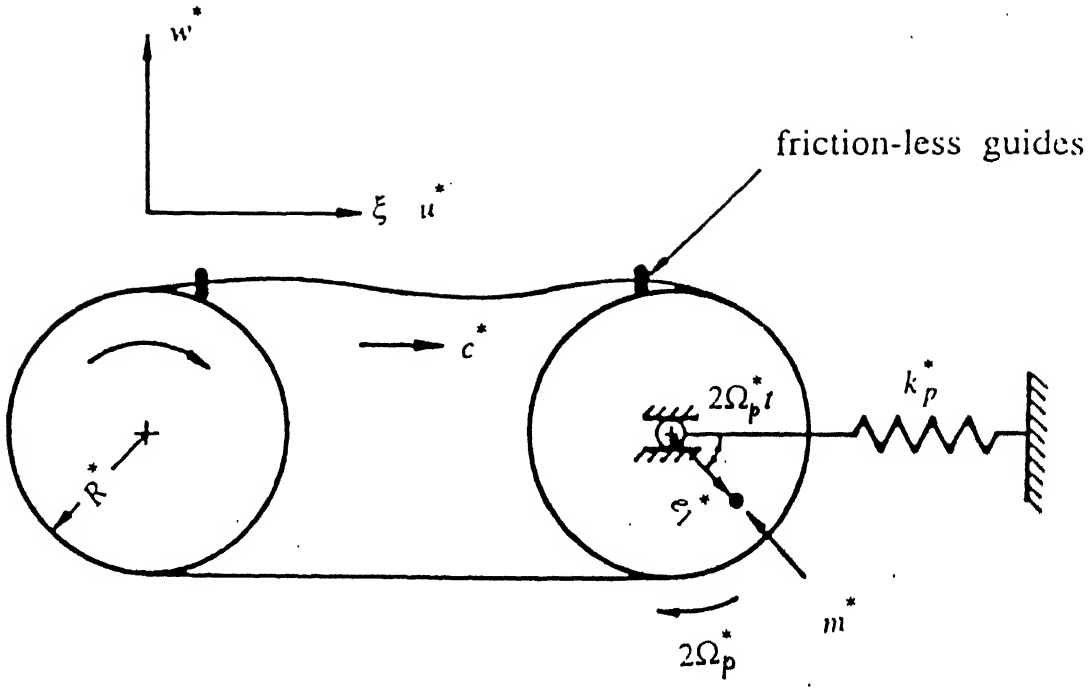

Figure 5.1: Schematic diagram of a travelling beam having parametric excitation.

and

$$\left[\frac{\partial u^*}{\partial \xi}+\frac{1}{2}\left(\frac{\partial w^*}{\partial \xi}\right)^2\right]_{\xi=l} EA+\frac{k_p^*}{2}u^*(l,t)=2m^*\Omega_p^{*^2}e_1^*\cos 2\Omega_p^* t, \tag{5.8}$$

where $m^*e_1^*$ is the unbalance of the pulley having a rotational speed $2\Omega_p^*$. Equation (5.8) is obtained by balancing the horizontal forces at the elastically mounted pulley.

Attention may be drawn to the fact that in the absence of any frictionless guide, the dynamics of the two spans of the beam/wheel system are coupled [43, 44, 46, 47] owing to the finite curvature at the beam-wheel interface. The coupling becomes less significant with increasing wheel radius and/or static tension and also with decreasing flexural rigidity of the beam. It is well known that the static deformation becomes significant at an axial speed close to the critical value. However, this deformation is reduced by incorporating the frictionless guides. Consequently, the simply-supported boundary conditions for the transverse vibration can now be used without much error.

The non-dimensional parameters used subsequently are given below:

$$u=\frac{u^*}{l},\ \gamma=\frac{r}{l},\ w=\frac{w^*}{l\gamma^2},\ x=\frac{\xi}{l},\ \tau=(\frac{E}{\rho})^{1/2}\gamma t/l,\ c=c^*(\frac{E}{\rho})^{-1/2}\frac{1}{\gamma},\ k_p=k_p^*l/(2EA),$$

$$\Omega_p^*t=\Omega_p\tau,\ 2m^*=m/(\rho Al),\ e_1=e_1^*/(\gamma^2 l),\ T_0=T_0^*/(EA\gamma^2),\ R=R^*/l. \tag{5.9}$$

It may be pointed out that the relative magnitudes of non-dimensionalized parameters u and w are now related as $u=O(\gamma^4 w^2)$.

Using equation (5.3) and the non-dimensional parameters, the equations of motion and the boundary conditions are rewritten as

$$\left[\frac{\partial^2 u}{\partial \tau^2}+2c\frac{\partial^2 u}{\partial x\partial \tau}+c^2\frac{\partial^2 u}{\partial x^2}\right]-\frac{1}{\gamma^2}\frac{\partial^2 u}{\partial x^2}=\gamma^2(1-\gamma^2T_0-\gamma^2c^2\eta)\frac{\partial w}{\partial x}\frac{\partial^2 w}{\partial x^2}, \tag{5.10}$$

$$\frac{\partial^2 w}{\partial \tau^2}+2c\frac{\partial^2 w}{\partial x\partial \tau}+(kc^2-T_0)\frac{\partial^2 w}{\partial x^2}+\frac{\partial^4 w}{\partial x^4}=(1-\gamma^2T_0-\gamma^2c^2\eta)\frac{\partial}{\partial \xi}\left[\frac{1}{\gamma^2}\frac{\partial u}{\partial x}\frac{\partial w}{\partial x}+\frac{\gamma^2}{2}\left(\frac{\partial w}{\partial x}\right)^3\right], \tag{5.11}$$

$$w(0,\tau)=w(1,\tau)=0, \tag{5.12}$$

$$\frac{\partial^2 w(0,\tau)}{\partial x^2} = \frac{\partial^2 w(1,\tau)}{\partial x^2} = 0, \tag{5.13}$$

$$u(0,\tau) = 0, \tag{5.14}$$

$$\left[\frac{\partial u}{\partial x} + \frac{\gamma^4}{2}\left(\frac{\partial w}{\partial x}\right)^2\right]_{x=1} + \frac{k_p}{2}u(1,\tau) = \gamma^4 m\Omega_p^2 e_1 \cos 2\Omega_p\tau, \tag{5.15}$$

where $k = 1 - \eta$. It is easy to see from equation (5.4) that $k = 1$ implies a rigidly mounted pulley i.e., $k_p^* \to \infty$. Moreover, from equations (5.4) and (5.9) one notes that k_p and k are related as

$$k_p/(1+k_p) = k \quad \text{and} \quad 1/(1+k_p) = 1 - k. \tag{5.16}$$

Since $\gamma \ll 1$ implies that the speed of the longitudinal waves is much higher than that of the transverse waves, one can neglect the longitudinal inertia term in equation (5.10) to get (neglecting terms of order higher than γ^2)

$$-\frac{1}{\gamma^2}\frac{\partial^2 u}{\partial x^2} = \gamma^2 \frac{\partial w}{\partial x}\frac{\partial^2 w}{\partial x^2}, \tag{5.17}$$

which when integrated twice results in

$$u(x,\tau) = -\frac{\gamma^4}{2}\int_0^x \left(\frac{\partial w}{\partial x_1}\right)^2 dx_1 + xq_1(\tau) + q_2(\tau). \tag{5.18}$$

The integration constants $q_1(\tau)$ and $q_2(\tau)$ are obtained, using boundary conditions (5.14) and (5.15) in equation (5.18), as

$$q_2(\tau) = 0, \tag{5.19}$$

and

$$q_1(\tau) = \left(\frac{k_p}{1+k_p}\right)\frac{\gamma^4}{2}\int_0^1 (\frac{\partial w}{\partial x})^2 dx + \frac{\gamma^4}{(1+k_p)} e_0 \cos 2\Omega_p\tau, \tag{5.20}$$

where $e_0 = m\Omega_p^2 e_1$.

Combining equations (5.11), (5.16), (5.18)-(5.20) and neglecting terms $O(\gamma^4)$, one gets

$$\frac{\partial^2 w}{\partial \tau^2} + 2c\frac{\partial^2 w}{\partial x \partial \tau} + (kc^2 - T_0 - 2\epsilon e_0(1-k)\cos 2\Omega_p\tau)\frac{\partial^2 w}{\partial x^2} + \frac{\partial^4 w}{\partial x^4}$$

$$= k\epsilon \left[\int_0^1 \left(\frac{\partial w}{\partial x} \right)^2 dx \right] \frac{\partial^2 w}{\partial x^2}, \tag{5.21}$$

where $\epsilon (= \gamma^2/2)$ will be treated as the small parameter, since $\epsilon \ll 1$.

The following points are at once observed from equation (5.21):

a) As expected, the spring flexibility makes the system softer.

b) For a rigidly mounted pulley (i.e., $k = 1$), the unbalance has no effect. This is because the unbalance force gets balanced by the reactive force at the pulley-support.

A small viscous damping force $\epsilon\mu(\partial w/\partial \tau)$ is introduced into equation (5.21) which can then be recast in the standard state-space form as

$$\mathbf{A}\frac{\partial W}{\partial \tau} + \mathbf{B}W = \epsilon \mathbf{N_1} + \epsilon \mathbf{N_2}, \tag{5.22}$$

where

$$\mathbf{A} = \begin{bmatrix} I & 0 \\ 0 & K \end{bmatrix}, \ \mathbf{B} = \begin{bmatrix} G & K \\ -K & 0 \end{bmatrix}, \ W = \begin{Bmatrix} \frac{\partial w}{\partial \tau} \\ w \end{Bmatrix},$$

$$\mathbf{N_1} = \left\{ 2e_0(1-k) \cos 2\Omega_p \tau \frac{\partial^2 w}{\partial x^2} - \mu \frac{\partial w}{\partial \tau}, 0 \right\}^T \tag{5.23}$$

and

$$\mathbf{N_2} = \left\{ k \left(\int_0^1 \left(\frac{\partial w}{\partial x} \right)^2 \mathrm{d}x \right) \frac{\partial^2 w}{\partial x^2}, 0 \right\}^T, \tag{5.24}$$

with I as the identity operator, $K \equiv (kc^2 - T_0)\frac{\partial^2}{\partial x^2} + \frac{\partial^4}{\partial x^4}$, $G \equiv 2c\frac{\partial}{\partial x}$.

In the presence of a harmonic excitation, expressed in the non-dimensional form as $f(x) \cos(\Omega_f \tau + \theta_f)$, the equation of motion (5.22) becomes

$$\mathbf{A}\frac{\partial W}{\partial \tau} + \mathbf{B}W = \epsilon \mathbf{N_1} + \epsilon \mathbf{N_2} + \mathbf{f}, \tag{5.25}$$

where

$$\mathbf{f} = \{ f(x) \cos(\Omega_f \tau + \theta_f), \ 0 \}^T. \tag{5.26}$$

5.3 Limit-Cycle Amplitude without External Forcing

Assuming that the amplitude of the solution to equation (5.22) changes slowly with time, one can write the response as

$$W(x,\tau) = \frac{1}{2}\Lambda_p e^{i\Omega_p \tau} + c.c., \tag{5.27}$$

with $\Lambda_p = \left\{ \begin{array}{c} i\Omega_p \lambda_p \\ \lambda_p \end{array} \right\}$ where λ_p is a complex shape function. The abbreviation *c.c.* denotes the complex conjugate of the preceeding term.

Depending upon the relation between Ω_p and the linear natural frequencies (ω_n^l) of the travelling beam, different kinds of parametric excitation may appear. In what follows, only the primary excitation is analysed.

To study the primary resonance, the following condition is first set

$$\Omega_p = \omega_n^l + \epsilon\sigma_n, \tag{5.28}$$

where σ_n is called the detuning parameter. In such a situation, the n-th mode is primarily excited and one can write

$$\Lambda_p = a_n(\tau)\Psi_n + \epsilon\left[\sum_{m\neq n} a_m(\tau)\Psi_m + \sum_{m=1}^{\infty} b_m(\tau)\overline{\Psi}_m\right], \tag{5.29}$$

where Ψ_n denotes the n-th non-linear complex modal vector with corresponding non-linear frequency ω_n. Following the steps outlined in Section 4.2 one can show that ω_n and Ψ_n are given by equations (4.13)-(4.17) with a factor k in $\lambda(\phi_m, \phi_n)$. Further, Ψ_n satisfies the following equation:

$$i\omega_n \frac{a}{2}\mathbf{A}\Psi_n + \frac{a}{2}\mathbf{B}\Psi_n = \epsilon \mathbf{N}_{2\psi}, \tag{5.30}$$

where

$$\mathrm{N}_{2\psi} = \left\{ \frac{ka^2\overline{a}}{8} \left[\left(\int_0^1 \left(\frac{\mathrm{d}\psi_n}{\mathrm{d}x} \right)^2 \mathrm{d}x \right) \frac{\mathrm{d}^2\overline{\psi}_n}{\mathrm{d}x^2} + 2 \left(\int_0^1 \frac{\mathrm{d}\psi_n}{\mathrm{d}x} \frac{\mathrm{d}\overline{\psi}_n}{\mathrm{d}x} \mathrm{d}x \right) \frac{\mathrm{d}^2\psi_n}{\mathrm{d}x^2} \right], 0 \right\}^T . \quad (5.31)$$

For a slowly-varying amplitude

$$\frac{\mathrm{d}a_j(\tau)}{\mathrm{d}\tau} = O(\epsilon) = \epsilon\alpha_j \text{ (say), for } j = 1, 2, \cdots, \quad (5.32)$$

and

$$\frac{\mathrm{d}b_j(\tau)}{\mathrm{d}\tau} = O(\epsilon) = \epsilon\delta_j \text{ (say), for } j = 1, 2, \cdots.$$

Now, equations (5.27), (5.28) and (5.32) are substituted in equation (5.22). Thereafter, equating the coefficients of $e^{i\Omega_p\tau}$ from both sides and neglecting terms $O(\epsilon^2)$, one gets

$$\epsilon\frac{\alpha_n}{2}\mathbf{A}\Phi_n + i\frac{a_n}{2}(\Omega_p - \omega_n)\mathbf{A}\Phi_n + \epsilon \left[\sum_{m\neq n} \frac{a_m}{2}(i\Omega_p\mathbf{A}\Phi_m + \mathbf{B}\Phi_m) \right.$$

$$\left. + \sum_{m=1}^{\infty} \frac{b_m}{2}(i\Omega_p\mathbf{A}\overline{\Phi}_m + \mathbf{B}\overline{\Phi}_m) \right] = \epsilon\mathrm{N}_1{}', \quad (5.33)$$

where

$$\mathrm{N}_1{}' = \left\{ e_0(1-k)\frac{\mathrm{d}^2\overline{\phi}_n}{\mathrm{d}x^2}\frac{\overline{a}_n}{2} - i\Omega_p\mu\phi_n\frac{a_n}{2}, 0 \right\}^T .$$

It is to be noted that while deriving equation (5.33), the fact that $(\Omega - \omega_n)$ is $O(\epsilon)$ (as can be easily seen from equations (5.29) and (4.17)), has been made use of.

Using the orthogonality relations between the linear modes (Φ_n) in equation (5.33), one gets

$$\epsilon\alpha_n + ia_n(\Omega_p - \omega_n) = \frac{2\epsilon\int_0^1 \overline{\Phi}_n^T \mathrm{N}_1{}' \mathrm{d}x}{t_n}, \quad (5.34)$$

where t_n is defined in Section 4.3. For notational simplicity, a_n is replaced by a, and the complex amplitude a is expressed as

$$a = \tilde{a}e^{i\theta}, \quad (5.35)$$

with $\tilde{a}$ as real.

Expanding ω_n as in equation (4.17) and using equations (4.13), (5.28), (5.32), and (5.35) in equation (5.34) and thereafter separating the real and imaginary parts, one gets

$$\frac{\mathrm{d}\tilde{a}}{\mathrm{d}\tau} = -\epsilon e_0^{'}\tilde{a}\left[G^I \cos 2\theta - G^R \sin 2\theta\right] - \epsilon\mu^{'}\tilde{a}, \tag{5.36}$$

and

$$\tilde{a}\frac{\mathrm{d}\theta}{\mathrm{d}\tau} = \epsilon\frac{\tilde{a}^3}{4}\frac{\omega_n^l}{t_n}d_n - \epsilon\tilde{a}\sigma_n + \epsilon e_0^{'}\tilde{a}\left[G^R \cos 2\theta + G^I \sin 2\theta\right], \tag{5.37}$$

where

$$d_n = k\left[\left(\int_0^1 \left(\frac{\mathrm{d}\phi_n}{\mathrm{d}x}\right)^2 \mathrm{d}x\right)\left(\int_0^1 \left(\frac{\mathrm{d}\overline{\phi}_n}{\mathrm{d}x}\right)^2 \mathrm{d}x\right) + 2\left(\int_0^1 \frac{\mathrm{d}\phi_n}{\mathrm{d}x}\frac{\mathrm{d}\overline{\phi}_n}{\mathrm{d}x}\,\mathrm{d}x\right)^2\right],$$

$$G = G^R + iG^I = \int_0^1 \left(\frac{\mathrm{d}\overline{\phi}_n}{\mathrm{d}x}\right)^2 \mathrm{d}x,$$

$$H = \int_0^1 \phi_n\overline{\phi}_n\,\mathrm{d}x,$$

$$e_0^{'} = \frac{e_0\omega_n^l(1-k)}{t_n}$$

and

$$\mu^{'} = \frac{\mu(\omega_n^l)^2 H}{t_n}. \tag{5.38}$$

The steady-state solutions of equation (5.34) correspond to the fixed points of equations (5.36) and (5.37) and are obtained by putting

$$\frac{\mathrm{d}\tilde{a}}{\mathrm{d}\tau} = 0 \quad \text{and} \quad \frac{\mathrm{d}\theta}{\mathrm{d}\tau} = 0 \text{ (if } \tilde{a} \neq 0). \tag{5.39}$$

A ready inspection reveals that $\tilde{a} = 0$ is a fixed point, which is called the 'trivial limit cycle' in the literature [145]. The amplitude ($\tilde{a}$) and the phase angle (θ) of non-trivial limit cycle(s) are obtained from equations (5.36)-(5.39). Thus, one finally obtains

$$\sin(2\theta - \delta) = \frac{\mu^{'}}{e_0^{'}\sqrt{(G^R)^2 + (G^I)^2}}, \tag{5.40}$$

$$\cos(2\theta - \delta) = \frac{1}{e_0'\sqrt{(G^R)^2 + (G^I)^2}} \left[\sigma_n - \frac{\tilde{a}^2}{4}\frac{\omega_n^l}{t_n} d_n\right], \tag{5.41}$$

with

$$\delta = \arctan\left(\frac{G^I}{G^R}\right).$$

Squaring and adding equations (5.40) and (5.41), one gets

$$(\tilde{a}\sqrt{\epsilon})^2 = \frac{4t_n}{\omega_n^l d_n}\left[\epsilon\sigma_n \pm \sqrt{(\epsilon e_0')^2\left[(G^R)^2 + (G^I)^2\right] - (\epsilon\mu')^2}\right]. \tag{5.42}$$

Remembering that $\tilde{a}^2$ should be positive, it is easy to note the following three possibilities from equation (5.42) :

(a) No non-trivial limit cycle exists :

(i) if

$$e_0' < \frac{\mu'}{\sqrt{(G^R)^2 + (G^I)^2}}, \tag{5.43}$$

(ii) even if condition (5.43) is violated but $\sigma_n < 0$ and

$$|\sigma_n| > \sqrt{e_0'^2(G^R)^2 + (G^I)^2 - \mu'^2}. \tag{5.44}$$

(b) Only one limit cycle exists, if condition (5.43) is violated and

$$|\sigma_n| < \sqrt{e_0'^2(G^R)^2 + (G^I)^2 - \mu'^2}. \tag{5.45}$$

(c) Two limit cycles exist, if both conditions (5.43) and (5.45) are violated for $\sigma_n > 0$.

It must be emphasized that even if a non-trivial limit cycle exists, it may not be stable. The analysis detailed below is then required to confirm the stability of the limit cycle.

5.3.1 Stability Analysis of Limit Cycles

The stability of the limit cycle(s), obtained in Section 5.3, is determined by linearizing equation (5.34) about the fixed points of $\tilde{a}$ and θ. Since for the trivial limit cycle

($\tilde{a} = 0$) no unique phase angle (θ) exists, the linear part of equation (5.34) is anlysed rather than using equations (5.36) and (5.37). However, for non-trivial limit cycles, linearization of equations (5.36) and (5.37) are carried out around $\tilde{a}$ and θ, given by equations (5.40) and (5.41). In what follows, first the stability of the trivial limit cycle and then that of the non-trivial one are discussed.

(1) TRIVIAL LIMIT CYCLE.

Expand a as

$$a = a_x + ia_y\,. \tag{5.46}$$

Now, equation (5.46) is substituted in equation (5.34) and Ψ_n is expanded as equation (4.16). Thereafter, neglecting the non-linear terms and equating the real and imaginary parts separately from both sides, one gets

$$\frac{\mathrm{d}}{\mathrm{d}\tau}\begin{Bmatrix} a_x \\ a_y \end{Bmatrix} = \epsilon \begin{bmatrix} (C-D) & (E-F) \\ -(E+F) & -(C+D) \end{bmatrix} \begin{Bmatrix} a_x \\ a_y \end{Bmatrix}, \tag{5.47}$$

where $C = e_0' G^I$, $D = \mu'$, $E = \sigma_n$, $F = e_0' G^R$.

The eigenvalues of the coefficient matrix are then given by

$$s_{1,2} = -D \pm \sqrt{D^2 + [(C^2 - D^2) - (E^2 - F^2)]}\,,$$

which implies that the trivial limit cycle is unstable if

$$\sigma_n^2 < \left[e_0'^2 \left((G^I)^2 + (G^R)^2\right) - \mu'^2\right]. \tag{5.48}$$

Comparing condition (5.48) with conditions (5.43)-(5.45), it is inferred that the trivial limit cycle is stable, if this is the only limit cycle or if two more non-trivial limit cycles exist. However, the trivial limit cycle is unstable, if there exists only one more non-trivial limit cycle.

(2) NON-TRIVIAL LIMIT CYCLE.

To ascertain the stability of the non-trivial limit cycles, one perturbs the amplitude

($\tilde{a}$) and phase (θ) in equations (5.36) and (5.37) in the form

$$\tilde{a}_p = \tilde{a} + \eta_p \tag{5.49}$$

and

$$\theta_p = \theta + \zeta_p \,. \tag{5.50}$$

Substituting equations (5.49) and (5.50) into equations (5.36) and (5.37) and using equations (5.40)-(5.42), the following results are obtained (after linearization) :

$$\frac{\mathrm{d}}{\mathrm{d}\tau}\begin{Bmatrix} \eta_p \\ \zeta_p \end{Bmatrix} = \epsilon \begin{bmatrix} 0 & 2e_0'\tilde{a}\sqrt{(G^R)^2+(G^I)^2}\cos(2\theta-\delta) \\ \frac{1}{2}\frac{\omega_n^l d_n}{t_n}\tilde{a} & -2\mu' \end{bmatrix} \begin{Bmatrix} \eta_p \\ \zeta_p \end{Bmatrix}. \tag{5.51}$$

The eigenvalues of the coefficient matrix of equation (5.51) are

$$s_{1,2} = -\mu' \pm \sqrt{\mu'^2 + e_0'\frac{\omega_n^l d_n}{t_n}\tilde{a}^2\left[(G^R)^2+(G^I)^2\right]^{\frac{1}{2}}\cos(2\theta-\delta)}\,. \tag{5.52}$$

From equation (5.52) one can show that the limit cycle is stable if $\cos(2\theta-\delta) < 0$. From equations (5.40) and (5.41) and conditions (5.43)-(5.45) the following conclusions are apparent:

(i) When two non-trivial limit cycles exist, the value of $\cos(2\theta-\delta)$ is negative for the limit cycle with the larger amplitude and positive for the one with the smaller amplitude. Hence the limit cycle with the larger amplitude is stable and the other one unstable.

(ii) When a single non-trivial limit cycle exists, it is always stable because the value of $\cos(2\theta-\delta)$ associated with it is negative.

5.3.2 Numerical Results and Discussion

Numerical results are presented to show the effects of various system parameters on the steady-state solution, i.e., the amplitude of the limit cycle. All the results have been

obtained with $T_0 = 1$. In what follows, the effects of only those parameters which can be independently controlled have been studied. These parameters are defined below :

(i) The axial speed of the beam, expressed as a speed parameter $c' = c/(c_{cr})_1$ where $(c_{cr})_1 = \sqrt{T_0 + \pi^2}$. It may be noted that c' varies linearly with both Ω_p and R, as $c' = 2\Omega_p R/\sqrt{T_0 + \pi^2}$.

(ii) The stiffness of the flexible pulley-support designated by the non-dimensional parameter k.

(iii) The amount of unbalance me_1, generating the parametric excitation, expressed by the non-dimensional parameter ϵe_0.

(iv) The external damping parameter $\epsilon\mu$.

For the primary parametric excitation, Ω_p should be in the neighbourhood of ω_n^l, which in turn depends on various system parameters, like c' and k. The results are, therefore, obtained for the ranges of values of c' and k, that yield $\omega_n^l \simeq \Omega_p$. Further, results are presented for $n = 1$, i.e., when the first mode is primarily excited through the parametric excitation.

Figure 5.2 shows the variation of the limit-cycle amplitudes with the axial speed for two different values of ϵe_0. It is indicated, as discussed in Section 5.3.1, that when two limit cycles exist, the trivial one is unstable. On the other hand, when three limit cycles exist, the trivial one and the one with the highest amplitude are stable. The amplitudes of the non-trivial and stable limit cycles are seen to increase with increasing axial speed. Moreover, if three limit cycles exist, then a jump phenomenon with decreasing axial speed occurs, as exhibited in Figure 5.2. This feature has also been exhibited by a parametrically excited Duffing oscillator, as reported in reference [145]. Similar observations were also made by varying the stiffness parameter k.

Figure 5.3 shows the effect of variation of the unbalance parameter ϵe_0 for two different axial speeds. At the lower speed, for which σ_n is negative, only the trivial

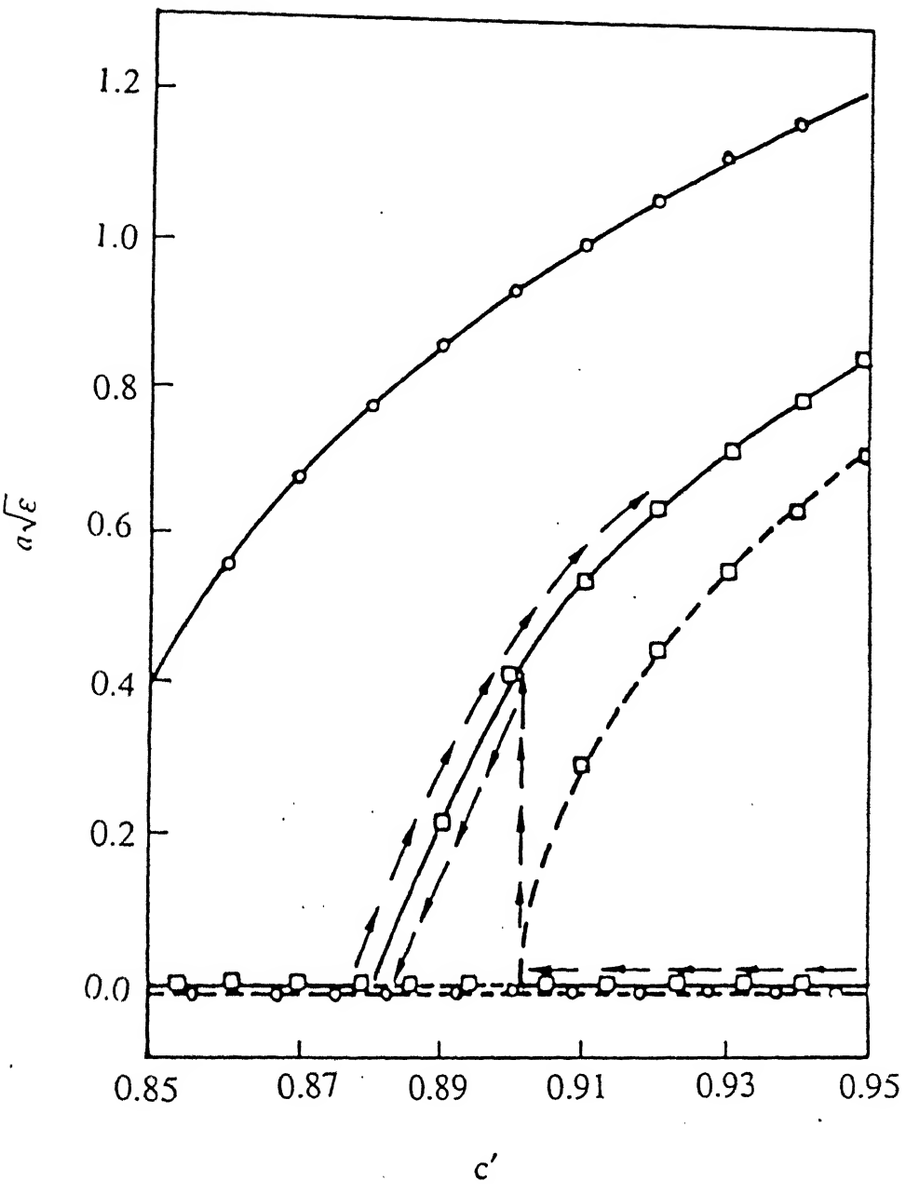

Figure 5.2: Variation of the limit-cycle amplitudes with c'. $R = 0.2$, $k = 0.5$, $\epsilon\mu = 0.0$
$\circ$:$\epsilon e_0 = 0.8$, $\square$:$\epsilon e_0 = 0.1$;—— stable, - - - - unstable.

limit cycle exists for low values of ϵe_0. With increasing ϵe_0, beyond a critical value, two limit cycles appear. When the axial speed is increased beyond a critical value, σ_n becomes positive. In such a situation, one, two or three limit cycles may exist depending on the value of ϵe_0. At such high speeds, the possibility of a two-way jump phenomenon, as ϵe_0 changes, is clearly indicated in Figure 5.3.

Figure 5.4 shows the effect of the external damping parameter at three different axial speeds. It may be noted, that with increasing damping, the non-trivial limit cycle vanishes at all speeds. The jump phenomenon is also exhibited as the damping parameter changes. Both one-way and two-way jumps are possible depending on the axial speed.

The effects of the non-linearity on the stability of a parametrically excited axially moving beam are summarized in Figure 5.5. The parameters used in this figure are defined in Sections 5.2 and 5.3. Using equation (5.48) one can draw the curve AB delineating the stable and unstable zones as predicted by the linear analysis, where the zone marked II refers to the unstable zone. When the non-linearities are included, in the zone marked I, the equilibrium position turns out to be stable, whereas in zone II the equilibrium position becomes unstable and a stable limit cycle (with finite amplitude) is approached. However, in the zone marked III, the system approaches either the equilibrium position or a stable limit cycle depending on the initial disturbance.

5.4 Near-Resonance Response with Simultaneous Parametric and Harmonic Excitations

In this section, the response $w(x, \tau)$ is obtained when an external harmonic force is present over and above the parametric excitation. Due to the simultaneous presence of both forms of excitations, the response usually turns out to be aperiodic. It is to be

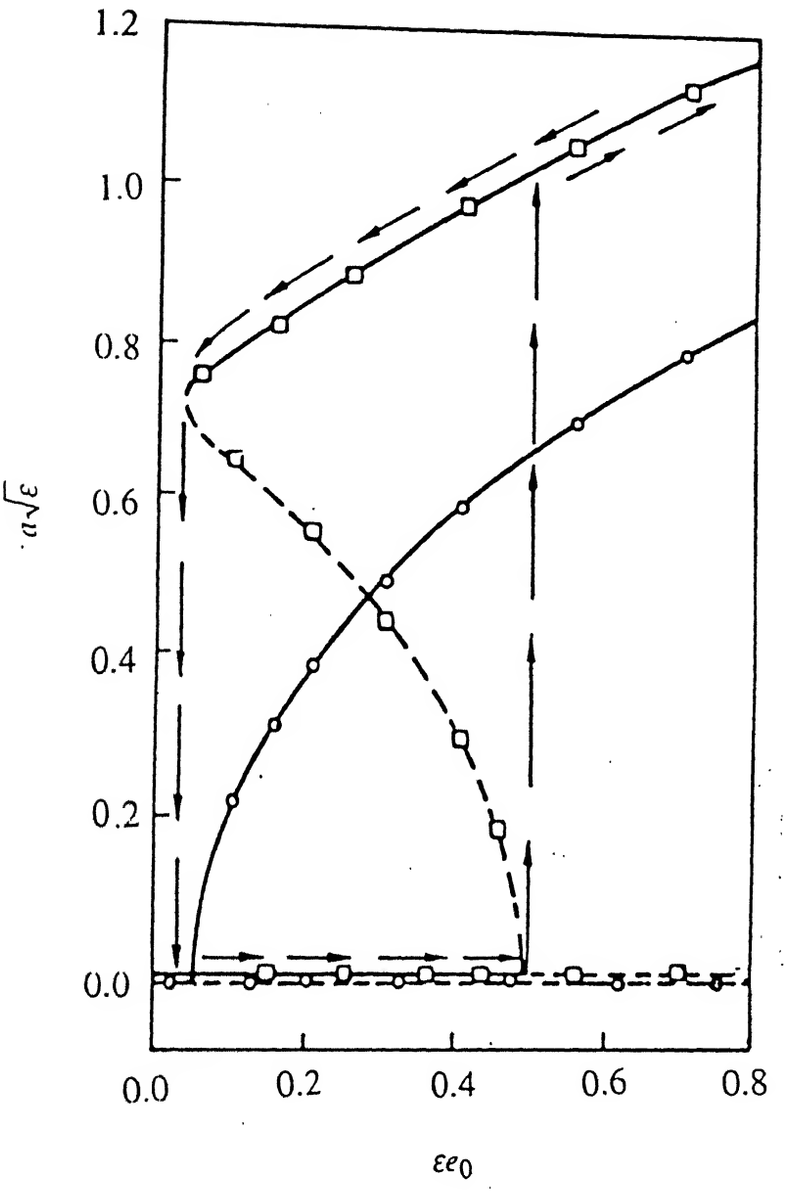

Figure 5.3: Variation of the limit-cycle amplitudes with εe_0. $R = 0.2$, $k = 0.5$, $\epsilon\mu = 0.05$; $\circ$:$c' = 0.89$, $\square$:$c' = 0.94$;—— stable, - - - - unstable.

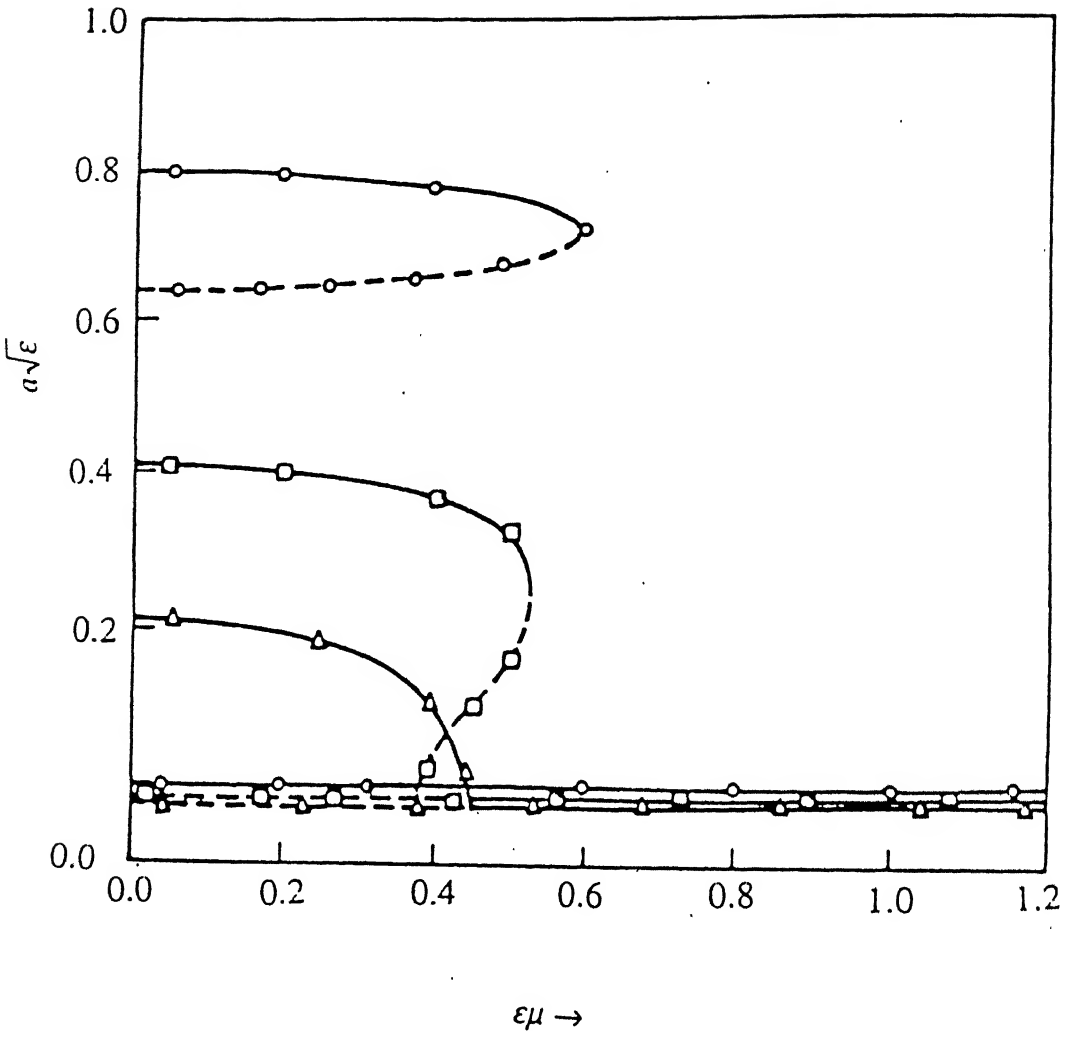

Figure 5.4: Variation of the limit-cycle amplitudes with $\epsilon\mu$. $R = 0.2$, $k = 0.5$, $\epsilon e_0 = 0.1$; $\circ$:$c' = 0.94$, $\square$:$c' = 0.90$, $\triangle$:$c' = 0.89$; —— stable, - - - - unstable.

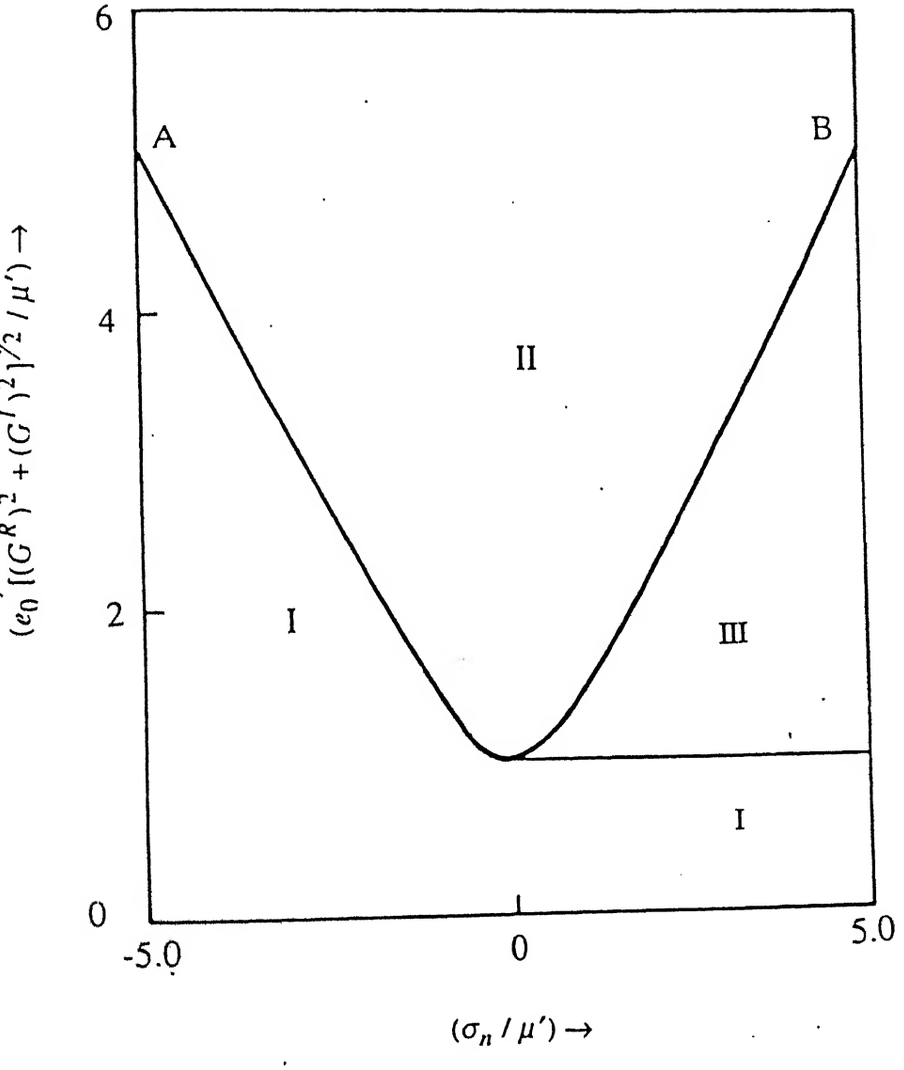

Figure 5.5: Stability boundaries of the parametrically excited system as predicted by the linear analysis.

noted that different combinations of frequencies of parametric and harmonic excitations are possible. These, in turn, may give rise to various complex patterns of the response. In what follows we shall consider a special case, where the exciting frequency is close to the natural frequency associated with the mode excited by the parametric excitation. Hence, along with equation (5.28) one can also assume that the forcing frequency Ω_f is given by

$$\Omega_f = \omega_n^l + \epsilon\sigma. \tag{5.53}$$

When $\sigma_n \neq \sigma$, the response is almost periodic. In the absence of any parametric excitation, the steady-state response is also harmonic having the same frequency as that of the excitation. But in the presence of a small parametric excitation, the response can be assumed as

$$W(x,\tau) = \sum_{n=1}^{\infty} \frac{a_n(\tau)}{2} \Psi_n e^{i\Omega_f \tau} + c.c. \; . \tag{5.54}$$

In view of equations (5.27) and (5.53), the following assumptions are justified :

$$a_m = O(\epsilon) = \epsilon a_m^{'} \;\; \text{(say), for} \;\; m \neq n, \tag{5.55}$$

and

$$\overline{a}_m = O(\epsilon) = \epsilon \overline{a}_m^{'} \;\; \text{(say), for} \;\; m = 1, 2, 3, \; \cdots, \tag{5.56}$$

with

$$\frac{\mathrm{d}}{\mathrm{d}\tau} a_n(\tau) = O(\epsilon). \tag{5.57}$$

First, equations (5.54)-(5.57) are substituted into equation (5.25) and the harmonics are balanced (i.e., the coefficients of $e^{i\Omega_f \tau}$ and $e^{-i\Omega_f \tau}$ are equated,separately, from both sides of the equation). Then using equations (5.30) and (5.31) and neglecting terms $O(\epsilon^2)$, one gets

$$\frac{1}{2}\frac{\mathrm{d}a_n}{\mathrm{d}\tau} \mathrm{A}\Psi_n + i(\Omega_f - \omega_n)\frac{a_n}{2}\mathrm{A}\Psi_n + \epsilon \left[\sum_{m \neq n} i\frac{a_m^{'}}{2}(\Omega_f - \omega_m^l)\mathrm{A}\Phi_m + \sum_{m=1}^{\infty} i\frac{\overline{a}_m^{'}}{2}(\Omega_f + \omega_m^l)\mathrm{A}\overline{\Phi}_m \right]$$

$$= \epsilon \mathbf{N_f} + \mathbf{f_1}, \tag{5.58}$$

where

$$\mathbf{N_f} = \left\{ e_0(1-k)\frac{\mathrm{d}^2\overline{\phi}_n}{\mathrm{d}x^2} e^{2i\epsilon(\sigma_n-\sigma)\tau}\frac{\overline{a}_n}{2} - i\omega_n^l \mu \phi_n \frac{a_n}{2}, 0 \right\}^T \tag{5.59}$$

and

$$\mathbf{f_1} = \left\{ \frac{f(x)}{2} e^{i\theta_f}, 0 \right\}^T . \tag{5.60}$$

Using equation (5.57) and orthogonality relations between the linear modes (see equations (2.27) and (2.28)) in equation (5.58), and excluding terms $O(\epsilon^2)$, one gets

$$\frac{\mathrm{d}a_n}{\mathrm{d}\tau} + ia_n(\Omega_f - \omega_n) = \frac{2\epsilon}{t_n}\int_0^1 \overline{\Phi}_n^T \mathbf{N_f}\,\mathrm{d}x + \frac{2}{t_n}\int_0^1 \overline{\Psi}_n^T \mathbf{f_1}\,\mathrm{d}x. \tag{5.61}$$

Further, the coefficients a_m' and $\overline{a}_m'$'s can be obtained as,

$$\epsilon a_m' = a_m = \frac{2\int_0^1 \overline{\Phi}_m^T(\mathbf{f_1} + \epsilon \mathbf{N_f})\,\mathrm{d}x}{i(\Omega_f - \omega_m^l)t_m} \quad \text{if } m \neq n, \tag{5.62}$$

and

$$\epsilon \overline{a}_m' = \overline{a}_m = \frac{2\int_0^1 \Phi_m^T(\mathbf{f_1} + \epsilon \mathbf{N_f})\,\mathrm{d}x}{i(\Omega_f + \omega_m^l)t_m} \quad \text{for } m = 1, 2, \cdots. \tag{5.63}$$

Since $\mathbf{N_f}$ contains a term having explicit time dependence, equation (5.61) does not exhibit any periodic solution unless $\sigma_n = \sigma$. Let us consider the special case when $\sigma_n = \sigma$, i.e., the frequencies of the parametric and external excitations are related. In this case, a steady-state solution to equation (5.61) exists. This solution can be obtained as explained below.

Substitution of $\frac{\mathrm{d}a_n}{\mathrm{d}\tau} = 0$ in equation (5.61) yields the complex algebraic equation

$$ia_n(\Omega_f - \omega_n) = \frac{2\epsilon}{t_n}\int_0^1 \overline{\Phi}_n^T \mathbf{N_f}\,\mathrm{d}x + \frac{2}{t_n}\int_0^1 \overline{\Psi}_n^T \mathbf{f_1}\,\mathrm{d}x. \tag{5.64}$$

For solving equation (5.64) to determine a_n, one substitutes $a_n = \tilde{a}_n e^{i\theta_n}$ in the above equation and equate the real and imaginary parts from both sides to obtain

$$\tilde{a}_n(\Omega_f - \omega_n^l - \epsilon \tilde{a}_n^2 S)\cos\theta_n = \epsilon e_0' \tilde{a}_n \left[G^R \cos\theta_n + G^I \sin\theta_n \right]$$

$$-\epsilon\mu'\tilde{a}_n \sin\theta_n + \frac{1}{t_n}\left[Q^R + \epsilon\tilde{a}_n^2 M^R\right] \tag{5.65}$$

and

$$\tilde{a}_n(\Omega_f - \omega_n^l - \epsilon\tilde{a}_n^2 S)\sin\theta_n = \epsilon e_0'\tilde{a}_n\left[G^I\cos\theta_n - G^R\sin\theta_n\right]$$
$$+\epsilon\mu'\tilde{a}_n\cos\theta_n + \frac{1}{t_n}\left[Q^I + \epsilon\tilde{a}_n^2 M^I\right], \tag{5.66}$$

where

$$S = \beta_1^{(n)}/\tilde{a}_n^2,\quad Q = Q^R + iQ^I = -\omega_n^l\int_0^1 \overline{\phi}_n f e^{i\theta_f}\,\mathrm{d}x$$

and

$$M = M^R + iM^I = \left\{-\sum_{m\neq n}\overline{g_m}\omega_m^l\int_0^1\overline{\phi}_m f e^{i\theta_f}\,\mathrm{d}x\right\} + \left\{\sum_{m=1}^{\infty}\overline{h_m}\omega_m^l\int_0^1\phi_m f e^{i\theta_f}\,\mathrm{d}x\right\}.$$

Now eliminating θ_n from equations (5.65) and (5.66) one gets, after some algebraic manipulations, a quintic polynomial in $\tilde{a}_n^2$. This polynomial for a concentrated external force (at $x = x_0$), i.e., when $f(x)$ is written as $F_0\delta(x - x_0)$, is given in Appendix C. For this particular loading, numerical results reveal one, three or five (positive) values of $\tilde{a}_n^2$. However, a subsequent stability analysis only can confirm whether the values so obtained are physically realisable (i.e., stable) or not.

The stability analysis can be carried out using the method outlined in Section 5.3.1. However, an alternative procedure, considering an arbitrary perturbation to the solution, which gives rise to Mathieu type equation, has been carried out.

5.4.1 Stability Analysis of the Steady-State Solution

The stability of the steady-state solution, $w(x,\tau)$ appearing in equation (5.54), is studied by perturbing it in the form

$$w_p(x,\tau) = w(x,\tau) + w_\delta(x,\tau). \tag{5.67}$$

Putting equation (5.67) into equation (5.25) and neglecting terms $O(\epsilon^2)$, one gets

$$\mathbf{A}\frac{\partial W_\delta}{\partial \tau} + \mathbf{B}W_\delta = \epsilon \mathbf{N}_{1\delta} + \epsilon \mathbf{N}_{2\delta}, \tag{5.68}$$

where $W_\delta = \left\{ \begin{array}{c} \frac{\partial w_\delta}{\partial \tau} \\ \\ w_\delta \end{array} \right\}$,

$$\mathbf{N}_{1\delta} = \left\{ 2e_0(1-k)\cos 2\Omega_p \tau \frac{\partial^2 w_\delta}{\partial x^2} - \mu \frac{\partial w_\delta}{\partial \tau}, 0 \right\}^T \tag{5.69}$$

and

$$\mathbf{N}_{2\delta} = \left\{ k \left[\left(\int_0^1 \left(\frac{\partial w}{\partial x} \right)^2 \mathrm{d}x \right) \frac{\partial^2 w_\delta}{\partial x^2} + 2 \left(\int_0^1 \frac{\partial w}{\partial x} \frac{\partial w_\delta}{\partial x} \mathrm{d}x \right) \frac{\partial^2 w}{\partial x^2} \right], 0 \right\}^T . \tag{5.70}$$

To analyse the stability of a_n, when $\Omega_f = \omega_n^l + \epsilon\sigma$, the following perturbation is considered :

$$W_\delta = \Phi_n(x)\xi_n(\tau) + c.c.. \tag{5.71}$$

Substituting the value of $w(x,\tau)$ from equations (5.54)-(5.56) one gets

$$\mathbf{A}\Phi_n \frac{\mathrm{d}\xi_n}{\mathrm{d}\tau} + \mathbf{B}\Phi_n \xi_n + \mathrm{c.c} = \epsilon \mathbf{L}_1 + \epsilon \mathbf{L}_2 + \epsilon \mathbf{L}_3 \frac{\mathrm{d}\xi_n}{\mathrm{d}\tau} + c.c., \tag{5.72}$$

where

$$\mathbf{L}_j = \{ l_j(x,\tau), 0 \}^T, \quad (j = 1,2,3),$$

with

$$\begin{aligned} l_1(x,\tau) &= \frac{k}{4}\tilde{a}_n^2 \left\{ 3 \left(\int_0^1 (\frac{\mathrm{d}\phi_n}{\mathrm{d}x})^2 \mathrm{d}x \right) \frac{\mathrm{d}^2\phi_n}{\mathrm{d}x^2} \right\} e^{2i(\Omega_p\tau + \theta_n)} \\ &+ \frac{k}{4}\tilde{a}_n^2 \left\{ \left(\int_0^1 (\frac{\mathrm{d}\overline{\phi}_n}{\mathrm{d}x})^2 \mathrm{d}x \right) \frac{\mathrm{d}^2\phi_n}{\mathrm{d}x^2} + 2 \left(\int_0^1 \frac{\mathrm{d}\overline{\phi}_n}{\mathrm{d}x} \frac{\mathrm{d}\phi_n}{\mathrm{d}x} \mathrm{d}x \right) \frac{\mathrm{d}^2\overline{\phi}_n}{\mathrm{d}x^2} \right\} e^{-2i(\Omega_p\tau + \theta_n)} \\ &+ \frac{k}{4}\tilde{a}_n^2 \left\{ 2 \left(\int_0^1 (\frac{\mathrm{d}\phi_n}{\mathrm{d}x})^2 \mathrm{d}x \right) \frac{\mathrm{d}^2\overline{\phi}_n}{\mathrm{d}x^2} + 4 \left(\int_0^1 \frac{\mathrm{d}\overline{\phi}_n}{\mathrm{d}x} \frac{\mathrm{d}\phi_n}{\mathrm{d}x} \mathrm{d}x \right) \frac{\mathrm{d}^2\phi_n}{\mathrm{d}x^2} \right\}, \end{aligned}$$

$$l_2(x,\tau) = 2e_0(1-k)\cos 2\Omega_p\tau \frac{\mathrm{d}^2\phi_n}{\mathrm{d}x^2}$$

and

$$l_3(x,\tau) = -\mu\phi_n.$$

Applying the orthogonality relations (i.e., equations (2.27) and (2.28)) one finally gets the following equation and its complex conjugate:

$$\frac{\mathrm{d}\xi_n}{\mathrm{d}\tau} - i\omega_n^l\xi_n = \frac{\epsilon}{t_n}\left(\int_0^1 \overline{\Phi}_n^T(\mathrm{L}_1+\mathrm{L}_2)\,\mathrm{d}x\right)\xi_n + \frac{\epsilon}{t_n}\left(\int_0^1 \overline{\Phi}_n^T\mathrm{L}_3\,\mathrm{d}x\right)\frac{\mathrm{d}\xi_n}{\mathrm{d}\tau}$$

$$+\frac{\epsilon}{t_n}\left(\int_0^1 \overline{\Phi}_n^T(\overline{\mathrm{L}}_1+\overline{\mathrm{L}}_2)\,\mathrm{d}x\right)\overline{\xi}_n + \frac{\epsilon}{t_n}\left(\int_0^1 \overline{\Phi}_n^T\overline{\mathrm{L}}_3\,\mathrm{d}x\right)\frac{\mathrm{d}\overline{\xi}_n}{\mathrm{d}\tau}. \tag{5.73}$$

Assuming $\tau' = \Omega_f\tau + \theta_n$ and $\eta = \frac{\omega_n^l}{\Omega_f}$, equation (5.73) can be written as

$$\Omega_f\left[\frac{\mathrm{d}\xi_n}{\mathrm{d}\tau'} - i\eta\xi_n\right] = \frac{\epsilon}{t_n}\left(\int_0^1 \overline{\Phi}_n^T(\mathrm{L}_1'+\mathrm{L}_2')\,\mathrm{d}x\right)\xi_n + \frac{\epsilon\Omega_f}{t_n}\left(\int_0^1 \overline{\Phi}_n^T\mathrm{L}_3'\,\mathrm{d}x\right)\frac{\mathrm{d}\xi_n}{\mathrm{d}\tau'}$$

$$+\frac{\epsilon}{t_n}\left(\int_0^1 \overline{\Phi}_n^T(\overline{\mathrm{L}}_1'+\overline{\mathrm{L}}_2')\,\mathrm{d}x\right)\overline{\xi}_n + \frac{\epsilon\Omega_f}{t_n}\left(\int_0^1 \overline{\Phi}_n^T\overline{\mathrm{L}}_3'\,\mathrm{d}x\right)\frac{\mathrm{d}\overline{\xi}_n}{\mathrm{d}\tau'}, \tag{5.74}$$

where

$$\mathrm{L}_j' = \{l_j(x,\tau'),0\}^T \quad j = 1,2,3,\cdots.$$

Using equation (5.53), one can write

$$\eta = 1 + \epsilon\eta_1 + \cdots. \tag{5.75}$$

Now, ξ_n is assumed in the following series form:

$$\xi_n = \xi_n^{(0)} + \epsilon\xi_n^{(1)} + \cdots \tag{5.76}$$

Substituting equations (5.75) and (5.76) into equation (5.74) and equating the coefficients of the like powers of ϵ from both sides, one gets:

$$\epsilon^0 : \frac{d\xi_n^{(0)}}{d\tau'} - i\xi_n^{(0)} = 0. \tag{5.77}$$

$$\epsilon^1 : \frac{\mathrm{d}\xi_n^{(1)}}{\mathrm{d}\tau'} - i\xi_n^{(1)} = i\eta_1\xi_n^{(0)} + \frac{1}{\omega_n^l t_n}\left(\int_0^1 \overline{\Phi}_n^T(\mathrm{L}_1'+\mathrm{L}_2')\,\mathrm{d}x\right)\xi_n + \frac{1}{t_n}\left(\int_0^1 \overline{\Phi}_n^T\mathrm{L}_3'\,\mathrm{d}x\right)\frac{\mathrm{d}\xi_n^{(0)}}{\mathrm{d}\tau'}$$

$$+\frac{1}{\omega_n^l t_n}\left(\int_0^1 \overline{\Phi}_n^T(\overline{\mathrm{L}}_1' + \overline{\mathrm{L}}_2')\,\mathrm{d}x\right)\overline{\xi}_n^{(0)} + \frac{1}{t_n}\left(\int_0^1 \overline{\Phi}_n^T \overline{\mathrm{L}}_3'\,\mathrm{d}x\right)\frac{\mathrm{d}\overline{\xi}_n^{(0)}}{\mathrm{d}\tau'}. \tag{5.78}$$

The following solution of equation (5.77),

$$\xi_n^{(0)} = be^{i\tau'},$$

is first substituted into equation (5.78). Then, to avoid secular terms in $\xi_n^{(1)}$, the following condition must hold good :

$$(\eta_1 - \Gamma_1)b - \Gamma_2\overline{b} + \left(\frac{e_0'}{\omega_n^l}\right)Ge^{-2i\theta_n}\overline{b} + i\left(\frac{\mu'}{\omega_n^l}\right)b = 0 \tag{5.79}$$

where

$$\Gamma_1 = \frac{k}{4}\tilde{a}_n^2\left[2\left(\int_0^1(\frac{\mathrm{d}\phi_n}{\mathrm{d}x})^2\,\mathrm{d}x\right)\left(\int_0^1 \frac{\mathrm{d}^2\overline{\phi}_n}{\mathrm{d}x^2}\overline{\phi}_n\,\mathrm{d}x\right) + 4\left(\int_0^1 \frac{\mathrm{d}\overline{\phi}_n}{\mathrm{d}x}\frac{\mathrm{d}\phi_n}{\mathrm{d}x}\,\mathrm{d}x\right)\left(\int_0^1 \frac{\mathrm{d}^2\phi_n}{\mathrm{d}x^2}\overline{\phi}_n\,\mathrm{d}x\right)\right]/t_n$$

and

$$\Gamma_2 = \frac{k}{4}\tilde{a}_n^2\left[\left(\int_0^1(\frac{\mathrm{d}\phi_n}{\mathrm{d}x})^2\,\mathrm{d}x\right)\left(\int_0^1 \frac{\mathrm{d}^2\overline{\phi}_n}{\mathrm{d}x^2}\overline{\phi}_n\,\mathrm{d}x\right) + \left(\int_0^1 \frac{\mathrm{d}\overline{\phi}_n}{\mathrm{d}x}\frac{\mathrm{d}\phi_n}{\mathrm{d}x}\,\mathrm{d}x\right)\left(\int_0^1 \frac{\mathrm{d}^2\phi_n}{\mathrm{d}x^2}\overline{\phi}_n\,\mathrm{d}x\right)\right]/t_n.$$

For the existence of a non-trivial solution of b $(= b_x + ib_y)$ from equation (5.79) one finally obtains, (after some algebraic manipulations)

$$\eta_1 = \Gamma_1 \pm \left[\Gamma_2^2 - 2\Gamma_2\left(\frac{e_0'}{\omega_n^l}\right)A_1 + \left(\frac{e_0'}{\omega_n^l}\right)^2\left((G^R)^2 + (G^I)^2\right) - \left(\frac{\mu'}{\omega_n^l}\right)^2\right]^{\frac{1}{2}} \tag{5.80}$$

with $A_1 = G^R\cos 2\theta_n + G^I \sin 2\theta_n$. In the $\tilde{a}_n - \Omega_f$ plane, equation (5.80) implies two curves

$$\Omega_{fs}^{(j)} = \omega_n^l(1 - \epsilon\eta_1^{(j)}), j = 1, 2,$$

where $\eta_1^{(j)}$ corresponds to either of the values of η_1 from equation (5.80) and $\Omega_{fs}^{(j)}$ denotes the associated stability boundary.

For a fixed value of $\tilde{a}_n$ and θ_n, $\Omega_{fs}^{(j)}$'s are calculated first ($\Omega_{fs}^{(1)} < \Omega_{fs}^{(2)}$, say) and then checked with the forcing frequency Ω_f. The amplitude is said to be unstable if

$$\Omega_{fs}^{(1)} < \Omega_f < \Omega_{fs}^{(2)}, \tag{5.81}$$

and stable otherwise.

It is to be noted from equation (5.80) that for some values of the parameters, η_1 does not exist. This implies a stable condition under such situations.

5.4.2 Numerical Results and Discussion

In this section, numerical results are presented to study the effects of several parameters on the steady-state response. All the results are obtained for $T_0 = 1$, $x_0 = 1/3$ and $\Omega_f \simeq \Omega_p \simeq \omega_1^I$.

At this stage it should be noted from equations (5.54)-(5.56) that the steady-state response of the beam is obtained (up to $o(1)$) as

$$w(x,\tau) = \tilde{a}_1 \phi_1^*(x) \cos(\Omega_f \tau + \theta_1 + \rho_1),$$

where $\tan \rho_1 = -\phi_1^I/\phi_1^R$, $\phi_1^* = \sqrt{(\phi_1^R)^2 + (\phi_1^I)^2}$. The values of $\tilde{a}_1$ and θ_1 are now obtained by solving equations (5.65) and (5.66). Subsequently the effects of different parameters on the value of $\tilde{a}_1$ are studied.

Figures 5.6-5.8 show the response variable $\tilde{a}_1$ with increasing speed for two different sets of values of F_0 and ϵe_0. It is seen from Figure 5.6 that if the external forcing predominates, then only one stable response is resulted. The value of $\tilde{a}_1$, while remaining insensitive to the amount of unbalance, increases with increasing speed. On the other hand, if the parametric excitation predominates, then depending on the value of ϵe_0 and c', one or three unstable roots for $\tilde{a}_1$ may be obtained (Figures. 5.7 and 5.8). However, the usual jump phenomenon, observed in a harmonically forced Duffing oscillator, is not altered. Figure 5.9 clearly indicates that, if a flexible pulley-support is used, then the steady-state response can be controlled by adjusting the phase relationship between the external and parametric excitations.

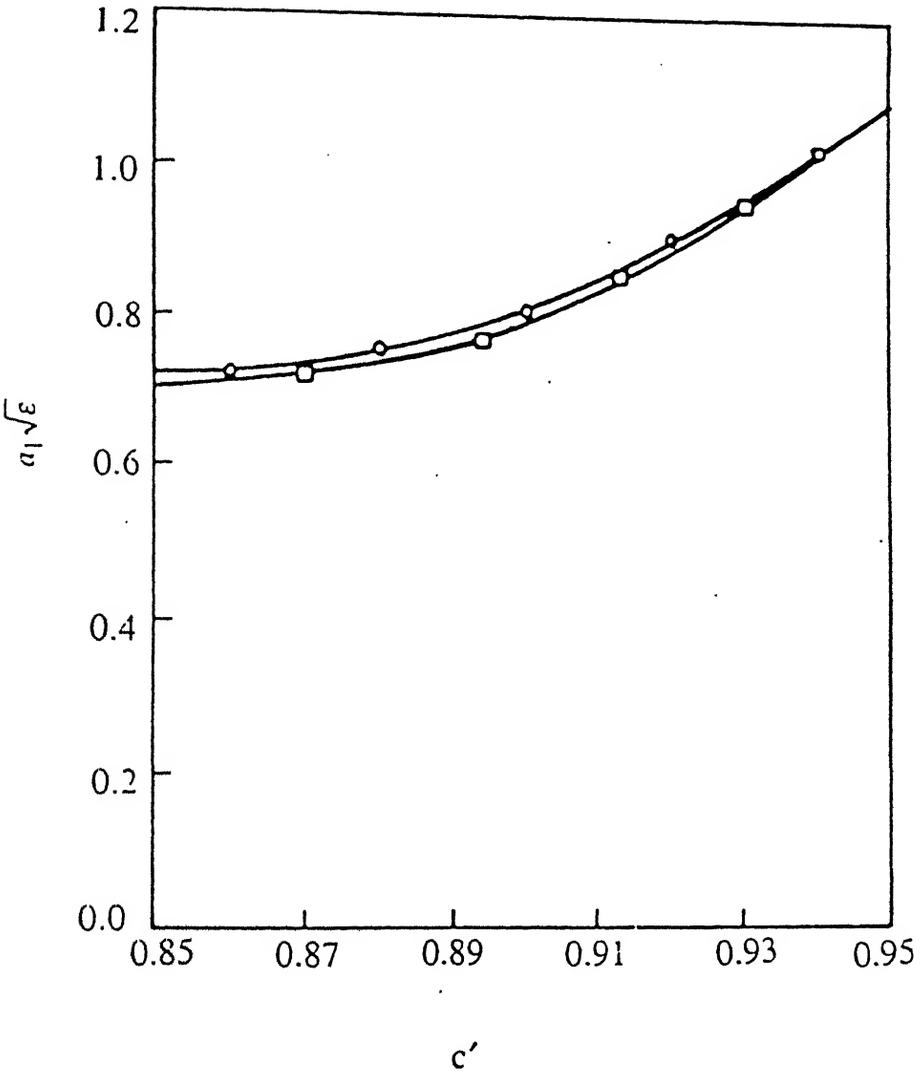

Figure 5.6: Variation of the roots of equations (5.65) and (5.66) with c'. $R = 0.2$, $k = 0.5$, $\theta_f = 0.0$, $\epsilon\mu = 0.05$, $F_0\sqrt{\epsilon} = 10.0$; $\circ$:$\epsilon e_0 = 0.8$, $\square$:$\epsilon e_0 = 0.1$.

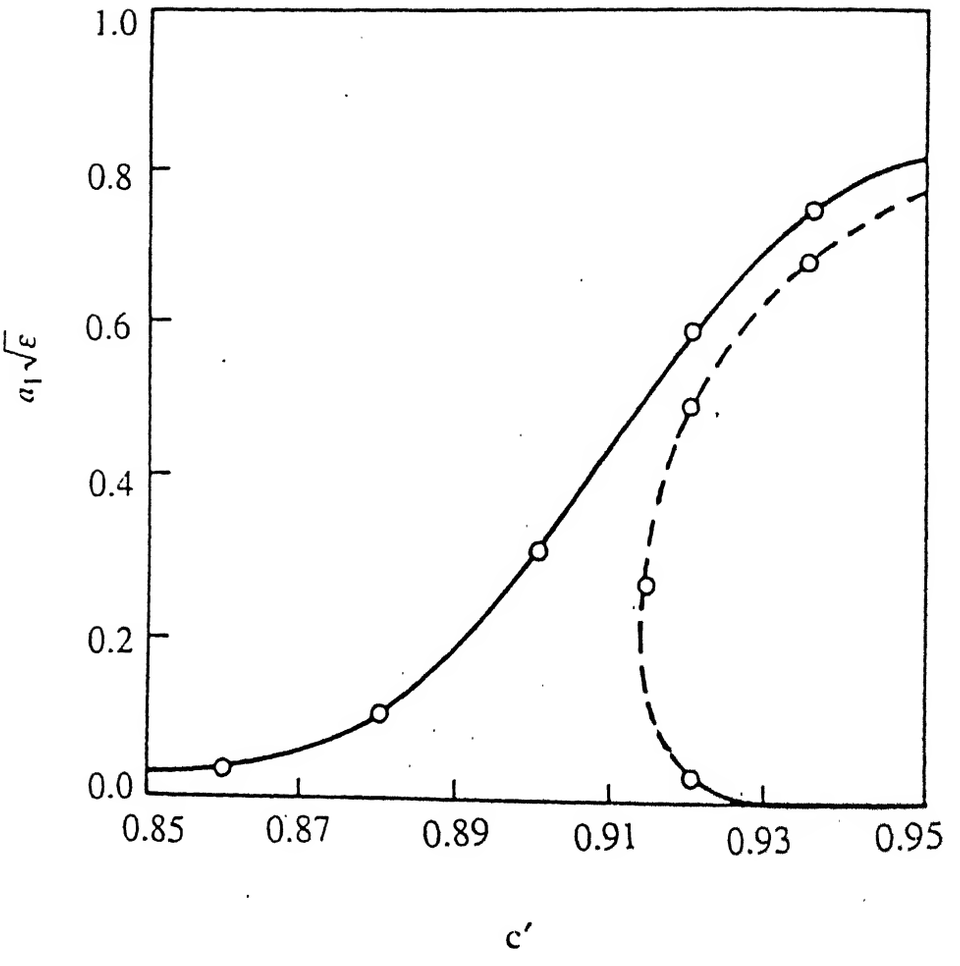

Figure 5.7: Variation of the roots of equations (5.65) and (5.66) with c'. $R = 0.2$, $k = 0.5$, $\theta_f = 0.0$, $\epsilon\mu = 0.05$, $F_0\sqrt{\epsilon} = 0.1$; $\circ$:$\epsilon e_0 = 0.1$; —— stable, - - - - unstable.

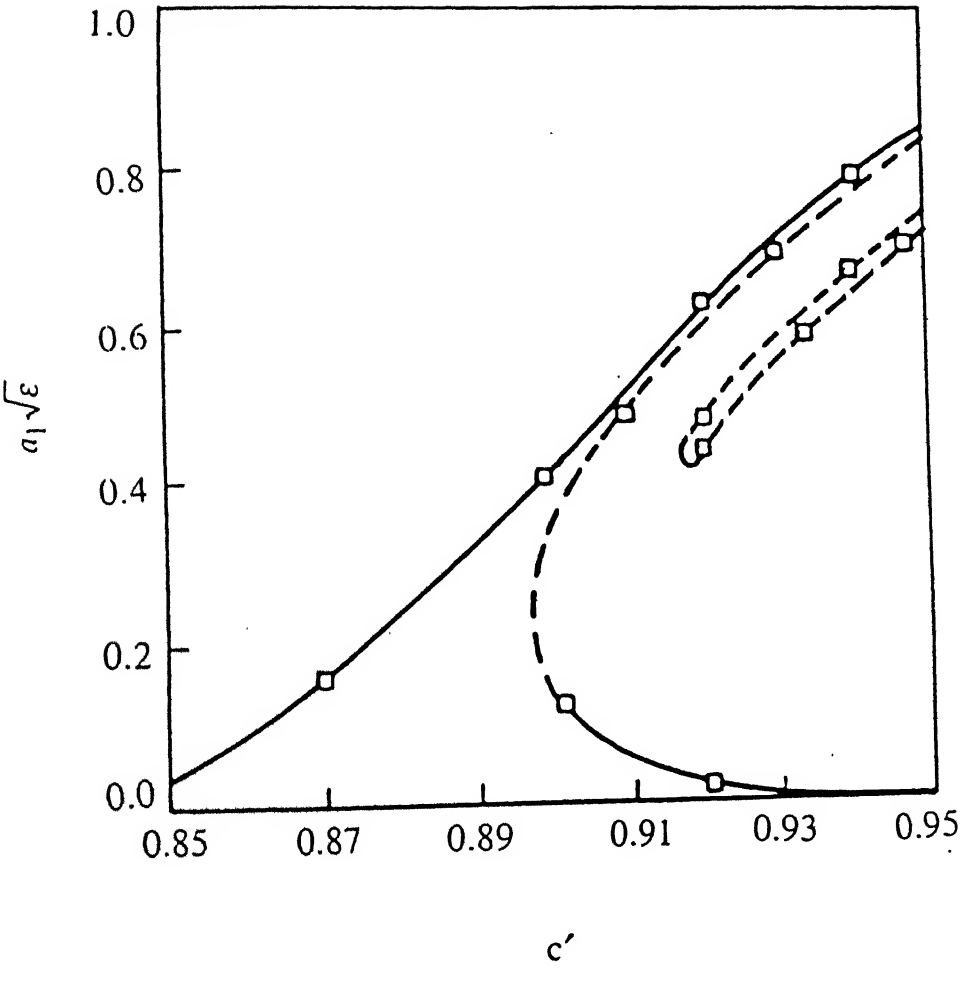

Figure 5.8: Variation of the roots of equations (5.65) and (5.66) with c'. $R = 0.2$, $k = 0.5$, $\theta_f = 0.0$, $\epsilon\mu = 0.05$, $F_0\sqrt{\epsilon} = 0.1$; $\circ$:$\epsilon e_0 = 0.8$; —— stable, - - - - unstable.

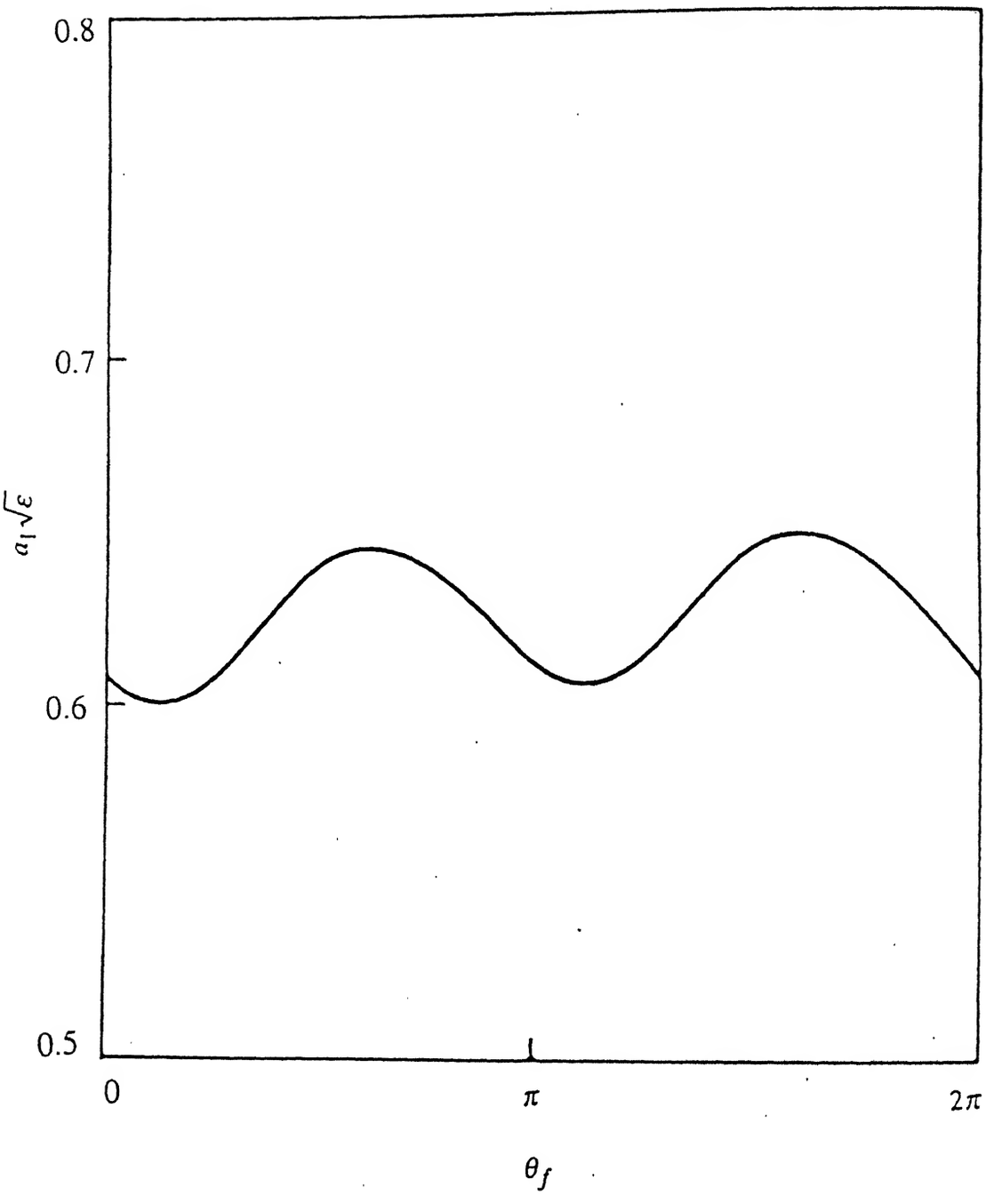

Figure 5.9: Variation of the roots of equations (5.65) and (5.66) with θ_f. $R = 0.2$, $k = 0.5$, $c' = 0.85$, $\epsilon\mu = 0.05$, $F_0\sqrt{\epsilon} = 10.0, \epsilon e_0 = 0.8$; —— stable, - - - - unstable.

Chapter 6

STABILITY OF AN ACCELERATING BEAM

6.1 Introduction

The studies on the non-linear vibrations of axially moving beams, carried out in Chapters 2 to 5, have been restricted to systems with uniform axial speed. Although the operating speed is normally maintained constant, the axial speed does vary considerably during the starting and stopping phases. It is the objective of the present chapter to bring out the effects of non-linearity on such an accelerating or decelerating beam.

For a travelling string, numerical studies reveal that the linear response builds up or decays as the string is accelerated or decelerated, respectively [149, 150]. An experiment with a pipe carrying fluid was also reported in reference [150] to validate the numerical results. However, the stability of a beam travelling with constant acceleration or deceleration has received less attention, though the parametric excitation caused by periodic variation of the axial speed has been studied [70].

The equation of motion for non-uniform axial speed is given in Section 6.2. In

Section 6.3, the Lyapunov's method is used to determine the sufficiency condition for asymptotic stability of a beam having any arbitrary acceleration. However, in some cases the method fails to ascertain the stability. An alternative method, based on Multiple Time Scale (MTS) is discussed in Section 6.4. Here, the change in the speed due to a constant acceleration or deceleration has been treated as a perturbation to the uniform speed.. Some numerical results are discussed in Section 6.5.

6.2 Equation of Motion

With the assumptions mentioned in Chapter 2, the non-linear equation of motion of a non-uniformly moving beam can be written in the following non-dimensional form:

$$\frac{\partial^2 w}{\partial \tau^2} + 2c\frac{\partial^2 w}{\partial x \partial \tau} + (c^2 - T_0)\frac{\partial^2 w}{\partial x^2} + \frac{\partial^4 w}{\partial x^4} + \frac{\mathrm{d}c}{\mathrm{d}\tau}\frac{\partial w}{\partial x} = \epsilon \left[\int_0^1 (\frac{\partial w}{\partial x})^2 \, dx\right] \frac{\partial^2 w}{\partial x^2}. \tag{6.1}$$

The non-dimensional symbols used in equation (6.1) have already been explained in Chapter 2. The boundary conditions due to simple supports are given by equations (2.10) and (2.11).

When a small viscous damping term $\delta\frac{\partial w}{\partial \tau}$ is present, the equation of motion turns out to be

$$\frac{\partial^2 w}{\partial \tau^2} + \delta\frac{\partial w}{\partial \tau} + 2c\frac{\partial^2 w}{\partial x \partial \tau} + (c^2 - T_0)\frac{\partial^2 w}{\partial x^2} + \frac{\partial^4 w}{\partial x^4} + \frac{\mathrm{d}c}{\mathrm{d}\tau}\frac{\partial w}{\partial x} = \epsilon \left[\int_0^1 (\frac{\partial w}{\partial x})^2 \, dx\right] \frac{\partial^2 w}{\partial x^2}, \tag{6.2}$$

which can be recast in the standard state-space form as

$$\mathbf{A}\frac{\partial W}{\partial \tau} + \mathbf{B}W + \mathbf{N} = 0 \tag{6.3}$$

where $\mathbf{A}$, $\mathbf{B}$ and W are given by equation (2.16) and

$$\mathbf{N} = \left\{\delta\frac{\partial w}{\partial \tau} + \frac{\mathrm{d}c}{\mathrm{d}\tau}\frac{\partial w}{\partial x} - \epsilon\left(\int_0^1 \left(\frac{\partial W}{\partial x}\right)^2 dx\right)\frac{\partial^2 W}{\partial x^2}, 0\right\}^T. \tag{6.4}$$

In the following, the stability of the response $w(x, \tau)$ is analysed using either equation (6.2) or (6.3) whichever is convenient depending on the method used.

6.3 Stability Analysis Using Lyapunov's Method

In this section, Lyapunov's direct method [151] is used to find the asymptotic nature of response of the system expressed by equation (6.2).

The following is taken as a Lyapunov function ,

$$V(w,\tau) = \frac{1}{2}\int_0^1 \left(\frac{\partial w}{\partial \tau}\right)^2 \mathrm{d}x + \frac{1}{2}(T_0 - c^2)\int_0^1 \left(\frac{\partial w}{\partial x}\right)^2 \mathrm{d}x + \frac{1}{2}\int_0^1 \left(\frac{\partial^2 w}{\partial x^2}\right)^2 \mathrm{d}x + \frac{\epsilon}{4}\left[\int_0^1 \left(\frac{\partial w}{\partial x}\right)^2 \mathrm{d}x\right]^2. \tag{6.5}$$

Assuming that the axial speed always remains positive (i.e., $c > 0$) and never crosses the first critical speed $\sqrt{T_0 + \pi^2}$, the chosen Lyapunov function is positive definite, since $\int_0^1 \left(\frac{\partial^2 w}{\partial x^2}\right)^2 \mathrm{d}x \geq \pi^2 \int_0^1 \left(\frac{\partial w}{\partial x}\right)^2 \mathrm{d}x$ for a continuous differentiable function with $w(0) = w(1) = 0$, [152].

Equation (6.5) is differentiated along the curve satisfying the equation of motion. Subsequent integration with the help of non-dimensionalized boundary conditions yields,

$$\frac{\mathrm{d}V}{\mathrm{d}\tau} = -\delta\int_0^1 \left(\frac{\partial w}{\partial \tau}\right)^2 \mathrm{d}x - 2c\int_0^1 \frac{\partial w}{\partial \tau}\frac{\partial^2 w}{\partial x \partial \tau}\,\mathrm{d}x - c\frac{\mathrm{d}c}{\mathrm{d}\tau}\int_0^1 \left(\frac{\partial w}{\partial x}\right)^2 \mathrm{d}x - \frac{\mathrm{d}c}{\mathrm{d}\tau}\int_0^1 \frac{\partial w}{\partial x}\frac{\partial w}{\partial \tau}\,\mathrm{d}x.$$

It can be seen by simple integration by parts that

$$\int_0^1 \frac{\partial w}{\partial \tau}\frac{\partial^2 w}{\partial x \partial \tau}\,\mathrm{d}x = 0,$$

for the given boundary conditions. Thus,

$$\frac{\mathrm{d}V}{\mathrm{d}\tau} = -\delta\int_0^1 \left(\frac{\partial w}{\partial \tau}\right)^2 \mathrm{d}x - c\frac{\mathrm{d}c}{\mathrm{d}\tau}\int_0^1 \left(\frac{\partial w}{\partial x}\right)^2 \mathrm{d}x - \frac{\mathrm{d}c}{\mathrm{d}\tau}\int_0^1 \frac{\partial w}{\partial x}\frac{\partial w}{\partial \tau}\,\mathrm{d}x. \tag{6.6}$$

Rearranging equation (6.6) as

$$\frac{\mathrm{d}V}{\mathrm{d}\tau} = -\left[\int_0^1 \left(\sqrt{\delta}\frac{\partial w}{\partial \tau} + \frac{1}{2\sqrt{\delta}}\frac{\mathrm{d}c}{\mathrm{d}\tau}\frac{\partial w}{\partial x}\right)^2 \mathrm{d}x + \left\{c\frac{\mathrm{d}c}{\mathrm{d}\tau} - \frac{1}{4\delta}\left(\frac{\mathrm{d}c}{\mathrm{d}\tau}\right)^2\right\}\int_0^1 \left(\frac{\partial w}{\partial x}\right)^2 \mathrm{d}x\right], \tag{6.7}$$

it can be seen that for a continuously accelerating beam, i.e., $(dc/d\tau) > 0$,

$$\frac{dV}{d\tau} < 0 \quad \text{if} \quad \left(\frac{dc}{d\tau}\right)^2 < 4\delta c\left(\frac{dc}{d\tau}\right). \tag{6.8}$$

When $(dc/d\tau) = 0$, it is observed from equation (6.7) that $(dV/d\tau) < 0$, i.e., the system is asymptotically stable. When $(dc/d\tau) \neq 0$, the system is stable if

$$\left(\frac{dc}{d\tau}\right) < 4\delta c. \tag{6.9}$$

Further, it is seen that the beam is stable (i.e., $\frac{dV}{d\tau} < 0$) when both $c < 0$ and $(dc/d\tau) < 0$ and the inequality (6.8) is satisfied. The situation corresponds to an acceleration in the direction of $-x$. Thus, considering the symmetric nature of the boundary conditions, these two cases are physically identical.

Although the stability is confirmed if condition (6.9) is satisfied, nothing can be said if the same condition is violated. Similarly, for a decelerating beam (i.e., $(dc/d\tau) < 0$), equation (6.7) can not be used to judge the asymptotic stability. This necessitates the choice of other functions.

6.4 Stability Analysis Using MTS Method

In this section, the stability of a uniformly accelerating or decelerating beam is analysed by the multiple-time-scale method. The change in speed is treated as a small perturbation to the uniform speed. Furthermore, the damping is also assumed to be small. Consequently, the speed of the beam and the damping factor are written, respectively, as

$$c = c_0 + \epsilon\alpha\tau \tag{6.10}$$

and

$$\text{and} \quad \delta = \epsilon\delta_0. \tag{6.11}$$

where $|\alpha|$ governs the magnitude of constant acceleration/deceleration. Using two time scales $t_0 = \tau$ and $t_1 = \epsilon\tau$, and neglecting terms $O(\epsilon^2)$, the partial differentials in time (τ) can be written as

$$\frac{\partial}{\partial \tau} = \frac{\partial}{\partial t_0} + \epsilon \frac{\partial}{\partial t_1}, \tag{6.12}$$

$$\frac{\partial^2}{\partial \tau^2} = \frac{\partial^2}{\partial t_0^2} + 2\epsilon \frac{\partial^2}{\partial t_0 \partial t_1}, \tag{6.13}$$

and the displacement as

$$w(x, t_0, t_1) = w_0(x, t_0, t_1) + \epsilon w_1(x, t_0, t_1). \tag{6.14}$$

Substituting equations (6.10)-(6.14) into equation (6.2) and equating the coefficients of the like powers of ϵ from both sides, the following equations are obtained in the state-space form:

$$\epsilon^0 : \mathbf{A}\frac{\partial W_0}{\partial t_0} + \mathbf{B}W_0 = 0, \tag{6.15}$$

$$\epsilon^1 : \mathbf{A}\frac{\partial W_1}{\partial t_0} + \mathbf{B}W_1 + \mathbf{N}_0 = 0, \tag{6.16}$$

where

$$\mathbf{N}_0 = \left\{ \delta_0 \frac{\partial w_0}{\partial t_0} + 2\alpha t_0 \frac{\partial^2 w_0}{\partial x \partial t_0} + 2c_0 \frac{\partial^2 w_0}{\partial x \partial t_1} + 2\frac{\partial^2 w_0}{\partial t_0 \partial t_1} + 2\alpha c_0 t_0 \frac{\partial^2 w_0}{\partial x^2} + \alpha \frac{\partial w_0}{\partial x} \right.$$
$$\left. - \left(\int_0^1 \left(\frac{\partial w_0}{\partial x} \right)^2 \mathrm{d}x \right) \frac{\partial^2 w_0}{\partial x^2}, 0 \right\}^T. \tag{6.17}$$

Equation (6.15) can be solved as

$$W_0(x, t_0, t_1) = \sum_{n=1}^{\infty} \left[\frac{a_n(t_1)}{2} \Phi_n(x) e^{i\omega_n^l t_0} + \frac{\overline{a}_n(t_1)}{2} \overline{\Phi}_n(x) e^{-i\omega_n^l t_0} \right], \tag{6.18}$$

where $a_n(t_1)$ is the complex amplitude and the bar at the top denotes the complex conjugate. To solve equation (6.16), equation (6.18) is first substituted into equation (6.17) and then $\mathbf{N}_0$ is expressed as

$$\mathbf{N}_0 = \sum_{n=1}^{\infty} \mathbf{P}_n(x) e^{i\omega_n^l t_0} + \mathbf{Q}(x, t_0) + c.c.,$$

where *c.c.* denotes the complex conjugate of the previous terms and $\mathbf{Q}$ contains terms having all other frequencies except ω_n^l. One readily finds $\mathbf{P}_n$ as

$$\begin{aligned}\mathbf{P}_n(x) &= \left\{ i\omega_n^l \delta_0 \frac{a_n}{2}\phi_n + i\pi\alpha a_n \frac{\mathrm{d}\phi_n}{\mathrm{d}x} + c_0 \frac{\mathrm{d}\phi_n}{\mathrm{d}x}\frac{\mathrm{d}a_n}{\mathrm{d}t_1} \right. \\ &+ i\omega_n^l \phi_n \frac{\mathrm{d}a_n}{\mathrm{d}t_1} + c_0\alpha a_n \frac{\pi}{\omega_n^l}\frac{\mathrm{d}^2\phi_n}{\mathrm{d}x^2} + \alpha\frac{a_n}{2}\frac{\mathrm{d}\phi_n}{\mathrm{d}x} \\ &\left. + \frac{a_n^2\overline{a}_n}{4}\left[\left(2\int_0^1 \frac{\mathrm{d}\phi_n}{\mathrm{d}x}\frac{\mathrm{d}\overline{\phi}_n}{\mathrm{d}x}\,\mathrm{d}x\right)\frac{\mathrm{d}^2\phi_n}{\mathrm{d}x^2} + \left(\int_0^1 \left(\frac{\mathrm{d}\phi_n}{\mathrm{d}x}\right)^2 \mathrm{d}x\right)\frac{\mathrm{d}^2\overline{\phi}_n}{\mathrm{d}x^2}\right], 0 \right\}^T . \end{aligned} \tag{6.19}$$

Using the orthogonality relations between the linear modal vectors Φ_n (see equations (2.27) and (2.28)) $\mathbf{P}_n$ is decomposed in terms of the linear modes as

$$\mathbf{P}_n(x) = \sum_{m=1}^{\infty} \left[p_{mn}\Phi_m(x) + q_{mn}\overline{\Phi}_n(x) \right],$$

where

$$p_{mn} = \frac{\int_0^1 \overline{\Phi}_m^T \mathbf{A}\mathbf{P}_n\,\mathrm{d}x}{\int_0^1 \overline{\Phi}_m^T \mathbf{A}\Phi_m\,\mathrm{d}x}$$

and

$$q_{mn} = \frac{\int_0^1 \Phi_m^T \mathbf{A}\mathbf{P}_n\,\mathrm{d}x}{\int_0^1 \overline{\Phi}_m^T \mathbf{A}\Phi_m\,\mathrm{d}x}.$$

Now, the secular terms in the solution of equation (6.16) can be avoided if,

$$p_{nn} = 0,$$

i.e.,

$$\int_0^1 \overline{\Phi}_n^T \mathbf{A}\mathbf{P}_n\,\mathrm{d}x = 0. \tag{6.20}$$

Equation (6.20) can be expanded with the help of equation (6.19) as,

$$\begin{aligned}&\frac{1}{2}\left(2\omega_n^l\int_0^1 \overline{\phi}_n\phi_n\,\mathrm{d}x - 2ic_0\int_0^1 \frac{\mathrm{d}\phi_n}{\mathrm{d}x}\overline{\phi}_n\,\mathrm{d}x\right)\frac{\mathrm{d}a_n}{\mathrm{d}t_1} = \\ &- \omega_n^l\frac{a_n}{2}\delta_0\int_0^1 \overline{\phi}_n\phi_n\,\mathrm{d}x - \pi\alpha a_n\int_0^1 \frac{\mathrm{d}\phi_n}{\mathrm{d}x}\overline{\phi}_n\,\mathrm{d}x + ic_0\alpha a_n\frac{\pi}{\omega_n^l}\int_0^1 \frac{\mathrm{d}^2\phi_n}{\mathrm{d}x^2}\overline{\phi}_n\,\mathrm{d}x\end{aligned}$$

$$+ \quad i\alpha\frac{a_n}{2}\int_0^1 \frac{\mathrm{d}\phi_n}{\mathrm{d}x}\overline{\phi}_n\,\mathrm{d}x - \frac{i}{8}a_n^2\overline{a}_n\left[\left(2\int_0^1 \frac{\mathrm{d}\phi_n}{\mathrm{d}x}\frac{\mathrm{d}\overline{\phi}_n}{\mathrm{d}x}\,\mathrm{d}x\right)\left(\int_0^1 \overline{\phi}_n\frac{\mathrm{d}^2\phi_n}{\mathrm{d}x^2}\,\mathrm{d}x\right)\right.$$
$$\left. + \quad \left(\int_0^1 \left(\frac{\mathrm{d}\phi_n}{\mathrm{d}x}\right)^2\mathrm{d}x\right)\left(\int_0^1 \overline{\phi}_n\frac{\mathrm{d}^2\overline{\phi}_n}{\mathrm{d}x^2}\,\mathrm{d}x\right)\right]. \tag{6.21}$$

It is to be noted that for a travelling beam,

$$\mathrm{Re}\left[\int_0^1 \overline{\phi}_n\frac{\mathrm{d}\phi_n}{\mathrm{d}x}\,\mathrm{d}x\right] = 0,\ \mathrm{Im}\left[\int_0^1 \overline{\phi}_n\phi_n\,\mathrm{d}x\right] = 0 \text{ and } \mathrm{Im}\left[\int_0^1 \overline{\phi}_n\frac{\mathrm{d}^2\phi_n}{\mathrm{d}x^2}\,\mathrm{d}x\right] = 0.$$

Now substituting $a_n = \tilde{a}_n e^{i\theta_n}$ into equation (6.21) and equating, separately, the real and imaginary parts from both sides, one obtains

$$\frac{1}{2}\left(2\omega_n^l\int_0^1 \overline{\phi}_n\phi_n\,\mathrm{d}x - 2ic_0\int_0^1 \frac{\mathrm{d}\phi_n}{\mathrm{d}x}\overline{\phi}_n\,\mathrm{d}x\right)\frac{\mathrm{d}\tilde{a}_n}{\mathrm{d}t_1} =$$
$$-\omega_n^l\frac{\tilde{a}_n}{2}\delta_0\int_0^1 \overline{\phi}_n\phi_n\,\mathrm{d}x + i\alpha\frac{\tilde{a}_n}{2}\int_0^1 \frac{\mathrm{d}\phi_n}{\mathrm{d}x}\overline{\phi}_n\,\mathrm{d}x, \tag{6.22}$$

and

$$\frac{1}{2}\left(2\omega_n^l\int_0^1 \overline{\phi}_n\phi_n\,\mathrm{d}x - 2ic_0\int_0^1 \frac{\mathrm{d}\phi_n}{\mathrm{d}x}\overline{\phi}_n\,\mathrm{d}x\right)\frac{\mathrm{d}\theta_n}{\mathrm{d}t_1}\tilde{a}_n = i\pi\alpha\tilde{a}_n\int_0^1 \frac{\mathrm{d}\phi_n}{\mathrm{d}x}\overline{\phi}_n\,\mathrm{d}x$$
$$+c_0\alpha\tilde{a}_n\frac{\pi}{\omega_n^l}\int_0^1 \frac{\mathrm{d}^2\phi_n}{\mathrm{d}x^2}\overline{\phi}_n\,\mathrm{d}x - \frac{1}{8}\tilde{a}_n^3\left[\left(2\int_0^1 \frac{\mathrm{d}\phi_n}{\mathrm{d}x}\frac{\mathrm{d}\overline{\phi}_n}{\mathrm{d}x}\,\mathrm{d}x\right)\left(\int_0^1 \overline{\phi}_n\frac{\mathrm{d}^2\phi_n}{\mathrm{d}x^2}\,\mathrm{d}x\right)\right.$$
$$\left. + \left(\int_0^1 \left(\frac{\mathrm{d}\phi_n}{\mathrm{d}x}\right)^2\mathrm{d}x\right)\left(\int_0^1 \overline{\phi}_n\frac{\mathrm{d}^2\overline{\phi}_n}{\mathrm{d}x^2}\,\mathrm{d}x\right)\right]. \tag{6.23}$$

Writing $\int_0^1 \overline{\phi}_n\frac{\mathrm{d}\phi_n}{\mathrm{d}x}\,\mathrm{d}x = iS_1\ (S_1 > 0)$, equation (6.22) takes the following form:

$$\frac{1}{2}\left(2\omega_n^l\int_0^1 \overline{\phi}_n\phi_n\,\mathrm{d}x - 2ic_0\int_0^1 \frac{\mathrm{d}\phi_n}{\mathrm{d}x}\overline{\phi}_n\,\mathrm{d}x\right)\frac{\mathrm{d}\tilde{a}_n}{\mathrm{d}t_1} =$$
$$-\omega_n^l\frac{\tilde{a}_n}{2}\delta_0\int_0^1 \overline{\phi}_n\phi_n\,\mathrm{d}x - \alpha\frac{\tilde{a}_n}{2}S_1. \tag{6.24}$$

Obvious from equation (6.24) is the fact that for $\alpha > 0$, i.e., during acceleration, $(\mathrm{d}\tilde{a}_n/\mathrm{d}t_1) < 0$ or the response decays. But for a decelerating beam (i.e., $\alpha < 0$), the response may be stable or unstable according as

$$\omega_n^l\delta_0\int_0^1 \overline{\phi}_n\phi_n\,\mathrm{d}x > |\alpha|\,S_1 \tag{6.25}$$

or

$$\omega_n^l \delta_0 \int_0^1 \overline{\phi}_n \phi_n \, dx < |\alpha| \, S_1, \tag{6.26}$$

respectively. However, the instability is only for a short time. The ephemerally observed characteristics of the instability can be explained as follows. As the beam becomes unstable, the amplitude grows but the speed also decreases since the beam decelerates. The numerically obtained value of S_1 is found to decrease monotonically with decreasing speed. Consequently, with decreasing speed the beam eventually regains its stability as $(d\tilde{a}_n/dt_1)$ becomes negative. Thus, the amplitude builds up to a limiting value after which it starts decreasing. This phenomenon was observed in a pipe carrying fluid when the flow was stopped [150]. It should be pointed out that the non-linear terms do not affect the stability but only change the frequency of oscillation. This can easily be seen from equation (6.23).

6.5 Numerical Results and Discussion

Numerical results are presented in this section for a beam having an initial tension $T_0 = 1$. For a beam with its axial speed given by equation (6.10), the asymptotic stability is confirmed using the Lyapunov's method (see equation (6.7)) if

$$\delta_0 > \frac{\alpha}{4c_0}.$$

The MTS method on the other hand predicts the stability for all possible values of δ_0 ($\delta_0 > 0$). For a decelerating beam, the chosen Lyapunov function (see equation (6.5)) fails to ascertain the stability. However, it is evident from the MTS method (see equations (6.25) and (6.26)) that the stability depends on the values of δ_0 and $|\alpha|$. Furthermore, it is obvious from equations (6.25) and (6.26) that in the parameter space (δ_0, $|\alpha|$) the boundary delineating the stable and unstable regions is a straight

line. Figure 6.1 shows these boundaries for three different values of c_0. The region above the line representing the boundary is stable. As expected, the damping required to prevent instability increases with increasing initial velocity.

The asymptotic or long-term stability, discussed in the previous section, is shown in Figure 6.2. The amplitude is approximately calculated as

$$\tilde{a}_n = \tilde{a}_n(0) e^{-\int_0^\tau \Delta(\tau_1) \mathrm{d}\tau_1},$$

where

$$\Delta = (\omega_n^l \delta_0 \int_0^1 \overline{\phi}_n \phi_n \, \mathrm{d}x + \alpha S_1) / \left(2\omega_n^l \int_0^1 \overline{\phi}_n \phi_n \, \mathrm{d}x - 2ic_0 \int_0^1 \frac{\mathrm{d}\phi_n}{\mathrm{d}x} \overline{\phi}_n \, \mathrm{d}x \right).$$

When the damping is not sufficiently large, the response amplitude shows a temporal rise. The results have been obtained by assuming that only the first mode is excited. For the values of damping and axial speed considered, other modes are found to be stable.

The effects of magnitude of deceleration on the maximum amplitude rise and the overshoot-time (i.e., the interval during which the response amplitude remains higher than the initial value) have been plotted in Figures 6.3 and 6.4, respectively.

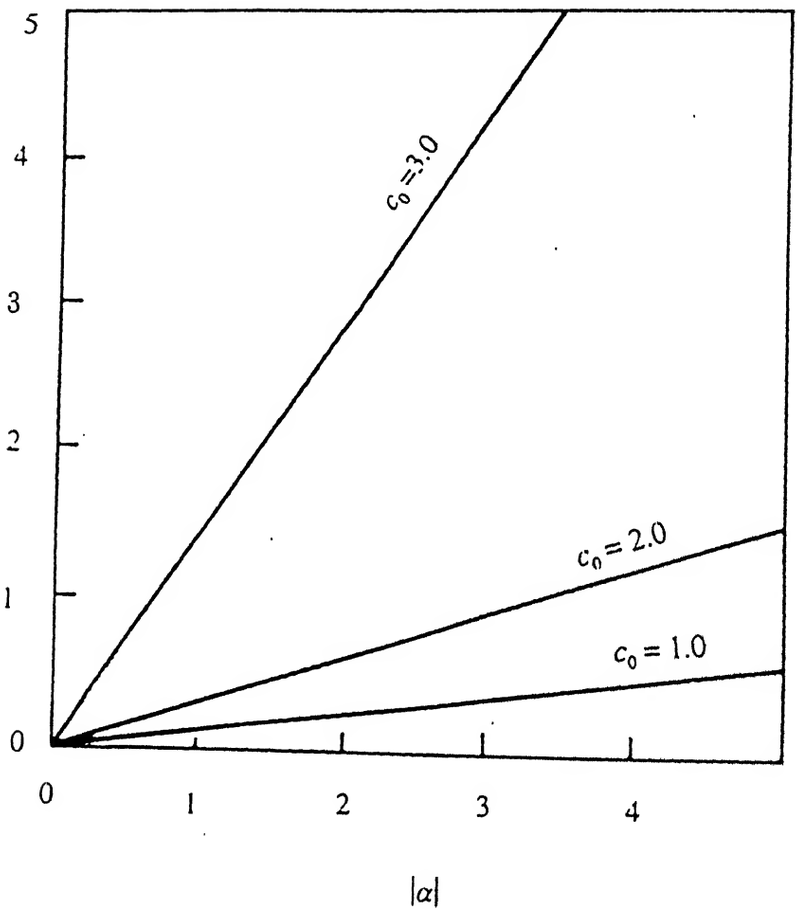

Figure 6.1: Stability boundaries for a uniformly decelerating beam.

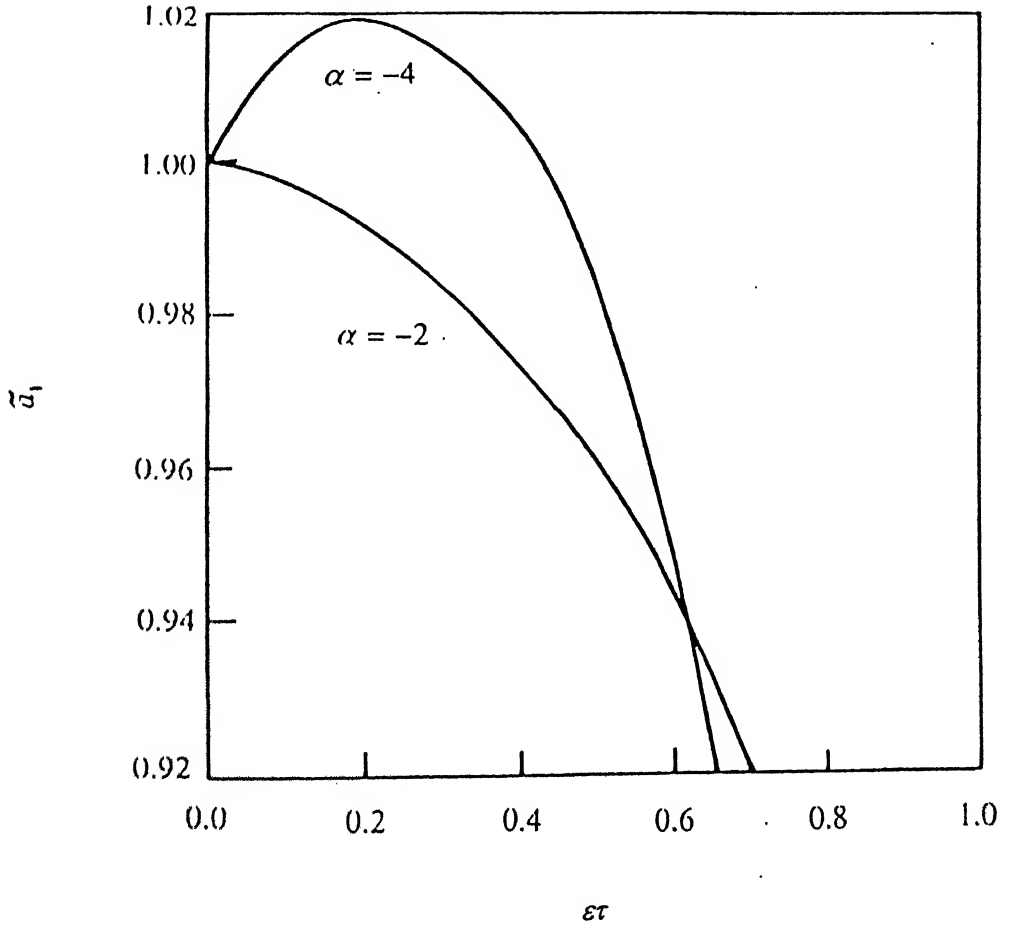

Figure 6.2: Variation of the response amplitude for a uniformly decelerating beam. $\delta_0 = 0.7$.

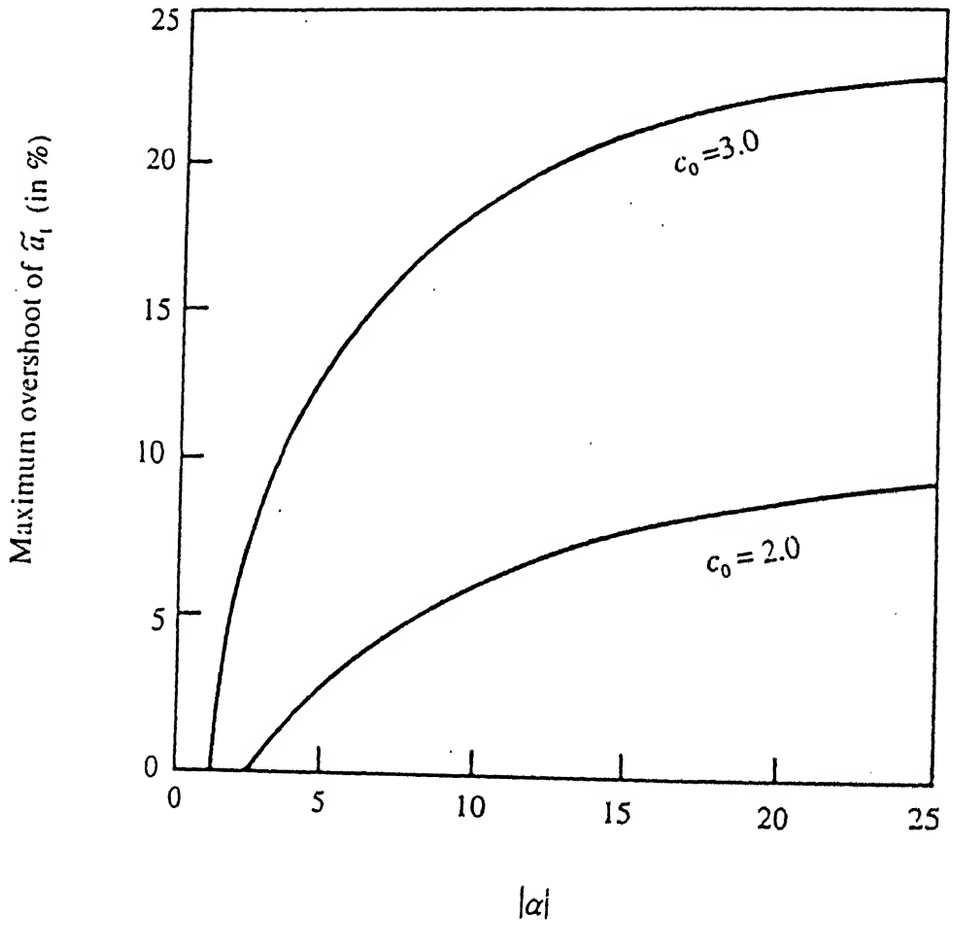

Figure 6.3: Variation of the maximum overshoot of response amplitude with the magnitude of uniform deceleration. $\delta_0 = 0.7$.

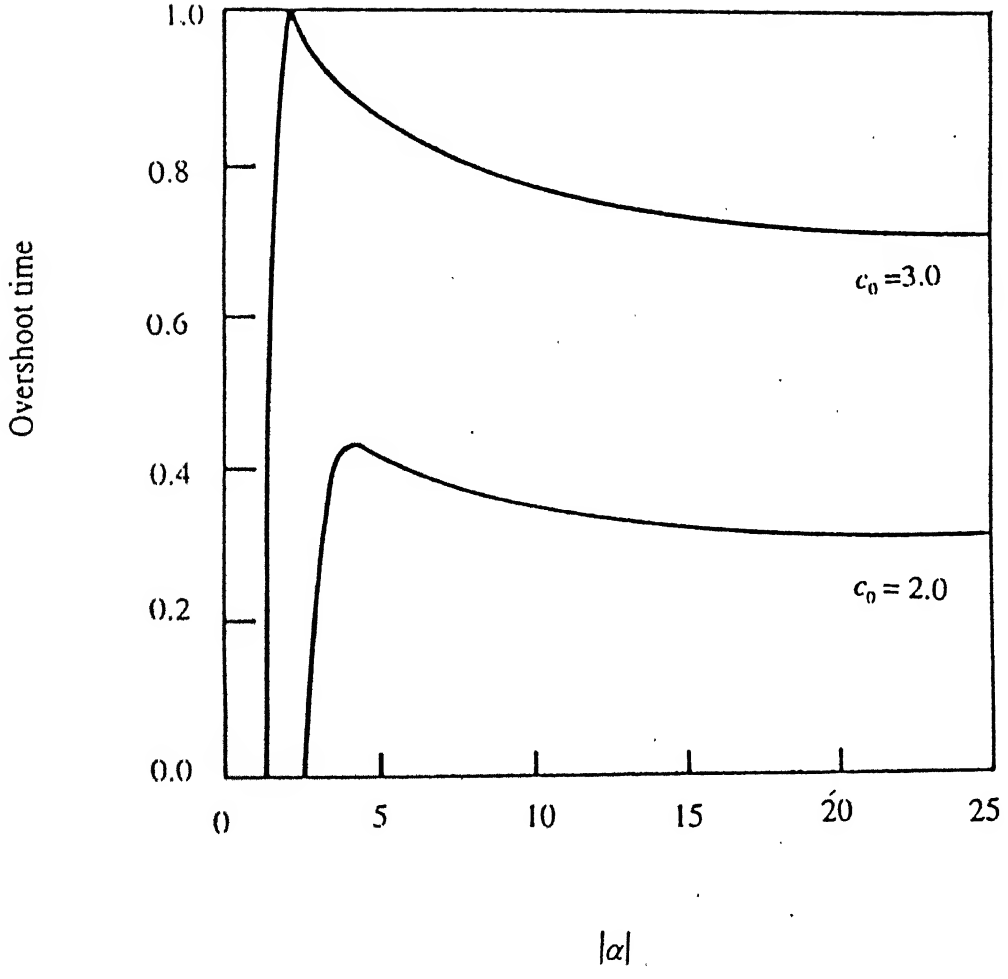

Figure 6.4: Variation of the overshoot time with the magnitude of uniform deceleration. $\delta_0 = 0.7$.

Chapter 7

VIBRATION OF A TRAVELLING BEAM HAVING AN INTERMEDIATE GUIDE

7.1 Introduction

The effects of the non-linear term on the free and forced transverse vibrations of a travelling beam under various operating conditions have been studied in the foregoing chapters. This chapter addresses to the problem of controlling these unwanted oscillations. A simple passive controller, in the form of an intermediate guide has been suggested. To analyse the effectiveness of such a controller, the response of a travelling beam to a harmonic excitation is considered with and without the guide. The equation of motion is derived in Section 7.2. The complex normal modes of the constrained system are obtained in Section 7.3 by neglecting the non-linear term. The near-resonance response is then obtained through a modal analysis. Both the stiffness of and dry friction in the guide are taken into consideration. Since the frictional force

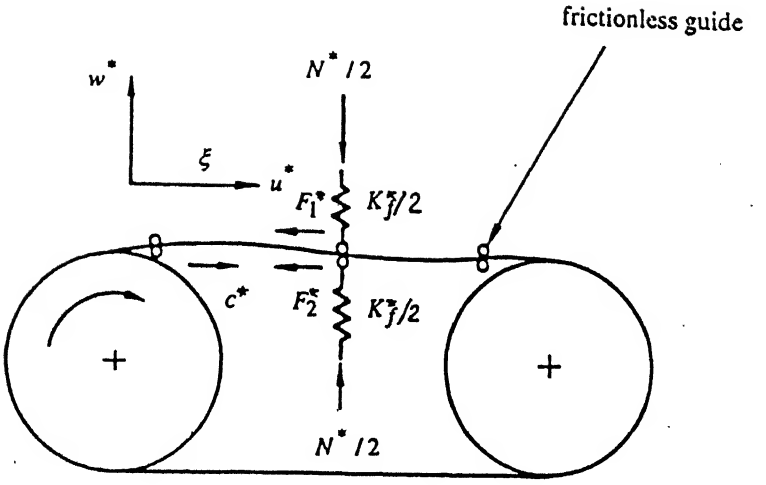

Figure 7.1: Schematic diagram of a travelling beam with an intermediate guide.

between the guide and the beam has a destabilizing effect, rollers can be used to maintain the contact between them. Similar analysis is carried out in Section 7.4 including the non-linear term. Numerical results are included to highlight the salient features.

7.2 Equation of Motion

Consider a slender beam moving axially between two frictionless guides as shown in Figure 7.1. The axial speed, c^*, is maintained by means of two rigidly mounted pulleys. An intermediate guide, consisting of two free rollers, with finite compliance is held in contact with the beam by means of an external force $N^*/2$, provided by the precompression of the compliant member. In addition, as indicated in the figure, the stiffness of the guides is assumed to be same in both the directions.

Under the usual assumption of small longitudinal vibration (in comparison to the transverse vibration, i.e., assuming $u^* = O(w^{*^2})$), the non-linear equations of motion for the coupled vibration in the axial and transverse directions are

$$\rho A\left[\frac{\partial^2 u^*}{\partial t^2}+2c^*\frac{\partial^2 u^*}{\partial \xi \partial t}+c^{*^2}\frac{\partial^2 u^*}{\partial \xi^2}\right]-EA\frac{\partial^2 u^*}{\partial \xi^2}=(EA-T_0^*)\frac{\partial w^*}{\partial \xi}\frac{\partial^2 w^*}{\partial \xi^2}-(F_1^*+F_2^*)\delta(\xi-d^*), \tag{7.1}$$

and

$$\rho A\left[\frac{\partial^2 w^*}{\partial t^2}+2c^*\frac{\partial^2 w^*}{\partial \xi \partial t}+c^{*^2}\frac{\partial^2 w^*}{\partial \xi^2}\right]-T_0^*\frac{\partial^2 w^*}{\partial \xi^2}+EI_z\frac{\partial^4 w^*}{\partial \xi^4}=(EA-T_0^*)\frac{\partial}{\partial \xi}[\frac{\partial u^*}{\partial \xi}\frac{\partial w^*}{\partial \xi}$$
$$+\frac{1}{2}(\frac{\partial w^*}{\partial \xi})^3]-K_f^* w^*\delta(\xi-d^*), \tag{7.2}$$

where F_1^* and F_2^* denote the frictional forces and are given by

$$F_1^*=\mu_f\left[\frac{N^*}{2}+\frac{K_f^*}{2}w^*(d^*,t)\right], \tag{7.3}$$

$$F_1^*=\mu_f\left[\frac{N^*}{2}-\frac{K_f^*}{2}w^*(d^*,t)\right]. \tag{7.4}$$

In equations (7.1)-(7.4), $K_f^*/2$ and μ_f denote the stiffness of the guide placed at $\xi = d^*$, and the coefficient of dynamic friction, respectively. The other symbols are explained in Chapter 2.

As discussed in Chapter 5, the vibration coupling between the two spans is neglected. The boundary conditions can then be written as

$$u^*(0,t)=u^*(l,t)=0, \tag{7.5}$$

$$w^*(0,t)=w^*(l,t)=0 \tag{7.6}$$

and

$$\frac{\partial^2 w^*(0,t)}{\partial \xi^2}=\frac{\partial^2 w^*(l,t)}{\partial \xi^2}=0. \tag{7.7}$$

Using the following non-dimensional parameters,

$F_i = F_i^*/(EA\gamma^2);\ i=1,2,\ N=N^*/(EA\gamma^2),\ K_f=K_f^* l/(EA),\ d=d^*/l,$

along with those given in Chapter 2 (see equation (2.6)), equations (7.1)-(7.7) can be written, respectively, as

$$\left[\frac{\partial^2 u}{\partial \tau^2} + 2c\frac{\partial^2 u}{\partial x \partial \tau} + c^2\frac{\partial^2 u}{\partial x^2}\right] - \frac{1}{\gamma^2}\frac{\partial^2 u}{\partial x^2} = \gamma^2(1-\gamma^2 T_0)\frac{\partial w}{\partial x}\frac{\partial^2 w}{\partial x^2} - (F_1+F_2)\delta(x-d), \quad (7.8)$$

$$\frac{\partial^2 w}{\partial \tau^2} + 2c\frac{\partial^2 w}{\partial x \partial \tau} + (c^2 - T_0)\frac{\partial^2 w}{\partial x^2} + \frac{\partial^4 w}{\partial x^4} = (1-\gamma^2 T_0)\frac{\partial}{\partial x}\left[\frac{1}{\gamma^2}\frac{\partial u}{\partial x}\frac{\partial w}{\partial x} + \frac{\gamma^2}{2}\left(\frac{\partial w}{\partial x}\right)^3\right] - K_f w\delta(x-d), \quad (7.9)$$

$$F_1 = \mu_f\left[\frac{N}{2} + \frac{K_f}{2}w(d,\tau)\right], \quad (7.10)$$

$$F_2 = \mu_f\left[\frac{N}{2} - \frac{K_f}{2}w(d,\tau)\right], \quad (7.11)$$

$$u(0,\tau) = u(1,\tau) = 0, \quad (7.12)$$

$$w(0,\tau) = w(1,\tau) = 0 \quad (7.13)$$

and

$$\frac{\partial^2 w(0,\tau)}{\partial x^2} = \frac{\partial^2 w(1,\tau)}{\partial x^2} = 0. \quad (7.14)$$

For a small value of γ (i.e., $\gamma \ll 1$), the longitudinal inertia in equation (7.8) is neglected to yield

$$-\frac{1}{\gamma^2}\frac{\partial^2 u}{\partial x^2} = \gamma^2\frac{\partial w}{\partial x}\frac{\partial^2 w}{\partial x^2} - (F_1+F_2)\delta(x-d),$$

which, when integrated twice with respect to x, results in

$$u(x,\tau) = -\frac{\gamma^4}{2}\int_0^x \left(\frac{\partial w}{\partial x_1}\right)^2 dx_1 + \gamma^2(F_1+F_2)\int_0^x H(x_1-d)dx_1 + xf_1'(\tau) + f_2'(\tau), \quad (7.15)$$

where

$$\begin{aligned} H(x-d) &= 0; \ x < d, \\ &= 1; \ x \geq d. \end{aligned}$$

Using equation (7.12) the unknown constants of integration $f_1'(\tau)$ and $f_2'(\tau)$ are obtained as

$$f_2'(\tau) = 0 \quad (7.16)$$

and

$$f_1'(\tau) = \frac{\gamma^4}{2}\int_0^1 (\frac{\partial w}{\partial x})^2\,\mathrm{d}x - \gamma^2(F_1+F_2)(1-d). \tag{7.17}$$

Now combining equations (7.10), (7.11), (7.15)-(7.17) and (7.9), the equation of motion for the transverse vibration can be written in the following simplified form:

$$\frac{\partial^2 w}{\partial \tau^2} + 2c\frac{\partial^2 w}{\partial x \partial \tau} + \left[c^2 - \{T_0 - \mu_f N(1-d) + \mu_f N H(x-d)\}\right]\frac{\partial^2 w}{\partial x^2} + \frac{\partial^4 w}{\partial x^4}$$
$$-(\mu_f N\frac{\partial w}{\partial x} - K_f w)\delta(x-d) = \epsilon\left[\int_0^1 (\frac{\partial w}{\partial x})^2\,\mathrm{d}x\right]\frac{\partial^2 w}{\partial x^2}, \tag{7.18}$$

where $\epsilon(=\frac{\gamma^2}{2})$ is a small parameter, i.e., $\epsilon \ll 1$. This equation can also be written in the familiar state-space form as

$$\mathrm{A}_1\frac{\partial W}{\partial \tau} + \mathrm{B}_1 W = \epsilon \mathrm{N}, \tag{7.19}$$

where $\mathrm{A}_1 = \begin{bmatrix} I & 0 \\ 0 & K_1 \end{bmatrix}$, $\mathrm{B}_1 = \begin{bmatrix} G & K_1 \\ -K_1 & 0 \end{bmatrix}$, $W = \begin{Bmatrix} \frac{\partial w}{\partial \tau} \\ w \end{Bmatrix}$, $K_1 \equiv (c^2 - T_0)\frac{\partial^2}{\partial x^2} + \frac{\partial^4}{\partial x^4} - \mu_f N H(x-d)\frac{\partial^2}{\partial x^2} - \delta(x-d)(\mu_f N\frac{\partial}{\partial x} - K_f)$, $G \equiv 2c\frac{\partial}{\partial x}$, I is the identity operator and

$$\mathrm{N} = \left\{\left(\int_0^1 \left(\frac{\partial w}{\partial x}\right)^2 \mathrm{d}x\right)\frac{\partial^2 w}{\partial x^2}, 0\right\}^T. \tag{7.20}$$

It is not difficult to verify that K_1 is a self-adjoint and positive definite operator. This fact is essential to obtain the orthogonality relations between the complex normal modes as discussed in the next section.

In order to facilitate computation, the non-analytic functions involved in equation (7.18) can be eliminated by writing the equation separately for two domains, namely, $0 < x_1 \le d$ and $d < x_2 < 1$ as

$$\frac{\partial^2 w_j}{\partial \tau^2} + 2c\frac{\partial^2 w_j}{\partial x_j \partial \tau} + [c^2 - T_j]\frac{\partial^2 w_j}{\partial x_j^2} + \frac{\partial^4 w_j}{\partial x_j^4} = \epsilon\left[\int_0^d (\frac{\partial w_1}{\partial x_1})^2\,\mathrm{d}x_1 + \int_d^1 (\frac{\partial w_2}{\partial x_2})^2\,\mathrm{d}x_2\right]\frac{\partial^2 w_j}{\partial x_j^2}, \tag{7.21}$$

for $j = 1, 2$, where w_j is the transverse displacement in the j-th domain and

$$\begin{aligned} T_1 &= T_0 - \mu_f N(1-d), \\ T_2 &= T_0 + \mu_f N d \end{aligned}$$

or

$$\Delta T = T_2 - T_1 = \mu_f N.$$

The matching conditions at $x = d$ can now be written as

$$\left.\begin{aligned} & w_1(d,\tau) = w_2(d,\tau), \\ & \tfrac{\partial w_1}{\partial x_1}(d,\tau) = \tfrac{\partial w_2}{\partial x_2}(d,\tau), \\ & \tfrac{\partial^2 w_1}{\partial x_1^2}(d,\tau) = \tfrac{\partial^2 w_2}{\partial x_2^2}(d,\tau), \\ \text{and } & \tfrac{\partial^3 w_1}{\partial x_1^3}(d,\tau) - \tfrac{\partial^3 w_2}{\partial x_2^3}(d,\tau) + \Delta T \tfrac{\partial w_1}{\partial x_1}(d,\tau) - K_f w_1(d,\tau) = 0. \end{aligned}\right\} \quad (7.22)$$

The non-linear response of the beam can be studied by solving equations (7.21) and (7.22). Since the non-linear term can be taken as a small perturbation to the linear equation of motion, the response of a linear beam is discussed first before taking up the non-linear one.

7.3 Free and Forced Responses of the Linear System

In this section, the free and forced responses of a linear travelling beam (i.e., with $\epsilon = 0$ in equation (7.19)) are discussed. As already mentioned in Chapter 2, no stationary mode shape exists for a travelling beam, but the harmonic oscillation is still possible at

some frequencies, known as the 'natural frequencies'. Considering the complex normal modes, the natural frequencies and the complex mode shapes can be obtained. The response of the beam, $w(x,\tau)$, at any one of the natural frequencies ω^l can be written as

$$W(x,\tau) = \frac{a}{2}\Phi(x)e^{i\omega^l\tau} + \frac{\overline{a}}{2}\overline{\Phi}(x)e^{-i\omega^l\tau}, \tag{7.23}$$

with $\Phi(x) = \left\{ \begin{array}{c} i\omega^l\phi \\ \phi \end{array} \right\}$, where $\phi(x)$ is the complex normal mode shape. Substituting equation (7.23) into equation (7.19) (with $\epsilon = 0$) and equating the coefficients of $e^{i\omega^l\tau}$ and $e^{-i\omega^l\tau}$ separately from both sides, one gets

$$i\omega^l \mathbf{A}_1\Phi + \mathbf{B}_1\Phi = \mathbf{0} \tag{7.24}$$

and its complex conjugate, respectively. It is to be pointed out that the partial derivatives appearing in $\mathbf{A}_1$ and $\mathbf{B}_1$ (see equation (7.19)) are replaced by total derivatives in equation (7.24) which is now solved together with the boundary conditions to determine ω^l's and ϕ's. The n-th natural frequency and mode shape so obtained are denoted by ω_n^l and ϕ_n, respectively.

It should be noted that the above solution is to be obtained numerically. In stead of solving equation (7.24), which contains several non-analytic functions, it is broken in two domains as explained in Section 7.2. Thus, equation (7.24) is reduced to

$$-(\omega^l)^2\phi_j + 2ic\omega^l\frac{\mathrm{d}\phi_j}{\mathrm{d}x_j} + (c^2 - T_j)\frac{\mathrm{d}^2\phi_j}{\mathrm{d}x_j^2} + \frac{\mathrm{d}^4\phi_j}{\mathrm{d}x_j^4} = 0, \tag{7.25}$$

with j=1, 2. The matching conditions at $x = d$ are still given by equation (7.22) with the partial derivatives replaced by the total derivatives and w replaced by ϕ. Assuming the solution in the form

$$\phi_j(x_j) = \sum_{k=1}^{4} \alpha_{jk}e^{p_{jk}x_j}, \quad j = 1,2$$

and applying the boundary conditions, one obtains

$$\left\{ \begin{array}{c} \alpha_{11} \\ \alpha_{12} \end{array} \right\} = [K_1] \left\{ \begin{array}{c} \alpha_{13} \\ \alpha_{14} \end{array} \right\}$$

and

$$\left\{ \begin{array}{c} \alpha_{21} \\ \alpha_{22} \end{array} \right\} = [K_2] \left\{ \begin{array}{c} \alpha_{23} \\ \alpha_{24} \end{array} \right\}.$$

The four unknowns α_{13}, α_{14}, α_{23} and α_{24} are now substituted in the matching conditions to obtain a relation like

$$[K_0] \left\{ \begin{array}{c} \alpha_{13} \\ \alpha_{14} \\ \alpha_{23} \\ \alpha_{24} \end{array} \right\} = 0. \tag{7.26}$$

The existence of a non-trivial solution implies

$$\det [K_0] = 0. \tag{7.27}$$

Since the matrix $[K_0]$ is a complex one, both the real and imaginary parts of the determinant must vanish simultaneously. The values of ω^l and p_{jk}'s $(j,k = 1,2,3,4)$ are obtaind numerically by solving equations (7.25) and (7.27).

Considering the symmetric and antisymmetric nature of the matrices A_1 and B_1, respectively, the following orthogonality relations amongst the complex modes ϕ_n's and their conjugates are easily obtained:

$$\int_0^1 \Phi_m^T \mathrm{A}_1 \Phi_n \, dx = 0 \text{ for all } m \text{ and } n, \tag{7.28}$$

and

$$\int_0^1 \overline{\Phi}_m^T \mathrm{A}_1 \Phi_n \, dx = 0 \text{ for all } m \neq n. \tag{7.29}$$

The above normal modes are used, as in Chapter 2, to derive the response of such a beam, when an external force $f(x,\tau)$ is applied. Following the procedure detailed

in Chapter 2, the steady-state response of the beam to a harmonic excitation, i.e., $f(x,\tau) = f(x)\cos\Omega\tau$, can be obtained by solving the following equation of motion:

$$\mathrm{A}_1\frac{\partial W}{\partial \tau} + \mathrm{B}_1 W = \mathrm{f}, \tag{7.30}$$

$$\text{with} \quad \mathrm{f} = \{f(x,\tau),\ 0\}^T. \tag{7.31}$$

The steady-state response $W(x,\tau)$ is finally given by

$$W(x,\tau) = \frac{1}{2}\sum_{n=1}^{\infty}(p_n\Phi_n + q_n\overline{\Phi}_n)e^{i\Omega\tau} + c.c., \tag{7.32}$$

where

$$p_n = \tilde{p}_n e^{i\theta_{pn}} = \frac{2\int_0^1 \overline{\Phi}_n^T \mathrm{f}_1\,\mathrm{d}x}{i(\Omega-\omega_n^l)\int_0^1 \overline{\Phi}_n^T \mathrm{A}_1\Phi_n\,\mathrm{d}x} \tag{7.33}$$

and

$$q_n = \tilde{q}_n e^{i\theta_{qn}} = \frac{2\int_0^1 \Phi_n^T \mathrm{f}_1\,\mathrm{d}x}{i(\Omega+\omega_n^l)\int_0^1 \overline{\Phi}_n^T \mathrm{A}_1\Phi_n\,\mathrm{d}x}, \tag{7.34}$$

with $\mathrm{f}_1 = \{f(x)/2,\ 0\}^T$. It is readily seen that at or near resonance the magnitude of p_n will be very high. Hence the aim of controlling the vibration is to reduce the value of p_n.

7.3.1 Numerical Results and Discussion

Numerical results obtained from the linear analysis (presented in the previous section) are now discussed. All the results, unless otherwise mentioned, apply to a travelling beam having a tension $T_2 = 1$. The important physical parameters which control the performance of the system are

1) the speed of the beam, expressed as a parameter $c' = c/(c_{cr})_1$ where $(c_{cr})_1 = \sqrt{\pi^2 + T_2}$,

2) the location of the guide, d,

3) the stiffness of the guide, K_f and

4) the coefficient of friction between the beam and the guide, μ_f.

As shown in Chapter 2, an increase in the axial speed reduces the natural frequencies of vibration of a beam without any intermediate guide. The same effect is also observed even in the presence of a guide. In Figure 7.2, the first and second natural frequencies are plotted against the axial speed for various values of K_f. For the chosen guide location, i.e., $d = 0.5$, the second natural frequency, ω_2^l, as expected, is insensitive to any change in the stiffness K_f. However, the first natural frequency ω_1^l, and consequently the first critical speed considerably increases with increasing K_f. Thus, for large values of K_f (i.e., when the guide behaves like a rigid support), the first natural frequency of the guided beam tends towards the second natural frequency of the unguided beam.

Figures 7.3 and 7.4 show the variation of the natural frequencies with the guide location. It is observed that the first natural frequency ω_1^l is maximum with $d = 0.5$, whereas the value of ω_2^l attains a maximum when $d = 0.25$ and $d = 0.75$. For a stationary simply-supported beam, the point $x = 0.5$ corresponds to the antinode of the first mode and the node of the second mode. Although the concepts of nodes and antinodes can not be used for a travelling beam, the response envelope, however, attains a maximum or minimum at $x = 0.5$ when the beam vibrates at its first or second natural frequency, respectively. Similarly, for the second natural frequency, the response envelope reaches a maximum value at $x = 0.25$ and $x = 0.75$. Thus, from this example, it is confirmed that the guide makes the system most stiff if it is placed where the response envelope reaches its maximum. Attention may be drawn to one of the general results for a constrained flexible system, known as the 'eigenvalue-inclusion principle'. For a gyroscopic system, it has been shown [30] that for a beam or string having a stiffness constraint, the n-th natural frequency of a constrained system (say

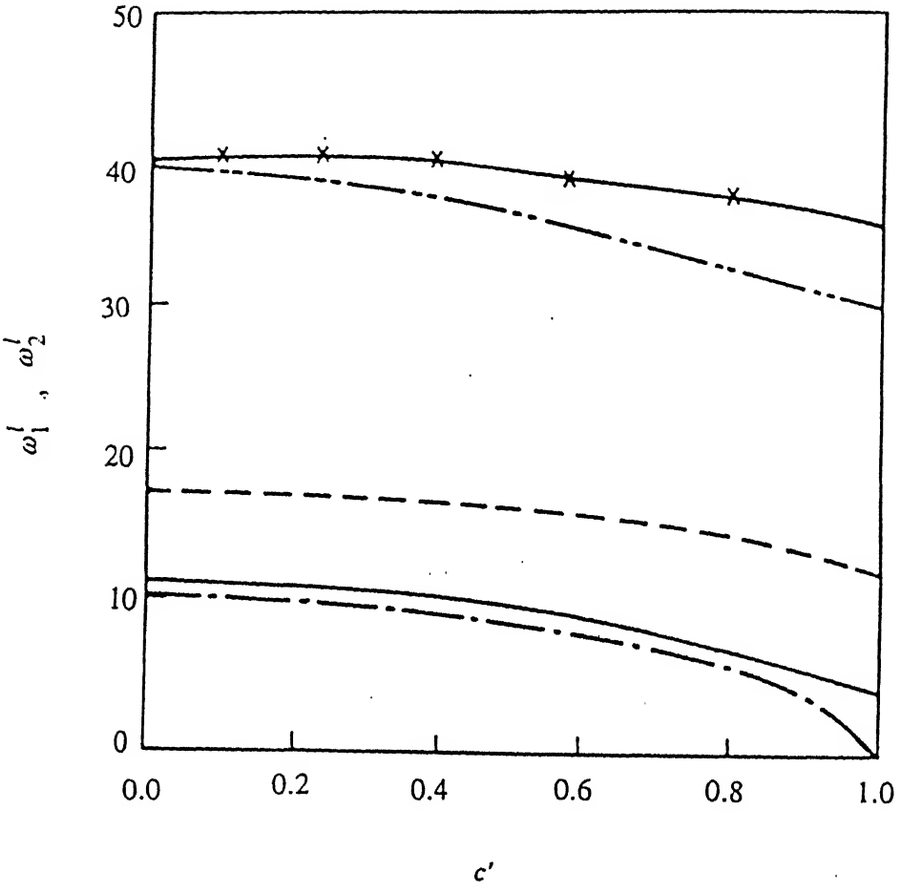

Figure 7.2: Variation of ω_1^l and ω_2^l with c'. $d = 0.5$, $\Delta T = 0$,— · — : ω_1^l with no guide; —— : ω_2^l, $K_f = 10$, - - - - : ω_1^l, $K_f = 100$, — - - — : ω_1^l, $K_f = 1000$, —×— : ω_2^l, $K_f = 0, 10, 100, 1000$.

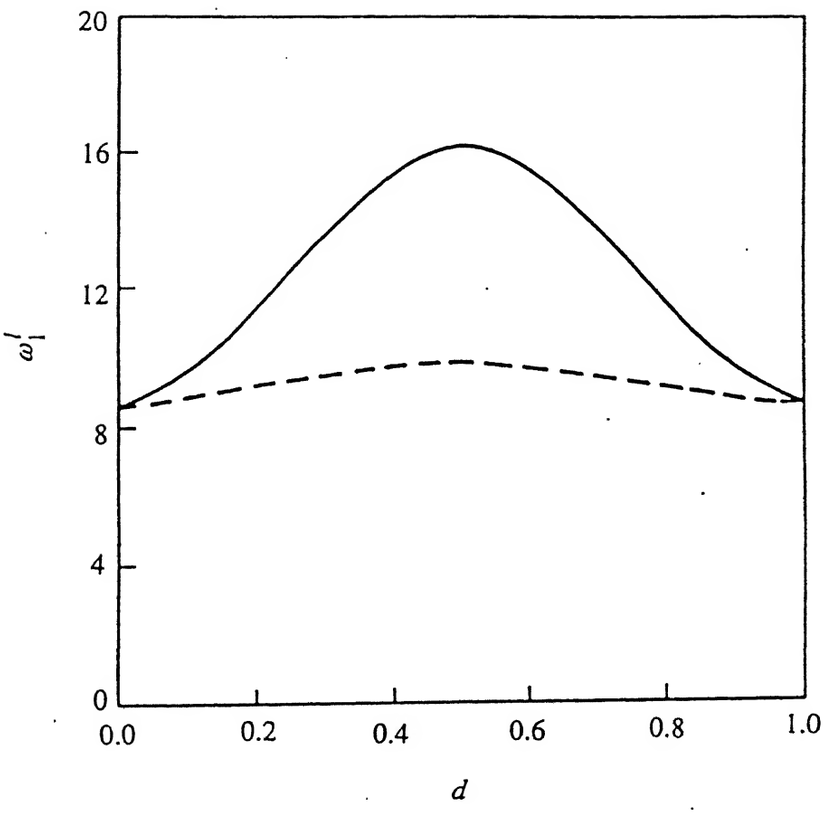

Figure 7.3: Variation of ω_1' with the guide-location. $c' = 0.5$, $\Delta T = 0$, - - - - : $K_f = 10$, —— : $K_f = 100$.

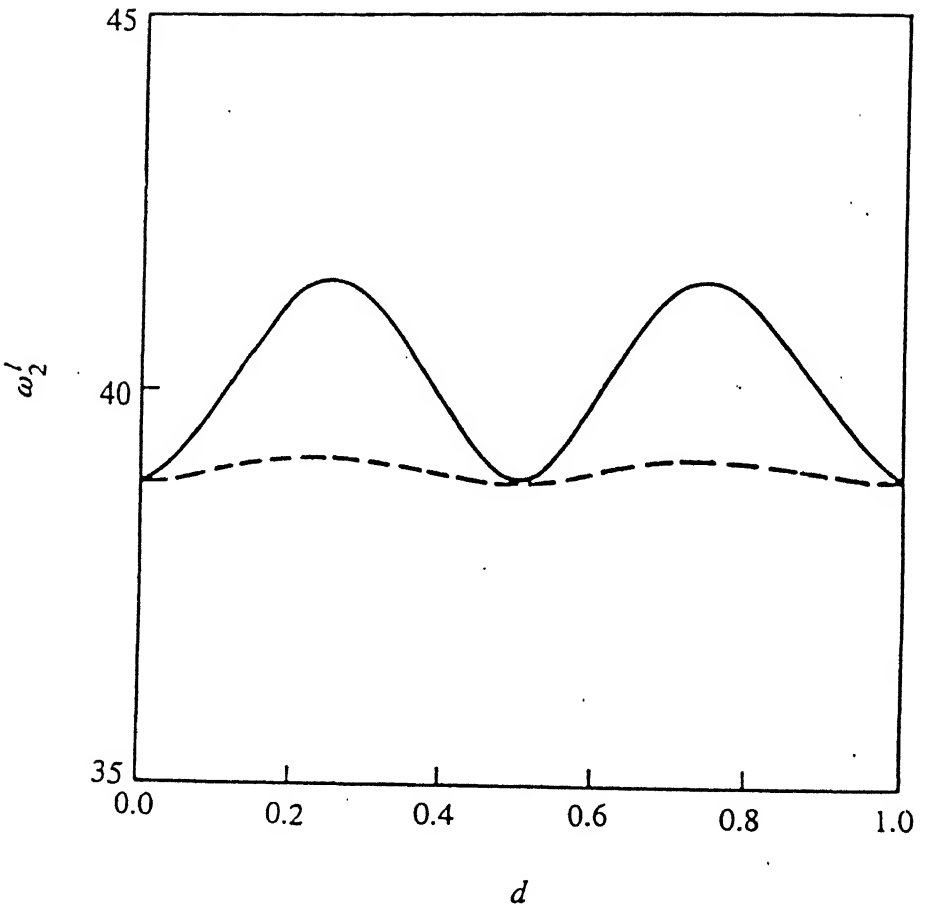

Figure 7.4: Variation of ω_2' with the guide-location. $c' = 0.5$, $\Delta T = 0$, - - - - : $K_f = 10$, —— : $K_f = 100$.

$\Omega_n^{(c)}$) satisfies the following inequalities

$$\omega_n^{(nc)} \leq \Omega_n^{(c)} \leq \omega_{n+1}^{(nc)},$$

where $\omega_n^{(nc)}$ is the n-th natural frequency of the unconstrained system. Numerical results obtained for the guided travelling beam are in conformity with the above result.

Figure 7.5 shows the variation of ω_1^l with the coefficient of guide friction, μ_f. It is seen that the friction reduces the stiffness of the system. From equation (7.21), it can be concluded that the friction introduces a compressive load in the first span $(0 < x < d)$. This compressive load may become so high that the span may undergo divergence instability, as shown in Figure 7.5. Thus, in addition to damaging the beam surface, the presence of friction may cause instability in the system.

For a guided travelling beam no 'frequency-loci veering' has been observed. This supportes the observation reported in reference [47]. The non-cyclic disordered beam discussed in this reference corresponds to the present model with $K_f \to \infty$ and $d = 0.5$. However, the phenomena of 'frequency-loci veering' and 'mode localization' have been observed for a guided travelling string [29].

The effect of the intermediate guide on the steady-state harmonic response is shown in Figure 7.6. Only the magnitude of p_1 is plotted for a beam excited by a point harmonic load $f(x) = F_0\delta(x-x_0)$ at $x_0 = 1/3$ with the excitation frequency $\Omega \approx \omega_1^l$. By changing the natural frequency, the guide helps to avoid the resonance at a particular speed. As expected, the near-resonance response decreases with increasing stiffness of the guide.

Figures 7.7 and 7.8 show the effects of the guide-location on the steady-state response. As seen from these figures, the guide when suitably placed can attenuate the response level of a resonantly excited beam. As the application of the guide shifts the natural frequency, the resonance condition can be avoided. If the guide is flexible, then

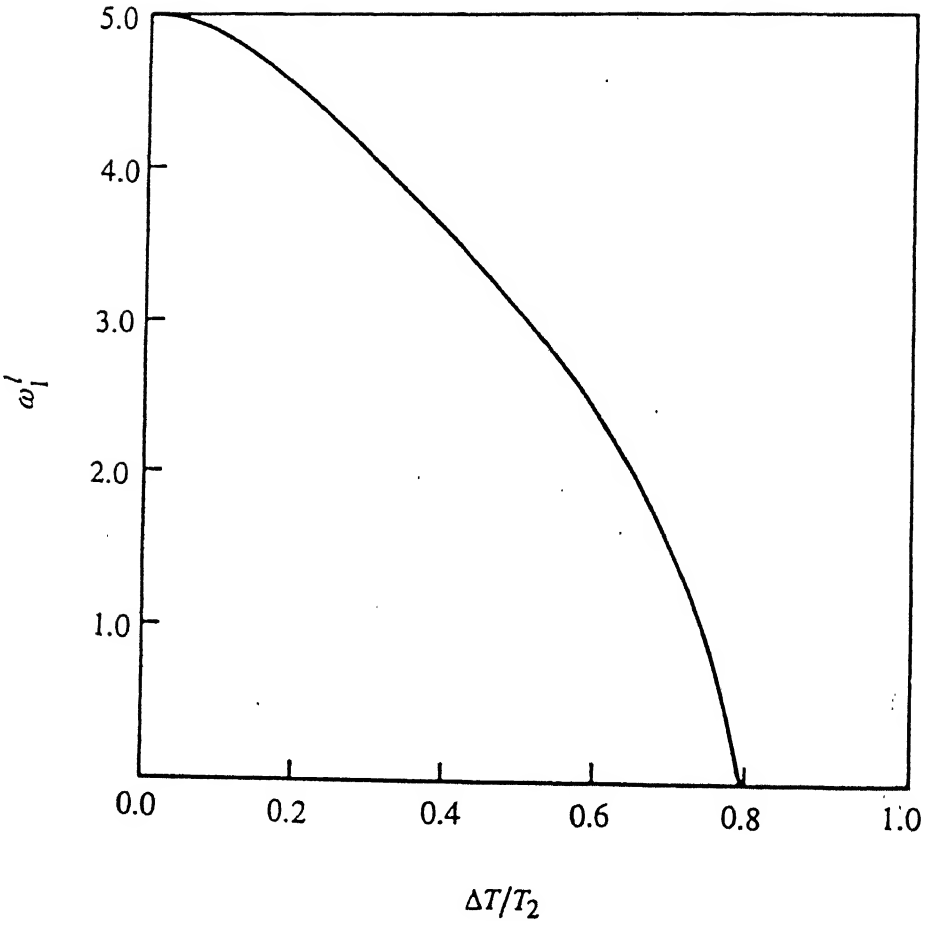

Figure 7.5: Variation of ω_1' with ΔT. $c' = 0.95$, $T_2 = 10.0$, $d = 0.5$, $K_f = 10$.

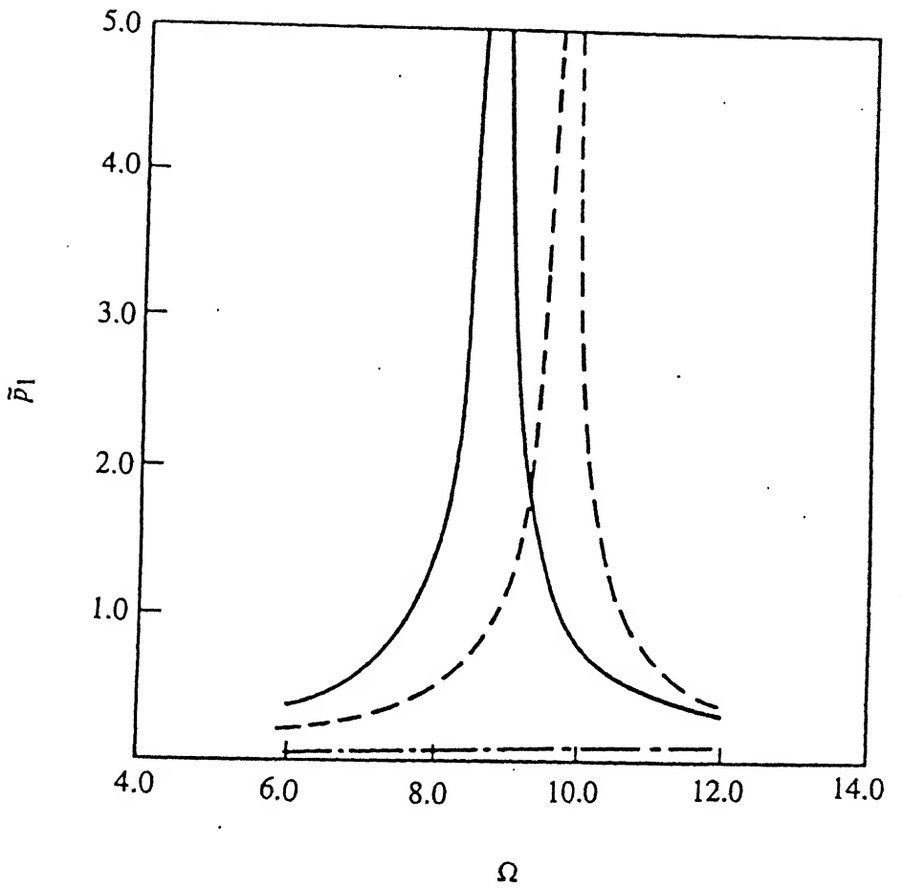

Figure 7.6: Amplitude of the frequency response of the first linear mode. $F_0 = 10$, $\Delta T = 0$, $c' = 0.5$, $d = 0.5$; —— : no guide ($K_f = 0$), - - - - : $K_f = 10$, — · — : $K_f = 100$.

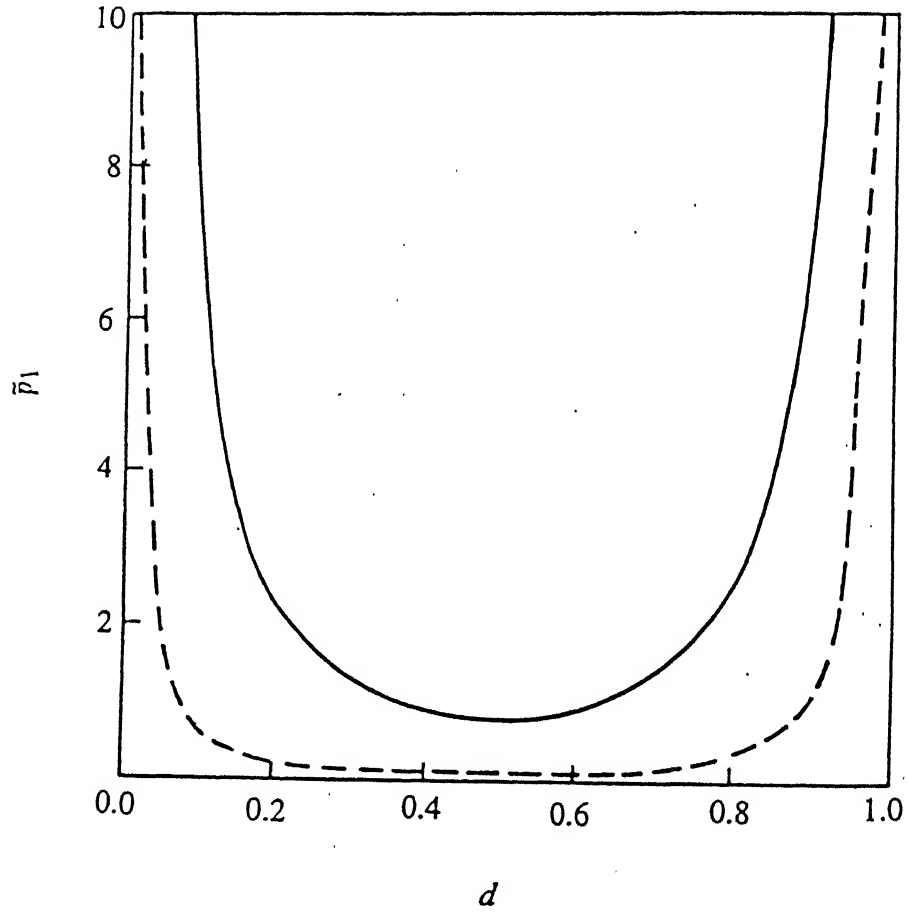

Figure 7.7: Effect of the guide-location on $\tilde{p}_1$. $c' = 0.5$, $\Delta T = 0$, $\Omega = 8.7$, $F_0 = 10$; —— : $K_f = 10$, - - - - : $K_f = 100$.

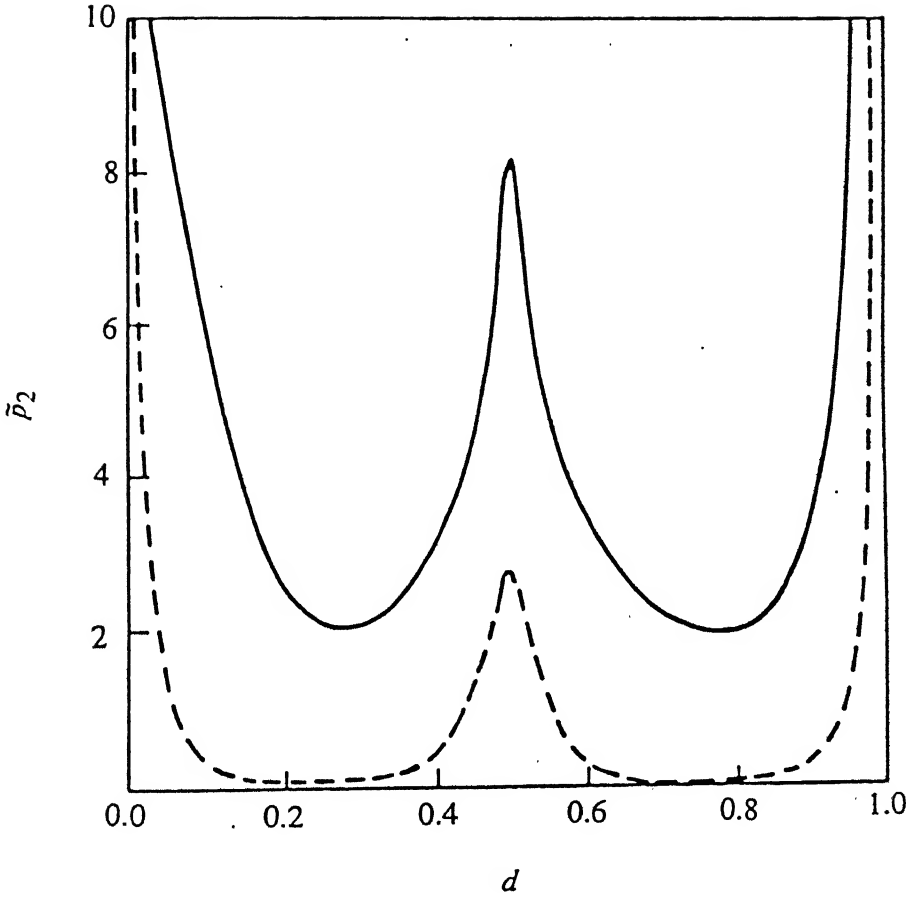

Figure 7.8: Effect of the guide-location on $\tilde{p}_2$. $c' = 0.5$, $\Delta T = 0$, $\Omega = 39.0$, $F_0 = 10$; —— : $K_f = 10$, - - - - : $K_f = 100$.

its optimal location corresponds to the position where the response envelope attains a maximum and depends on the mode which is resonantly excited. In other words, to minimize the vibration, the guide is placed at a location where the response of the uncontrolled system is maximum. However, as the stiffness of the guide increases, the location of the guide looses its importance as long as it does not coincide with any of the nodal points of the response envelope. The shift of the natural frequency, after placing the stiff guide anywhere within two successive nodal points, is so large that the response amplitude becomes practically insensitive to the guide-location.

7.4 Effects of Non-Linearity

In this section, the effects of non-linearity on the free and near-resonance forced responses are presented. It may be mentioned that the relationship between different linear natural frequencies depends on the various system parameters. Some typical relationships may give rise to internal and combinatorial resonances, which are not considered in this work. Thus, only such combinations of parameters are taken where all the natural frequencies are distinct and no special relation between them exists. For such a system, the free and near-resonance forced harmonic responses are analysed.

In the absense of any internal resonance, the harmonic response of a free travelling beam has already been presented in Chapter 4. Following similar method first the complex non-linear normal modes are obtained for this constrained system. For free vibration in the n-th non-linear normal mode, the response is assumed as

$$W(x,\tau) = \frac{a}{2}\Psi_n(x)e^{i\omega_n\tau} + \frac{\overline{a}}{2}\overline{\Psi}_n(x)e^{-i\omega_n\tau}, \tag{7.35}$$

where $\Psi_n = \left\{ \begin{array}{c} i\omega_n\psi_n \\ \\ \psi_n \end{array} \right\}$, with ψ_n and ω_n as the n-th non-linear mode shape and the corresponding frequency, respectively. Both these quantities, however, are amplitude

dependent. Following the method outlined in Chapter 4, ω_n and Ψ_n can be derived, respectively, as

$$\omega_n = \omega_n^l + \epsilon\beta_1^{(n)} + \cdots, \tag{7.36}$$

$$\Psi_n = \Phi_n + \epsilon\Delta_1 + \cdots, \tag{7.37}$$

where

$$\beta_1^{(n)} = -\frac{\omega_n^l}{4} a\bar{a}\frac{\lambda(\overline{\phi}_n, \phi_n)}{t_n}, \tag{7.38}$$

$$\Delta_1 = a\bar{a}\left[\sum_{m\neq n} g_m\Phi_m + \sum_{m=1}^{\infty} h_m\overline{\Phi}_m\right], \tag{7.39}$$

with

$$g_m = -\frac{1}{4}\frac{\omega_m^l}{\omega_n^l - \omega_m^l}\frac{\lambda(\overline{\phi}_m, \phi_n)}{t_n}, \quad m \neq n$$

$$h_m = \frac{1}{4}\frac{\omega_m^l}{\omega_n^l + \omega_m^l}\frac{\lambda(\phi_m, \phi_n)}{t_n}, \quad m = 1, 2, 3, \cdots$$

$$t_n = \int_0^1 \overline{\Phi}_n^T \mathbf{A}_1 \Phi_n \, \mathrm{d}x, \quad n = 1, 2, 3, \cdots$$

and

$$\lambda(\phi_m, \phi_n) = 2\left(\int_0^1 \phi_m \frac{\mathrm{d}^2\phi_n}{\mathrm{d}^2x}\,\mathrm{d}x\right)\left(\int_0^1 \frac{\mathrm{d}\phi_n}{\mathrm{d}x}\frac{\mathrm{d}\overline{\phi}_n}{\mathrm{d}x}\,\mathrm{d}x\right) + \left(\int_0^1 \phi_m \frac{\mathrm{d}^2\overline{\phi}_n}{\mathrm{d}x^2}\,\mathrm{d}x\right)\left(\int_0^1 \left(\frac{\mathrm{d}\phi_n}{\mathrm{d}x}\right)^2 \mathrm{d}x\right).$$

The above-mentioned non-linear complex normal modes can be used to obtain the near-resonance harmonic response of the beam when excited by an external force $f(x)\cos\Omega\tau$, i.e., to solve the equation of motion

$$\mathbf{A}_1\frac{\partial W}{\partial \tau} + \mathbf{B}_1 - \epsilon\mathbf{N} = \mathbf{f}, \tag{7.40}$$

where $\mathbf{f} = \{f(x)\cos\Omega\tau\ ,\ 0\}^T$.

The principal harmonic response of the beam can be assumed as

$$W(x,\tau) = \frac{1}{2}\left(\Lambda(x)e^{i\Omega\tau} + \overline{\Lambda}(x)e^{-i\Omega\tau}\right). \tag{7.41}$$

For the near-resonance excitation $\Omega \approx \omega_n^l$, the following response is obtained :

$$\Lambda = a_n \Psi_n + \epsilon \sum_{m \neq n}^{\infty} a_m \Psi_m + \epsilon \sum_{m=1}^{\infty} b_m \overline{\Psi}_m + O(\epsilon^2). \tag{7.42}$$

One can follow the steps detailed in Chapter 4 (see Section 4.3) to get the following results, valid up to $o(\epsilon)$:

$$a_n = \frac{2 \int_0^1 \overline{\Psi}_n^T \mathbf{f}_1 \, dx}{i(\Omega - \omega_n) \int_0^1 \overline{\Psi}_n^T \mathbf{A}_1 \Psi_n \, dx}, \tag{7.43}$$

$$\epsilon a_m = \frac{2 \int_0^1 \overline{\Phi}_m^T \mathbf{f}_1 \, dx}{i(\Omega - \omega_m^l) \int_0^1 \overline{\Phi}_m^T \mathbf{A}_1 \Phi_m \, dx}; \; m \neq n$$

and

$$\epsilon b_m = \frac{2 \int_0^1 \Phi_m^T \mathbf{f}_1 \, dx}{i(\Omega + \omega_m^l) \int_0^1 \overline{\Phi}_m^T \mathbf{A}_1 \Phi_m \, dx}; \; m = 1, 2 \cdots,$$

where $\mathbf{f}_1 = \{f(x)/2, \; 0\}^T$. The complex cubic equation (7.43) can be solved numerically. Assuming

$$a_n = \tilde{a}_n e^{i\theta_n},$$

equation (7.43), for a point load $f(x) = F_0 \delta(x - x_0)$, takes the form of equation (4.35) which is reproduced below:

$$A^6 + \left[\frac{2\omega_n^l (1 - r_1)}{S} - \nu \left((M_1^R)^2 + (M_1^I)^2 \right) \right] A^4 + \left[\frac{(\omega_n^l)^2 (1 - r_1)^2}{S^2} - 2\nu (M_1^R Q_1^R + M_1^I Q_1^I) \right] A^2$$
$$- \nu \left[(Q_1^R)^2 + (Q_1^I)^2 \right] = 0, \tag{7.44}$$

where

$$Q_1 = -\frac{\omega_n^l}{F_0} \int_0^1 \overline{\phi}_n f \, dx = Q_1^R + i Q_1^I,$$

$$M_1 = \frac{1}{F_0} \left\{ - \sum_{m \neq n} \overline{g}_m \omega_m^l \int_0^1 \overline{\phi}_m f \, dx \right\} + \frac{1}{F_0} \left\{ \sum_{m=1}^{\infty} \overline{h}_m \omega_m^l \int_0^1 \phi_m f \, dx \right\} = M_1^R + i M_1^I,$$

$$S = \frac{\beta_1^{(n)}}{\tilde{a}_n^2} \; r_1 = \frac{\Omega}{\omega_n^l}, \; \nu = \left(\frac{F_0}{t_n} \right)^2 \frac{\epsilon}{S^2}, \; A = \sqrt{\epsilon} \tilde{a}_n.$$

It may be mentioned that depending upon the system parameters, either one, or three roots may exist. As shown in Chapter 4, the intermediate root is always unstable and is not observable in reality. It was also shown in Chapter 4 that the steady-state response of the beam, up to the order $o(1)$, is

$$w(x,\tau) = \tilde{a}_n \phi_1^*(x) \cos(\Omega\tau + \theta_n + \rho_n),$$

where $\tan \rho_n = -\phi_1^I/\phi_1^R$ and $\phi_1^* = \sqrt{(\phi_1^R)^2 + (\phi_1^I)^2}$.

7.4.1 Numerical Results and Discussion

In this section, numerical results showing the effect of non-linearity on the free and forced responses of a guided travelling beam are presented. The tension of the beam, T_2, is again taken as unity, i.e., $T_2 = 1$.

Owing to the presence of the non-linear term, the natural frequency shows a hardening characteristics, since the term $\beta_1^{(n)}/a\overline{a}$ (see equation (7.36)) is positive. In Figure 7.9, the variation of $\beta_1^{(1)}/a\overline{a}$ with the guide location, d, is shown. As seen from the figure, the non-linear effects depend strongly on the location and the stiffness of the guide.

As is well known, the linear theory, when compared with the non-linear theory for such a hard system, over-estimates the steady-state response when the excitation frequency is equal to the natural frequency i.e,. $\Omega = \omega_n^l$ and under estimates the response when $\Omega > \omega_n^l$. Therefore, special attention should be given to the response for $\Omega > \omega_n^l$. Figure 7.10 shows the variation of amplitude with the guide location. Where more than one value of the amplitude A are obtained from equation (7.44) (with $n = 1$), the higher stable amplitude is plotted. Three excitation frequencies $\Omega = 8.7, 12$ and 15 are considered. These frequencies are such that the first mode is primarily excited. The significance of the choice of the guide location, so far as the

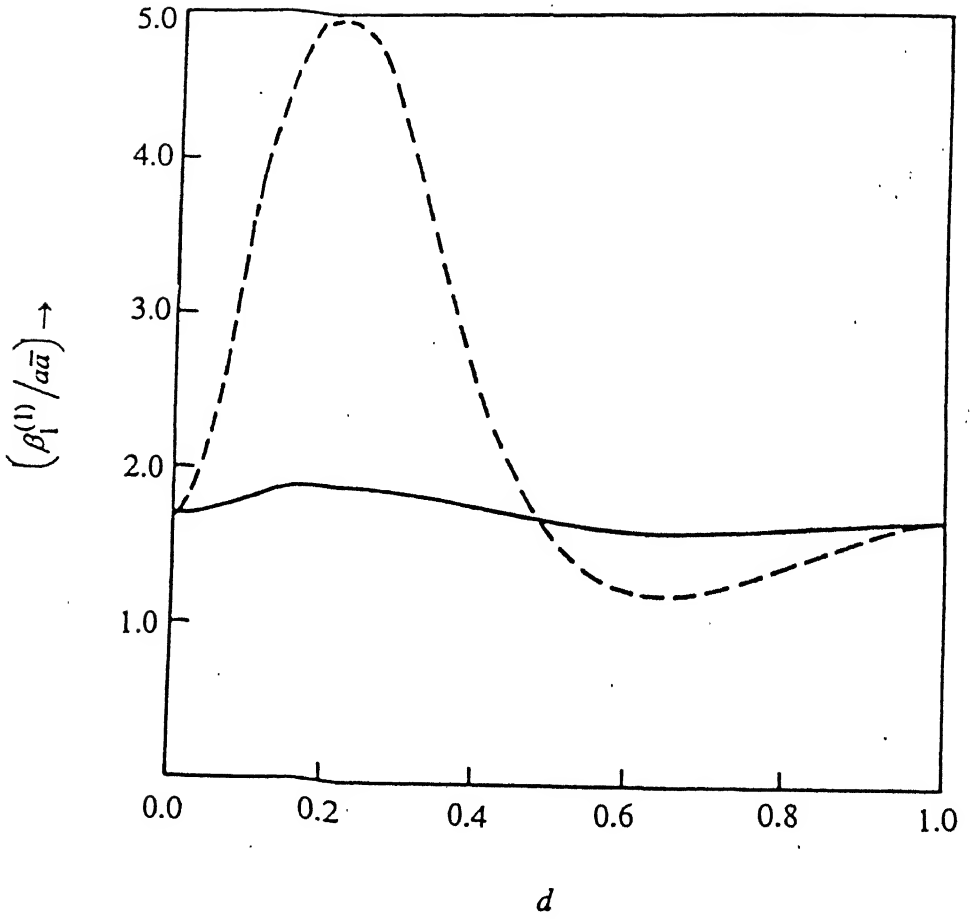

Figure 7.9: Effect of the guide-location on $\beta_1^{(1)}/a\bar{a}$. $c' = 0.5$, $\Delta T = 0$; —— : $K_f = 10$, - - - - : $K_f = 100$.

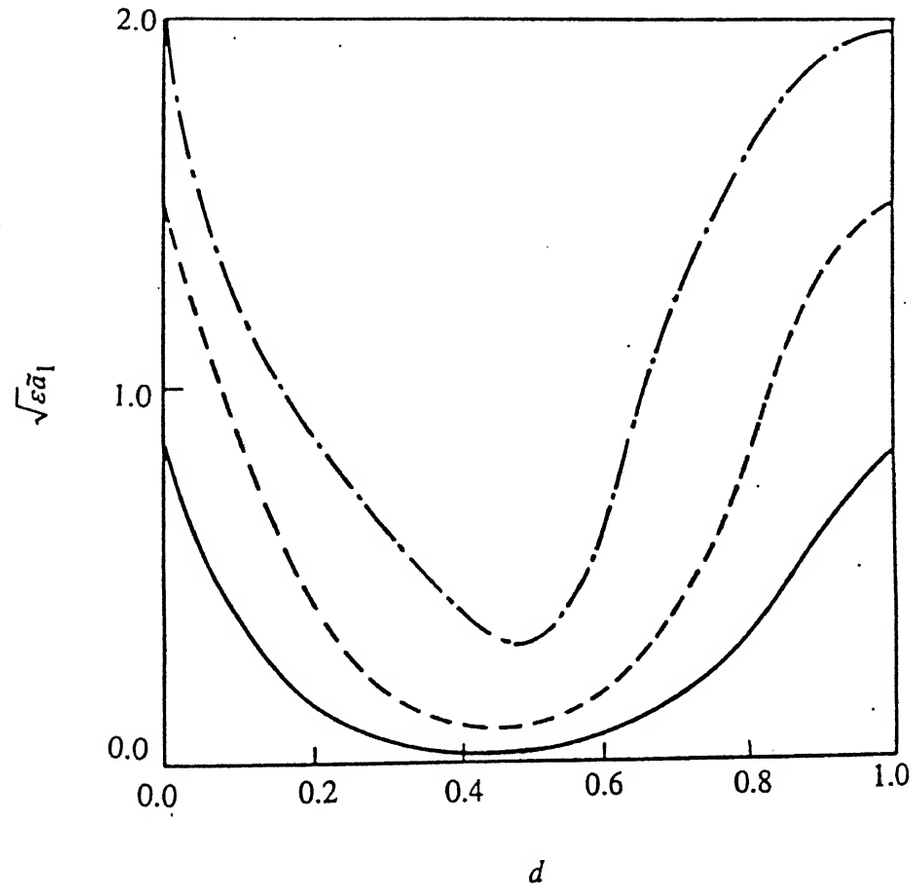

Figure 7.10: Effect of the guide-location on the maximum value of the roots of equation (7.44). $c' = 0.5$, $\Delta T = 0$, $K_f = 100$, $F_0\sqrt{\epsilon} = 10$; —— : $\Omega = 8.7$, - - - - : $\Omega = 12$, — · — : $\Omega = 15$.

maximum amplitude is concerned, can be clearly seen in Figure 7.10. It is seen that for $\Omega = 8.7$ (i.e., $\Omega < \omega_1^l = 10.87$), the non-linear response is less compared to the linear response. If a guide is placed, the linear natural frequency increases (see Section 7.3) and the excitation frequency becomes much less compared to the natural frequency, i.e., the frequency at which the resonance occurs. For a suitable guide-location, the difference between the excitation and the natural frequencies becomes so large that the effect of non-linearity is hardly perceptable. When $\Omega > \omega_1^l$ (for example, $\Omega = 12$ or 15), the response amplitude predicted by the linear theory is much smaller than that obtained by the non-linear analysis. If a guide is now placed, ω_1^l approaches Ω and the response amplitude decreases which is a typical characteristic of a hard system. It is to be pointed out that even if the linear theory may not suggest the requirement of a guide by under-estimating the response, a guide may be required because of the presence of the non-linear term.

Chapter 8

CONCLUSIONS

8.1 Conclusions

Different aspects of non-linear vibration of a travelling beam are studied in this thesis. The effects of the geometrical non-linear term taken as a small perturbation to the linear equation of motion of the beam are obtained by extending the results of linear vibration. Both complex modal analysis and wave-propagation theory are used to study the free and forced vibrations of a linear travelling beam. An idea of 'non-linear complex normal modes', similar to the 'non-linear normal modes' for axially stationary systems, has been introduced. These non-linear complex normal modes are used to obtain the near-resonance response under an external harmonic and/or parametric excitations. For a non-resonantly excited beam, the non-linear response is obtained using the results of the wave-propagation analysis. The effects of non-linearity on a non-uniformly moving beam has also been studied. A simple vibration controller in the form of a roller guide has been suggested. The major conclusions of the analyses presented in the thesis can be summarized as listed below:

(i) The natures of the waves associated with the free modal vibration of a travelling

beam change depending upon the relations between various system parameters. During linear modal vibration, either two propagating and two evanescent waves (one of each kind in both upstream and downstream directions) or four propagating waves (one in the upstream direction and the remaining three in the downstream direction) appear depending on the axial speed. The well-known 'phase-closure' principle is satisfied for both the cases. The 'phase-closure' principle is also satisfied during non-linear modal oscillations of such a beam.

(ii) The near-resonance response to an external harmonic and/or parametric excitation can be obtained easily using the non-linear complex normal modes. This method is computationally more efficient than the commonly-used Galerkin's technique.

(iii) The steady-state response of the beam to a non-resonant hard excitation can be obtained by wave-propagation analysis. In this method, a closed form transfer function, i.e., the Laplace transform of a point-impulse response, is first obtained. The linear response obtained using this transfer function is then perturbed to get the effects of the small non-linear term. The present method is shown to be more accurate and computationally more efficient than either Galerkin's technique or non-linear complex modal analysis.

(iv) The non-linear natural frequencies of a travelling beam increase with the amplitude of vibration. The 'jump' of the amplitude of the response envelope can be observed under a near-resonant excitation. Further, one or multiple 'limit cycle's of the amplitude of the response envelope are possible when the beam is parametrically excited. These three phenomena show striking resemblance with those exhibited by a hard Duffing oscillator.

(v) For a parametrically excited travelling beam with an external harmonic excitation, the effects of various system parameters depend on the relative strengths of the two forms of excitation. Moreover, a particular phase relationship between the two forms

of excitations (whose frequencies are related) results in a minimum value of the steady-state response.

(vi) A continuously accelerating beam remains stable, but for a decelerating beam instability may appear depending upon the magnitudes of damping and deceleration. However, the amplitude of a decelerating beam does not grow unboundedly and the beam regains its stability in the long run. The non-linear term does not play any role so far as the stability is concerned. It merely changes the frequencies of oscillations.

(vii) An intermediate guide can be effectively used as a passive controller of vibration. The choice of the suitable guide-location plays a very important role in reducing the level of vibration. The guide also has a stabilizing effect so far as the divergence instability is concerned. But the frictional force between the guide and beam may add to instability. Thus, to use the controller effectively, the friction has to be minimised. Towards this end, a roller-guide is suggested.

8.2 Scope of Future Work

The follwing are the directions along which future researches can be motivated:

(i) The vibrations of the travelling beam having a single span have been considered in this thesis. A natural extension of these studies to multi-span beams (for example, band/wheel systems) can be carried out.

(ii) The equilibrium configuration of the beam has been taken to be trivial. However, the case where the beam has initial transverse deflection deserves further attention.

(iii) The study can be extended to the beams having imperfections like weld melts etc..

(iv) Chaotic behaviour and the associated statistical properties of the non-linear response have not been considered in the present work. These can be taken as the subjects for further investigations.

Appendix A

Proof of Identity (2.23) and (2.47)

The identity can be easily proved by first noting the following fact [153]. For a block matrix

$$[M] = \begin{bmatrix} [M_1] & [M_2] \\ [M_3] & [M_4] \end{bmatrix},$$

$$\det[M] = \det[M_1]\det[M_4]\det\left(I - [M_4]^{-1}[M_3][M_1]^{-1}[M_2]\right).$$

Assuming the members of matrix $[M]$ as,

$$[M_1] = \begin{bmatrix} e^{ik_2} & e^{ik_4} \\ k_2^2 e^{ik_2} & k_4^2 e^{ik_4} \end{bmatrix}, \; [M_2] = \begin{bmatrix} e^{ik_1} & e^{ik_3} \\ k_1^2 e^{ik_1} & k_3^2 e^{ik_3} \end{bmatrix},$$

$$[M_3] = \begin{bmatrix} 1 & 1 \\ k_2^2 & k_4^2 \end{bmatrix}, \; [M_4] = \begin{bmatrix} 1 & 1 \\ k_1^2 & k_3^2 \end{bmatrix},$$

and performing a few row operations, one can easily verify that equation (2.23) turns out to be identical with the following :

$$\det[M] = 0.$$

Further, it can also be noticed that $[R_4][R_3][R_2][R_1] = [M_4]^{-1}[M_3][M_1]^{-1}[M_2]$, where $[R_j]$'s are the same as appearing in equation (2.47). Thus, $\det[M] = 0$ also implies

equation (2.23).

Appendix B

Forced Response of a Travelling String

For a linear travelling string, equation (2.60) is replaced by

$$s^2\hat{w} + 2sc\frac{\partial \hat{w}}{\partial x} + (c^2 - 1)\frac{\partial^2 \hat{w}}{\partial x^2} = \delta(x - x_0)e^{-s\tau_0}. \tag{B.1}$$

The response, from the wave-propagation analysis, formulated in Section 2.4.2, is obtained as

$$\hat{w}(x,s) = C_1 e^{\lambda_1 x} + C_2 e^{\lambda_2 x} + D_2 e^{\lambda_2(x-x_0)} \text{ for } x \geq x_0\,, \tag{B.2}$$

$$= C_1 e^{\lambda_1 x} + C_2 e^{\lambda_2 x} - D_1 e^{\lambda_1(x-x_0)} \text{ for } x < x_0\,, \tag{B.3}$$

where $\lambda_1 = ik_1 = s/(1-c)$, $\lambda_2 = ik_2 = -s/(1+c)$, $D_1 = -e^{-s\tau_0}/2s$, $D_2 = e^{-s\tau_0}/2s$.

Applying the boundary conditions $\hat{w}(0,s) = \hat{w}(1,s) = 0$, the following expressions of C_1 and C_2 are obtained:

$$C_1 = e^{-s\tau_0}\left[e^{\lambda_2 - \lambda_1 x_0} - e^{\lambda_2(1-x_0)}\right]/2s(e^{\lambda_1} - e^{\lambda_2})$$

and

$$C_2 = e^{-s\tau_0}\left[e^{\lambda_2(1-x_0)+\lambda_1} - e^{\lambda_1(1-x_0)}\right]/2s(e^{\lambda_1} - e^{\lambda_2}),$$

which, when substituted into equations (B.2) and (B.3), yield

$$\hat{w}(x,s) = \left[e^{\lambda_2(x-x_0)} - e^{\lambda_2 x-\lambda_1 x_0} - e^{\lambda_2(1-x_0)-\lambda_1(1-x)} + e^{\lambda_2-\lambda_1(1+x_0-x)}\right] \times \frac{e^{-s\tau_0}}{2s(1-e^{\lambda_2-\lambda_1})} \quad \text{for } x \geq x_0, \tag{B.4}$$

$$= \left[-e^{\lambda_2 x-\lambda_1 x_0} + e^{\lambda_2(1-x-x_0)-\lambda_1} + e^{-\lambda_1(x_0-x)} - e^{\lambda_2(1-x_0)-\lambda_1(1-x)}\right] \times \frac{e^{-s\tau_0}}{2s(1-e^{\lambda_2-\lambda_1})} \quad \text{for } x < x_0. \tag{B.5}$$

For $\tau_0 = 0$, the above equations are identical with the transfer function obtained by Yang and Tan [60]. As mentioned therein, $s = 0$ is not a singular point since $\hat{w}(x,s)$ is finite as $s \to 0$. The only singular points are $s = \pm i\omega_n^l = \pm in\pi(1-c^2)$, when $\lambda_1 = \pm in\pi(1+c) = \lambda_1^{(n)}$, and $\lambda_2 = \mp in\pi(1-c) = \lambda_2^{(n)}$.

The temporal response is obtained by inverse Laplace transform of equations (B.4) and (B.5) as:

$$w(x,\tau) = \sum_{n=1}^{\infty} \left[\frac{(e^{\lambda_2^{(n)}x} - e^{\lambda_1^{(n)}x})(e^{-\lambda_2^{(n)}x_0} - e^{-\lambda_1^{(n)}x_0})}{2(1-e^{\lambda_2^{(n)}-\lambda_1^{(n)}}) + 2s\left(\frac{\partial\lambda_1^{(n)}}{\partial s} - \frac{\partial\lambda_2^{(n)}}{\partial s}\right)e^{\lambda_2^{(n)}-\lambda_1^{(n)}}}\right] e^{i\omega_n^l(\tau-\tau_0)} + \text{c.c.} \quad \text{for } \tau \geq \tau_0,$$

or

$$w(x,\tau) = \sum_{n=1}^{\infty} \frac{(e^{\lambda_2^{(n)}x} - e^{\lambda_1^{(n)}x})(e^{-\lambda_2^{(n)}x_0} - e^{-\lambda_1^{(n)}x_0})}{4in\pi} e^{i\omega_n^l(\tau-\tau_0)} + \text{c.c.} \quad \text{for } \tau \geq \tau_0. \tag{B.6}$$

Since for a travelling string, the linear normal mode ϕ_n can be written as $\phi_n = e^{\lambda_2^{(n)}x} - e^{\lambda_1^{(n)}x}$, one can verify that

$$2\omega_n^l \int_0^1 \phi_n \overline{\phi}_n \, \mathrm{d}x - 2ic \int_0^1 \overline{\phi}_n \frac{\mathrm{d}\phi_n}{\mathrm{d}x} \, \mathrm{d}x = 4n\pi. \tag{B.7}$$

Using equations (B.6) and (B.7) the response is finally obtained as

$$w(x,\tau) = \sum_{n=1}^{\infty} \frac{\phi_n(x)\overline{\phi}_n(x_0)}{2\omega_n^l \int_0^1 \phi_n\overline{\phi}_n \, \mathrm{d}x - 2ic\int_0^1 \overline{\phi}_n \frac{\mathrm{d}\phi_n}{\mathrm{d}x} \, \mathrm{d}x} e^{i\omega_n^l(\tau-\tau_0)} + \text{c.c.} \quad \text{for } \tau \geq \tau_0. \tag{B.8}$$

Equation (B.8) is identical to equation (2.55).

Appendix C

Algebraic Equation for Obtaining the Near-Resonance Response

The final algebraic equation, after eliminating θ_n from equations (5.66) and (5.67) for $f(x) = F_0\delta(x - x_0)$, is obtained as

$$
\begin{aligned}
A^5 \;+\; & A^4\left[-\frac{4(\Omega_f-\omega_n^l)}{S}-\nu\left\{(M_1^R)^2+(M_1^I)^2\right\}\right]+A^3\left[\frac{4(\Omega_f-\omega_n^l)^2}{S^2}\right. \\
+\; & \frac{2l_1}{S^2}-2\nu(Q_1^RM_1^R+Q_1^IM_1^I)+\frac{2\nu}{S}\left\{(M_1^R)^2l_2+(M_1^I)^2l_3\right\} \\
+\; & \left.2\nu\frac{M_1^RM_1^I}{S}(l_5-l_4)\right]+A^2\left[-\frac{4(\Omega_f-\omega_n^l)l_1}{S^3}-\nu\left\{(Q_1^R)^2+(Q_1^I)^2\right\}\right. \\
-\; & \frac{\nu}{S^2}\left\{l_2^2(M_1^R)^2+l_3^2(M_1^I)^2+l_4^2(M_1^I)^2+l_5^2(M_1^R)^2\right\} \\
+\; & \frac{4\nu}{S}(l_2Q_1^RM_1^R+l_3Q_1^IM_1^I)+\frac{2\nu}{S^2}M_1^RM_1^I(l_4l_2-l_5l_3) \\
+\; & \left.\frac{2\nu}{S}(l_5-l_4)(M_1^RQ_1^I+Q_1^RM_1^I)\right]+A\left[\frac{l_1^2}{S^4}+\frac{2\nu}{S}\left\{l_2(Q_1^R)^2\right.\right. \\
+\; & \left.l_3(Q_1^I)^2\right\}-\frac{2\nu}{S^2}Q_1^RM_1^R(l_2^2+l_5^2)-\frac{2\nu}{S^2}Q_1^IM_1^I(l_4^2+l_3^2) \\
+\; & \left.\frac{2\nu}{S}Q_1^IQ_1^R(l_5-l_4)+\frac{2\nu}{S^2}(Q_1^IM_1^R+Q_1^RM_1^I)(l_2l_4-l_5l_3)\right] \\
+\; & \left[-\frac{\nu}{S^2}\left\{(Q_1^R)^2(l_2^2+l_5^2)+(Q_1^I)^2(l_4^2+l_3^2)-2Q_1^RQ_1^I(l_2l_4-l_3l_5)\right\}\right]=0\,,
\end{aligned}
$$

(C.1)

where $M_1 = M/F_0$, $Q_1 = Q/F_0$, $A = \epsilon\tilde{a}_n^2$, $l_1 = (\Omega_f - \omega_n^l)^2 - \epsilon^2 e_0^{'2}\left[(G^R)^2 + (G^I)^2\right] + \epsilon^2\mu^{'2}$, $l_2 = (\Omega_f - \omega_n^l) + \epsilon e_0^{'} G^R$, $l_3 = (\Omega_f - \omega_n^l) - \epsilon e_0^{'} G^R$, $l_4 = \epsilon\mu^{'} - \epsilon e_0^{'} G^I$, $l_5 = \epsilon\mu^{'} + \epsilon e_0^{'} G^I$, $\nu = \epsilon(F_0/t_n)^2/S^2$.

REFERENCES

1. J. Aitken 1878 *Philosophical Magazines* **5**, 83-105. An accounts of some experiments on rigidity produced by centrifugal force.

2. C. D. Mote, Jr. 1972 *Shock and Vibration Digest* **4**(4), 2-11. Dynamic stability of axially moving materials.

3. A. G. Ulsoy and C. D. Mote, Jr. 1978 *Shock and Vibration Digest* **10**(1),3-15. Band saw vibration and stability.

4. C. D. Mote, Jr., W. Z. Wu and G. S. Schajer 1982 *Shock and Vibration Digest* **14**(2), 19-25. Band saw and circular saw vibration and stability.

5. C. D'Angelo, N. T. Alvarado, K. W. Wang and C. D. Mote, Jr. 1985 *Shock and Vibration Digest* **17**(5), 11-23. Current research on circular saw and band saw vibration and stability.

6. J. A. Wickert and C. D. Mote, Jr. 1988 *Shock and Vibration Digest* **20**(5), 3-13. Current research on the vibration and stability of axially moving materials.

7. M. P. Paidoussis 1987 *Applied Mechanics Review* **40**(2), 163-175. Flow induced instabilities of cylindrical structures.

8. J. A. Wickert and C. D. Mote, Jr. 1989 *Journal of Acoustic Society of America* **85**(3), 1365-1367. On the energetics of axially moving continua.

9. S. -Y. Lee and C. D. Mote, Jr. 1997 *Journal of Sound and Vibration* **204**(5), 717-734. A generalized treatment of the energetics of translating continua, Part I: Strings and second order tensioned pipes.

10. S. -Y. Lee and C. D. Mote, Jr. 1997 *Journal of Sound and Vibration* **204**(5), 735-753. A generalized treatment of the energetics of translating continua, Part II: Beams and fluid conveying pipes.

11. A. A. Renshaw, C. D. Rahn, J. A. Wickert and C. D. Mote, Jr. 1998 *ASME Journal of Vibration and Acoustics* **120**, 634-636. Energy and conserved functional for axially moving materials.

12. R. Skutch 1897 *Annalen der Physik und Chemie* **61**, 190-195. Uber die Bewegung eines gespannten Faden, whelcher gezwungen ist, durch zwei feste Punkte, mit einer constanten Geschwindigkeit Zugchen, und zwischen denselben in transversalschwingungen von gerlinger Amplitude verstetzwire.

13. R. A. Sack 1954 *British Journal of Applied Physics* **5**, 224-226. Transverse oscillations in travelling strings.

14. S. Mahalingam 1957 *British Journal of Applied Physics* **8**, 145-148. Transverse vibrations of power transmission chains.

15. F. R. Archibald and A. G. Emslie 1958 *ASME Journal of Applied Mechanics* **25**, 347-348. Vibration of a string having a uniform motion along its length.

16. J. A. Wickert and C. D. Mote, Jr. 1990 *ASME Journal of Applied Mechanics* **57**, 738-744. Classical vibration analysis of an axially moving continua.

17. W. L. Mirankar 1960 *IBM Journal of Research and Development* **4**, 36-42. The wave equation in a medium in motion.

18. L. Meirovitch 1974 *AIAA Journal* **12**(10), 1337-1342. A new method of solution for the eigenvalue problem for gyroscopic systems.

19. L. Meirovitch 1975 *ASME Journal of Applied Mechanics* **42**, 446-450. A modal analysis for the responses of linear gyroscopic systems.

20. G. M. T. D'Eleuterio and P. C. Hughes 1984 *ASME Journal of Applied Mechanics* **51**, 415-422. Dynamics of gyroelastic continua.

21. N. C. Perkins 1990 *ASME Journal of Vibration and Acoustics* **112**, 2-7. Linear dynamics of a translating string on an elastic foundation.

22. J. A. Wickert 1993 *ASME Journal of Vibration and Acoustics* **115**, 145-151. Free linear vibration of self-pressurized foil bearings.

23. C. A. Tan and L. Zhang 1994 *ASME Journal of Vibration and Acoustics* **116**, 319-325. Dynamic characteristics of a constrained string translating across an elastic foundation.

24. W. D. Zhu and C. D. Mote, Jr. 1995 *ASME Journal of Applied Mechanics* **62**, 873-879. Propagation of boundary disturbances in an axially moving strip in contact with rigid and flexible constraints.

25. A. V. Laksmikumaran and J. A. Wickert 1996 *ASME Journal of Vibration and Acoustics* **118**, 398-405. On the vibration of coupled travelling string and air bearing system.

26. J. -S. Chen 1997 *ASME Journal of Vibration and Acoustics* **119**, 152-157. Natural frequency and stability of an axially travelling string in contact with a stationary load system.

27. S. -Y. Lee and C. D. Mote, Jr. 1998 *Journal of Sound and Vibration* **212**(1), 1-22. Travelling wave dynamics in a translating string coupled to stationary constraints : energy transfer and mode localization.

28. K. F. Graff 1975 *Wave Motions in Elastic Solids.* Ohio State University Press.

29. S. -P. Cheng and N. C. Perkins 1991 *Journal of Sound and Vibration* **144**(2), 281-291. The vibration and stability of a friction guided travelling string.

30. B. Yang 1992 *ASME Journal of Applied Mechanics* **59**, 650-656. Eigenvalue inclusion principles for distributed gyroscopic systems.

31. W. D. Zhu, C. D. Mote, Jr. and B. Z. Guo 1997 *ASME Journal of Applied Mechanics* **64**, 613-619. Asymptotic distribution of eigenvalues of a constrained translating string.

32. A. Simpson 1972 *Journal of Sound and Vibration* **20**, 177-189. On the oscillating motions of travelling elastic cables.

33. M. S. Triantafyllou 1985 *Journal of Sound and Vibration* **103**, 171-182. The dynamics of translating cables.

34. N. C. Perkins and C. D. Mote, Jr. 1987 *Journal of Sound and Vibration* **114**(2), 325-340. Three dimensional vibration of travelling elastic cables.

35. N. C. Perkins and C. D. Mote, Jr. 1989 *Journal of Sound and Vibration* **128**, 397-410. Theoretical and experimental stability of two translating cable equilibria.

36. N. C. Perkins 1989 *Journal of Sound and Vibration* **135**, 375-383. Asymptotic analysis of a translating cable arch.

37. C. D. Mote, Jr. 1965 *Journal of Franklin Institute* **279**(6), 430-444. A study of band saw vibrations.

38. R. Barakat 1967 *Journal of Acoustic Society of America* **43**, 533-539. Transverse vibrations of a moving thin rod.

39. A. Simpson 1973 *Journal of Mechanical Engineering Science* **15**(3). Transverse modes and frequencies of beams translating between fixed end supports.

40. H. M. Nelson 1979 *Journal of Sound and Vibration* **65**(3), 381-389. Transverse vibration of a moving strip.

41. K. W. Wang 1991 *ASME Journal of Vibration and Acoustics* **113**, 62-68. Dynamic stability analysis of high speed axially moving bands with end-curvatures.

42. S. -J. Hwang and N. C. Perkins 1992 *Journal of Sound and Vibration* **154**(3), 381-409. Supercritical stability of an axially moving beam. Part I : Model and equilibrium analysis. Part II : Vibration and stability analysis.

43. C. D. Mote, Jr. and W. Z. Wu 1985 *Journal of Sound and Vibration* **102**(1), 1-9. Vibration coupling in belt and band systems.

44. K. W. Wang and C. D. Mote, Jr. 1986 *Journal of Sound and Vibration* **109**(2), 237-258. Vibration coupling analysis of band/wheel mechanical systems.

45. K. W. Wang 1990 *Journal of Sound and Vibration* **143**(1), 75-91. Indirect damping analysis and synthesis of band/wheel mechanical systems.

46. A. G. Ulsoy 1986 *ASME Journal of Vibration, Acoustics, Srtess and Reliability in Design* **108**, 207-212. Coupling between spans in the vibration of axially moving materials.

47. A. A. N. Al-Jawi, C. Pierre and A. G. Ulsoy 1995 *Journal of Sound and Vibration* **179**(2), 243-287. Vibration localization in dual-span axially moving beams. Part I : Formulation and results. Part II : Perturbation analysis.

48. N. C. Perkins and C. D. Mote, Jr. 1986 *Journal of Sound and Vibration* **106**, 451-463. Comments on curve veering in eigenvalue problems.

49. A. A. N. Al-Jawi, C. Pierre and A. G. Ulsoy 1995 *Journal of Sound and Vibration* **179**(2), 289-312. Vibration localization in band-wheel systems : theory and experiment.

50. P. W. Anderson 1958 *Journal of Experimental and Theoretical Physics* **109**, 1492-1505. Absence of diffusion in certain random lattices.

51. C. D. Hodges 1982 *Journal of Sound and Vibration* **82**, 411-424. Confinement of vibration by structural irregularity.

52. C. Pierre, E. H. Dowell and D. M. Tang 1987 *AIAA Journal* **25**, 1249-1257. Localized vibrations of disordered multi-span beams : theory and experiment.

53. D. Bouzit and C. Pierre 1992 *ASME Journal of Vibration and Acoustics* **114**, 521-530. Vibration confinement phenomena in disordered, mono-coupled multispan beams.

54. Y. K. Lin 1996 *Applied Mechanics Review* **49**(2), 57-64. Dynamics of disordered periodic structures.

55. J. A. Wickert and C. D. Mote, Jr. 1988 *Journal of Acoustics Society of America* **84**, 963-969. Linear transverse vibration of an axially moving string particle system.

56. W. D. Zhu and C. D. Mote, Jr. 1994 *Journal of Sound and Vibration* **117**(5), 591-560. Free and forced response of an axially moving string transporting a damped linear oscillator.

57. J. A. Wickert and C. D. Mote, Jr. 1991 *Journal of Sound and Vibration* **149**, 267-284. Travelling load response of an axially moving string.

58. K. W. Wang and C. D. Mote, Jr. 1987 *Journal of Sound and Vibration* **115**(2), 203-216. Band/wheel system vibration under impulsive boundary excitation.

59. J. A. Wickert 1994 *ASME Journal of Vibration and Acoustics* **116**, 137-139. Response solution for the vibration of a travelling string on an elastic foundation.

60. B. Yang and C. A. Tan 1992 *ASME Journal of Applied Mechanics* **59**, 1009-1014. Transfer function of one dimensional distributed parameters ststems.

61. C. A. Tan and C, H. Chung 1993 *ASME Journal of Applied Mechanics* **60**, 1004-1019. Transfer function formulation of constrained distributed parameter systems. Part I : Theory. Part II : Applications.

62. E. A. Coddington and N. Levinson 1955 *Theory of Ordinary Differential Equations.* New York: McGraw-Hill.

63. C. A. Tan and S. Ying 1997 *ASME Journal of Applied Mechanics* **64**. 394-400. Dynamic analysis of the axially moving string based on wave propagation.

64. J. A. Wickert and C. D. Mote, Jr. 1991 *Applied Mechanics Review* **44**, s279-s284. Responses and discretization methods for axially moving materials.

65. S. Chonan 1986 *Journal of Sound and Vibration* **107**(1), 155-165. Steady state response of an axially moving strip subjected to a stationary lateral load.

66. S. Naguleswaran and C, J. H. Williams 1968 *International Journal Mechanical Sciences* **10**, 239-250. Lateral vibration of ban-saw blades, pulley belts and the like.

67. S. F. Asokanthan and S. T. Ariaratnam 1994 *ASME Journal of Vibration and Acoustics* **116**, 275-279. Flexural instabilities in axially moving bands.

68. M. Pakdemirli and H. Batan 1993 *Journal of Sound and Vibration* **168**(2), 371-378. Dynamic stability of a constantly accelerating strip.

69. M. Pakdemirli, A. G. Ulsoy and A. Ceranoglu 1994 *Journal of Sound and Vibration* **169**(2), 179-196. Transverse vibration of an axially accelerating string.

70. M. Pakdemirli and A. G. Ulsoy 1997 *Journal of Sound and Vibration* **203**(5), 815-832. Stability analysis of an axially accelerating string.

71. H. R. Oz, M. Pakdemirli and E Ozkaya 1998 *Journal of Sound and Vibration* **215**(3), 571-575. Transition behaviour from string to beam for an axially accelerating material.

72. F. Kozin and R. M. Milstead 1979 *ASME Journal of Applied Mechanics* **46**(2), 404-410. The stability of moving elastic strip subjected to random parametric excitation.

73. S. T. Ariaratnam and S. F. Asokanthan 1993 *Journal of Sound and Vibration* **167**(3), 421-432. Instabilities in moving bands under random tension fluctuation.

74. R. L. Stratonovitch 1963 *Topics in the Theory of Random Noise* vol. I. New York : Gordon and Breach.

75. A. G. Ulsoy, J. E. Whitesell and M. D. Hooven 1985 *ASME Journal of Vibration, Acoustics, Stress and Reliability in Design* **107**, 282-290. Design of belt-tensioner systems for dynamic stability.

76. B. Ravindra and W. D. Zhu 1998 *Applied Mechanics Archieve* **68**, 195-205. Low dimensional chaotic response of axially accelerating continuum in the supercritical regime.

77. A. K. Mallik 1990 *Principles of Vibration Control.* New Delhi : Affiliated East-West Press Pvt. Ltd.

78. C. H. Hansen and S. D. Snyden 1997 *Active Control of Noise and Vibration.* London : E & FN.

79. C. A. Tan, B. Yang and C. D. Mote, Jr. 1990 *ASME Journal of Vibration and Acoustics* **112**, 337-345. On the vibration of a translating string coupled to hydrodynamic bearings.

80. C. A. Tan, B. Yang and C. D. Mote, Jr. 1993 *ASME Journal of Vibration and Acoustics* **115**, 9-15. Dynamic response of an axially moving beam coupled to hydrodynamic bearing.

81. K. V. Ingard and A. Akay 1987 *ASME Journal of Vibration, Acoustics, Stress and Reliability in Design* **109**, 178-184. On the vibration damping of a plate by means of a viscous fluid layer.

82. C. A. Tan and C. D. Mote, Jr. 1990 *ASME Journal of Tribology* **112**, 514-523. Analysis of a hydrodynamic bearing under transverse vibration of an axially moving band.

83. F. Y. Huang and C. D. Mote, Jr. 1995 *Journal of Sound and Vibration* **181**(2), 251-260. On the translating damping caused by a thin viscous fluid layer between a translating string and a translating rigid surface.

84. A. E. Jai and A. J. Pritchand 1987 *International Journal of Control* **46**(4), 1139-1153. Sensors and actuators in distributed systems.

85. B. Yang and C. D. Mote, Jr. 1991 *ASME Journal of Dynamic Systems, Measurement, and Control* **113**, 11-17. Controllability and observability of distributed gyroscopic systems.

86. L. Meirovitch and H. Oz 1980 *Journal of Guidance, Control and Dynamics* **3**(2), 140-150. Modal space control of distributed gyroscopic systems.

87. H. Oz and L. Meirovitch 1980 *Journal of Guidance, Control and Dynamics* **3**(3), 218-226. Optimal modal space control of flexible gyroscopic systems.

88. L. Meirovitch and H. Baruh 1985 *Journal of Guidance, Control, and Dynamics* **8**, 707-716. The implementation of modal filters for control of structures.

89. M. J. Balas 1978 *IEEE Transactions of Automatic Control* AC-**23**, 673-679. Feedback control of flexible systems.

90. M. J. Balas 1978 *Journal of Optimization Theory and Application* **25**, 415-436. Active control of flexible systems.

91. A. G. Ulsoy 1984 *ASME Journal of Dynamic Systems, Measurement, and Control*, **106**, 6-14. Vibration control in rotating or translating elastic systems.

92. B. Yang and C. D. Mote, Jr. 1991 *ASME Journal of Applied Mechanics* **58**, 189-196. Active vibration control of the axially moving string in the s-domain.

93. B. Yang and C. D. Mote, Jr. 1991 *ASME Journal of Dynamic Systems, Measurement, and Control* **113**, 18-25. Frequency domain vibration control of distributed gyroscopic systems.

94. S. M. Shahruz and S. A. Parasurama 1986 *Journal of Sound and Vibration* **214**(3), 567-575. Suppression of vibration in the axially moving Kirchoff string by boundary control.

95. C. H. Chung and C. A. Tan 1995 *ASME Journal of Vibration and Acoustics* **117**, 49-55. Active vibration control of the axially moving string by wave cancellation.

96. S. -Y. Lee and C. D. Mote, Jr. 1996 *ASME Journal of Dynamic Systems, Measurement, and Control* **118**, 66-74. Vibration control of an axially moving string by boundary control.

97. A. H. von-Flotow 1986 *Journal of Guidance, Control and Dynamics* **9**(4), 463-468. Travelling wave control for large space-craft structures.

98. A. H. von-Flotow and B. Schafer 1986 *Journal of Guidance, Control and Dynamics* **9**(6), 673-680. Wave absorbing controller for a flexible beam.

99. B. Yang and C. D. Mote, Jr. 1992 *ASME Journal of Dynamic Systems, Measurement, and Control* **114**, 409-414. On time-delay in non-colocated control of flexible mechanical systems.

100. S. Ying and C. A. Tan 1996 *ASME Journal of Vibration and Acoustics* **118**, 306-312. Active vibration control of the axially moving string using space feedforward and feedback controller.

101. B. Tabarrok, C. M. Leech and Y. I. Kim 1974 *Journal of Franklin Institute* **297**(3), 201-220. On the dynamics of an axially moving beam.

102. P. K. C Wang and J. Wei 1987 *Journal of Sound and Vibration* **116**, 149-160. Vibration of a moving flexible robot arm.

103. M. C. Stylianou and B. Tabarrok 1994 *Journal of Sound and Vibration* **178**, 433-453. Finite element analysis of an axially moving beam. Part I : time integration.

104. J. Zajaczkowski and J. Lipinski 1979 *Journal of Sound and Vibration* **63**, 9-18. Instability of the motion of a beam of periodically varying length.

105. J. Zajaczkowski and G. Yamada 1980 *Journal of Sound and Vibration* **68** 173-180. Further results on the instability of the motion of a beam of periodically varying length.

106. M. C. Stylianou and B. Tabarrok 1994 *Journal of Sound and Vibration* **178**, 455-481. Finite element analysis of an axially moving beams. Part II : Stability analysis.

107. C. Bardos and G. Chen 1981 *SIAM Journal of Control and Optimization* **19**, 123-138. Control and stabilization for the wave equation, Part III : Domain with moving boundary.

108. J. Yuh and T. Young 1991 *ASME Journal of Dynamic Systems, Measurement, and Control* **113**, 34-40. Dynamic modelling of an axially moving beam in rotation : simulation and experiment.

109. Y. K. Kim and J. S. Gibson 1991 *IEEE Transactions on Robotics and Automation* **7**, 818-827. A variable-order adaptive controller of a manipulator with a sliding flexible link.

110. C. D. Mote, Jr. 1966 *ASME Journal of Applied Mechanics* **33**, 463-464. On the nonlinear oscillation of an axially moving string.

111. W. F. Ames, S. Y. Lee and J. N. Zaiser 1968 *International Journal of Non-linear Mechanics* **3**, 449-469. Non-linear vibration of a travelling threadline.

112. L. Y. Shih 1971 *International Journal of Non-linear Mechanics* **6**(4), 427-434. Three-dimensional non-linear vibration of a travelling string.

113. L. Y. Shih 1975 *International Journal of Non-linear Mechanics* **10**(3), 183-191. Motion of elliptic ballooning for a travelling string.

114. A. L. Thurman and C. D. Mote, Jr. 1969 *ASME Journal of Applied Mechanics* **36**, 83-91. Free peiodic non-linear oscillation of an axially moving strip.

115. C. G. Reuter and P. Hagedorn 1995 *Proceedings of the ASME Design Engineering Conference* DE-84-1, part A, 585-593. On the non-linear dynamics of a travelling cable with small sag.

116. O. M. O'Reilly 1996 *ASME Journal of Applied Mechanics* **63**, 180-189. Steady Motions of a drawn cable.

117. J. A. Wickert 1992 *International Journal of Non-linear Mechanics* **27**(3), 503-517. Non-linear vibration of a travelling tensioned beam.

118. J. Moon and J. A. Wickert 1997 *Journal of Sound and Vibration* **200**(4), 419-431. Non-linear vibration of power transmission belts.

119. M. A. Mostafa and F. K. Salman 1976 *ASME Journal of Engineering for Industry* **98**, 868-875. Dynamic properties of a moving threadlines.

120. K. R. Korde 1985 *ASME Journal of Applied Mechanics* **52**, 493-494. On non-linear oscillation of moving string.

121. D. B. McIver 1973 *Journal of Engineering Mathematics* **7**, 249-261. Hamilton's principle for systems of changing mass.

122. S. Dost and B. Tabarrok 1979 *ASME Journal of Applied Mechanics* **46**, 285-290. Application of Hamilton's principle to large deformation and flow problems.

123. L. Vu-Quoc and S. Li 1995 *Computer Methods in Applied Mechanics and Engineering* **120**, 65-118. Dynamics of sliding geometrically exact beams : large angle maneuver and parametric resonances.

124. K. Behdinan, M. C. Stylianou and B. Tabarrok 1997 *Journal of Sound and Vibration* **208**(4), 517-539. Dynamics of flexible sliding beams - non-linear analysis. Part I : Formulation.

125. T. R. Kane and D. A. Levinson 1985 *Dynamics : Theory and Applications.* New York : McGraw-Hill Book Company.

126. K. W. Buffinton 1992 *ASME Journal of Dynamic Systems, Measurement, and Control* **114**, 41-49. Dynamics of elastic manipulators with prismatic joints.

127. K. W. Buffinton and T. R. Kane 1985 *International Journal of Solids and Structures* **21**(7), 617-643. Dynamics of a beam moving over supports.

128. C. W. Wampler, K. W. Buffinton and S. H. Jia 1985 *ASME Journal of Applied Mechanics* **52**, 465-470. Formulation of equations of motion for systems subjected to contraints.

129. K. Behdinan and B. Tabarrok 1997 *Journal of Sound and Vibration* **208**(4), 541-565. Dynamics of flexible sliding beams – non-linear analysis. Part II : Transient response.

130. R. S. beikmann, N. C. Perkins and A. G. Ulsoy 1996 *ASME Journal of Vibration and Acoustics* **118**, 567-574. Non-linear coupled vibration response of serpentine belt drive systems.

131. W. Z. Wu and C. D. Mote, Jr. 1986 *Journal of Sound and Vibration* **110**(1), 27-39. Parametric excitation of an axially moving band by periodic edge-loading.

132. E. M. Mockenstrum, N. C. Perkins and A. G. Ulsoy 1996 *ASME Journal of Vibration and Acoustics* **118**, 346-350. Stability and limit cycles of parametrically excited, axially moving strings.

133. P. J. Holmes 1978 *ASME Journal of Applied Mechanics* **45**, 619-622. Pipes supported at both end cannot flutter.

134. P. Berge, Y. Pomeau and C. Vidal 1984 *Order within Chaos.* New Yprk : John Wiley & Sons.

135. D. J. Mead 1994 *Journal of Sound and Vibration*, **171**, 695-702. Waves and modes in finite beams : application of the phase-closure principle.

136. E. J. Barbeau 1988 *Polynomials.* Berlin: Springer Verlag.

137. S. Timoschenko and D. H. Young 1959 *Vibration Problems in Engineering.* Princeton: Van Nostrand.

138. E. Kreyszig 1983 *Advanced Engineering Mathematics.* John Wiley & Sons, Inc.

139. G. Doetsh 1961 *Guide to the Application of Laplace Transformations.* London : D. van Nostrand Company Ltd..

140. R. M. Rosenberg 1966 *Advances in Applied Mechanics* **9**, 155-243. On non-linear vibration of systems with many degrees of freedom.

141. W. Szemplinska-Stupcicka 1990 *The Behavior of Nonlinear Vibrating Systems* Volume II. London : Kluwer Academic Publishers

142. S. W. Shaw and C. Pierre 1994 *Journal of Sound and Vibration* **169**, 319-347. Normal modes of vibration for non-linear continuous systems.

143. A. H. Nayfeh and S. A. Nayfeh, 1994, *ASME Journal of Vibration and Acoustics*, **116**, 129-136. On nonlinear modes of continuous systems.

144. M. E. King and A. F. Vakakis, 1994, *ASME Journal of Vibration and Acoustics*, **116**, 332-340. An energy-based formulation for computing non-linear normal modes in undamped continuous systems.

145. A. H. Nayfeh and D. T. Mook 1979 *Non-linear Oscillations.* New York: Wiley.

146. J. A. Bennet and J. G. Eisley 1970 *AIAA Journal* 8(4), 734-739. A multiple degree-of-freedom approach to non-linear beam vibrations.

147. H. Troger and C. S. Hsu 1977 *ASME Journal of Applied Mechanics* **44**, 179-181. Response of a nonlinear system under combined parametric and forcing excitation.

148. L. D. Zavodney, A. H. Nayfeh and N. E. Sanchez 1989 *Journal of Sound and Vibration* **129**(3), 417-422. The response of a single-degree-of-freedom system with quadratic and cubic non-linearities to a principal parametric resonance.

149. C. D. Mote, Jr. 1975 *Trans ASME Journal of Dynamic Systems, Measurement, and Control* **97**, 96-98. Stability of systems transporting accelerating axially moving materials.

150. H. S. Lin and C. D. Mote, Jr. 1974 *Trans ASME Journal of Engineering for Industry* **96**, 591-596. Dynamic response of pipes transporting fluids.

151. W. Hahn 1967 *Stability of Motion.* Berlin: Springer-Verlag.

152. P. C. Perks 1966 *Differential Equations and Dynamical Systems, eds. J. K. Hale and J. P. LaSalle*, Academic Press. A stability criterion for a panel flutter problem via the second method of Lyapunov.

153. T. Kailath 1980 *Linear Systems.* Englewood Cliffs: Prentice-Hall.

LIST OF PUBLICATIONS OUT OF THE THESIS

1. G. Chakraborty, A. K. Mallik and H. Hatwal 1998 *Journal of Sound and Vibration* **210**(1), 19-36. Normal modes and near-resonance response of beams with non-linear effects.
2. G. Chakraborty, A. K. Mallik and H. Hatwal 1999 *International Journal of Non-Linear mechanics* **34**, 655-670. Non-linear vibration of a travelling beam.
3. G. Chakraborty and A. K. Mallik 1998 *Nonlinear Dynamics* **17**, 301-324. Parametrically excited non-linear traveling beams with and without external forcing.
4. G. Chakraborty and A. K. Mallik 1999 *Journal of Sound and Vibration* (in press). Stability of an accelerating beam.
5. G. Chakraborty and A. K. Mallik 1999 *Nonlinear Dynamics* (accepted for publication). Non-linear vibration of a travelling beam having an intermediate guide.
6. G. Chakraborty and A. K. Mallik 1999 *Journal of Sound and Vibration* (communicated). Wave propagation in and vibration of a travelling beam with and without non-linear effects: Part I: Free Vibration, Part II: Forced vibration.